Defence Research and Development Canada
Recherche et développement pour la défense Canada

DRDC | RDDC
technologysciencetechnologie

Range of motion measurement reliability for the Canadian Load Effects Assessment Program

Andrew Morton

Carlie Sorgini, Jordan Bray-Miners, Melissa Yu, Neha Sam

Prepared by:
Human Systems Incorporated
111 Farquhar St #202
Guelph, (ON)
Canada

PSPC Contract Number: W7701-166107/001/QCL
Technical Authority: Thomas Karakolis and Linda Bossi
Contractor's date of publication: March 2018

Defence Research and Development Canada

Contract Report
DRDC-RDDC-2018-C120
October 2018

Canada

IMPORTANT INFORMATIVE STATEMENTS

DRDC No. DRDC-RDDC-2018-C120

RANGE OF MOTION MEASUREMENT RELIABILITY FOR THE CANADIAN LOAD EFFECTS ASSESSMENT PROGRAM

by:

Andrew Morton, Carlie Sorgini, Jordan Bray-Miners, Melissa Yu, Neha Sam

Human*Systems*® Incorporated
111 Farquhar Street
Guelph, ON N1H 3N4

HSI® Project Manager: Andrew Morton
(519) 836-5911

PWGSC Contract No. W7701-166107/001/QCL
Task Authorization No. 04

On Behalf of

Department of National Defence

As represented by

DRDC Toronto Research Centre
1133 Sheppard Ave
Toronto, ON, M3K 2C9

Project Scientific Authority:

Thomas Karakolis
416.635.2000 ext.3068

Linda Bossi
416.635.2197

March, 2018

Author

Andrew Morton
Human*Systems*® Incorporated

Approved by

Thomas Karakolis and Linda Bossi
Scientific Authority

Approved for release by

Document Review Chair
Chair, Document Review and Library Committee

Abstract

The Canadian Load Effects Assessment Program (CAN-LEAP) was created to study the implications of "Soldier Burden" on mobility and combat tasks and to determine the threshold at which a degradation in performance occurs. In addition to completing the mobility course and ancillary stands, the flexibility of each soldier while wearing the various equipment configurations is characterized. These Range of Motion (ROM) measurements encompass movements such as trunk rotation, lateral bending, trunk flexion, hip flexion, and shoulder abduction. To date, a standardized approach to taking ROM measures has not been developed. Of the seven experimental studies that have taken place at DRDC-Toronto, there have been four different ROM approaches used, making it difficult to consistently relate ROM to mobility performance. In order to better understand the association between ROM and operational performance, a standardized, accurate, and reliable ROM approach must be developed.

Thirty regular force volunteers participated over six weeks of data collection. Each week a new set of participants completed range of motion exercises in three different equipment conditions and completed the CAN-LEAP course in six different equipment conditions. The first three conditions included a baseline condition, a full fighting order (FFO) condition, and an extended-FFO condition, while the last three conditions were slight modifications to the first three. Participants not only completed multiple runs of the CAN-LEAP course but they also participated in five ROM stations where multiple range of motion measurements were taken using different ROM methods. In addition to completing the typical CAN-LEAP analysis to determine the effect of wearing extended body armour, multiple statistical analysis techniques were employed to determine the effect on soldier ROM of: extended body armour, running the LEAP course, and doffing/donning equipment. An Analysis of Variance (ANOVA) was used to determine the effect on soldier ROM of wearing extended body armour while a combination of ANOVAs and intra-class correlations were employed to determine which methods were most reliable when taking the various ROM measures. Linear regression models were computed using a two-stage cluster bootstrap technique to determine the strength of the relationship between ROM measures and CAN-LEAP performance metrics

Significant differences were observed between conditions in total obstacle course time and individual obstacle times, subjective ratings of performance, ratings of perceived exertion and, to a lesser degree, marksmanship and the other ancillary stands. As expected, soldiers posted the fastest course times in the slick condition and the slowest course times in the more encumbered extended armour condition. While the overall course times and subjective ratings of performance showed a significant decrease in timings and ratings between the extended body armour and the traditional body armour, only select course obstacles showed this statistically significant difference. Significant differences were also observed between conditions in all ROM measures. As expected, soldiers had the greatest ROM in the slick condition and typically had the lowest ROM in the fully encumbered condition. The only ROM measures that showed a significant decrease in ROM between the extended body armour and the traditional body armour were front forward flexion and high knee lift. While all measurement methods were deemed to have good reliability, the Natick protocol of ROM measurement was deemed to be the most reliable measurement method for front forward flexion, high knee lift, and shoulder abduction while the iRoM electronic system was deemed to be the most reliable measurement method for trunk rotation and lateral bending. Right and left high knee lift were found to be most strongly related to obstacle course time, while for subjective ratings it was right/left high knee lift and right/left lateral bend. There was little relationship found between ROM and ratings of perceived exertion.

Executive Summary

Range of Motion Measurement Reliability for the Canadian Load Effects Assessment Program

Andrew Morton, Carlie Sorgini, Jordan Bray-Miners, Melissa Yu, Neha Sam
Human*Systems*® Incorporated; DRDC Toronto DRDC-RDDC-2018-C120; Defence R&D Canada – Toronto; March, 2018.

Aim:

The Canadian Load Effects Assessment Program (CAN-LEAP) experimentation series has been conducted in the past to evaluate the effect of various worn kit and equipment configurations on the soldiers' performance. The objectives of this experimentation campaign remain the same, this time examining the effect of wearing extended body armour on soldier Range of Motion (ROM) and the associated effect on CAN-LEAP performance. The primary objectives of this study are:

1. To assess both previously developed and novel approaches to assessing ROM to determine which approach is most precise, repeatable, and most highly correlated with CAN-LEAP performance.
2. To evaluate the effect of wearing extended body armour on soldier ROM and the associated effect on CAN-LEAP performance.

Background:

The CAN-LEAP was created to determine the implications of "Soldier Burden" on mobility and combat tasks and to determine the threshold at which a degradation in performance occurs. In addition to completing the mobility course and ancillary stands, the flexibility of each soldier while wearing the various equipment configurations is characterized prior to the start of each run. The ROM measurements taken encompass movements such as trunk rotation, lateral bending, trunk flexion, hip flexion, and shoulder abduction.

To date, a standardized approach to taking ROM measures has not been developed. Of the seven experimental studies that have taken place at DRDC-Toronto, there have been four different ROM approaches used, making it difficult to consistently relate ROM to mobility performance. In order to better understand the association between ROM and operational performance, a standardized, precise, and reliable ROM approach must be developed.

Methods:

Thirty regular force volunteers participated over six weeks of data collection. Each week a new set of participants completed range of motion exercises in three different equipment conditions and completed the CAN-LEAP course in six different equipment conditions. The first three conditions included a baseline condition, a full fighting order (FFO) condition, and an extended-FFO condition, while the last three conditions were slight modifications to the first three.

The CAN-LEAP course consisted of the mobility course, a marksmanship component, vertical and horizontal weight transfer, vertical and horizontal (long) jump, and a subjective questionnaire. The results of each component were analyzed to determine the effects of the load condition on performance and user acceptability. Before the CAN-LEAP course is run, typically range of motion measurements are made.

As part of this protocol, five ROM methods were used. The methods were titled as follows:

1. Original LEAP ,
2. United States Marine Corps (USMC) Inertial Measurement Units ROM (iROM),
3. Modified LEAP,
4. NATICK Manual,
5. Functional Reach[1].

In addition to completing the typical LEAP analysis to determine the effect of wearing extended body armour, multiple statistical analysis techniques were employed to determine the effect on soldier ROM of: extended body armour, running the LEAP course, and doffing/donning equipment. Statistical methods were also employed to determine which methods were most reliable when taking the various ROM measures. Using an analysis of variance (ANOVA), the ROM measurement methods were compared to determine the effect, if any, condition, iteration, direction, and trial had on the soldiers' range of motion. An intra-class correlation (ICC) technique was then used to compare methods and determine which was the most reliable, repeatable, and precise for each ROM measure. After determining the most reliable method for a given ROM measure, those ROM values were then regressed against LEAP performance metrics (overall LEAP time, overall subjective ratings of LEAP performance, and ratings of perceived exertion) using a two-stage cluster bootstrap technique to determine which ROM measure was most highly predictive of LEAP performance.

Results and Discussion:

For the total obstacle course times and overall subjective ratings of LEAP performance, significant differences were observed between all conditions with participants performing best in the slick condition and worst when wearing the shoulder brassards and Protective Under Garment (PUG) / Protective Over Garment (POG). Subjectively, the same pattern was observed with participants rating both the slick condition and FFO condition significantly more acceptable than when wearing the shoulder brassards and PUG/POG. The ratings of perceived exertion followed this same general trend, however, participants' perceived exertion when wearing the PUG/POG and shoulder brassards was not significantly lower than when wearing just their Fragmentation Protective Vest (FPV) and Tactical Assault Vest (TAV). For individual obstacle timings and transition timings, the only significant decreases in timings when wearing the PUG/POG and shoulder brassards as opposed to just their FPV and TAV was observed for the tunnel to sprint transition time, the stairs and ladder obstacle, the agility run, the bounding rushes, and the inner wall obstacle. All other obstacles and transition times saw a significant decrease in timings between the slick condition and the FFO condition, but no additional significant decrease in timings with the addition of the PUG/POG and shoulder brassards.

For range of motion, the general trend observed was that ROM decreased as encumbrance increased. The only two measures that were able to tease out a significant decrease in ROM when shoulder brassards and PUG/POG were added to their FFO was front forward flexion and high knee lift. These findings make sense since movements that are potentially restricted by the extended body armour are captured with these two measures, not trunk rotation and lateral bending. Surprisingly, there was not a significant decrease in shoulder abduction between the two encumbered conditions suggesting that the shoulder brassards may be more restrictive in the forward reach motion which is more accentuated in the front forward flexion stations.

[1] Statistical analyses were not completed for Functional Reach as the analysis and reporting of these ROM results were outside the scope of this report.

When analyzing the reliability of the methods, for all measures each method proved to have good reliability (ICC>0.75) with the exception of the modified LEAP and USMC iROM method for front forward flexion. The most reliable, repeatable, and precise methods, determined from ICCs calculated between iterations and ICCs calculated between trials, were as follows:

- Trunk rotation: iRoM
- Lateral Bending: iRoM
- Front Forward Flexion: Natick
- High Knee Lift: Natick
- Shoulder Abduction: Natick

Using the ROM values captured by these methods, a two-stage cluster bootstrapping technique was used to compute regression equations correlating ROM with LEAP performance metrics (overall LEAP time, overall subjective ratings of performance, and ratings of perceived exertion) with each ROM measure. The highest correlations were found between right/left high knee lift and overall LEAP course time, right/left high knee lift and subjective ratings, and right/left lateral bend and subjective ratings. The regressions between ROM and RPE were all very low indicating little to no relationship.

Conclusion:

In conclusion, an increase in encumbrance significantly decreased LEAP course performance times and subjective ratings. The addition of extended body armour specifically decreased LEAP performance timings when completing obstacles like the stairs and ladder, agility run, bounding rushes, and inner wall. An increase in encumbrance also significantly decreased soldier range of motion. The addition of extended body armour specifically decreased ROM for front forward flexion and high knee lift. Some ROM measures were reasonably correlated with the chosen LEAP performance metrics, with right and left high knee lift being the most highly correlated with overall LEAP times, right and left high knee lift/right and left lateral bend being most highly correlated with subjective ratings, and none of the ROM measurements showing a strong correlation with RPE.

Table of Contents

This page intentionally left blank.

List of Figures

List of Tables

Acknowledgements

We would like to acknowledge the soldiers from the Canadian Armed Forces for their participation in this study. Linda Bossi has been instrumental in advising and assisting throughout the project. We would like to thank the data collection team, including Adrienne Sy, Alison Kelly, Caitlin Yee, Cerys McGuiness, Christopher Apostoli, Dan Wong, Dorothy Wojtarowicz, Eric Kramkowski, Michael Thomson, Sean Denroche, and additional reserve force soldiers. Finally, we would like to thank Jeanette O'Hara Hines for her expert advice in the statistical analysis of results.

1. Background

The Canadian Load Effects Assessment Program (CAN-LEAP) was created to determine the implications of "Soldier Burden" on mobility and combat tasks and to determine the threshold at which a degradation in performance occurs. The CAN-LEAP was developed by Human*Systems* Incorporated® (HSI®) in consultation with subject matter experts (SMEs) in combat activities and the Program Manager of the Marine Expeditionary Rifle Squad (MERS) of the United States Marine Corps (USMC). The CAN-LEAP consists of a timed mobility course and a series of ancillary stands specifically designed to evaluate soldier performance. The obstacles were designed to replicate or represent real life obstacles in the field, such as traversing through windows, over walls, over logs and ditches, etc. In general, the course serves to provide an accurate and repeatable method of measuring performance in a controlled environment. The major component of the CAN-LEAP is the course itself, which consists of a series of ten sequential test segments separated by Fitlight timing sensors. An additional three stations (firing accuracy, jump and weight transfer station, and a questionnaire kiosk) are performed independently of the obstacle course. The ten course obstacles are:

1. Tunnel and hatch;
2. Sprint;
3. Stair and ladder;
4. Agility run;
5. Casualty drag;
6. Windows (two);
7. Bounding rushes.
8. Balance beam;
9. Low crawl;
10. Inner and outer courtyard walls;

The ancillary stands are:

1. Weight transfer;
2. Vertical jump;
3. Horizontal jump;
4. NOPTEL firing accuracy;
5. Questionnaire kiosk.

The specifications, assembly, disassembly, care, maintenance and operational instruction of these CAN-LEAP sections, as well as the specifications, start-up, placement, and operation of the Fitlight sensor, NOPTEL firing accuracy, vertical and horizontal jump, weight transfer and, and questionnaire stations are outlined in the CAN-LEAP User Manual.

In addition to completing the mobility course and stands, the flexibility of each soldier, while wearing the various equipment configurations is characterized prior to the start of each run. The range of motion (ROM) measurements taken encompass movements such as trunk rotation, lateral bending, trunk flexion, hip flexion, and shoulder abduction. Typically, manual measurement methods have been used to capture participants' ROM using tools such as inclinometers and goniometers however emerging technologies are enabling scientists to digitally capture range of motion measurements as well. To date, DRDC Toronto has conducted seven experimental studies using the CAN-LEAP course

and stands. ROM measurements have been taken during each experimental study; however, a standardized approach to taking ROM measures has not been developed. Of the seven experimental studies that have taken place, there have been four different ROM approaches used which has made it difficult to consistently relate ROM to mobility performance (Bossi, Jones, Kelly, & Tack, 2016). In order to better understand the association between ROM and operational performance, a standardized, accurate, and more reliable ROM approach must be developed.

1.1 Goal

The CAN-LEAP experimentation series has been conducted in the past to evaluate the effect of various worn kit and equipment configurations on the soldiers' performance. The objectives of this experimentation campaign remain the same, this time examining the effect of wearing extended body armour on soldier ROM and the associated effect on CAN-LEAP performance. The primary objectives of this study are:

1. To assess both previously developed and novel approaches to assessing ROM to determine which approach is most precise, repeatable, and most highly correlated with CAN-LEAP performance.
2. To evaluate the effect of wearing extended body armour on soldier ROM and the associated effect on CAN-LEAP performance.

2. Methods

The following section describes the methodology for all facets of the 2017 CAN-LEAP experimentation campaign, including participants and participant characterization, load configurations, course and station descriptions, ROM methods, and protocols.

2.1 Participant Characterization

Thirty regular force combat arms personnel (aged 22 to 35) were participants in this study. The participants were recruited from combat arms units of the Canadian Army. The study was 6 weeks in duration; a different group of five participants travelled from their home base to DRDC Toronto for the study each week. All participants were required to be physically fit enough for deployment (as determined by their units) and were required to complete the Canadian Armed Forces (CAF) minimum fitness requirements tests (FORCES test) within three months of the study.

2.1.1 Demographics

Participant factors such as size, age, weight, strength, aerobic fitness (VO_2 max), and military experience may have had an influence on the soldiers' performance. Therefore, it was important to characterize the soldiers for these factors to help explain any associated variability in the data and to aid in the interpretation of the results. The following background information was collected for all participants during the study:

- Rank,
- MOSID,
- Age,
- Length of service (regular or reserve),
- Handedness, shooting hand, shooting eye,
- Marksmanship level,
- Combat experience,
- Operational experience,
- Fragmentation Protective Vest (FPV) experience (training and operations),
- Hard Ballistic Plate (HBP) experience (training and operations),
- Vision testing,
- Body composition (percent body fat) using ultrasound,

2.1.2 Physical Characteristics

Participant physical characteristics such as anthropometry may have had an influence on their performance. Therefore, weight, height, front length (standing), back length (standing), waist circumference (iliac crest), and chest circumference (thelion) were measured.

2.1.2.1 ***Physical Capabilities***

Participant physical capabilities such as fitness, adiposity, heart rate, and strength may have had an influence on their performance. Therefore, it was important to characterize the soldiers for these factors. The physical capabilities collected are explained in the sections below.

2.1.2.1.1 Fitness Testing

A sub-maximal fitness test (Modified Canadian Aerobic Fitness Test, mCAFT) was conducted to estimate each participant's aerobic (endurance) fitness, usually referred to as the maximal rate of oxygen consumption (VO_2 max). Sub-maximal fitness testing was conducted as described in Annex A: Sub-Maximal Fitness Testing.

2.1.2.1.2 Adiposity Testing

Participants had their body composition (percent body fat) assessed using ultrasound. Subcutaneous fat thickness was measured using the BodyMetrix portable ultrasound over seven sites: triceps, chest, axilla, scapula, hip, waste, and thigh.

2.1.2.1.3 Strength Testing

Static strength was measured using three different protocols: upper limb static strength, shoulder strength, and lower limb static strength. Each of these tests involved the participant grasping a handle that is sturdily attached to the ground and pulling on it in a series of different postures. A force gauge is in series with the chain and measures the force the participant is able to apply. Refer to Annex B: Static Strength Testing for full details on the static strength testing protocols.

2.1.2.1.4 Heart Rate

The participant's heart rate (HR) was monitored using a Polar Heart Rate Monitor (Polar Electro Canada, Lachine, QC) that was strapped to the participant's chest under their clothing and monitored remotely through a wrist-watch that the participant wore. The participant's HR was monitored to ensure it had returned to within 15% of the resting HR prior to being permitted to commence their LEAP run-through. An alarm was set on the HR monitor whereby an audible signal was emitted if the participant exceeded 95% of his/her maximum HR. This value had been determined as an upper safe limit of exercise for a healthy, fit adult by the American College of Sports Medicine. HR data was recorded, but the analysis of this data is beyond the scope of this report.

2.1.2.2 ***Range of Motion***

As part of this protocol, five separate ROM methods were used. The methods were titled as follows:

1. Original LEAP
2. USMC IMU
3. Modified LEAP
4. NATICK Manual
5. Functional Reach

Each method is described in more detail in the sections below.

2.1.2.2.1 Original LEAP

The original LEAP ROM protocol involved manual measurements of trunk rotation, lateral bending, and front forward flexion using an inclinometer, digital level, and a Wells and Dillon Sit and Reach apparatus. The full details of the ROM protocol is described in Annex C: Original LEAP Method. Throughout the results, this method is referred to as the Manual method.

2.1.2.2.2 USMC IMU

The USMC IMU ROM protocol involved the digital collection of trunk rotation, lateral bending and front forward flexion measurements using six inertial measurement units (IMU) that communicated through motion capture software. This digital protocol used the instrumented range of motion (iRoM) software developed by PM-MERS of the USMC in collaboration with HSI® which collects angular measurements while monitoring the participant's posture to ensure they are using the correct technique for the test. Further detail of this protocol is described in Annex D: USMC IMU Method. Throughout the results, this method is referred to as the iRoM method.

2.1.2.2.3 Modified LEAP

The Modified LEAP method was similar to both the Original LEAP method (Section 2.1.2.2.1) and the USMC IMU method (Section 2.1.2.2.2). For this method, the same IMU setup was used as described previously in the USMC IMU method; however, the custom iRoM software was not used to ensure that participants were not flexing or extending other joints in the body, other than the joint of interest for the specific range of motion exercise. The ROM exercises were identical to those described in the Original LEAP method; however, the advantage of this method was hypothesized to be in the collection of the ROM measures through digital IMUs rather than traditional analog tools as described in Section 2.1.2.2.1. Throughout the results, this method is referred to as the Digital method.

2.1.2.2.4 Natick Manual

The Natick Manual ROM protocol involved manual measurements of trunk forward flexion, trunk lateral flexion, trunk rotation, hip flexion and shoulder abduction using an anthropometer, GoPro camera, and inclinometer. The full, detailed ROM protocol is described in Annex F: Natick Manual Method. Throughout the results, this method is referred to as the Natick method.

2.1.2.2.5 Functional Reach

This functional reach ROM protocol collected data for arm abduction/adduction, flexion/extension, and horizontal flexion/extension. The functional reach apparatus included a small handle attached via four taut strings to potentiometers that the participant would hold when completing the range of motions; this allowed the experimenter to track the position of the participant's hand in three-dimensional space. The functional reach protocol is described in more detail in Annex E: Dalhousie Functional Reach Method. The analysis and reporting of the functional reach ROM results is outside of the scope of this report.

2.2 Experimental Conditions and General Procedures

Participants were involved in five consecutive days of testing at DRDC Toronto Research Centre. The five days are summarized in Table 1 and Table 2. During Days 1 and 2, participants attended a briefing session, provided their informed consent, demographic information, and completed anthropometric measures, sub-maximal fitness testing, strength and body composition testing, and four training runs of the CAN-LEAP course. During days 3-5, participants completed a series of five ROM measuring methods (described in Section 2.1.2.2), multiple times, before and after running the CAN-LEAP course to test the repeatability of the ROM measures as well as their association with CAN-LEAP performance. On each day (Days 3-5), the participants wore one of three different equipment conditions that are described in the following paragraphs. Equipment conditions were assigned to participants in a counterbalanced order. On Day 5, participants also provided feedback to the experimenters in the form of a focus group.

Table 1: Test stand/activity sequence for ROM reliability study

Day	Test Stand/Activity in Sequence
1	Intake Session
1	Detailed briefings, demonstrations, safety brief, consent forms, training, anthropometry
1 & 2	Sub-Maximal Fitness Testing and Strength Testing
1 & 2	LEAP training runs (x4)
3	Condition 1 rotation (described in Table 2)
4	Condition 2 rotation (described in Table 2)
5	Condition 3 rotation (described in Table 2)
5	Wrap-up session and exit focus group discussion

Table 2: Condition rotation flow

Order	
1	ROM taken at all 5 ROM stations (Original LEAP, USMC IMU, Modified LEAP, Natick, and Functional Reach).
2	ROM taken at all 5 ROM stations (Original LEAP, USMC IMU, Modified LEAP, Natick, and Functional Reach).
3	Complete 1st run of LEAP course.
4	ROM taken at all 5 ROM stations (Original LEAP, USMC IMU, Modified LEAP, Natick, and Functional Reach).
5	Lunch (doff body armour and re-don body armour).
6	ROM taken at all 5 ROM stations (Original LEAP, USMC IMU, Modified LEAP, Natick, and Functional Reach).
7	Complete 2nd run of LEAP course in secondary load configuration condition.

2.2.1 Participant Briefing and Safety

Participants were provided with a briefing the first morning where they got background information on the CAN-LEAP, the aim of the project, and the study protocol. If interested in participating, they were required to review and sign the informed consent as well as complete a personal demographic information form (refer to Annex G: Demographic Information Questionnaire). The brief concluded with a participant number assignment.

Prior to any use of the CAN-LEAP course, participants were given a safety briefing and walk through of each obstacle and ancillary stand. Proper and safe techniques of traversing each obstacle were discussed and demonstrated. During this time (and any other time), participants were free to ask any questions they had concerning the obstacles or the method of traversing them.

Participants were given two days to practice and familiarize themselves with the obstacle course. They ran two training runs each day in order to accomplish this. No participant was asked to complete the course more than twice in one day. The safety of the participants was a top priority during the entire study. Participants were given a minimum of 60 minutes of recovery time between the two obstacle course runs in order for the cardiovascular and thermoregulatory systems to adequately recover.

No more than two participants were permitted to run on the course at any one time. This prevented participants from passing/colliding into one another, as well as prevented the attention of human

factors observers and safety personnel from becoming divided. There was always at least one researcher or assistant present on the course, walking alongside the participants. The researcher provided the participant with reminders of the correct course path and proper protocol, observed the participant for any signs of unsafe levels of fatigue or exhaustion, and watched the course for any other safety concerns.

2.2.2 Load Configurations and Participant Matrix

Six equipment conditions were configured in order to examine the effect of extended body armour on the soldier. The six equipment conditions are outlined in Table 3. The conditions will be referred to by their assigned letter for all of the data analysis in this report.

Table 3: Load configuration by condition for first run

Condition	Description
A	The baseline condition consisted of: • combat trousers, • t-shirt, • combat shirt, • combat boots, • in-service helmet; and • C7A2 assault rifle with C79 sight and sling.
B	The FFO condition consisted of the same articles as Condition A, plus: • fragmentation vest, • ballistic plates (front and back); and • tactical vest with standard combat load (4 loaded dummy magazines, 2 dummy frag grenades, 2 dummy smoke grenades, 1 litre of water, personal role radio, and two field dressings).
C	Consisted of the same articles as Condition B, plus: • protective undergarment groin protection (PUG); and • protective overgarment groin protection (POG).
D	Consisted of the same articles as Condition B, plus: • bi-lateral shoulder brassards.
E	The FFO extended armour condition consisted of the same articles as Conditions B, C, and D.
F	Consisted of the same articles as Condition B, plus: • PUG.

Conditions A, B, and E were worn for the ROM portion of the study as well as the first LEAP run of the day. For the second LEAP run each day, participants' load conditions were altered slightly from their morning run. Since these conditions (C, D and F) were not part of the initial trial plan, they were not properly counterbalanced and therefore inferential statistics will not be done for these conditions. Instead, descriptive plots are reported in Annex K: Additional LEAP Results for Conditions C, D, and F.

2.3 CAN-LEAP Course and Activity Sequence

Participants followed the same flow-through of stations for each condition being tested. The following sections describe each station and its methodology, and the order in which each station was completed.

2.3.1 Activity Sequence

After the briefings and safety demonstrations on Day 1 participants were asked to perform a sub-maximal fitness test and undergo basic anthropometric measures (e.g., weight, height, etc.), an adiposity measurement, and strength testing, as described in Section 2.1.2.1. Anthropometric measures were completed while the participant was wearing boots, combat pants and a t-shirt. These stations were completed in a round robin sequence.

On Days 1 and 2, participants completed a dynamic warm up (as described in Annex H: LEAP Station Descriptions) and were then given time to perform two training runs (during Week 1 both training runs were completed in Condition E however for the remainder of the weeks, the first run was done in Condition B and the second run was done in Condition E) on the course. Ample rest time was given between the two runs.

The third day of each testing week marked the official start of LEAP and ROM data collection, where each participant was provided with one of the three test conditions (A, B, or E). A summary of the sequence of events for each day (days 3-5) can be seen in Figure 1.

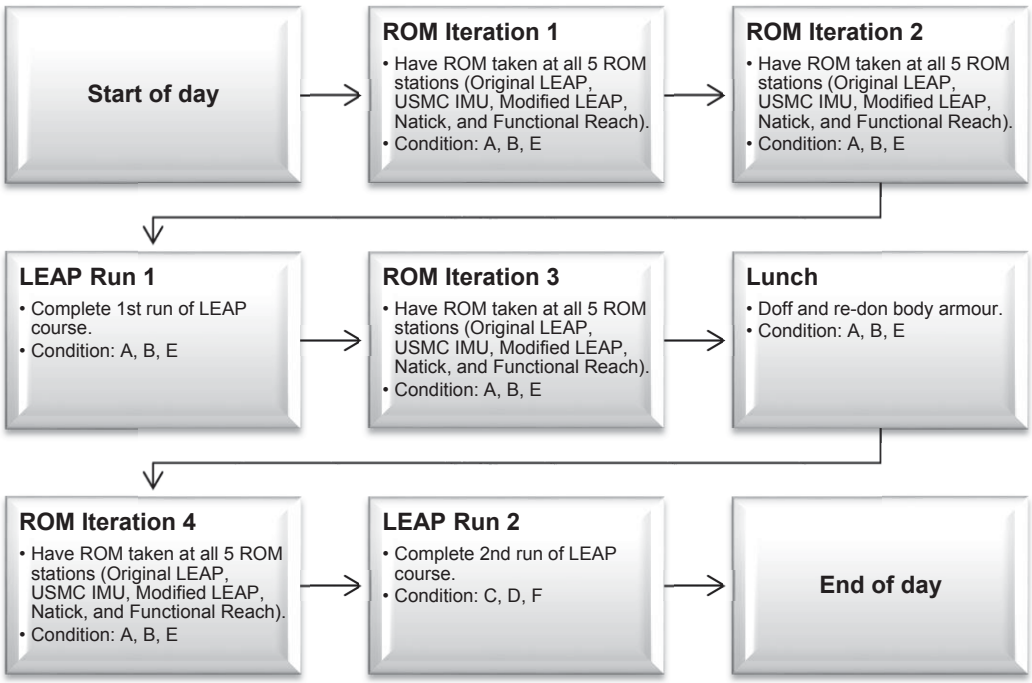

Figure 1: Activity Sequence for Testing Days (Days 3-5)

Each participant would complete the 5 ROM stations twice, they would then complete a dynamic warm up and run the LEAP course. After completing their first LEAP course run they would then complete all 5 ROM stations for a third time. After having completed all 5 ROM stations for a third time they would then doff their equipment and take a break (typically lunch). After their break, participants would re-don their equipment condition (A, B, or E) and complete all 5 ROM stations for the fourth and final time. After the final ROM iteration, the LEAP course was then run for a second time; this run was done in a slightly different equipment condition (C, D, or F). Condition A was always altered to become Condition C, Condition B was always altered to become Condition D, and Condition E was always altered to become Condition F. This sequence of events was completed again

for the next two days but wearing a different equipment condition (A, B or E) so that each participant completed all ROM rotations and LEAP runs in each of the three conditions.

2.3.2 LEAP Flow through of Stations

Participants completed the LEAP once they completed their second ROM iteration and again after they completed their fourth ROM iteration. Prior to commencing the obstacle course portion of LEAP, participants performed a dynamic warm up, followed by the shooting task, the horizontal jump, vertical weight transfer, horizontal weight transfer, and then the vertical jump task. These activities, as well as the Questionnaire kiosk (which is only completed after the obstacle course) are referred to as the ancillary stations.

After finishing the warm up and ancillary stations in the rested state, participants completed the obstacle course comprised of sequential test segments and the ancillary stands. The CAN-LEAP course is traversed in the following order:

- Hatch and Tunnel
- Sprint
- Stair and Ladder
- Agility Run
- Casualty Drag
- Windows
- Bounding Rushes
- Balance Beam
- Crawl
- Courtyard Walls

Immediately following the last obstacle, participants gave a rating of perceived exertion (RPE) and then commenced the same rotation of ancillary stands as before, this time in the fatigued state. A diagram of the CAN-LEAP course configuration and its sequential test segments can be seen in Figure 2.

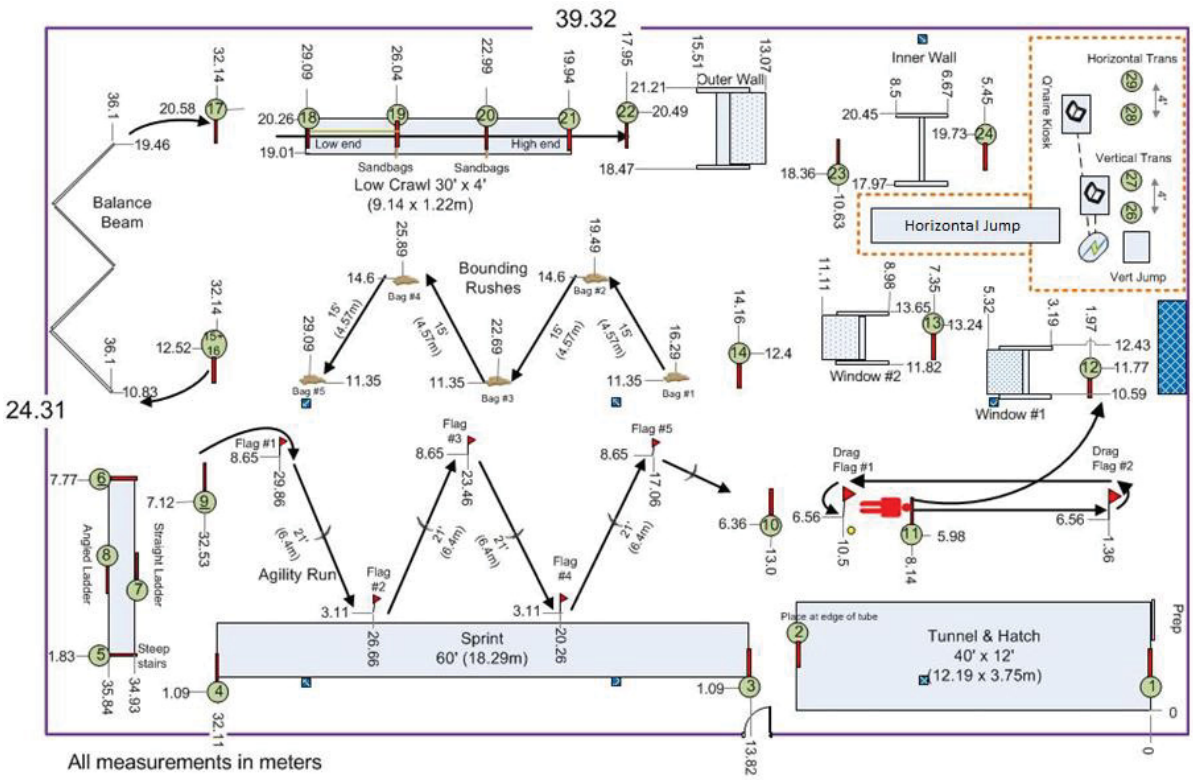

Figure 2: CAN-LEAP Course Configuration

Each of the obstacle course segments are separated by a wireless timing system (Fitlight Trainer™); the additional ancillary stations (firing accuracy, vertical and horizontal weight transfer, vertical and horizontal jump) are performed independently of the Fitlight timing system. Performance in each of the physical tasks was measured and recorded, and included total obstacle course completion time, completion time of individual obstacles and transitions, firing accuracy (shot score and shot X and Y coordinates), jump distance, weight transfer times, jump height, and subjective ratings.

2.3.3 Station Descriptions

The physical specifications and the method of traversing each of the ten obstacles (segments) within the CAN-LEAP course, instrumented with the Fitlight™ timing system, and each of the ancillary stations are described in Annex H: LEAP Station Descriptions. Participants complete all obstacles, in sequence, with no rest breaks.

2.4 Environmental Factors

Wet Bulb Globe Temperature (WBGT), an index calculated from the dry and wet bulb temperatures, the humidity, and the solar radiation, was measured throughout the experimentation campaign. These environmental conditions were measured and recorded using the QuestTemp 36 Heat Stress Monitor.

2.5 Statistical Approach

For this ROM reliability report, multiple different analyses were planned for the various data collected in order to respond to its aims.

2.5.1 LEAP Analysis

Figure 3 shows the analysis plan for the data collected from the first and second LEAP runs, the types of data collected, and which aim the analysis was targeting. For all LEAP analyses, a $p<0.05$ was used to determine whether results were significant.

Due to the ordering of conditions and lack of counterbalancing as mentioned in Section 2.2.2, inferential statistics could not be run on data collected from the second LEAP run. Instead, descriptive plots were completed and presented in Annex K: Additional LEAP Results. All other results for the LEAP data can be seen in Section 3.3.

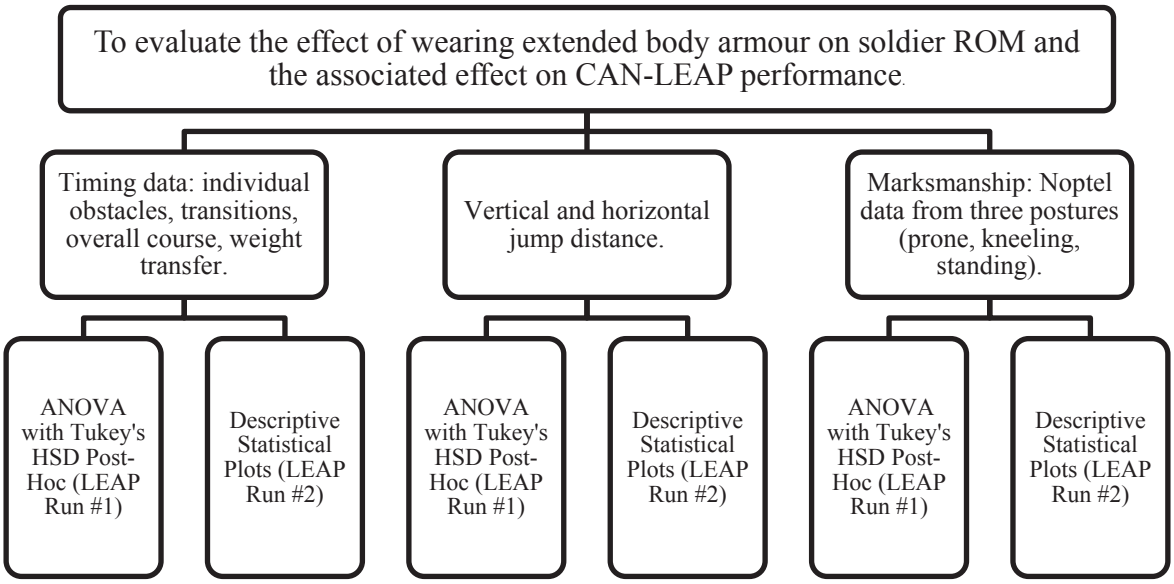

Figure 3: Analysis Plan for LEAP Data Collected During the Winter Experimentation Campaign

2.5.2 ROM Analysis

Figure 4 shows the analysis plan for the data collected during the ROM iterations, the types of data collected, and which aim the analysis was targeting. For all ROM analyses, a $p<0.05$ was used to determine whether results were significant.

For the ROM data, two different analyses were completed to address the corresponding aim. Firstly, the ROM data was filtered for any transcription errors to ensure clean data was being analyzed. Then an analysis of variance (ANOVA) was computed, separately for each measure (trunk rotation, lateral bending, front forward flexion, high knee lift, and shoulder abduction). The purpose of this analysis was to determine, any significant differences between methods, conditions, iterations, trials, or sides.

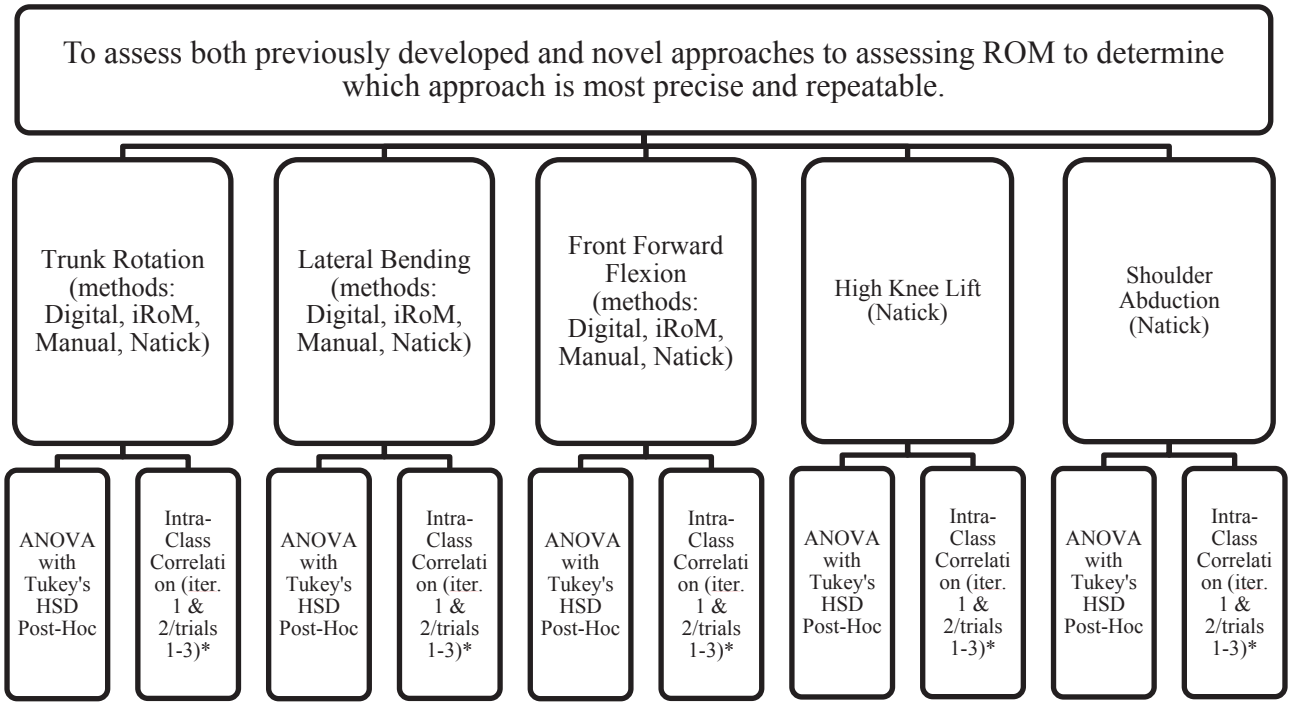

* This method is described in more detail in Annex I: Intra-Class Correlation Method.

Figure 4: Analysis Plan for ROM Data Collected During the Winter Experimentation Campaign

Due to unit inconsistencies, not all methods could be analyzed together for certain ROM measures. More specifically, methods for lateral bending and front forward flexion were analyzed separately depending on units. Figure 5 shows which methods were analyzed separately for these two measures and the corresponding within effects. High knee lift and shoulder abduction were only completed as part of the Natick protocol so there was no comparison between methods for these two measures.

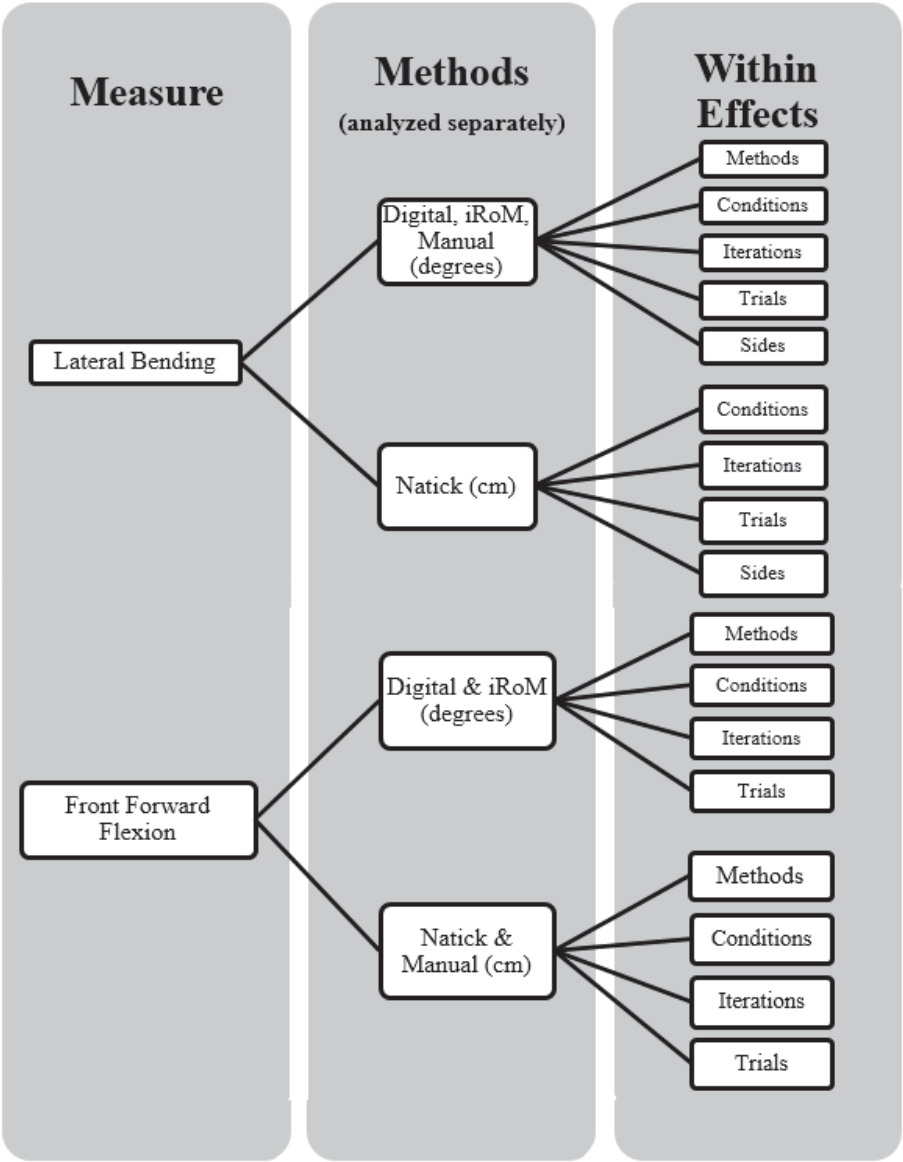

Figure 5: Methods Analyzed Separately for Lateral Bending

Due to experimental design, the assumption of sphericity may have been violated for the repeated-measure ANOVAs. In Statistica, Mauchly's test was run on all computed ANOVAs to determine whether the assumption of sphericity had been violated for each factor and interaction. For Mauchly's test, sphericity is assumed if $p>0.05$. For any cases where Mauchly's test revealed a significant result (i.e. $p<0.05$), the degrees of freedom were adjusted appropriately using either the Greenhouse-Geisser correction (Greenhouse & Geisser, 1959) or the Huynh-Feldt correction (Huynh & Feldt, 1976). The appropriate correction method for adjusting the degrees of freedom was chosen using the epsilon values; for $\varepsilon > 0.75$ the Huynh-Feldt correction was applied and for $\varepsilon < 0.75$ the Greenhouse-Geisser correction was applied (Girden, 1992). By altering the degrees of freedom, a valid F-ratio was obtained for any within-subject factors that violated the assumption of sphericity.

The second part of the ROM analysis involved calculating and comparing intra-class correlation coefficients (ICCs) for each ROM method and measure to determine the reliability of the measurement method. Two different ICCs were calculated: an ICC between trials (1-3) and an ICC between iterations (1 & 2). The equations used, brief methodology, and reasoning for selection are described in Table 4.

Table 4: ICC Equations, Methodology, and Reasoning

	ICC between Trials 1-3	ICC between Iterations 1& 2
ICC Equation	$ICC(A,1)^* = \frac{MS_R - MS_E}{MS_R + (k-1)\cdot MS_E + \frac{k}{n}\cdot(MS_C - MS_E)}$	$ICC(A,k)^* = \frac{MS_R - MS_E}{MS_R - \frac{MS_C - MS_E}{n}}$
Method	Within each condition (A,B,E)/iteration(1-4) the three trials were compared to one another.	For each condition, Trials 1-3 were averaged for Iteration 1 and compared with the averaged trials from Iteration 2.
Reasoning	This ICC was looking at absolute agreement between the three trials in order to determine the precision of each measurement method.	This ICC was looking at absolute agreement between iterations 1 and 2 (the test-retest case) in order to determine the repeatability of the measurement method.

*The ICC form selection and methodology is described in more detail in Annex I: Intra-Class Correlation Method.

The rule of thumb used for interpreting the ICCs was as follows: ICCs less than 0.5 indicated poor reliability, ICCs between 0.5 and 0.75 indicated moderate reliability, ICCs between 0.75 and 0.9 indicated good reliability, and ICCs greater than 0.9 indicated excellent reliability (Koo & Li, 2016).

In order to create a visual comparison of reliability across methods for each ROM measure, all ICCs were then transformed using Fisher's *z*-transformation and plotted (McGraw & Wong, 1996). The methods that were determined to have the best reliability from this portion of the ROM analysis were then carried over to be used for the correlation analysis described in Section 2.5.3 below.

2.5.3 Correlation Analysis

Figure 6 shows the analysis plan for determining which ROM measure was most highly correlated with CAN-LEAP performance.

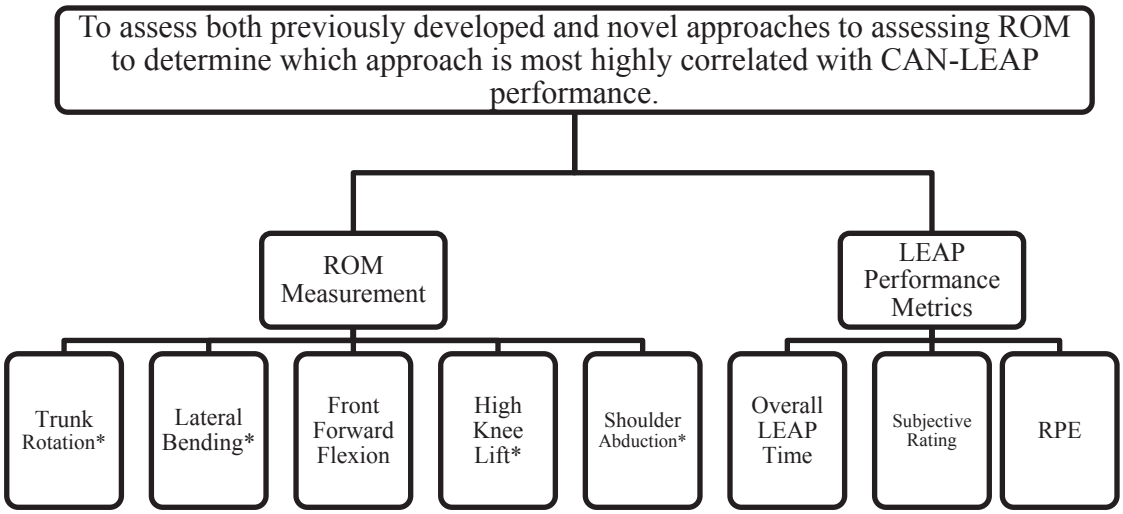

*Right and left sides.

Figure 6: Analysis Plan for Correlating ROM with LEAP Performance

To determine which ROM measure was most highly correlated with CAN-LEAP performance a two-stage cluster bootstrapping method was used to develop a regression model for each ROM measure correlating them with overall LEAP time, subjective rating, and RPE separately (Solow, 1985). For this method, the first stage required that three points were randomly selected, with replacement, for each participant (Field & Welsh, 2007). The second stage then involved the random selection of 29 participants with replacement, meaning that the same participant could be chosen more than once (Field & Welsh, 2007). Finally, using these 87 data points, a linear regression was computed outputting a slope, intercept, and R^2. This process was computed 10,000 times to have a sufficient number of iterations run for this multi-stage bootstrapping method and the averaged coefficients, from these 10,000 iterations, were used as the regression model. A regression coefficient analysis (RCA) was also completed to determine the strength of the within subject relationship between ROM and LEAP performance. This method, and its results, are described in more detail in Annex J: Regression Coefficient Analysis.

The ROM measure values were obtained from the method that was deemed to be most precise and repeatable; this was determined using the results of the ANOVA and ICCs computed for the ROM measurements (see Section 2.5.2). Given the number of methods used for each ROM measure, various parameters from the ROM analysis were used to determine the most precise, repeatable, and reliable method. Figure 7 shows the decision-making process that was used to choose which method most reliably measured each range of motion.

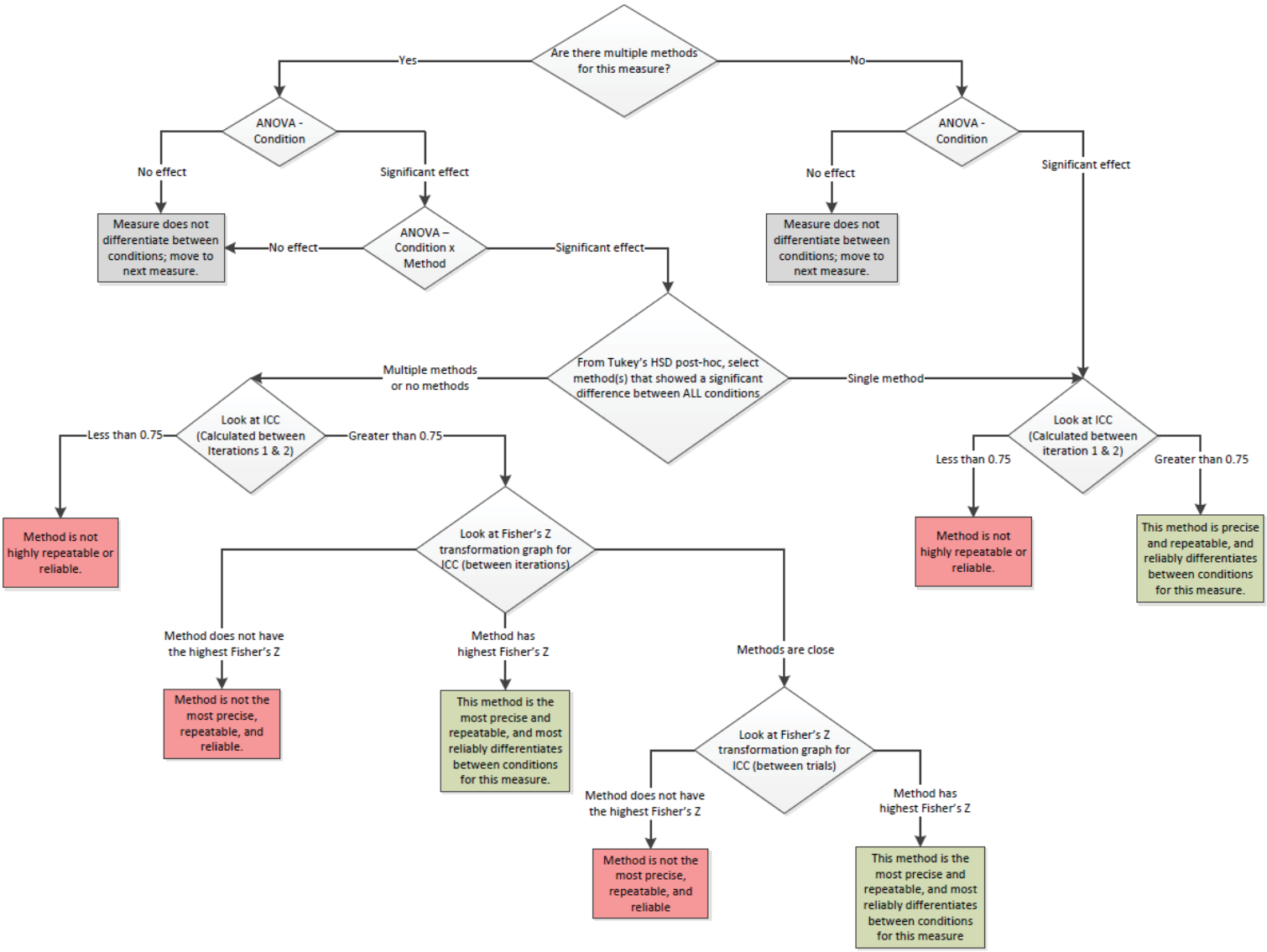

Figure 7: Flow Chart of Decision Process for Best Method for Each ROM Measure

Based on this process, the most precise, repeatable, and reliable method for each ROM measure was chosen and subsequently correlated to overall LEAP time, LEAP subjective ratings, and LEAP RPE using a RCA to determine which ROM measure was most highly correlated with CAN-LEAP performance.

3. Results

The following results section displays all the information obtained throughout the ROM reliability study including participant and environmental characterization (Sections 3.1 and 3.2 respectively). Section 3.3 displays all the information obtained from the CAN-LEAP course and Section 3.4 displays all the information obtained from the ROM stations. Section 3.5 summarizes the correlation between soldier range of motion and LEAP performance.

3.1 Participant Characterization

Several different measures were recorded in order to characterize the soldier population that participated in this experimentation campaign. These results are outlined below.

3.1.1 Demographics

The all-male group of participants (n = 29) ranged in age from 22 to 35, with a mean age of 26.3 years (SD = 3.4). All but four of the participants were right-handed, 23 of the 29 were right-handed for shooting and 21 of the 29 were right-eye dominant for shooting. Participants were also asked their C7A2 marksmanship level; one participant was Personal Weapons Test (PWT) 1 qualified, eight participants were PWT 3, six participants were PWT 3 Supplement, 11 participants were PWT 4 and three participants were PWT 4 Supplement. The participants' mean number of years in the regular force was 5.9 years (SD = 3.3). Eight participants had operational experience; two of those had experienced three deployments, while the remainder had 1-2 deployments. Table 5 presents a summary of rank, and Table 6 presents a summary of MOS.

Table 5: Participant Rank

Rank	Participants
Warrant Officer	1
Sergeant	1
Master Corporal	1
Corporal	20
Private	6
Total	**29**

Table 6: Military Occupational Speciality

MOS ID	Occupation	Participants
0010	Infantryman	14
0005	Crewman	5
0368	Artilleryman	5
0339	Combat Engineer	5
	Total	**29**

Vision testing data revealed that six participants wear prescription glasses and two participants wear contacts. Table 7 presents a summary of far acuity.

Table 7: Far Acuity Results

	Left Eye	Binocular	Right Eye
	Participants	Participants	Participants
20/20	16	27	21
20/30	9	2	6
20/40	3	0	1
20/50	1	0	1

3.1.2 Physical characteristics

The participants' mean weight and height was 93.0 kg (min = 62.2 kg, max = 120.8 kg, SD = 13.1), and 178.0 cm (min = 166.9 cm, max = 194.3 cm, SD = 6.7). Height was measured unshod. Additional anthropometric measurements included front length (standing), back length (standing), waist circumference (iliac crest) and chest circumference (thelion). Descriptive statistics on these measurements are outlined in Table 8.

Table 8: Anthropometric Measurements

	Front Length (standing) (cm)	Back Length (standing) (cm)	Waist Circumference (iliac crest) (cm)	Chest Circumference (thelion) (cm)
Average	36.3	46.2	97.2	109.0
Minimum	32.2	42.6	75.3	93.7
Maximum	41	52.0	120.4	123.8
Standard Deviation	2.0	2.5	10.4	6.4

3.1.2.1 ***Physical capabilities***

Physical capability measures comprised of the mCAFT step test, adiposity testing and strength testing.

3.1.2.1.1 Fitness Testing

mCAFT step test results showed that the participant's average VO_2 max was 44.3 mL/(kg·min), with minimum and maximum VO_2 max scores being observed at 33.1 and 52.3 mL/(kg·min) respectively (SD = 5.9).

3.1.2.1.2 Adiposity Testing

Adiposity testing revealed a range of participant body fat values from a minimum of 11.6% to a maximum of 28.5%, with an overall mean of 19.2% (SD = 4.3).

3.1.2.1.3 Strength Testing

Three different strength values (peak forces) were measured: arm lift, shoulder lift, and leg lift. The results of these tests are outlined in Table 9.

Table 9: Strength Testing Results

	Arm Lift (lb-ft)	Shoulder Lift (lb-ft)	Leg Lift (lb-ft)
Average	107	185	319
Minimum	72.5	97	224.5
Maximum	144.5	270.5	439
Standard Deviation	17.5	32.1	67.8

3.2 Environmental Characterization

Throughout the duration of the study, the indoor conditions were monitored using a WBGT instrument. The average daily temperature was 13.4°C, the average daily dry bulb temperature was 18.5°C, and the average daily relative humidity was 25.1%. The results can be seen in Figure 8. Wind speed was not recorded, as the air movement in the indoor environment was considered negligible.

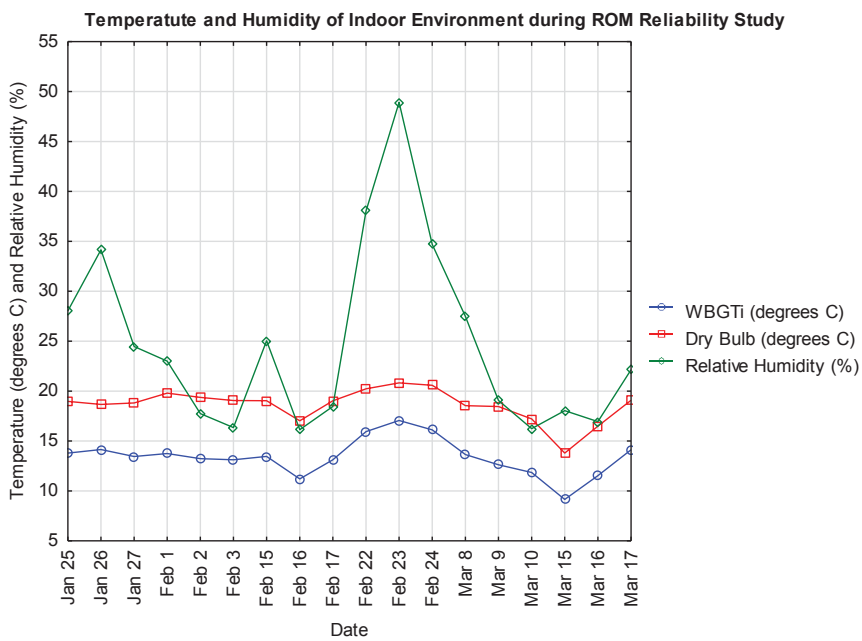

Figure 8: Daily Temperature and Humidity Readings from the Indoor Test Environment

3.3 LEAP Results

The following section displays all the information obtained from the CAN-LEAP course during the ROM Reliability study, including obstacle course performance by total time, individual obstacle times, transition times, and the results of all ancillary stands. For all statistical analyses completed, $p \leq 0.05$ was used as the threshold of statistical significance and for all charts, error bars denote the upper and lower levels of standard error, unless otherwise stated. Technical issues throughout the data collection period resulted in missing interval times or shooting scores for some participant conditions. In these cases, the data was resolved using the replace by mean technique, where the mean was obtained from the known participant data for the given condition at that obstacle.

Statistical analyses are only shown for Conditions A, B, and E since they were properly counterbalanced. Descriptive statistics and plots for the remaining conditions (C, D and F) are presented in Annex K: Additional LEAP Results.

3.3.1 Total Course Performance

The results for the total course time, the participants' subjective performance rating, and their ratings of perceived exertion are outlined below. Figure 9 displays the results for the total obstacle course time.

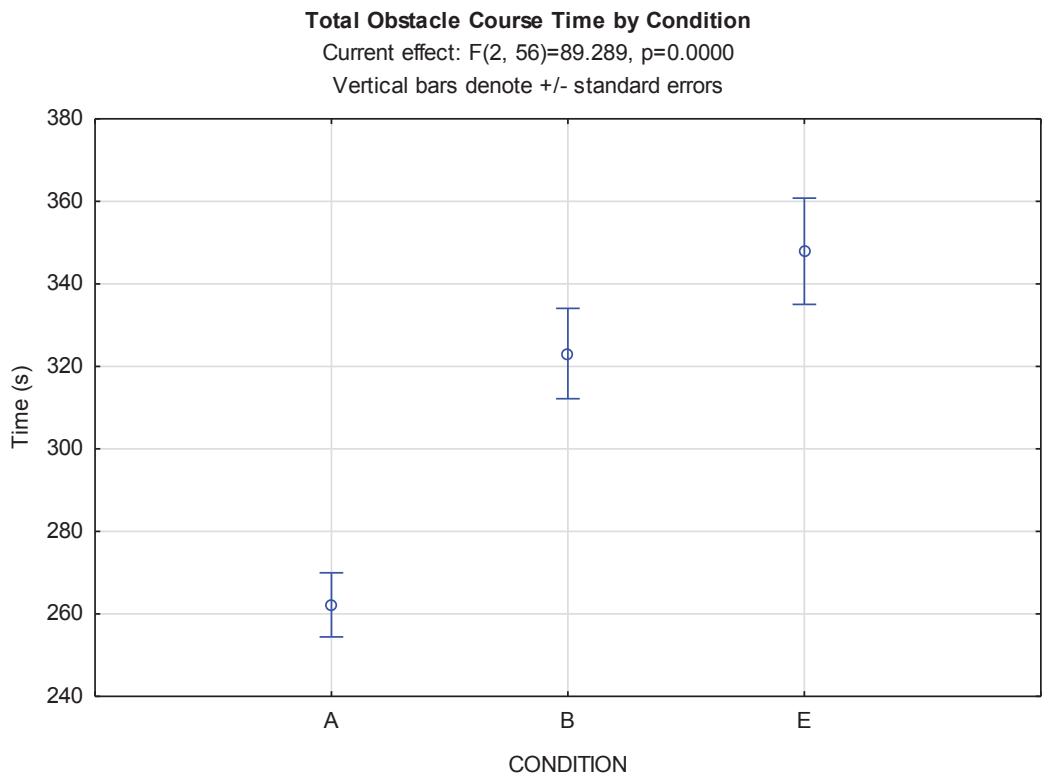

Figure 9: Average Total Obstacle Course Time for each Condition

A repeated-measures analysis of variance (ANOVA) of total obstacle course time identified a significant difference between conditions (n=29, F(2, 56)=89.29, p=0.0000). A Tukey HSD post-hoc analysis revealed that all conditions were significantly different from each other. The post-hoc results are summarized in Annex K: Additional LEAP Results.

The descriptive statistics for total obstacle course time, in seconds, can be found in Table 10.

Table 10: Descriptive statistics for total obstacle course time

Condition	Mean	Min	Max	Std Dev
A	262.19	193.58	390.53	41.80
B	323.10	224.26	499.30	58.94
E	347.91	241.81	550.47	69.36

Figure 10 shows the average subjective rating of overall performance.

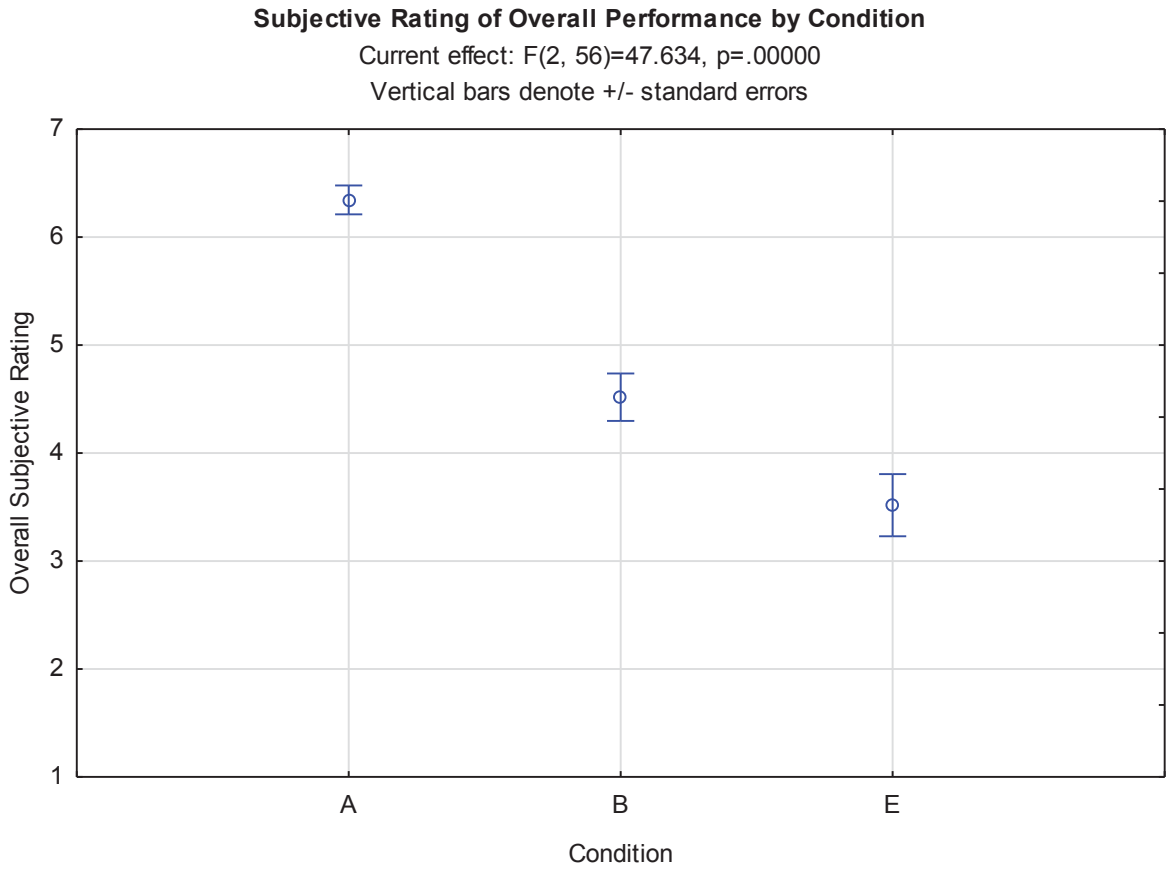

Figure 10: Average participant subjective rating of overall performance

A repeated-measures ANOVA of the subjective ratings of overall performance identified a significant difference between armour conditions (n=29, F(2, 56)=47.63, p=0.0000). A Tukey HSD post-hoc analysis revealed that all conditions were significantly different from each other. The post-hoc results are summarized in Annex K: Additional LEAP Results.

The descriptive statistics for subjective rating of overall performance can be found in Table 11.

Table 11: Descriptive statistics for subjective rating of overall performance

Condition	Mean	Min	Max	Std Dev
A	6.34	5.00	7.00	0.72
B	4.52	1.00	6.00	1.18
E	3.52	1.00	7.00	1.55

3.3.1.1 *RPE (Borg Scale Rating)*

Immediately after completion of the obstacle course, the soldier gave their Rating of Perceived Exertion (RPE) to the researcher using the "Borg Scale". The average RPE rating for each condition is in Figure 11 below.

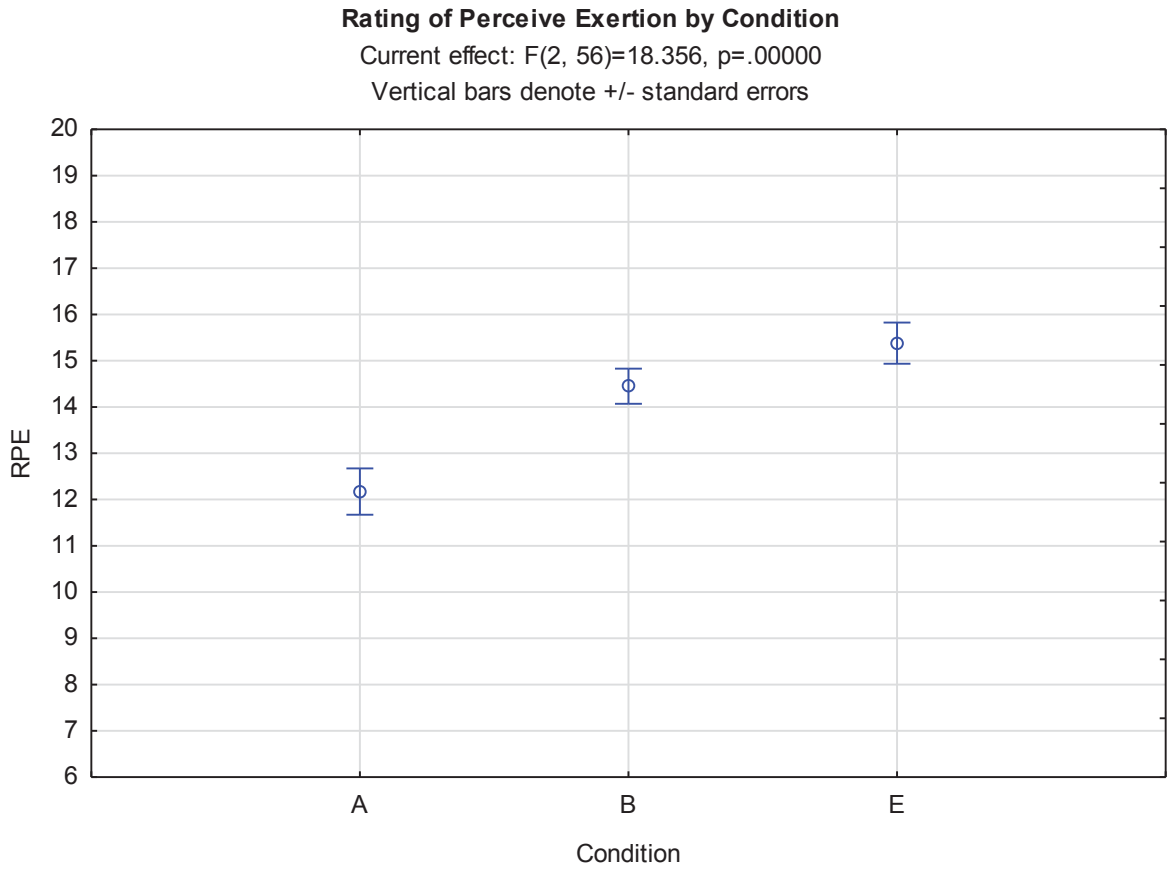

Figure 11: Average subjective Borg Scale rating for each condition

A repeated measures ANOVA of the RPEs identified a significant difference between conditions (n=29, F(2, 56)=18.36, p=0.0000). A Tukey HSD post-hoc analysis revealed that only Condition A was significantly different from all other conditions. There was no significant difference between Conditions B and E. The post-hoc results are summarized in Annex K: Additional LEAP Results.

The descriptive statistics for RPE can be found in Table 12.

Table 12: Descriptive statistics for RPE

Condition	Mean	Min	Max	Std Dev
A	12.17	8.00	20.00	2.70
B	14.45	10.00	18.00	2.05
E	15.38	10.00	20.00	2.40

3.3.2 Course Performance by Obstacle

Figure 12 shows the average Tunnel and Hatch interval time for each condition.

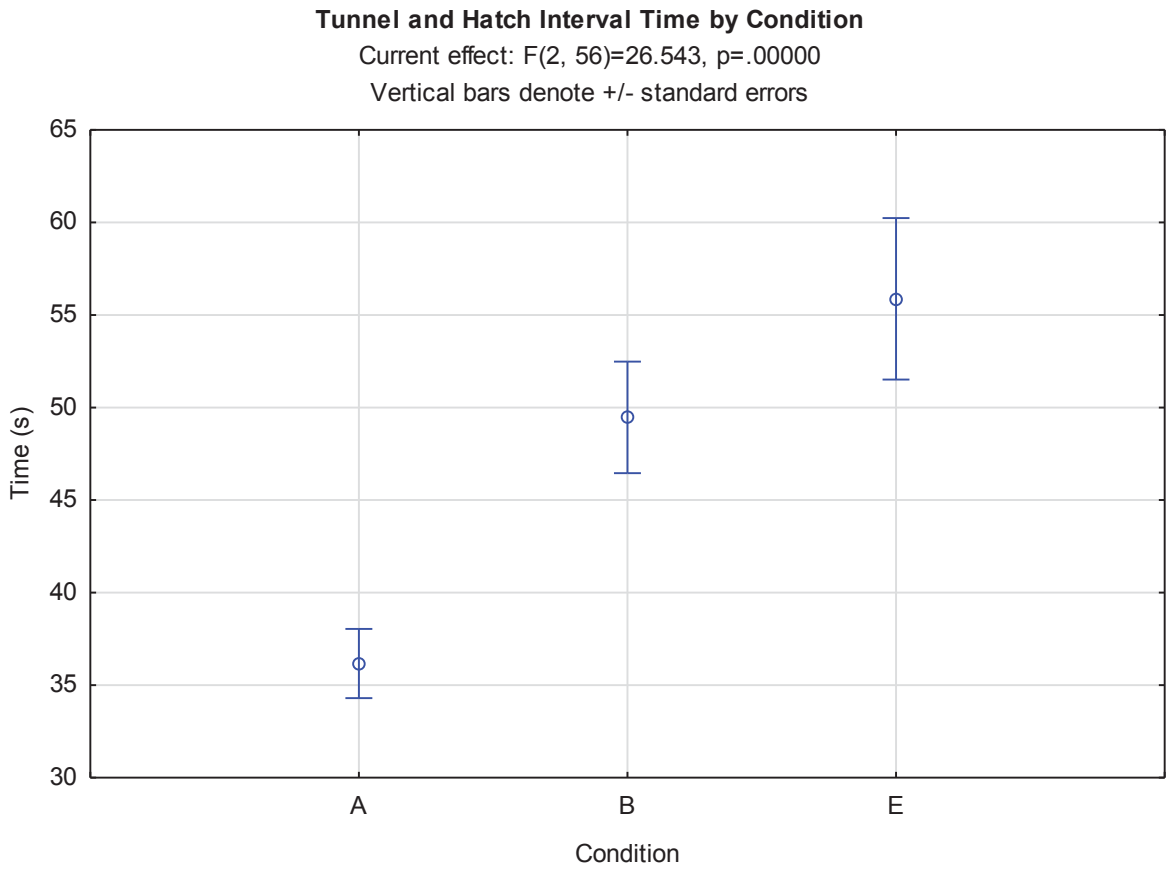

Figure 12: Average Tunnel and Hatch Interval Time for each Condition

A repeated-measures ANOVA of Tunnel and Hatch interval times identified a significant difference between armour conditions (n=29, F(2, 56)=26.54, p=0.0000). A Tukey HSD post-hoc analysis revealed that Condition A was significantly different from all other conditions. There was no significant difference observed between Conditions B and E. The post-hoc results are summarized in Annex K: Additional LEAP Results.

The descriptive statistics for the tunnel and hatch can be found in Table 13.

Table 13: Descriptive statistics for the tunnel and hatch

Condition	Mean	Min	Max	Std Dev
A	36.1	23.33	71.32	10.08
B	49.47	28.67	106.84	16.22
E	55.87	32.06	153.05	23.49

Figure 13 shows the average Sprint interval time for each condition.

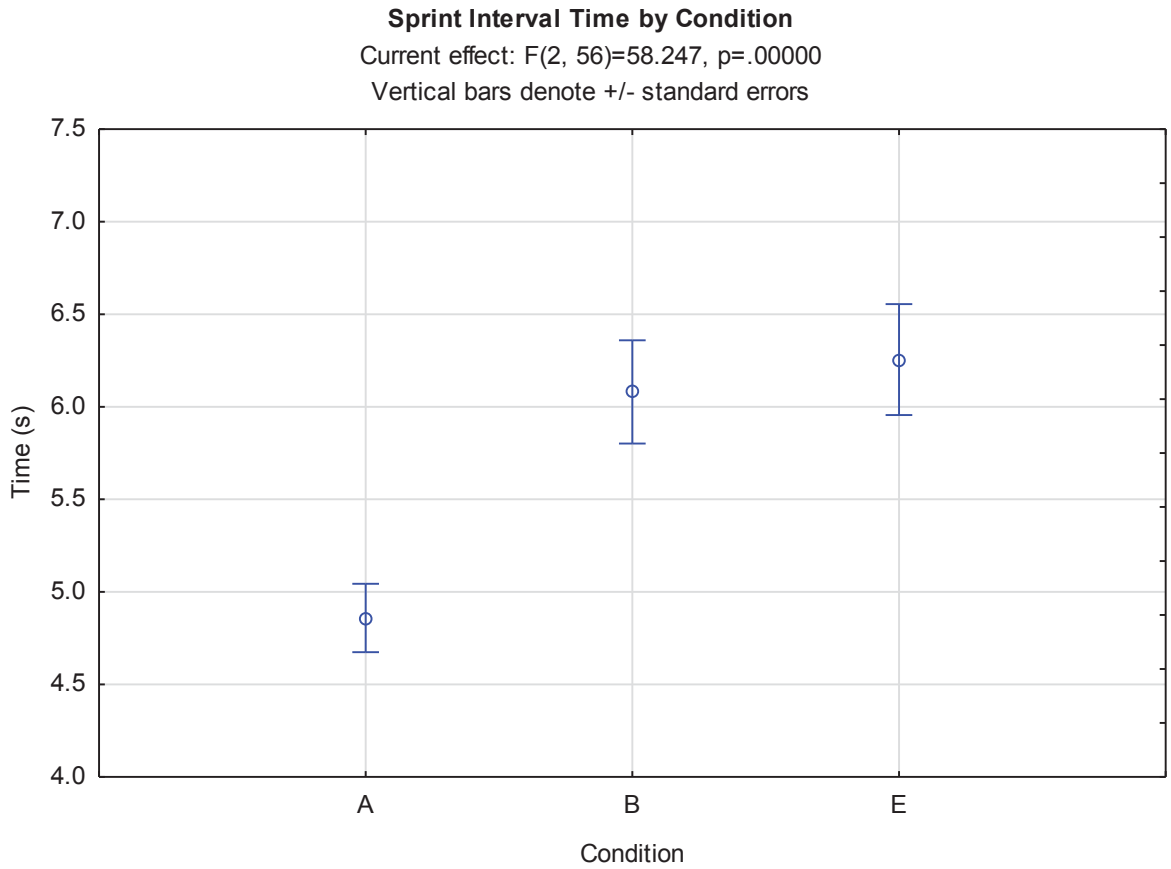

Figure 13: Average Sprint Interval Time for each Condition

A repeated-measures ANOVA of Sprint interval times identified a significant difference between armour conditions (n=29, F(2, 56)=58.25, p=0.0000). A Tukey HSD post-hoc analysis revealed that Condition A differed significantly from all other conditions. There were no significant differences observed between Conditions B and E. The post-hoc results are summarized in Annex K: Additional LEAP Results.

The descriptive statistics for the sprint interval, in seconds, can be found in Table 14.

Table 14: Descriptive statistics for the sprint interval

Condition	Mean	Min	Max	Std Dev
A	4.86	3.53	7.25	0.99
B	6.08	3.70	10.18	1.50
E	6.26	3.82	10.55	1.61

Figure 14 shows the average time to ascend the steep stairs and descend the shallow stairs for each condition.

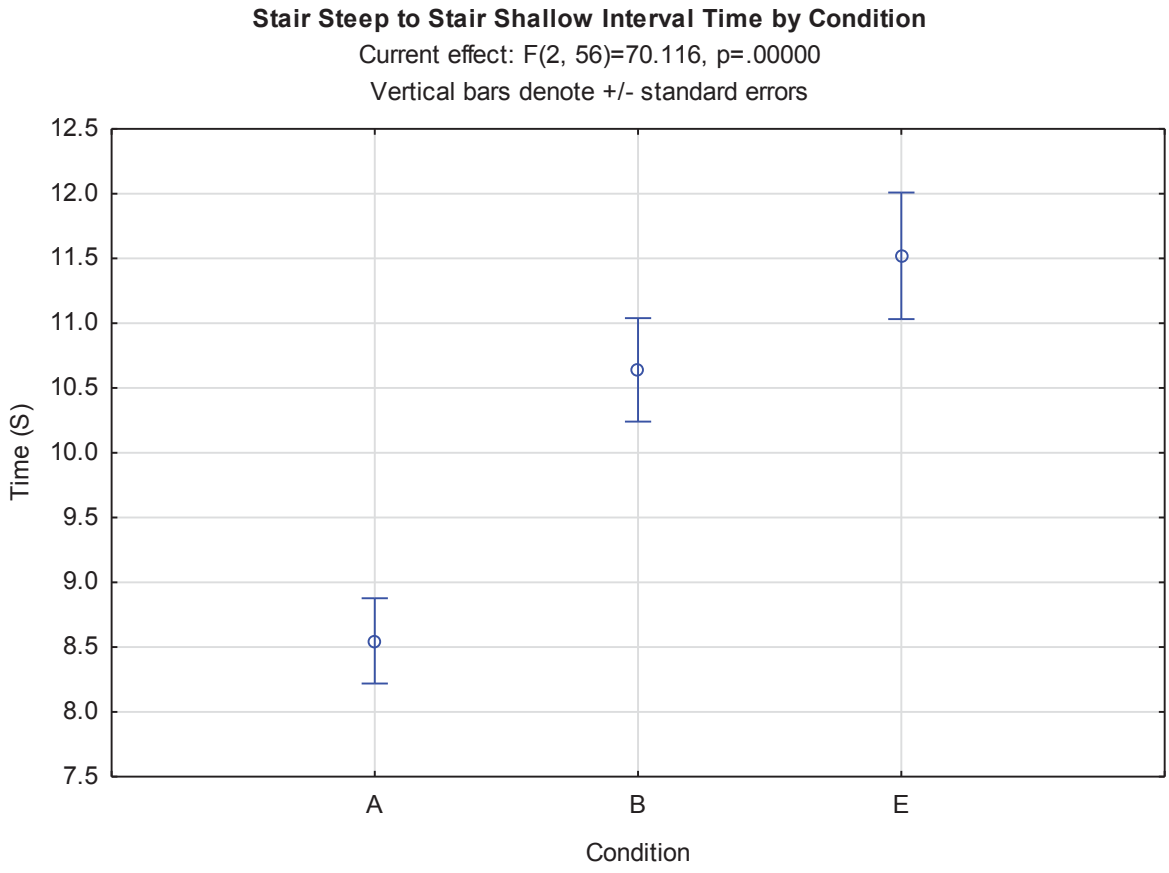

Figure 14: Average Stair Steep to Stair Shallow Interval Time for each Condition

A repeated-measures ANOVA of the Steep to Shallow Stair interval times identified a significant difference between armour conditions (n=29, F(2, 56)=70.12, p=0.0000). A Tukey HSD post-hoc analysis revealed that all conditions were significantly different. The post-hoc results are summarized in Annex K: Additional LEAP Results.

The descriptive statistics for the stair steep to stair shallow interval time, in seconds, can be found in Table 15.

Table 15: Descriptive Statistics for Stair Steep to Stair Shallow

Condition	Mean	Min	Max	Std Dev
A	8.55	5.30	12.78	1.77
B	10.64	5.74	16.90	2.15
E	11.52	6.31	18.44	2.63

Figure 15 shows the average time to ascend the shallow stairs and descend the steep stairs for each condition.

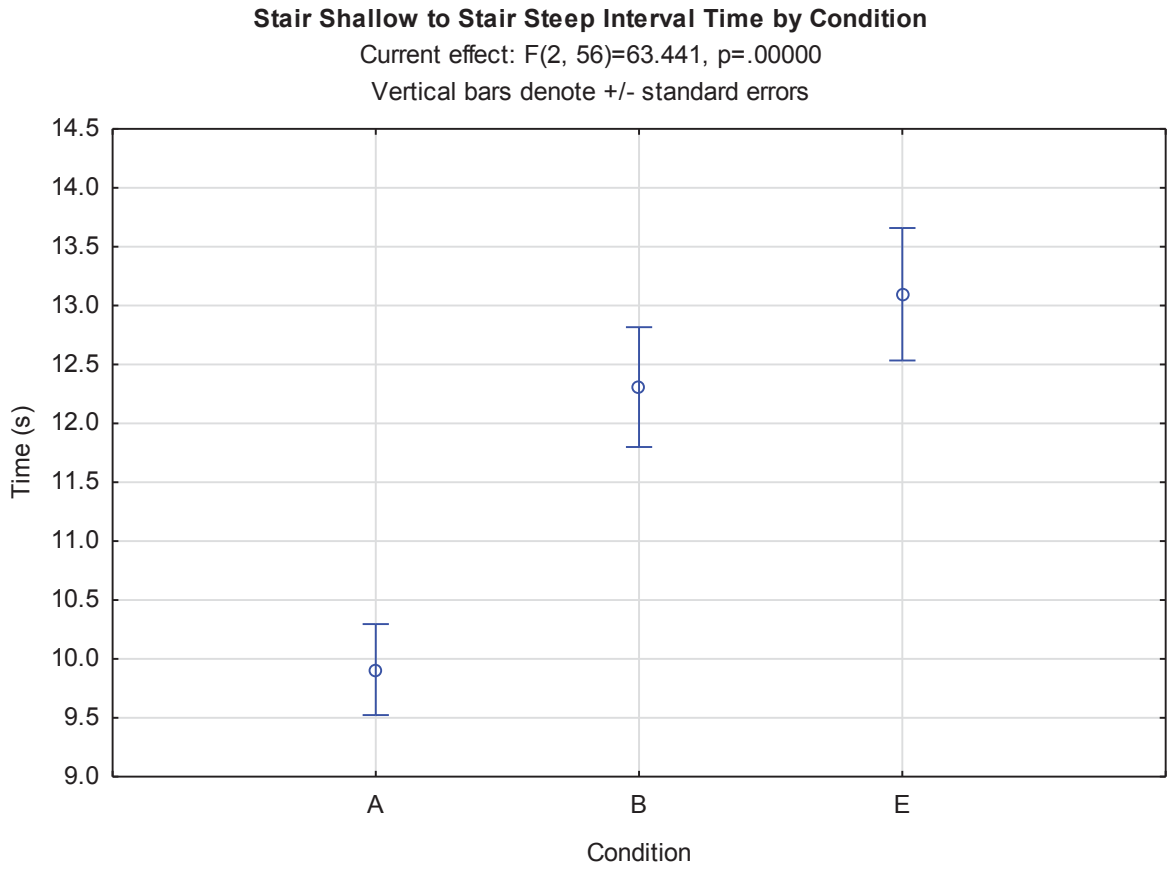

Figure 15: Average Stair Shallow to Stair Steep Interval Time for each Condition

A repeated-measures ANOVA of the Shallow to Steep Stair interval times identified a significant difference between armour conditions (n=29, F(2, 56)=63.44, p=0.0000). A Tukey HSD post-hoc analysis revealed that significant differences were observed across all conditions. The post-hoc results are summarized in Annex K: Additional LEAP Results.

The descriptive statistics for the stair shallow to stair steep interval time, in seconds, can be found in Table 16.

Table 16: Descriptive Statistics for Stair Shallow to Stair Steep

Condition	Mean	Min	Max	Std Dev
A	9.91	7.09	17.25	2.08
B	12.31	8.72	22.09	2.74
E	13.10	9.55	23.56	3.03

Figure 16 shows the time to ascend the straight ladder and descend the angled ladder for each condition.

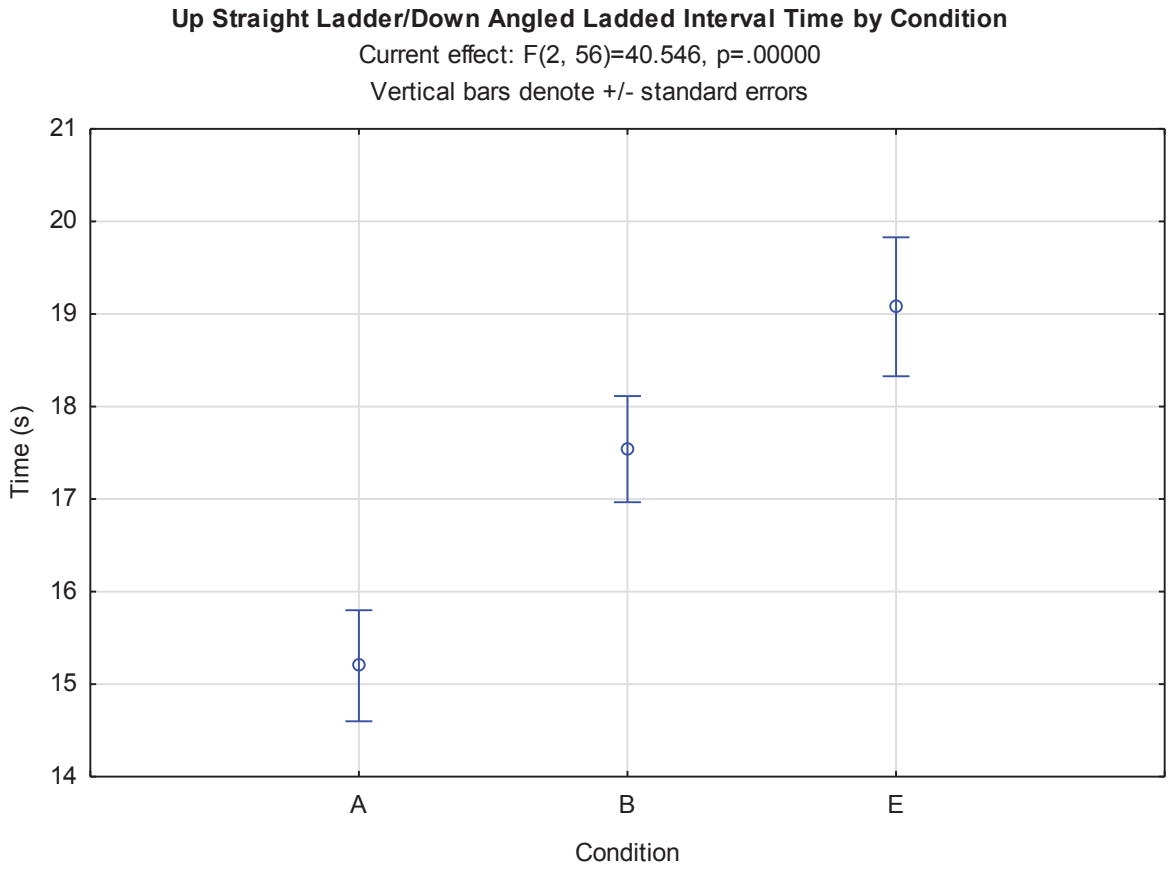

Figure 16: Average for Up Straight/Down Angled Ladder Interval Time for each Condition

A repeated-measures ANOVA of the Up Straight and Down Angled Ladder interval times identified a significant difference between armour conditions (n=29, F(2, 56)=40.55, p=0.0000). A Tukey HSD post-hoc analysis revealed that significant differences were observed across all conditions. The post-hoc results are summarized in Annex K: Additional LEAP Results.

The descriptive statistics for up straight ladder/down angled ladder interval time, in seconds, can be found in Table 17.

Table 17: Descriptive Statistics for Up Straight Ladder/Down Angled Ladder

Condition	Mean	Min	Max	Std Dev
A	15.20	10.86	24.05	3.23
B	17.54	13.25	26.59	3.09
E	19.08	13.39	31.49	4.04

Figure 17 shows the average time to ascend the angled ladder and descend the straight ladder for each condition.

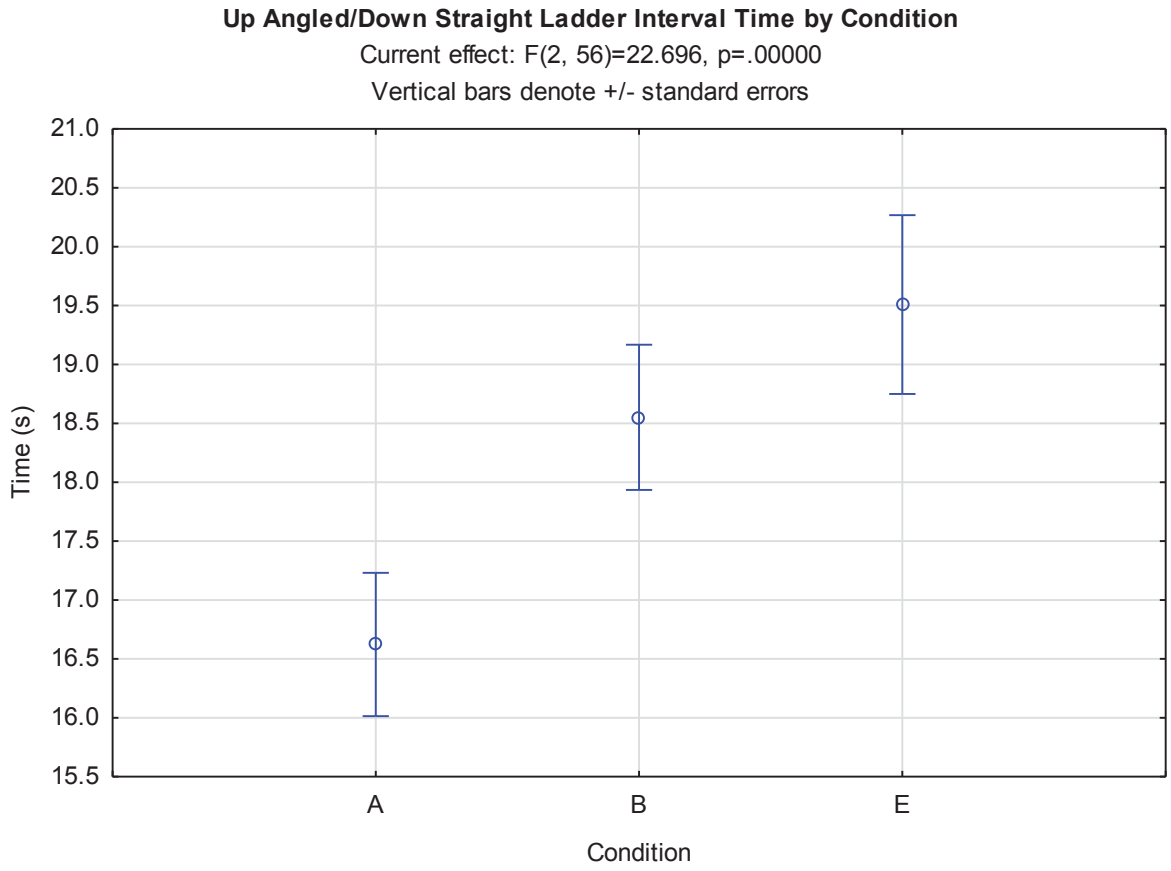

Figure 17: Average for Up Angled/Down Straight Ladder Interval Time for each Condition

A repeated-measures ANOVA of the Up Angled and Down Straight Ladder interval times identified a significant difference between armour conditions (n=29, F(2, 56)=22.70, p=0.0000). A Tukey HSD post-hoc analysis revealed a significant difference between Condition A and all other conditions. There was no significant difference observed between Conditions B and E. The post-hoc results are summarized in Annex K: Additional LEAP Results.

The descriptive statistics for up angled ladder/down straight ladder interval time, in seconds, can be found in Table 18.

Table 18: Descriptive Statistics for Up Angled Ladder/Down Straight Ladder

Condition	Mean	Min	Max	Std Dev
A	16.62	10.63	25.96	3.28
B	18.55	11.60	25.45	3.32
E	19.51	11.61	31.70	4.09

Figure 18 shows the average Agility run interval time for each condition.

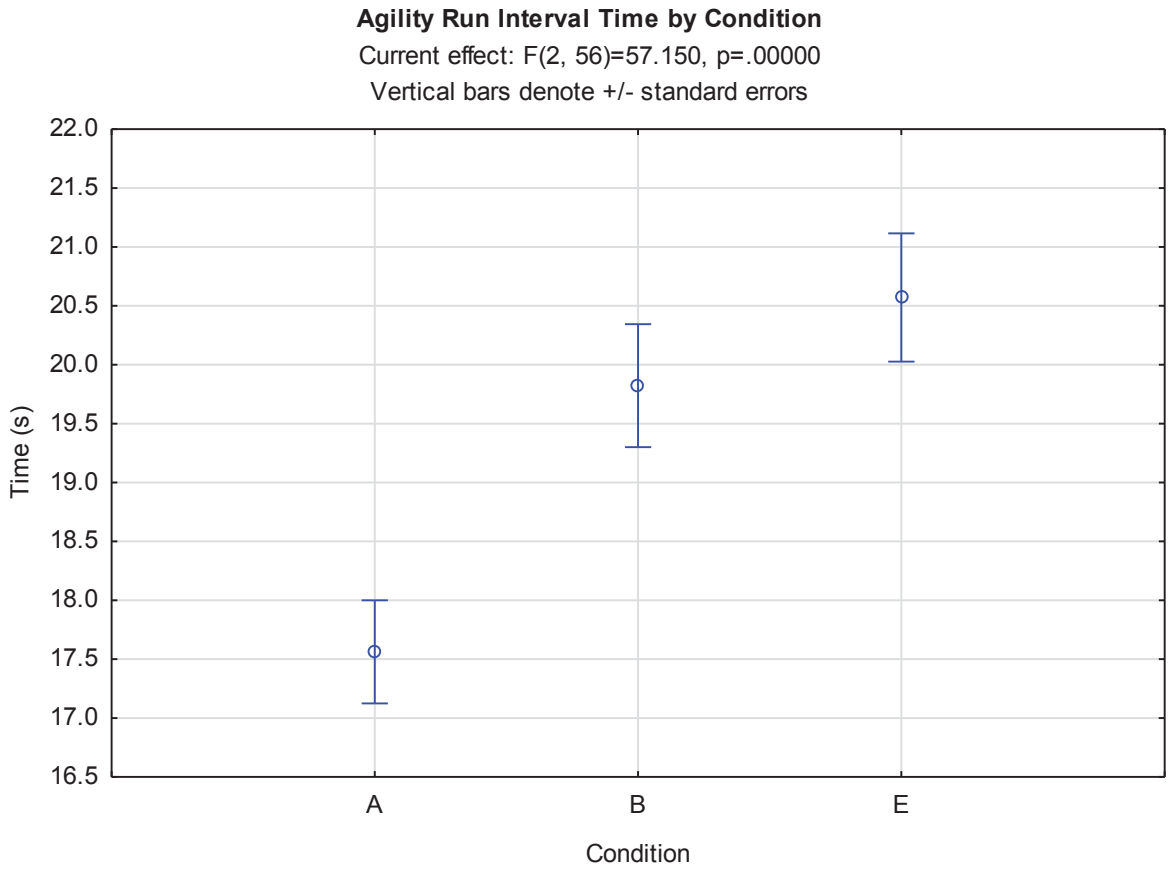

Figure 18: Average Agility Interval Time for each Condition

A repeated-measures ANOVA of Agility interval times identified a significant difference between armour conditions (n=29, F(2, 56)=57.15, p=0.0000). A Tukey HSD post-hoc analysis revealed that all conditions were significantly different from each other. The post-hoc results are summarized in Annex K: Additional LEAP Results.

The descriptive statistics for the agility run interval time, in seconds, can be found in Table 19.

Table 19: Descriptive Statistics for the Agility Interval

Condition	Mean	Min	Max	Std Dev
A	17.56	13.48	24.24	2.36
B	19.82	15.06	27.09	2.81
E	20.57	16.71	28.97	2.93

Figure 19 shows the average Casualty Drag interval time for each condition.

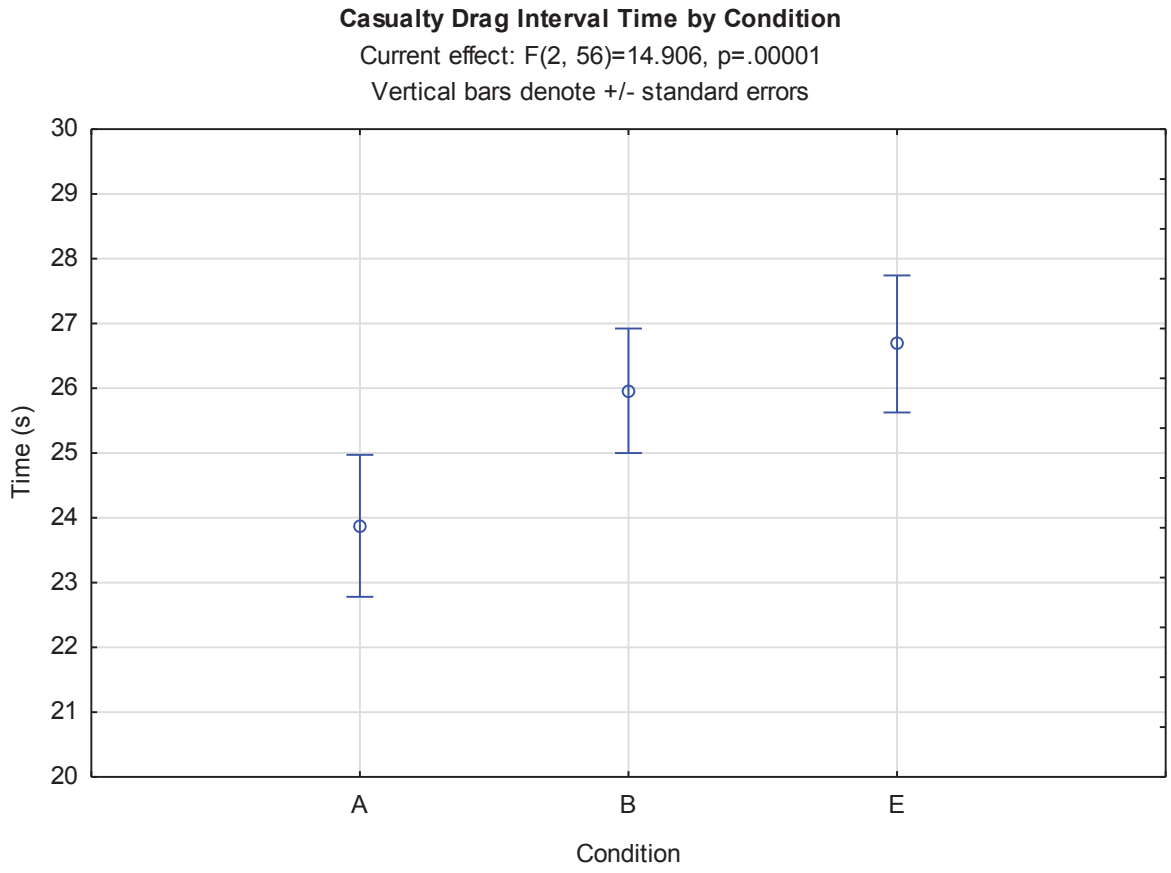

Figure 19: Average Casualty Drag Interval Time for each Condition

A repeated-measures ANOVA of Casualty Drag interval time identified a significant difference between armour conditions (n=29, F(2, 56)=14.91, p=0.0000). A Tukey HSD post-hoc analysis revealed that only Condition A was significantly different from all other conditions. There was no significant difference observed between Conditions B and E. The post-hoc results are summarized in Annex K: Additional LEAP Results.

The descriptive statistics for the casualty drag interval times, in seconds, can be found in Table 20.

Table 20: Descriptive Statistics for the Casualty Drag Interval

Condition	Mean	Min	Max	Std Dev
A	23.88	14.97	40.69	5.90
B	25.96	15.41	40.33	5.18
E	26.68	16.20	42.68	5.70

Figure 20 shows the average Window #1 interval time for each condition.

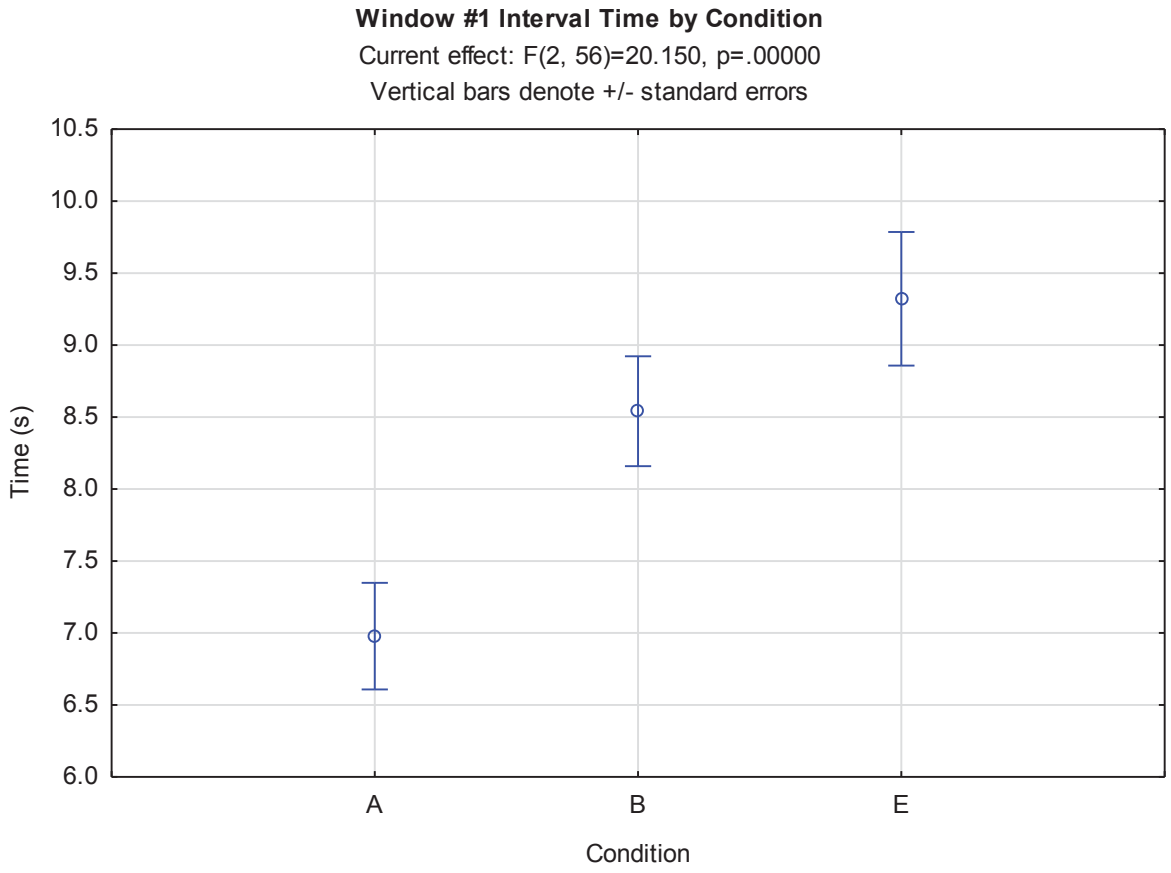

Figure 20: Average Window #1 Interval Time for each Condition

A repeated-measures ANOVA of Window #1 interval time identified a significant difference between armour conditions (n=29, F(2, 56)=20.150, p=0.0000). A Tukey HSD post-hoc analysis revealed that only Condition A was significantly different from all other conditions. There was no significant difference observed between Conditions B and E. The post-hoc results are summarized in Annex K: Additional LEAP Results.

The descriptive statistics for the first window interval times, in seconds, can be found in Table 21.

Table 21: Descriptive Statistics for Window #1

Condition	Mean	Min	Max	Std Dev
A	6.98	4.17	11.90	1.99
B	8.54	5.15	13.43	2.05
E	9.32	5.55	15.80	2.50

Figure 21 shows the average Window #2 interval time for each condition.

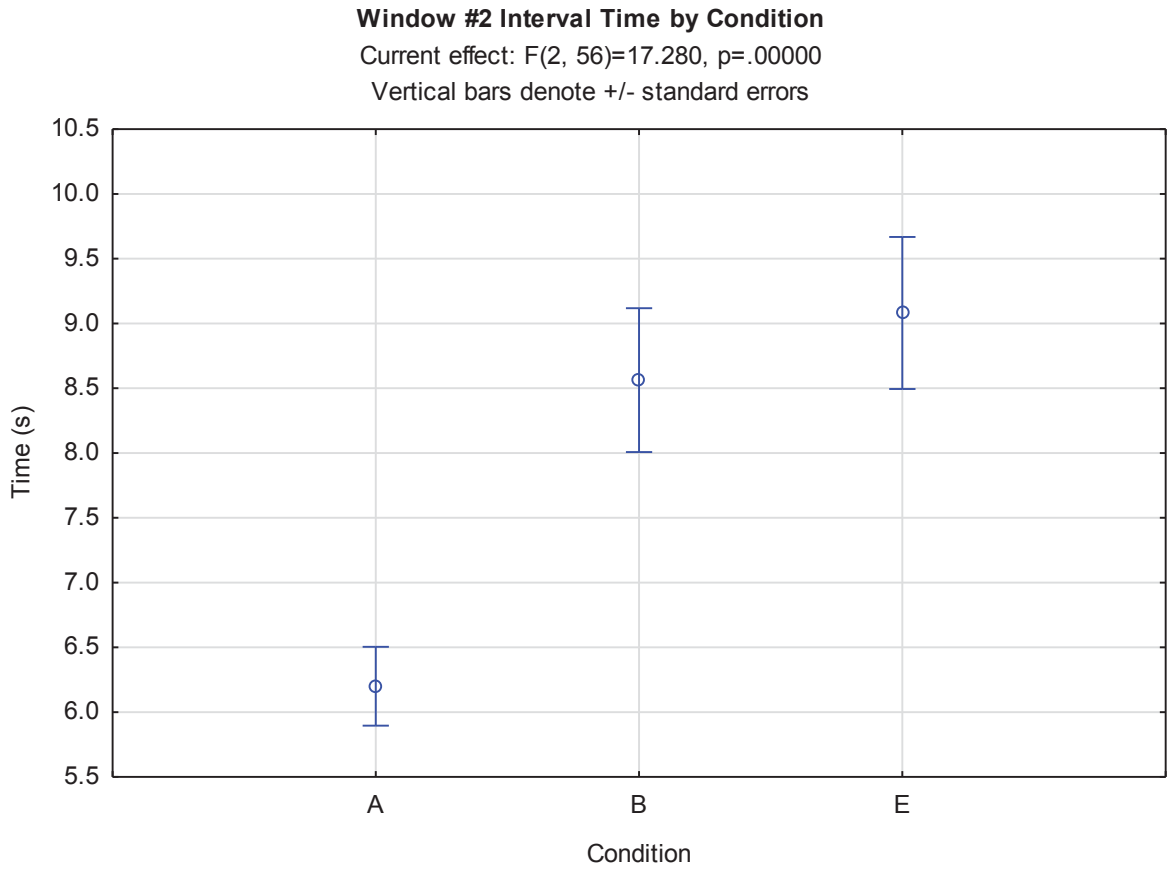

Figure 21: Average Window #2 Interval Time for each Condition

A repeated-measures ANOVA of the Window #2 interval time identified a significant difference between armour conditions (n=29, F(2, 56)=17.28, p=0.0000). A Tukey HSD post-hoc analysis revealed that Condition A was significantly different from all other conditions. There was no significant difference observed between Conditions B and E. The post-hoc results are summarized in Annex K: Additional LEAP Results.

The descriptive statistics for the second window interval times, in seconds, can be found in Table 22.

Table 22: Descriptive Statistics for Window #2

Condition	Mean	Min	Max	Std Dev
A	6.20	4.10	9.94	1.64
B	8.56	5.27	17.79	2.99
E	9.08	5.77	21.52	3.16

Figure 22 shows the average Bounding Rush interval time for each condition.

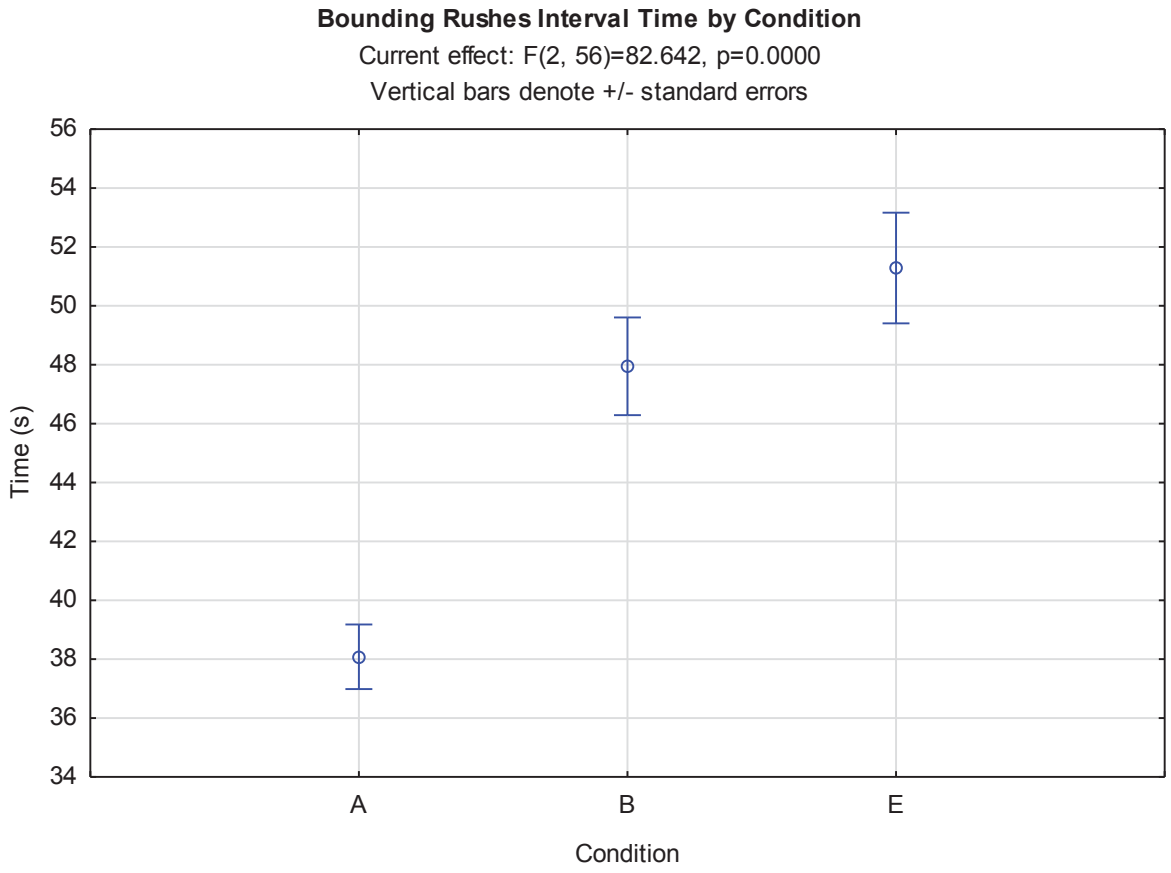

Figure 22: Average Bounding Rush Interval Time for each Condition

A repeated-measures ANOVA of the Bounding Rush interval time identified a significant difference between armour conditions (n=29, F(2, 56)=82.64, p=0.0000). A Tukey HSD post-hoc analysis revealed that all conditions were significantly different from each other. The post-hoc results are summarized in Annex K: Additional LEAP Results.

The descriptive statistics for the bounding rush interval times, in seconds, can be found in Table 23.

Table 23: Descriptive Statistics for the Bounding Rush Interval

Condition	Mean	Min	Max	Std Dev
A	38.08	27.71	55.02	5.91
B	47.95	32.45	66.79	8.94
E	51.28	33.99	76.32	10.12

Figure 23 shows the average Balance Beam interval time for each condition.

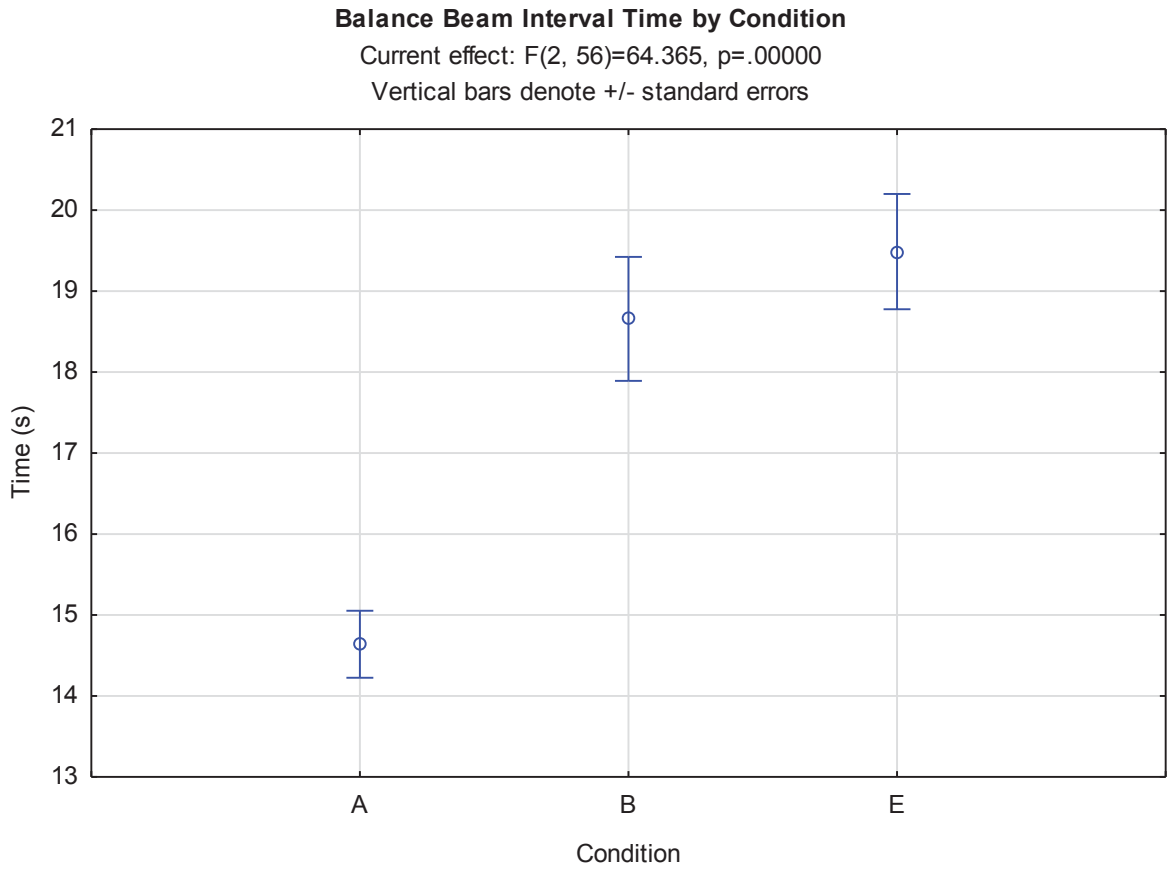

Figure 23: Average Balance Beam Interval Time

A repeated-measures ANOVA of Balance Beam interval time identified a significant difference between armour conditions (n=29, F(2, 56)=64.37, p=0.0000). A Tukey HSD post-hoc analysis revealed that only Condition A was significantly different from all other conditions. There was no significant difference observed between Conditions B and E. The post-hoc results are summarized in Annex K: Additional LEAP Results.

The descriptive statistics for the balance beam interval times, in seconds, can be found in Table 24.

Table 24: Descriptive Statistics for the Balance Beam

Condition	Mean	Min	Max	Std Dev
A	14.64	10.09	19.14	2.23
B	18.66	12.90	29.42	4.12
E	19.49	12.96	29.00	3.83

Figure 24 shows the average Low Crawl interval time for each condition.

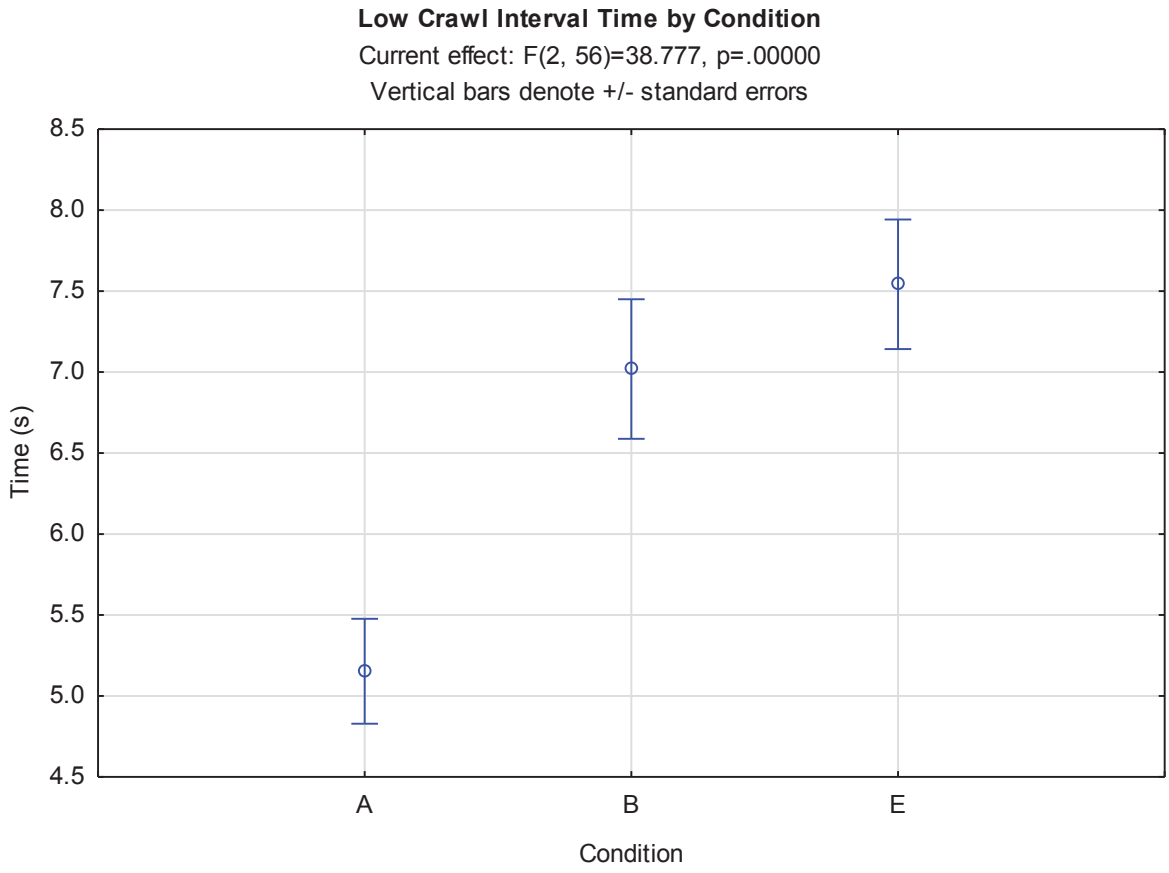

Figure 24: Average Low Crawl Interval Time for each Condition

A repeated-measures ANOVA of Low Crawl interval time identified a significant difference between conditions (n=29, F(2, 56)=38.78, p=0.0000). A Tukey HSD post-hoc analysis revealed that Condition A was significantly different from all other conditions. There was no significant difference observed between Conditions B and E. The post-hoc results are summarized in Annex K: Additional LEAP Results.

The descriptive statistics for the low crawl interval times, in seconds, can be found in Table 25.

Table 25: Descriptive Statistics for the Low Crawl

Condition	Mean	Min	Max	Std Dev
A	5.15	2.89	9.31	1.75
B	7.02	3.65	13.60	2.32
E	7.54	4.92	14.00	2.15

Figure 25 shows the average Back Crawl interval time for each condition.

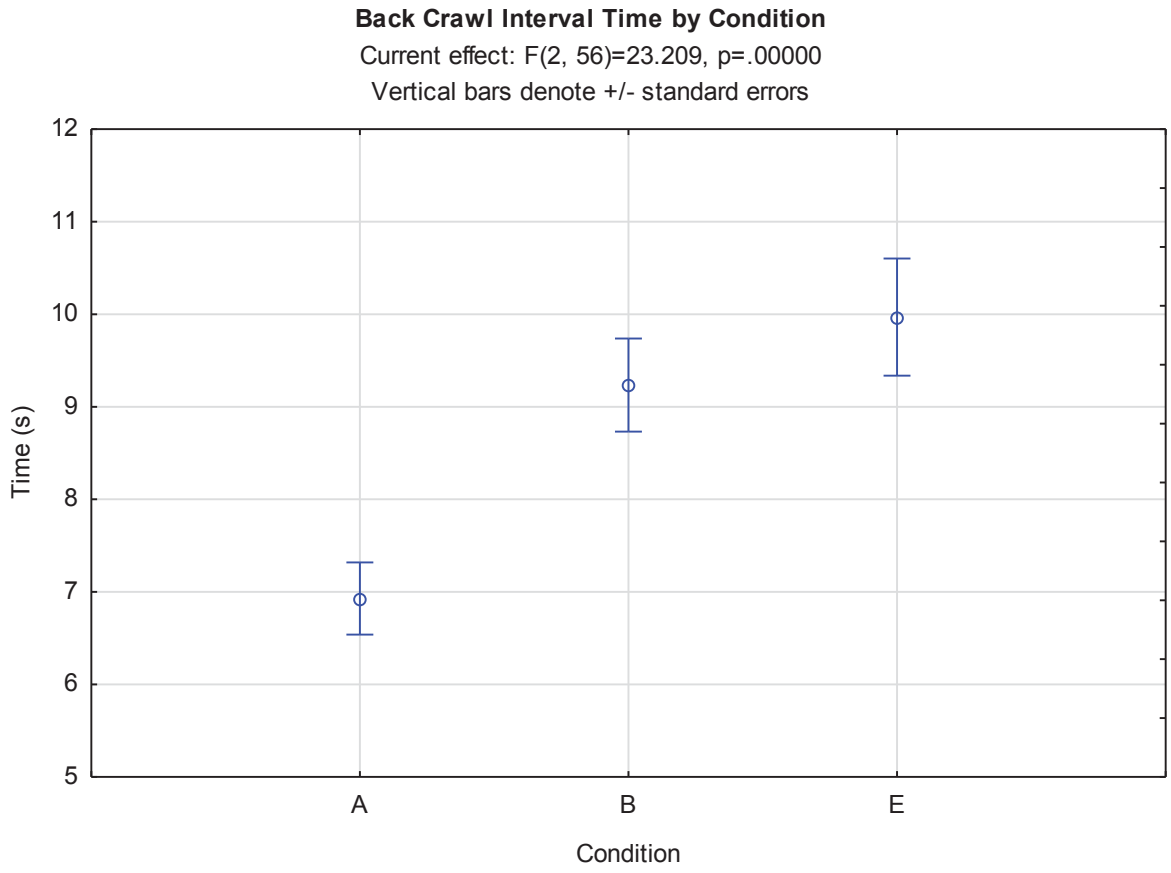

Figure 25: Average Back Crawl Interval Time

A repeated-measures ANOVA of Back Crawl interval times identified a significant difference between armour conditions (F(2, 56)=23.21, p=0.0000). A Tukey HSD post-hoc analysis revealed that Condition A was significantly different from all other conditions. There was no significant difference observed between Conditions B and E. The post-hoc results are summarized in Annex K: Additional LEAP Results.

The descriptive statistics for the back crawl interval times, in seconds, can be found in Table 26.

Table 26: Descriptive Statistics for the Back Crawl

Condition	Mean	Min	Max	Std Dev
A	6.93	3.72	11.72	2.10
B	9.24	5.21	16.39	2.71
E	9.97	4.71	19.90	3.41

Figure 26 shows the average High Crawl interval time for each condition.

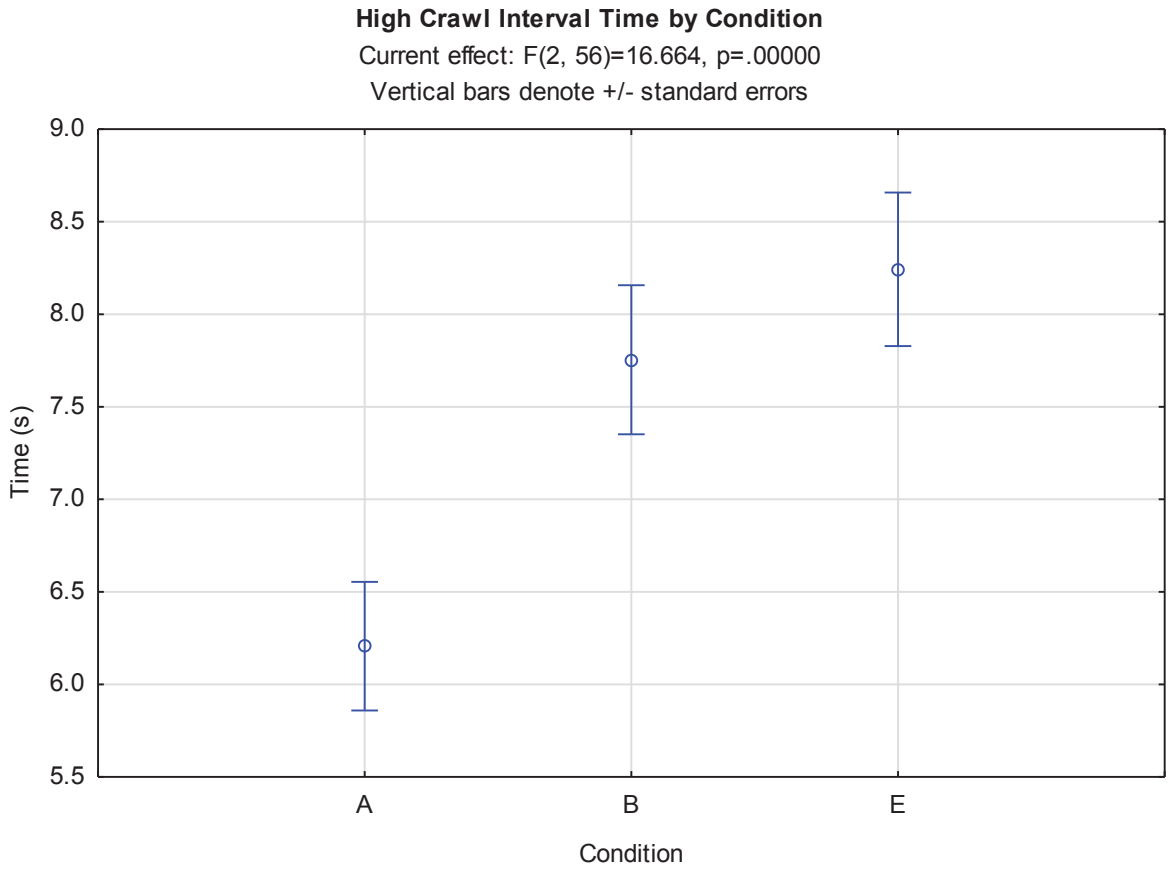

Figure 26: Average High Crawl Interval Time

A repeated-measures ANOVA of High Crawl interval time identified a significant difference between armour conditions (n=29, F(2, 56)=16.66, p=0.0000). A Tukey HSD post-hoc analysis revealed that Condition A was significantly different from all other conditions. There was no significant difference observed between Conditions B and E. The post-hoc results are summarized in Annex K: Additional LEAP Results.

The descriptive statistics for the high crawl interval times, in seconds, can be found in Table 27.

Table 27: Descriptive Statistics for the High Crawl

Condition	Mean	Min	Max	Std Dev
A	6.21	2.91	10.21	1.87
B	7.75	3.64	12.01	2.17
E	8.24	4.14	12.98	2.23

Figure 27 shows the average Outer Wall interval time for each condition.

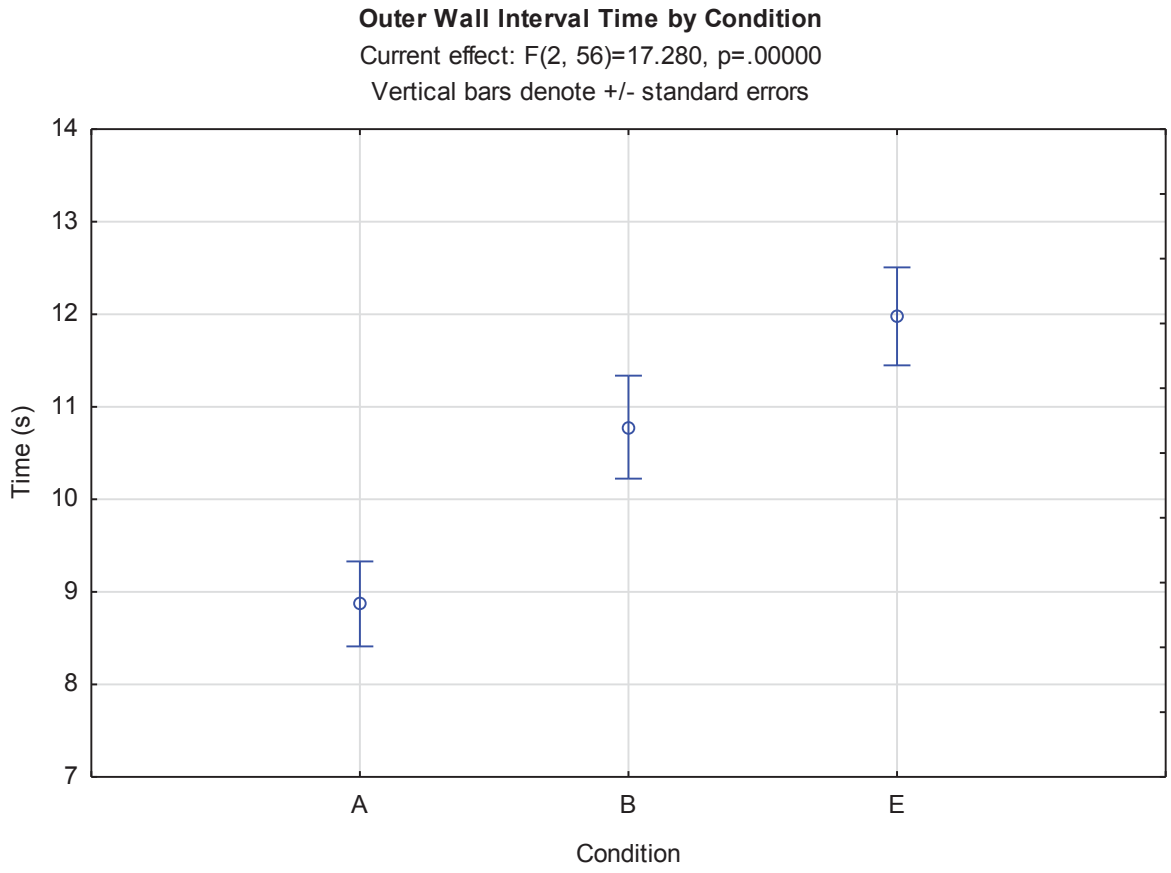

Figure 27: Average Outer Wall Interval Time for each Condition

A repeated-measures ANOVA of Outer Wall interval time identified a significant difference between armour conditions (n=29, F(2, 56)=17.28, p=0.0000). A Tukey HSD post-hoc analysis revealed that Condition A was significantly different from all other conditions. There was no significant difference observed between Conditions B and E. The post-hoc results are summarized in Annex K: Additional LEAP Results.

The descriptive statistics for the outer wall interval times, in seconds, can be found in Table 28.

Table 28: Descriptive Statistics for the Outer Wall

Condition	Mean	Min	Max	Std Dev
A	8.87	4.99	17.11	2.47
B	10.78	6.13	19.78	2.99
E	11.98	7.52	20.06	2.85

Figure 28 shows the average Inner Wall interval time for each condition.

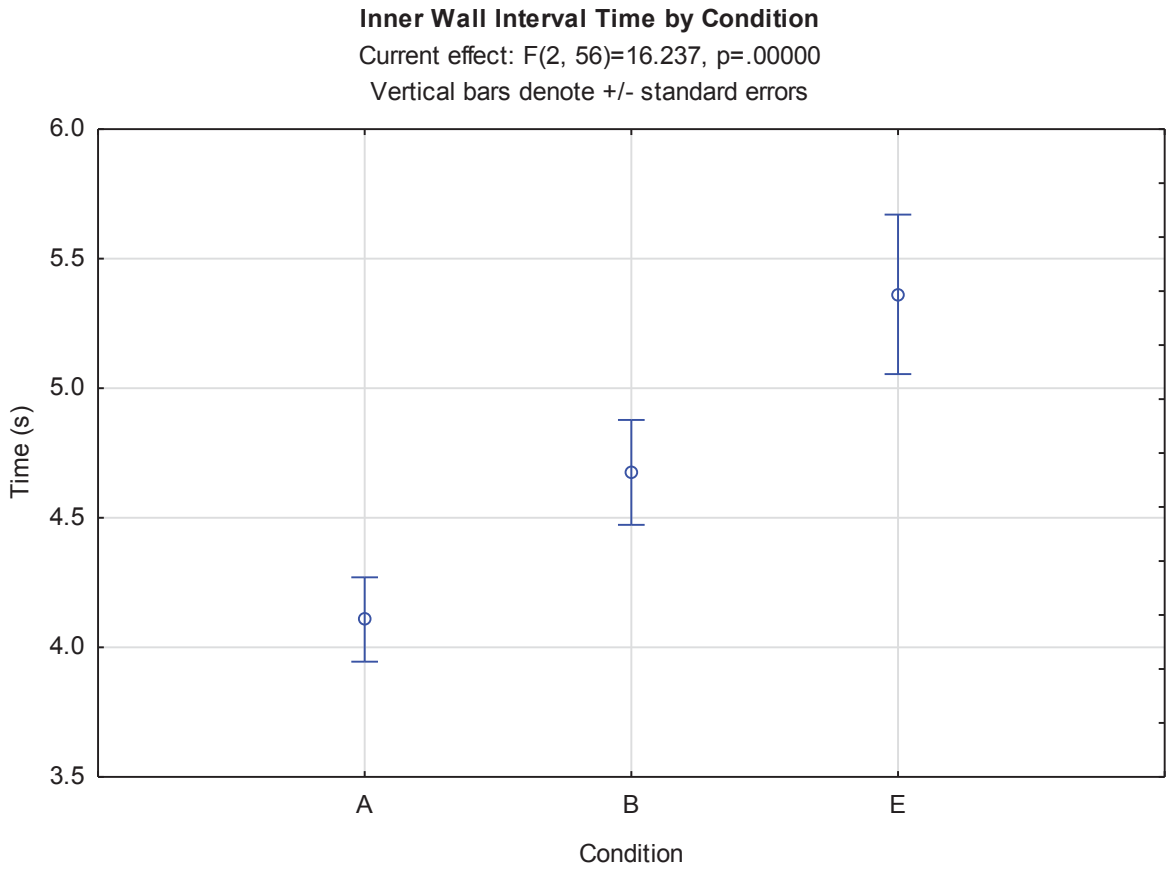

Figure 28: Average Inner Wall Interval Time for each Condition

A repeated-measures ANOVA of Inner Wall interval time identified a significant difference between armour conditions (n=29, F(2, 56)=16.24, p=0.0000). A Tukey HSD post-hoc analysis revealed that all conditions were significantly different from each other. The post-hoc results are summarized in Annex K: Additional LEAP Results.

The descriptive statistics for the inner wall interval times, in seconds, can be found in Table 29.

Table 29: Descriptive Statistics for the Inner Wall

Condition	Mean	Min	Max	Std Dev
A	4.11	2.59	5.64	0.88
B	4.68	3.09	6.90	1.10
E	5.36	3.60	11.81	1.66

3.3.3 Course Performance by Transition Time

Figure 29 shows the average Tunnel to Sprint transition time for each condition.

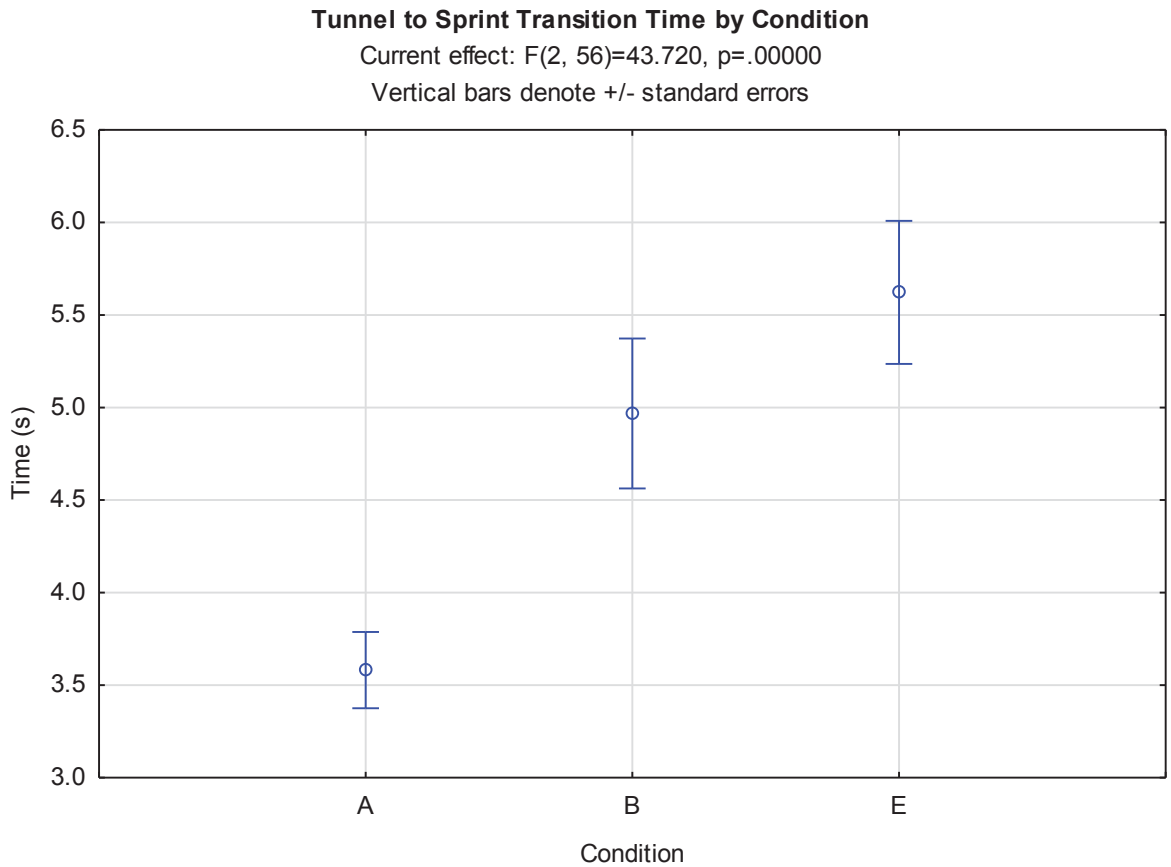

Figure 29: Average Hatch to Sprint Transition Time for each Condition

A repeated-measures ANOVA of the Hatch to Sprint Transition Time identified a significant difference between armour conditions (n=29, F(2, 56)=43.72, p=0.0000). A Tukey HSD post-hoc analysis revealed that all conditions were significantly different from each other. The post-hoc results are summarized in Annex K: Additional LEAP Results.
The descriptive statistics for the Tunnel to Sprint transition times, in seconds, can be found in Table 30.

Table 30: Descriptive statistics for the Tunnel to Sprint Transition Times

Condition	Mean	Min	Max	Std Dev
A	3.58	2.03	7.76	1.11
B	4.97	2.67	13.81	2.18
E	5.62	3.53	13.52	2.08

Figure 30 shows the average Sprint to Stairs transition time for each condition.

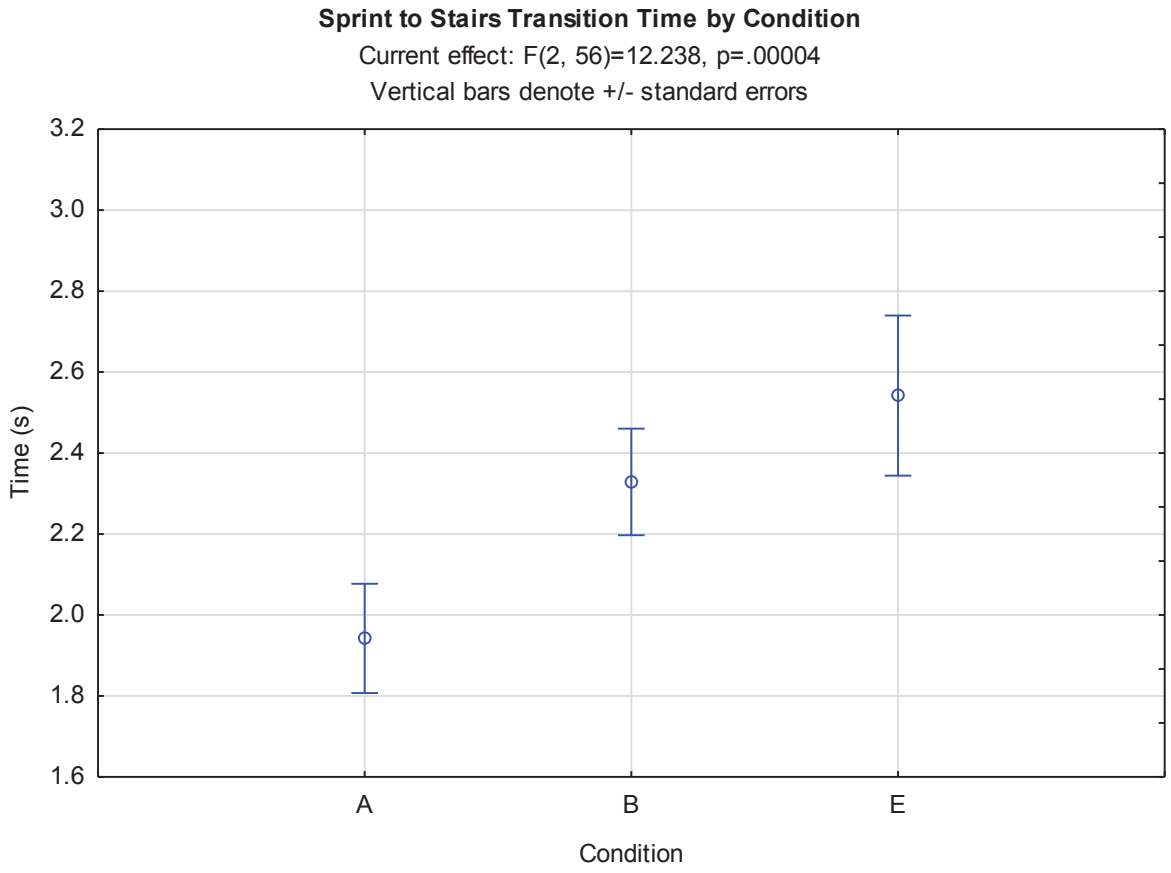

Figure 30: Average Sprint to Stairs Transition Time for each Condition

A repeated-measures ANOVA of the Sprint to Stairs Transition Time identified a significant difference across armour conditions (n=29, F(2, 56)=12.24, p=0.0000). A Tukey HSD post-hoc analysis revealed a significant difference between Condition A and all other conditions. There was no significant difference observed between Conditions B and E. The post-hoc results are summarized in Annex K: Additional LEAP Results.
The descriptive statistics for the sprint to stairs transition times, in seconds, can be found in Table 31.

Table 31: Descriptive statistics for the Sprint to Stairs Transition Times

Condition	Mean	Min	Max	Std Dev
A	1.94	1.27	4.34	0.73
B	2.33	1.39	4.42	0.71
E	2.54	1.52	6.04	1.07

Figure 31 shows the average Stairs to Agility transition time for each condition.

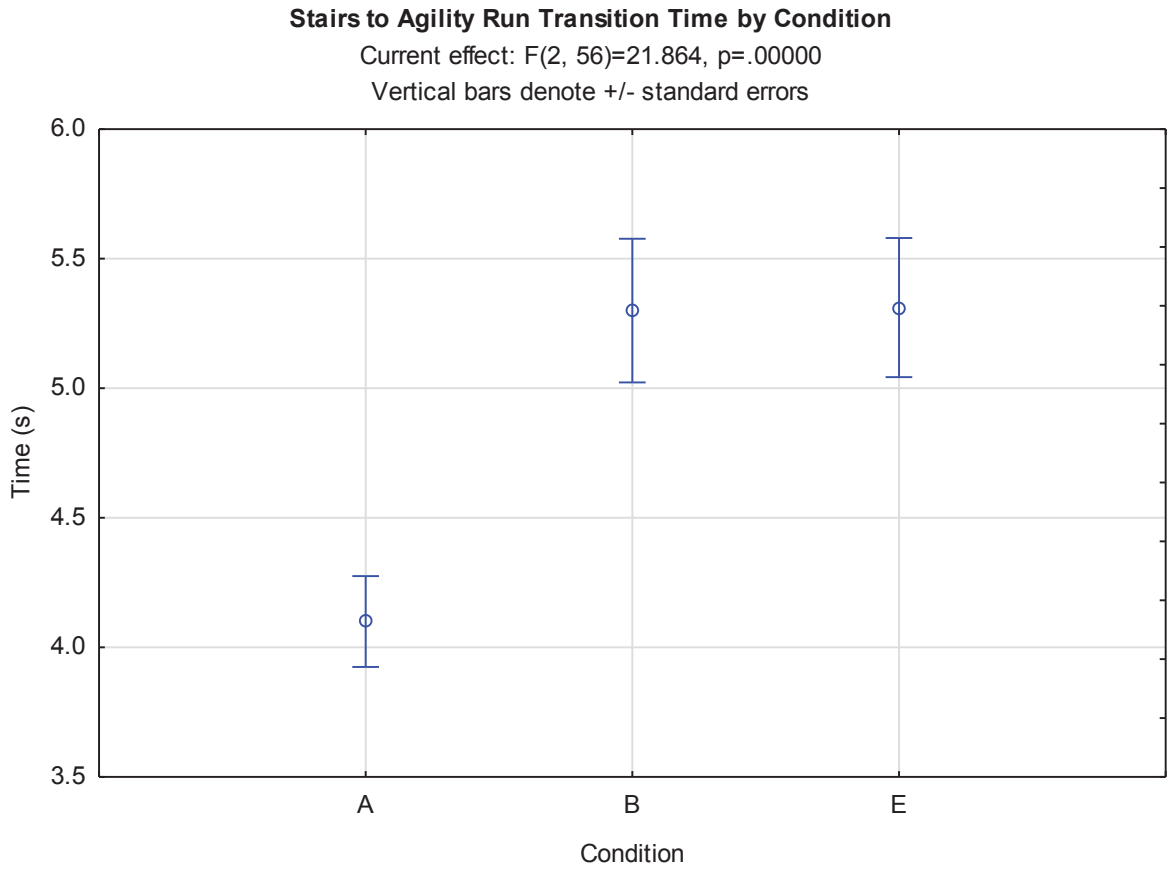

Figure 31: Average Stairs to Agility Transition Time for each Condition

A repeated-measures ANOVA of the Stairs to Agility Transition Time identified a significant difference between conditions (n=29, F(2, 56)=21.86, p=0.0000). A Tukey HSD post-hoc analysis revealed that there was only a significant difference between Condition A and all other conditions. There was no significant difference observed between Conditions B and E. The post-hoc results are summarized in Annex K: Additional LEAP Results.

The descriptive statistics for the stairs to agility run transition times, in seconds, can be found in Table 32.

Table 32: Descriptive statistics for the Stairs to Agility Run Transition Times

Condition	Mean	Min	Max	Std Dev
A	4.10	2.75	6.84	0.94
B	5.30	3.31	8.14	1.49
E	5.31	3.15	8.47	1.45

Figure 32 shows the average Casualty Drag to Window transition time for each condition.

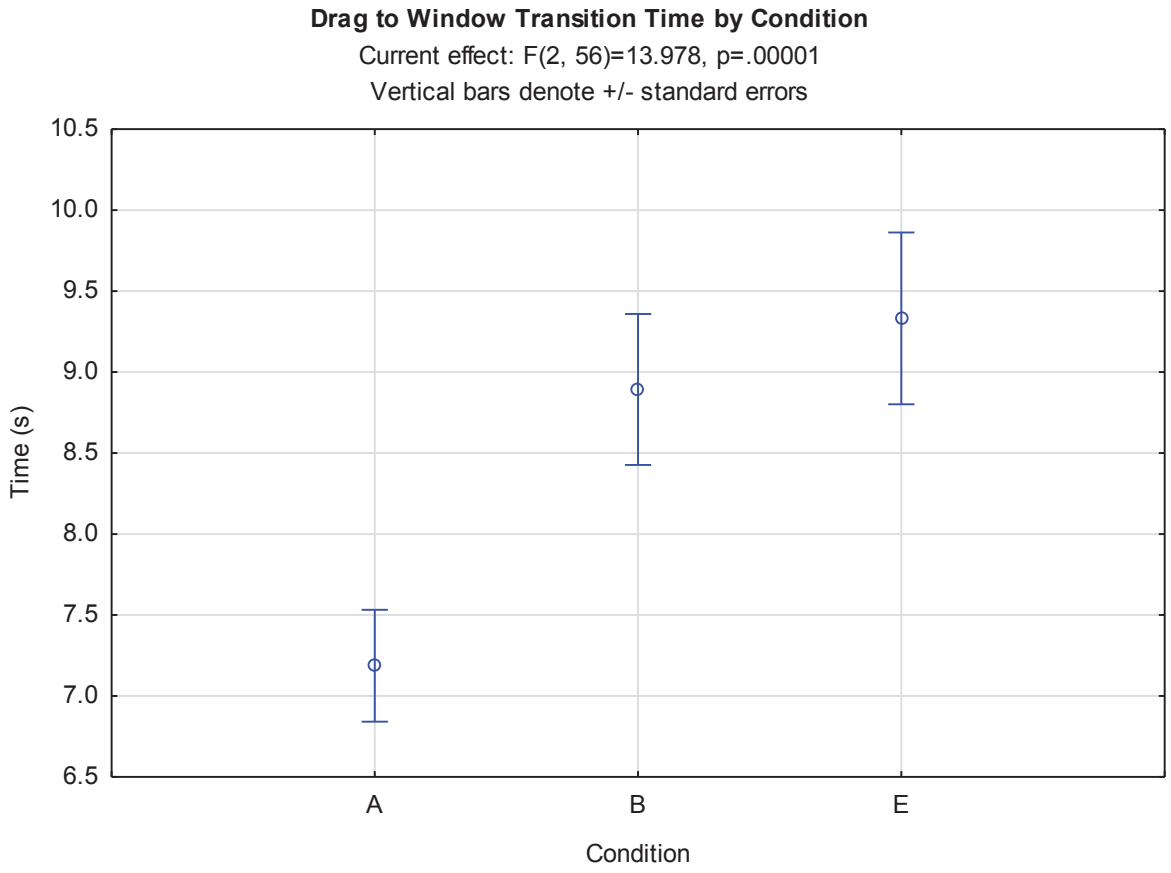

Figure 32: Average Casualty Drag to Window Transition Time

A repeated-measures ANOVA of the Drag to Window Transition Time identified a significant difference between armour conditions (n=29, F(2, 56)=13.98, p=0.0000). A Tukey HSD post-hoc analysis revealed that Condition A was significantly different from all other conditions. There was no significant difference observed between Conditions B and E. The post-hoc results are summarized in Annex K: Additional LEAP Results.

The descriptive statistics for the casualty drag to window transition times, in seconds, can be found in Table 33.

Table 33: Descriptive statistics for the Casualty Drag to Window Transition Times

Condition	Mean	Min	Max	Std Dev
A	7.19	4.31	13.10	1.86
B	8.89	4.93	14.85	2.51
E	9.33	5.54	19.10	2.86

Figure 33 shows the average Beam to Crawl transition time for each condition.

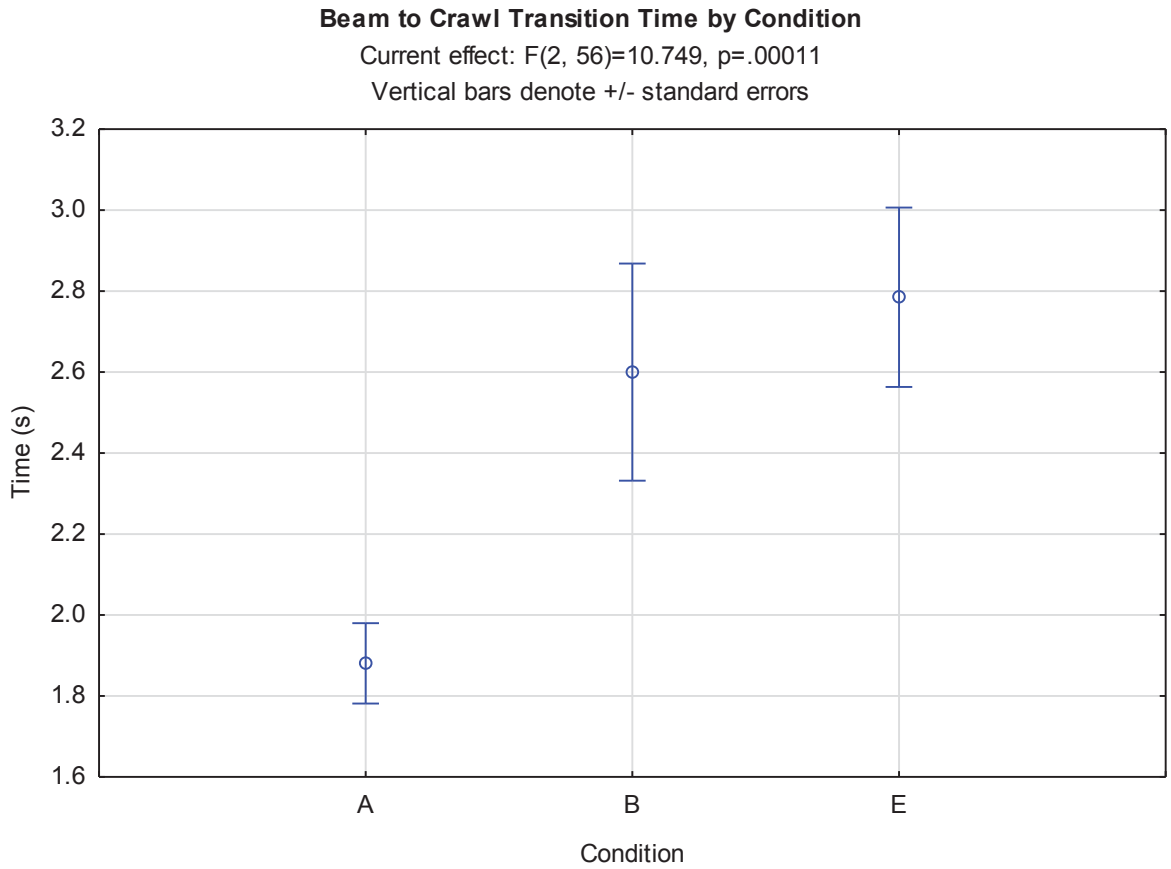

Figure 33: Average Beam to Crawl Transition Time for each Condition

A repeated-measures ANOVA of the Beam to Crawl Transition Time identified a significant difference between armour conditions (n=29, F(2, 56)=10.75, p=0.0001). A Tukey HSD post-hoc analysis revealed that only Condition A was significantly different from all other conditions. There was no significant difference observed between Conditions B and E. The post-hoc results are summarized in Annex K: Additional LEAP Results.
The descriptive statistics for the balance beam to low crawl transition times, in seconds, can be found in Table 34.

Table 34: Descriptive statistics for the Balance Beam to Low Crawl Transition Times

Condition	Mean	Min	Max	Std Dev
A	1.88	1.07	3.69	0.53
B	2.60	1.39	9.10	1.44
E	2.78	1.52	6.30	1.19

Figure 34 shows the average Crawl to Wall transition time for each condition.

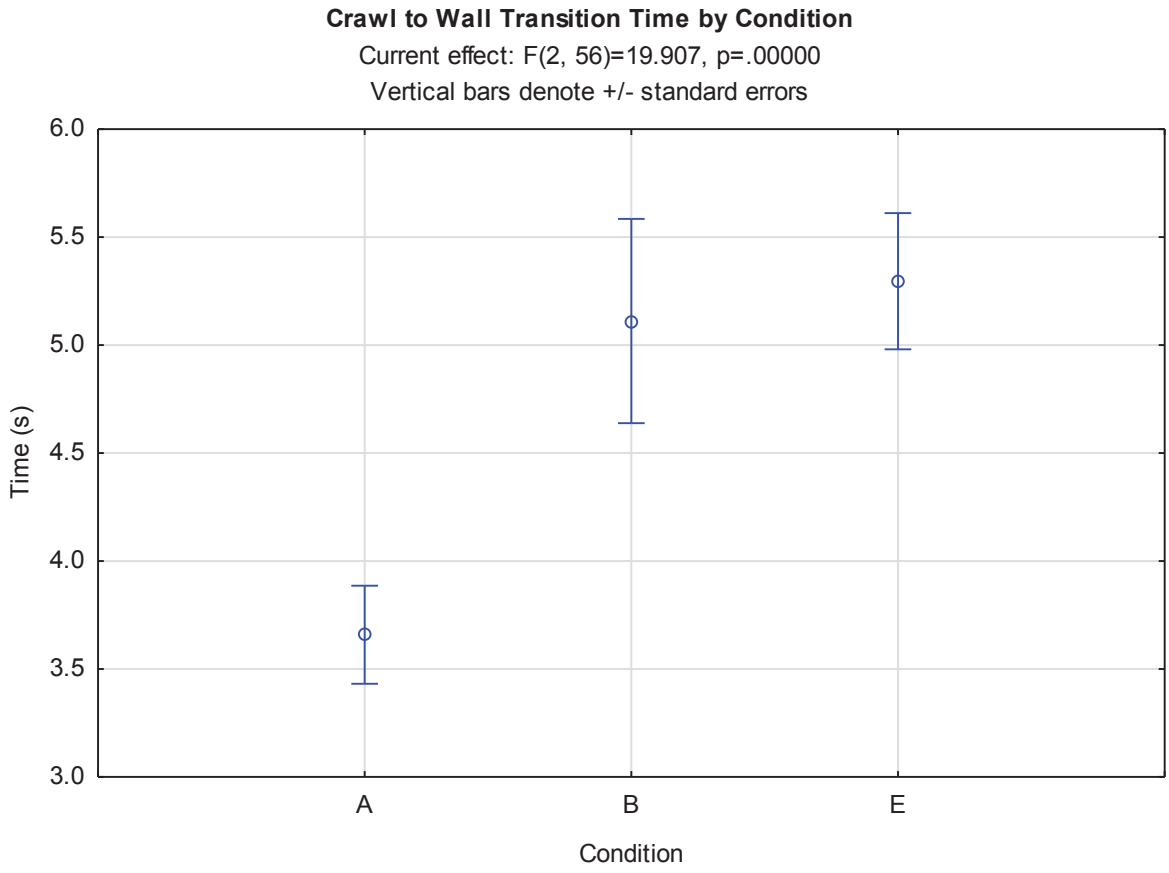

Figure 34: Average Crawl to Wall Transition Time for each Condition

A repeated-measures ANOVA of the Crawl to Wall Transition Time identified a significant difference between armour conditions (n=29, F(2, 56)=19.91, p=0.0000). A Tukey HSD post-hoc analysis revealed that Condition A was significantly different from all other conditions. There was no significant difference observed between Conditions B and E. The post-hoc results are summarized in Annex K: Additional LEAP Results.
The descriptive statistics for the crawl to wall transition times can be found in Table 35.

Table 35: Descriptive statistics for the Crawl to Wall Transition Times

Condition	Mean	Min	Max	Std Dev
A	3.66	2.08	6.87	1.22
B	5.11	2.74	14.42	2.55
E	5.30	3.65	12.23	1.70

3.3.4 Ancillary Stand Performance and Results

3.3.4.1 *Noptel Marksmanship*

Figure 35 displays the average distance between shots and aiming point across conditions, broken down by shooting posture and state of fatigue. The rested state is on the left and the fatigued state is on the right.

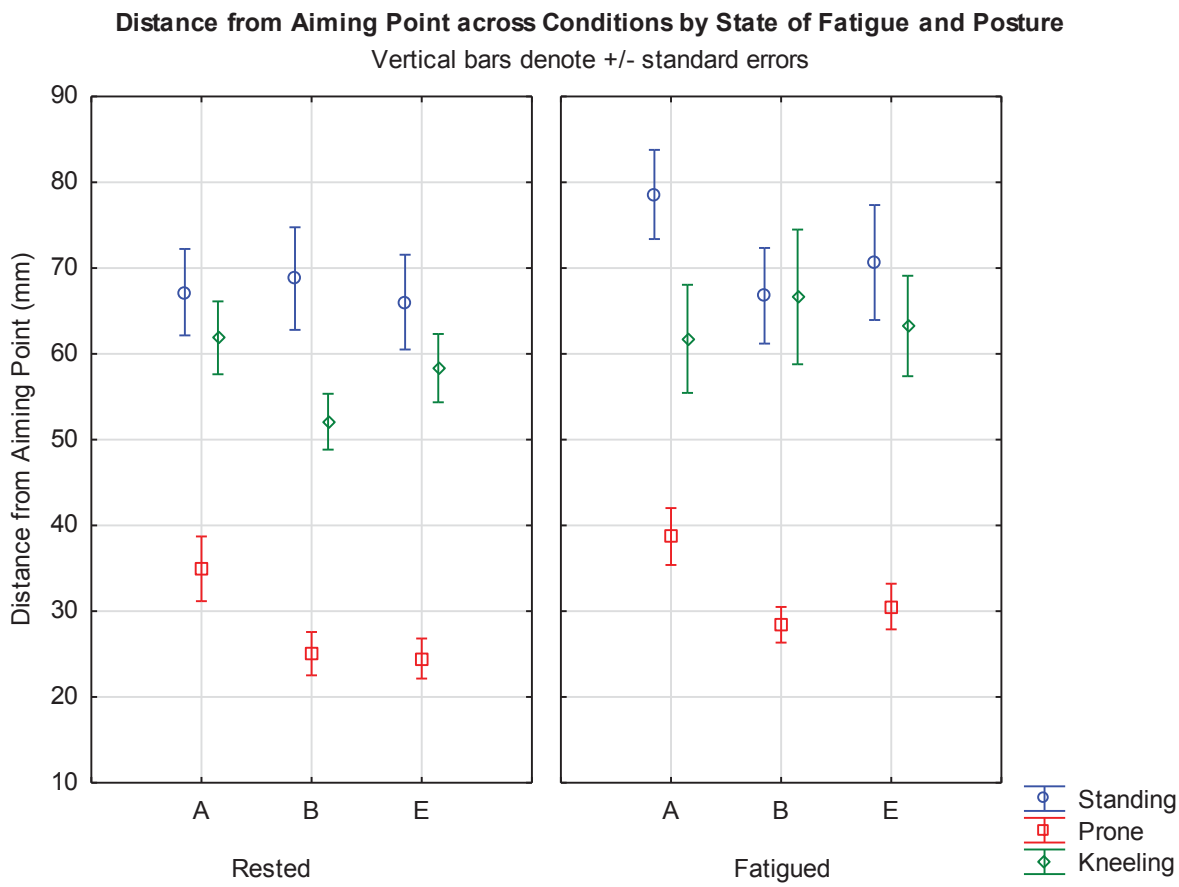

Figure 35: Average Distance Between Shot and Aiming Point Across Conditions by State of Fatigue and Posture

A repeated-measures ANOVA of the distance between aiming point and participant shots identified a significant difference between postures (n=29, F(2, 56)=77.12, p=0.0000), states of fatigue (n=29, F(1, 28)=8.33, p=0.0074), and conditions (n=29, F(2, 56)=3.52, p=0.0362). Because there was a significant difference between rested and fatigued states, the condition and postural analyses were analyzed separately within each state of fatigue. Figure 36 shows the average distance between shot and aiming point across postures for the rested state.

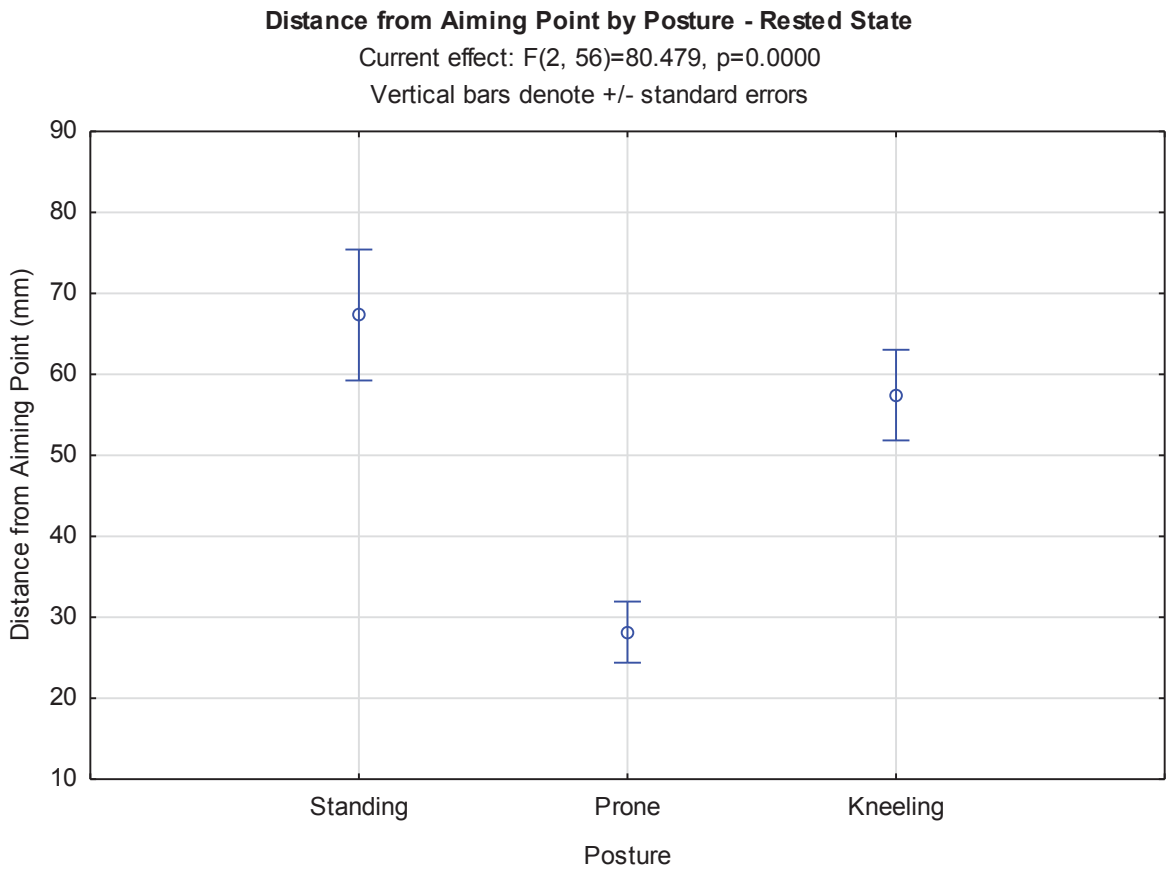

Figure 36: Average Distance between Shot and Aiming Point Across Postures (Rested State)

A repeated measures ANOVA identified a significant effect of posture on the average distance between shot and aiming point (n=29, F(2,26)=80.48, p=0.0000). A Tukey HSD post-hoc analysis revealed that all postures were significantly different than each other with the smallest distance being observed in prone, followed by kneeling. There was no significant effect of condition in the rested state. The post-hoc results are summarized in Annex K: Additional LEAP Results.

Figure 37 shows the average distance between shot and aiming point across postures for the fatigued state.

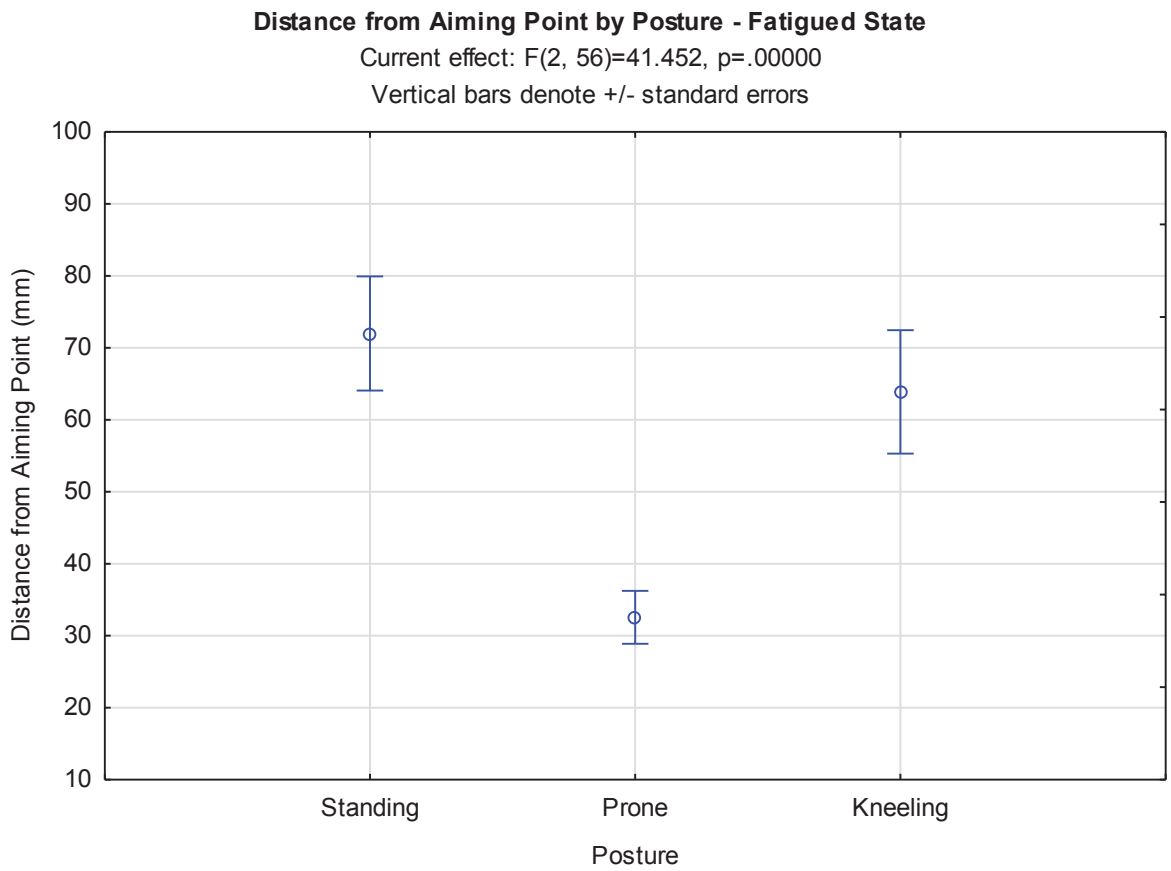

Figure 37: Average Distance Between Shot and Aiming Point Across Postures (Fatigued State)

A repeated measures ANOVA identified a significant effect of posture on the average distance between shot and aiming point in the fatigued state (n=29, F(2,26)=41.45, p=0.0000). A Tukey HSD post-hoc analysis revealed that standing and prone were significantly different and that prone and kneeling were significantly different. Standing and kneeling were not significantly different. There was no significant effect of condition in the fatigued state. The post-hoc results are summarized in Annex K: Additional LEAP Results.

3.3.4.2 *Vertical Weight Transfer*

Figure 38 shows the average time to complete the vertical weight transfer station for each state of fatigue (rested or fatigued).

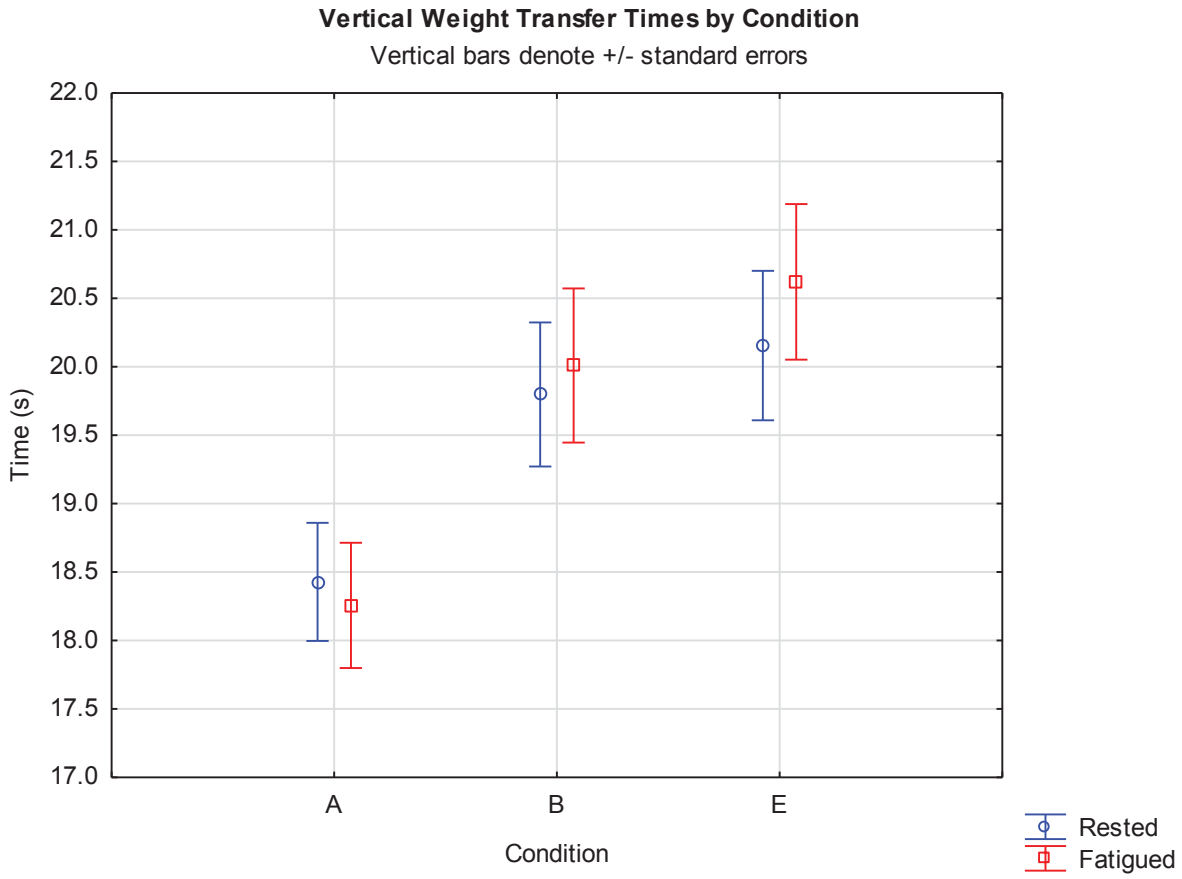

Figure 38: Vertical Weight Transfer Times Across all Conditions by State of Fatigue

A repeated measures ANOVA did not identify a significant difference between states, therefore rested and fatigued results were collapsed together for the analysis of the results across conditions. The repeated measures ANOVA identified a significant difference between conditions (n=29, $F(2, 56)=24.58$, $p=0.0000$).

Figure 39 shows the effect of condition on weight transfer times.

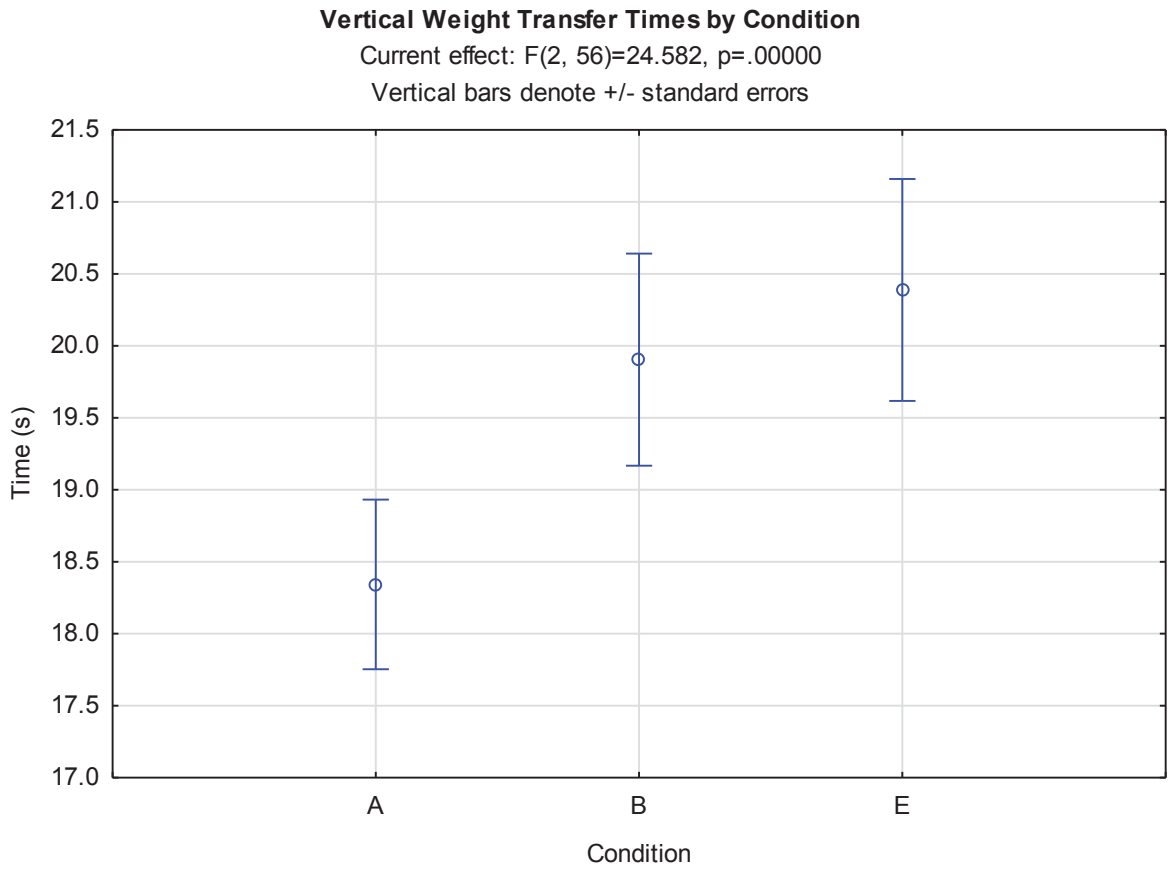

Figure 39: Vertical Weight Transfer Times by Condition

A Tukey HSD post-hoc analysis revealed that Condition A was significantly different than all other conditions but Conditions B and E were not significantly different, with soldiers performing the task fastest in Condition A. The post-hoc results are summarized in Annex K: Additional LEAP Results.

Descriptive statistics for the vertical weight transfer times for the fatigued and rested states can be found in Table 36 and Table 37 respectively.

Table 36: Descriptive Statistics for Vertical Weight Transfer Times (Rested State)

Condition	Mean	Min	Max	Std Dev
A	18.43	15.40	23.89	2.32
B	19.80	16.11	26.08	2.84
E	20.16	15.58	26.62	2.94

Table 37: Descriptive Statistics for Vertical Weight Transfer Times (Fatigued State)

Condition	Mean	Min	Max	Std Dev
A	18.26	13.97	23.72	2.47
B	20.01	15.83	26.54	3.03
E	20.62	15.45	26.00	3.06

3.3.4.3 *Horizontal Weight Transfer*

Figure 40 shows the average time to complete horizontal weight transfer station for each state of fatigue (rested or fatigued).

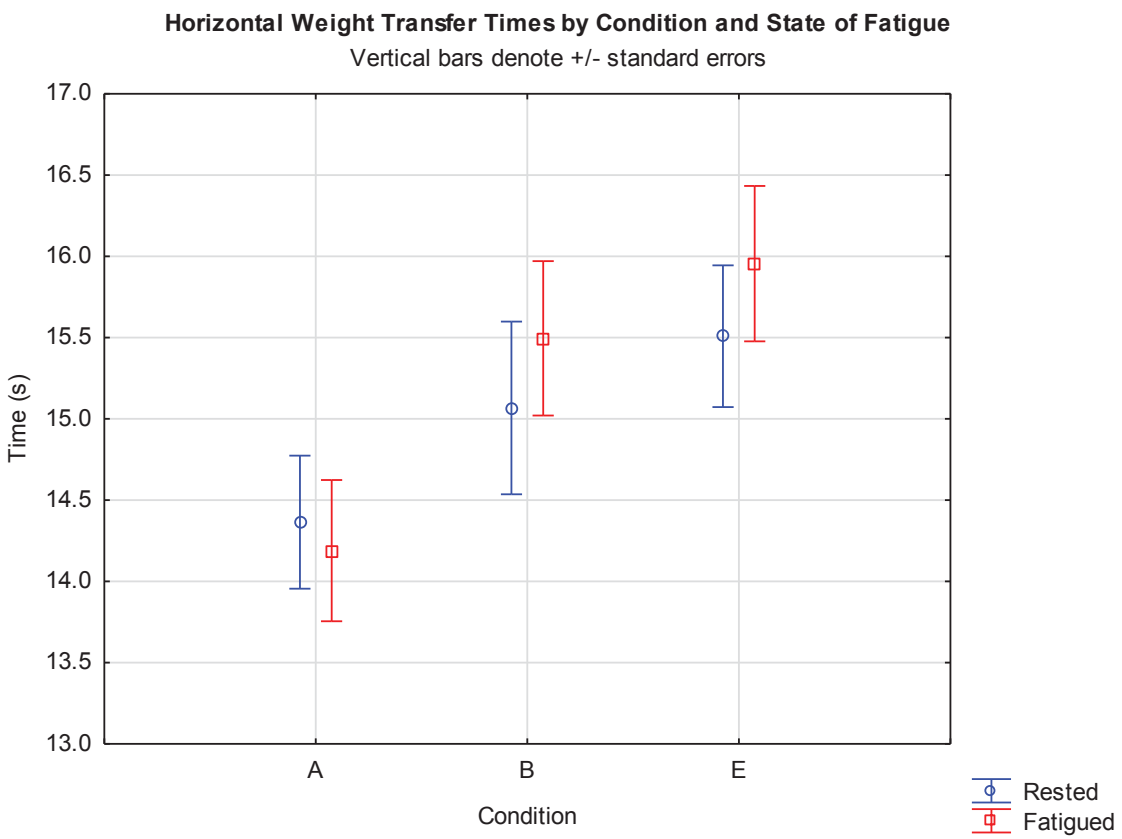

Figure 40: Horizontal Weight Transfer Times across all Conditions by State of Fatigue

A repeated measures ANOVA did not identify a significant difference between states, therefore rested and fatigued results were collapsed together for the analysis of the results across conditions. The repeated measures ANOVA identified a significant difference between conditions (n=29, F(2, 56)=11.48, p=0.0001).

Figure 41 shows the effect of condition on weight transfer times.

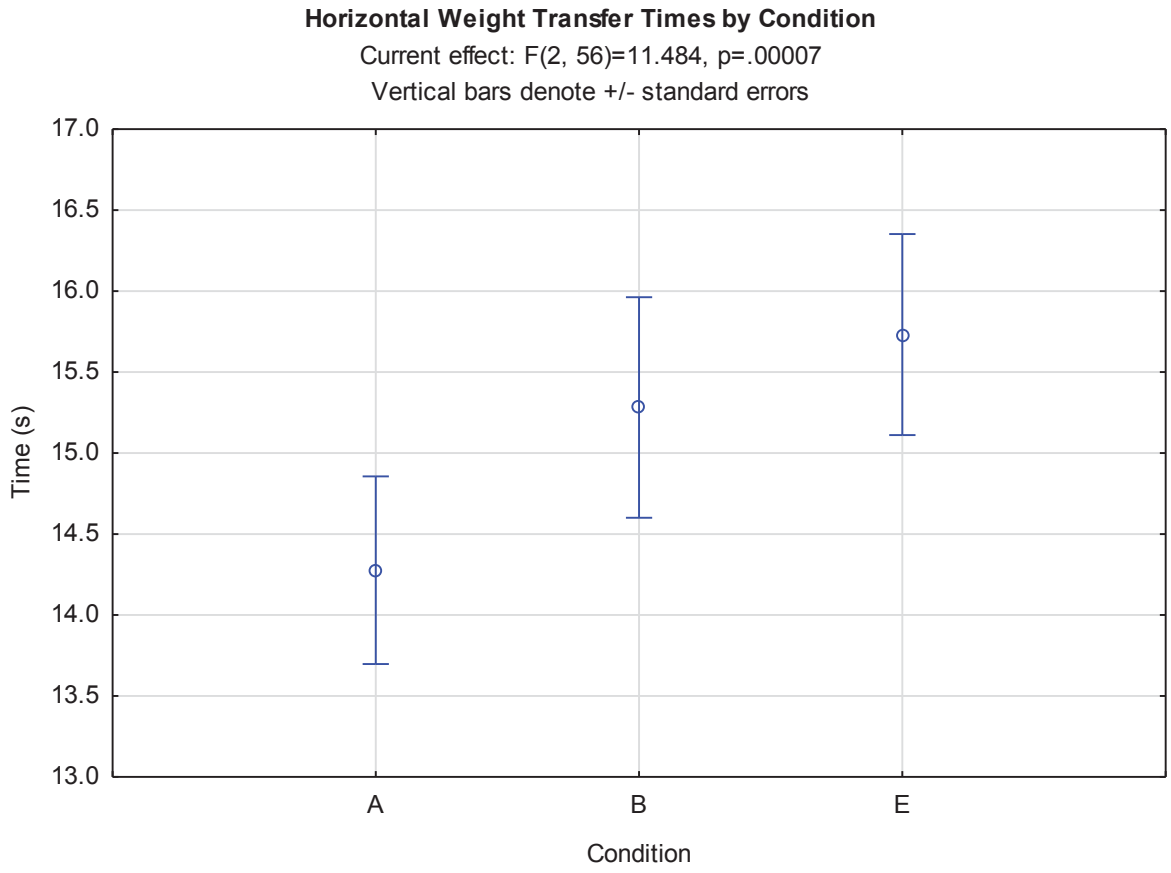

Figure 41: Horizontal Weight Transfer Time by Condition

A Tukey HSD post-hoc analysis revealed that Condition A was significantly different than all other conditions but Conditions B and E were not significantly different, with soldiers performing the task fastest in Condition A. The post-hoc results are summarized in Annex K: Additional LEAP Results.

Descriptive statistics for the horizontal weight transfer times for the fatigued and rested states can be found in Table 38 and Table 39 respectively.

Table 38: Descriptive Statistics for Horizontal Weight Transfer Times (Rested State)

Condition	Mean	Min	Max	Std Dev
A	14.36	11.89	20.47	2.20
B	15.07	11.14	22.06	2.86
E	15.51	12.11	21.19	2.35

Table 39: Descriptive Statistics for Horizontal Weight Transfer Times (Fatigued State)

Condition	Mean	Min	Max	Std Dev
A	14.19	10.56	20.36	2.34
B	15.50	11.89	21.47	2.56
E	15.95	12.11	20.54	2.57

3.3.4.4 *Vertical Jump*

Figure 42 shows the results of the vertical jump across conditions by state of fatigue.

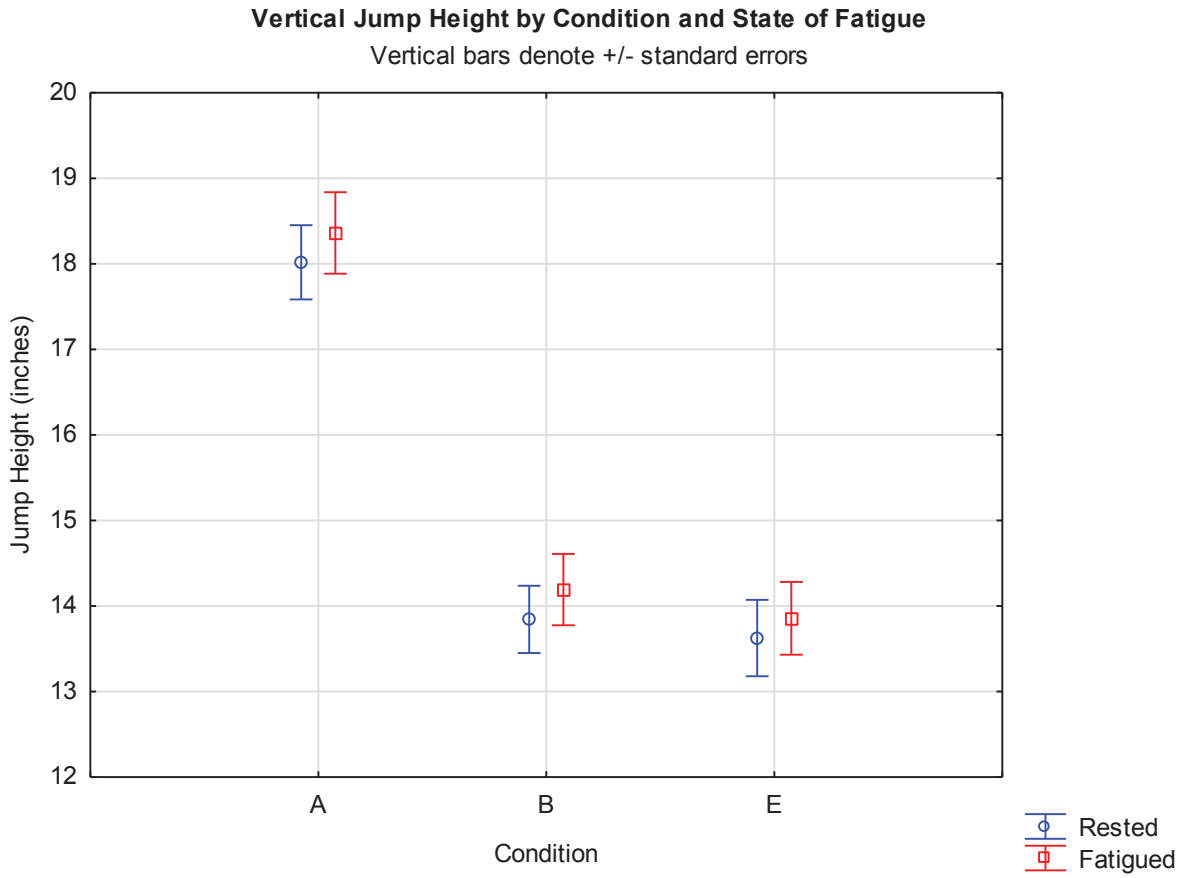

Figure 42: Vertical Jump Heights across Conditions by State of Fatigue

A repeated-measures ANOVA was performed on the vertical jump height results. Mauchly's test indicated that the assumption of sphericity had been violated for between conditions ($\chi^2(2)=6.78$, $p=0.0336$). The degrees of freedom were adjusted using the Huynh-Feldt correction. There was a statistically significant difference observed between conditions ($n=29$, $F(1.72, 48.28)=263.40$, $p=0.0000$), and between states of fatigue ($n=29$, $F(1, 28)=6.7114$, $p=.01504$). Because there was a significant difference between rested and fatigued states, the effects of condition on jump height were analyzed separately within each state of fatigue. Figure 43 shows the average jump height by condition in the rested state.

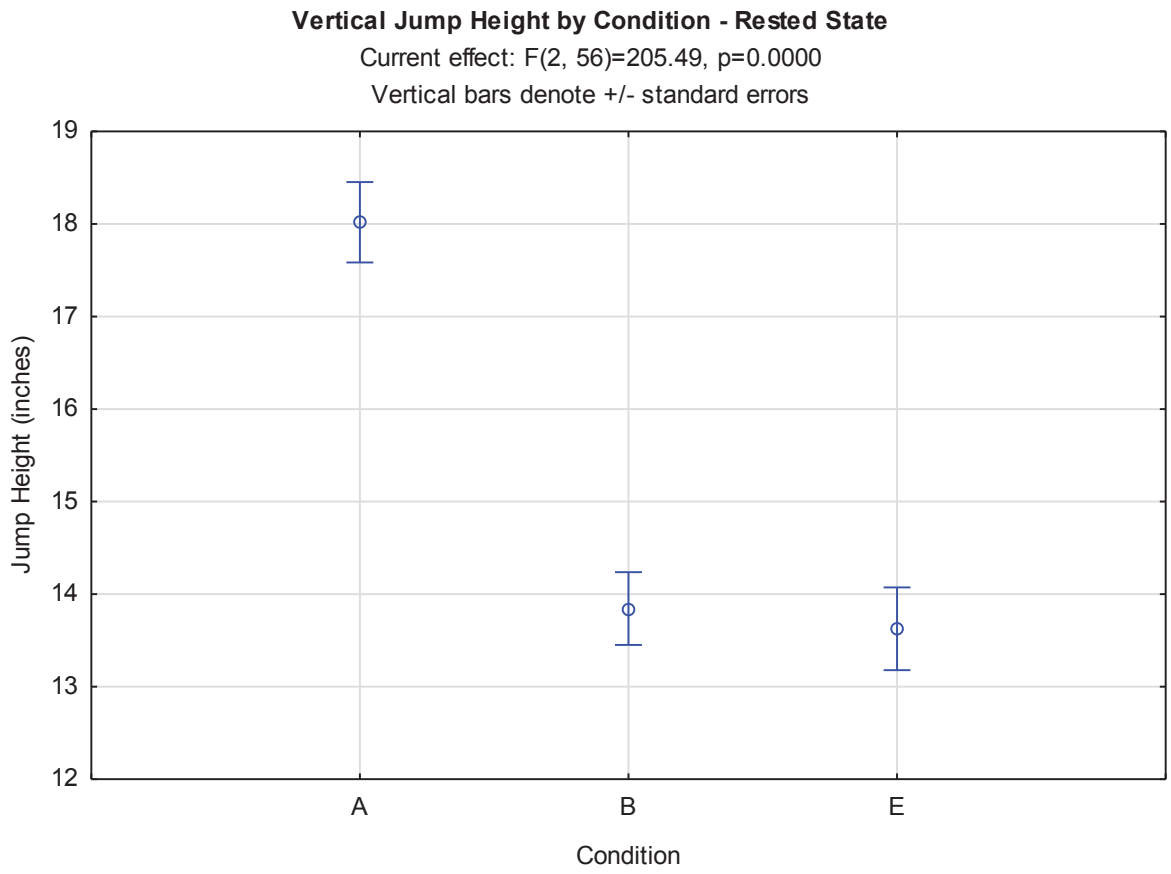

Figure 43: Jump Height by Condition in the Rested State

A repeated measures ANOVA showed a significant difference between conditions in the rested state (n=29, F(2, 56)=205.49, p=0.0000). A Tukey's HSD post-hoc analysis revealed that Condition A was significantly different than all other conditions, but Conditions B and E were not significantly different than each other with Condition A allowing the highest jump. The post-hoc results are summarized in Annex K: Additional LEAP Results.

Descriptive statistics for vertical jump height in the rested state can be seen in Table 40.

Table 40: Descriptive Statistics for Vertical Jump Height (Rested State)

Condition	Mean	Min	Max	Std Dev
A	18.02	14.13	22.20	2.34
B	13.84	10.37	17.30	2.12
E	13.63	8.67	18.10	2.41

Figure 44 shows the average jump height by condition in the fatigued state.

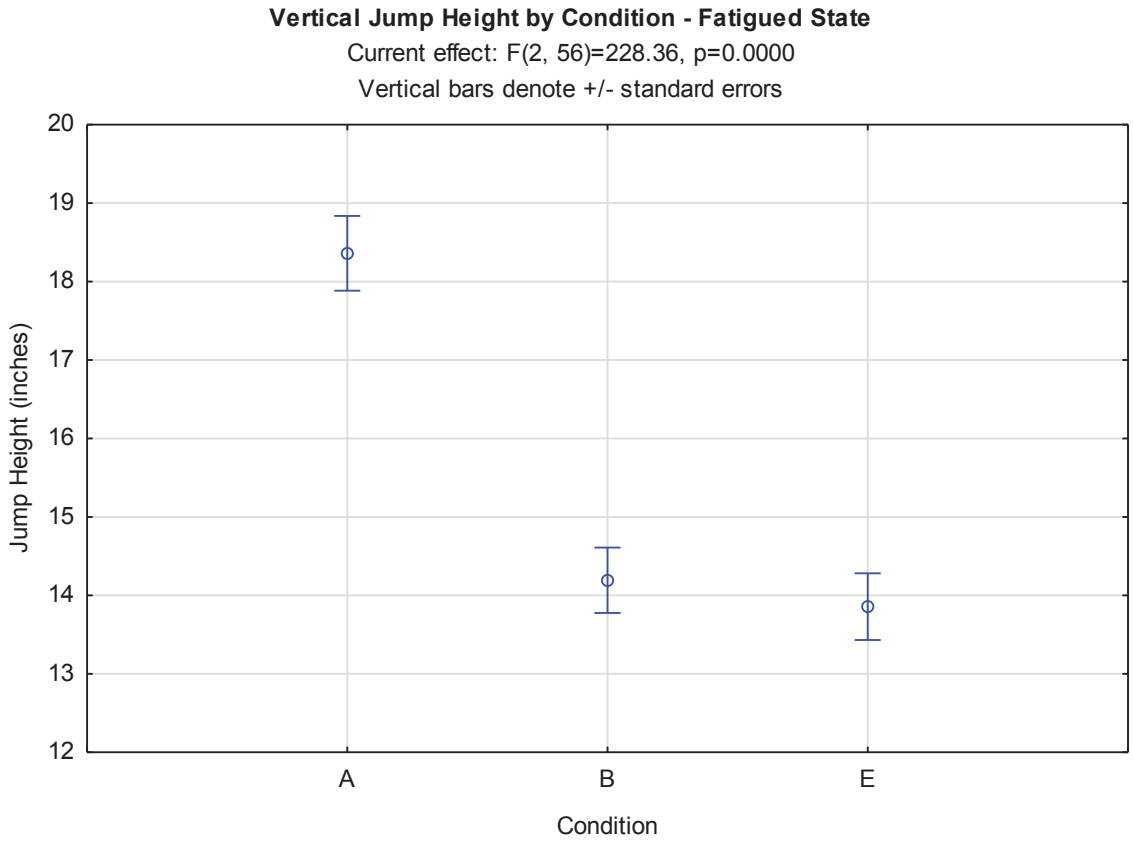

Figure 44: Jump Height by Condition in the Fatigued State

A repeated measures ANOVA showed a significant difference between conditions in the fatigued state (n=29, F(2, 56)=228.36, p=0.0000). A Tukey's HSD post-hoc analysis revealed that Condition A was significantly different than all other conditions, but Conditions B and E were not significantly different than each other with Condition A allowing the highest jump. The post-hoc results are summarized in Annex K: Additional LEAP Results.

Descriptive statistics for vertical jump height in the fatigued state can be seen in Table 41.

Table 41: Descriptive Statistics for Vertical Jump Height (Fatigued State)

Condition	Mean	Min	Max	Std Dev
A	18.36	13.57	22.77	2.57
B	14.19	10.60	18.70	2.24
E	13.86	9.73	17.97	2.29

3.3.4.5 *Horizontal Jump*

Figure 45 below shows the results of the horizontal jump across conditions by states of fatigue.

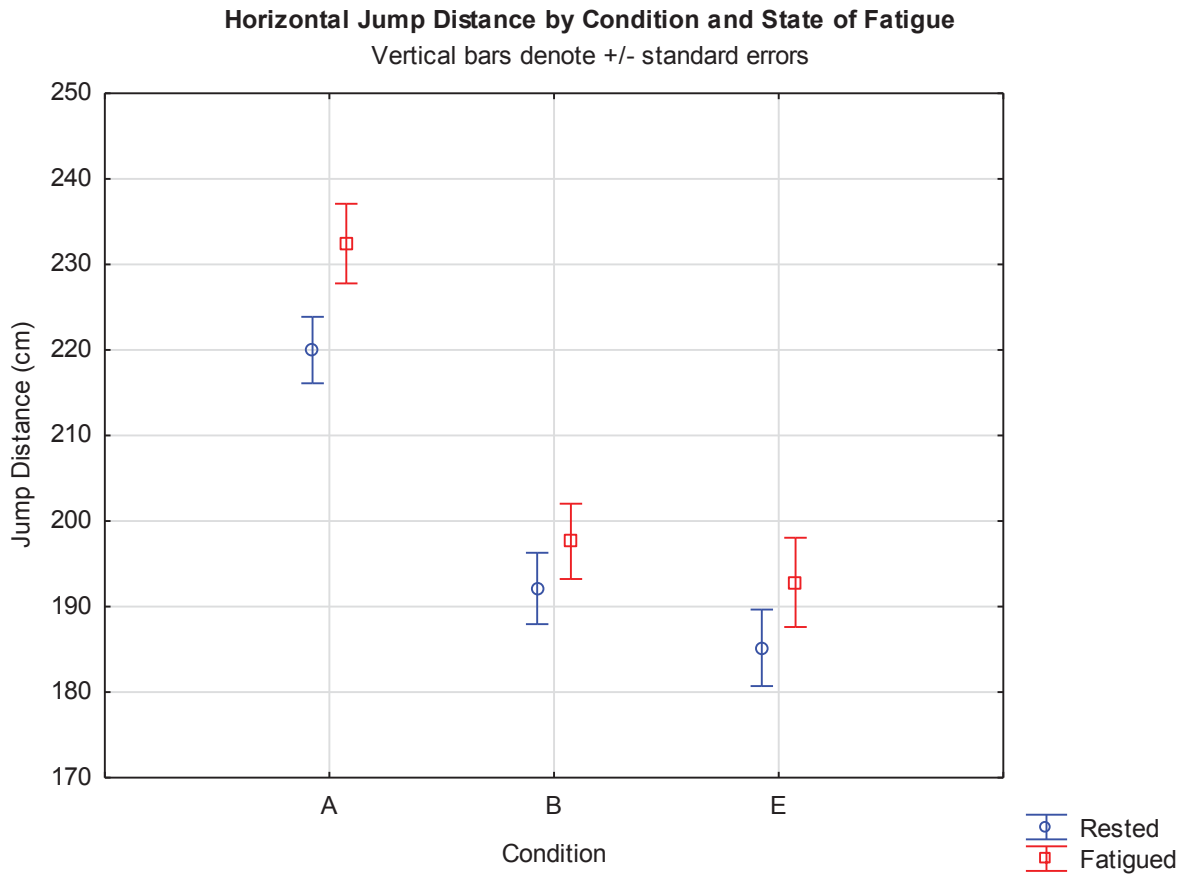

Figure 45: Horizontal Jump Distances Across Conditions by State of Fatigue

Repeated-measure ANOVAs were carried out on the horizontal jump distance results. There was a significant difference observed between conditions (n=29, F(2, 56)=126.63, p=0.0000), states of fatigue (n=29, F(1, 28)=19.88, p=0.0001), and state by condition (n=29, F(2, 56)=3.72, p=0.0304). Because there was a significant difference between rested and fatigued states, the effects of condition on horizontal jump distance were analyzed separately within each state of fatigue. Figure 46 shows the effect of condition on horizontal jump distance in the rested state.

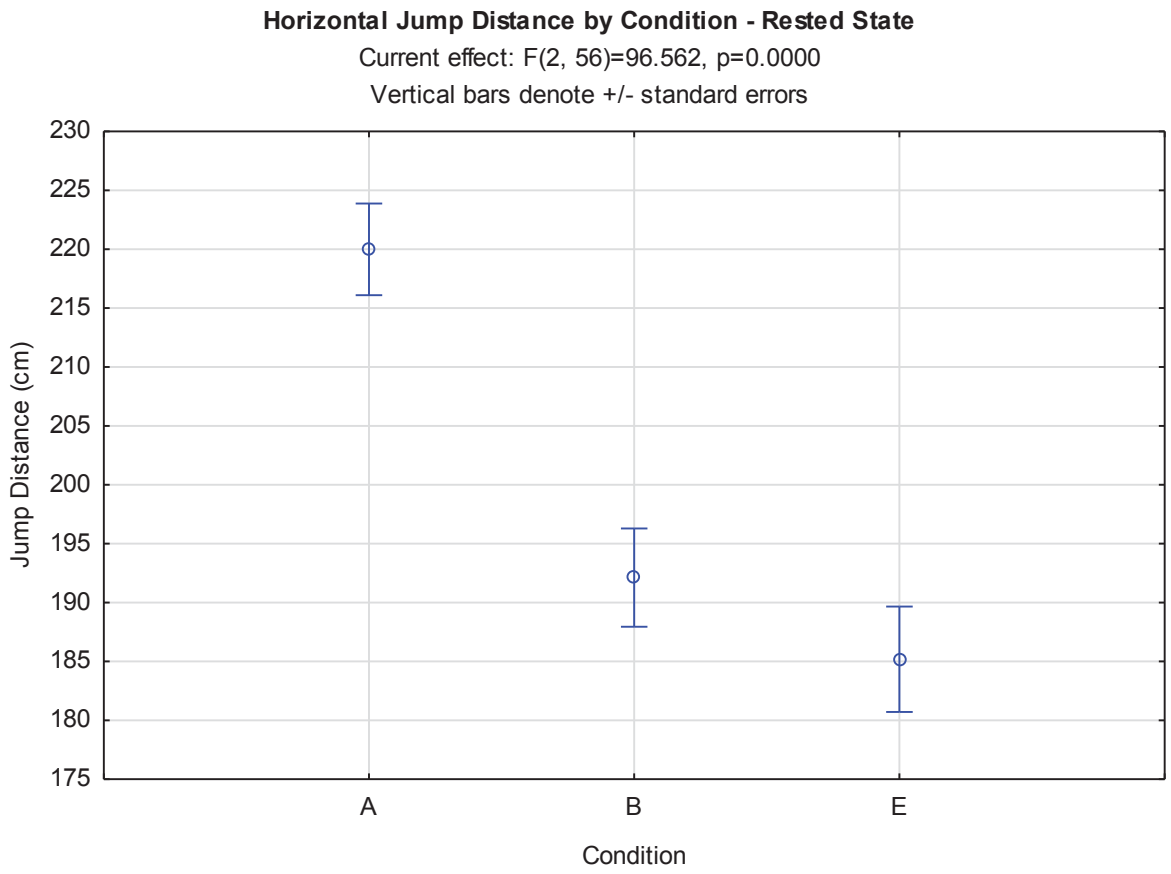

Figure 46: Horizontal Jump Distance by Condition in the Rested State

A repeated measures ANOVA showed a significant difference between conditions in the rested state (n=29, F(2, 56)=96.56, p=0.0000). A Tukey's HSD post-hoc analysis revealed that all conditions were significantly different than each other with Condition A allowing for the furthest horizontal jump distance. The post-hoc results are summarized in Annex K: Additional LEAP Results.

Descriptive statistics for horizontal jump distance in the rested state are shown in Table 42.

Table 42: Descriptive Statistics for Horizontal Jump Distance in the Rested State

Condition	Mean	Min	Max	Std Dev
A	219.99	177.20	254.50	20.96
B	192.12	145.10	235.40	22.45
E	185.19	130.90	228.10	24.10

Figure 47 shows the effect of condition on horizontal jump distance in the fatigued state.

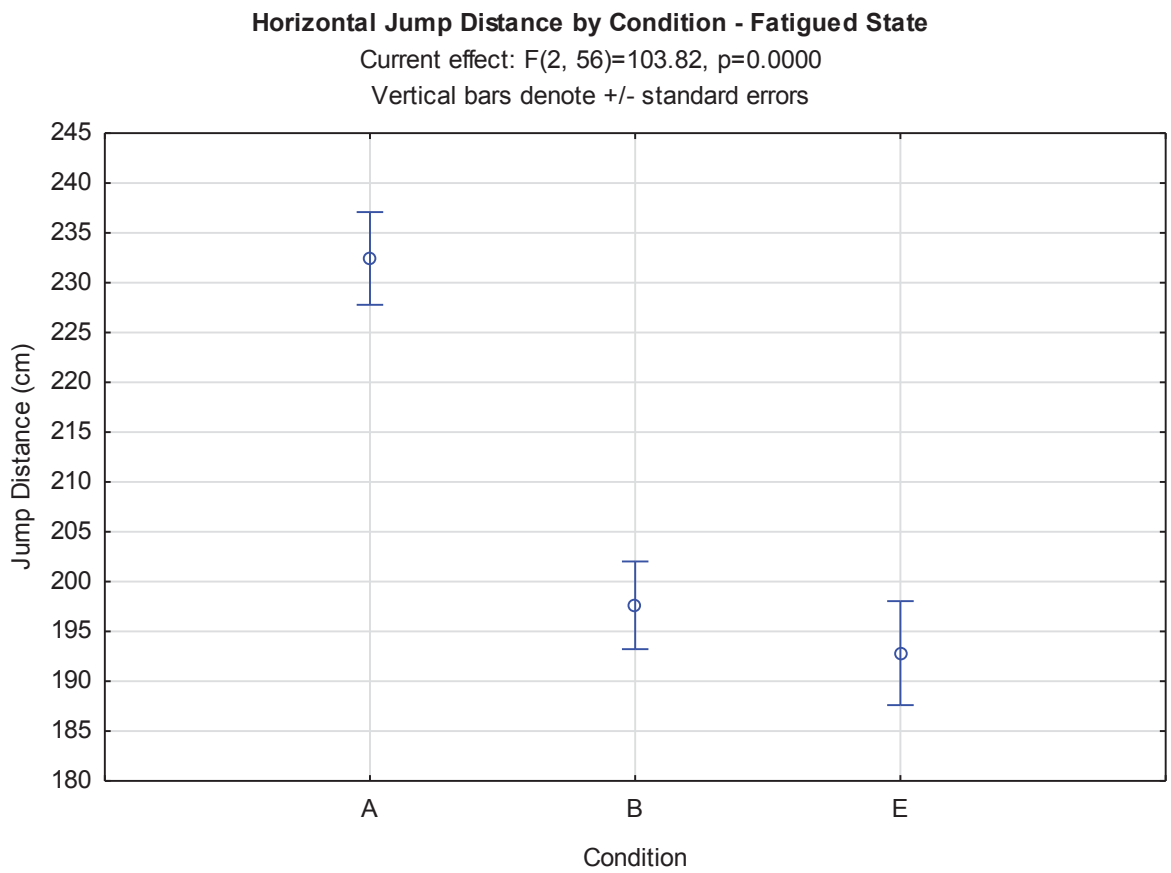

Figure 47: Horizontal Jump Distance by Condition in the Fatigued State

A repeated measures ANOVA showed a significant difference between conditions in the fatigued state (n=29, F(2, 56)=103.82, p=0.0000). A Tukey's HSD post-hoc analysis revealed that Condition A was significantly different than all other conditions, but Conditions B and E were not significantly different. The post-hoc results are summarized in Annex K: Additional LEAP Results.

Descriptive statistics for horizontal jump distance in the fatigued state are shown in Table 43.

Table 43: Descriptive Statistics for Horizontal Jump Distance in the fatigued State

Condition	Mean	Min	Max	Std Dev
A	232.43	173.60	276.60	25.04
B	197.63	128.50	238.90	23.69
E	192.82	131.60	249.80	28.09

3.4 ROM Results

The following section displays all the information obtained from four of the five ROM stations during the ROM Reliability study, including the original LEAP (manual), modified LEAP (digital), USMC IMU (iRoM), and Natick protocols. Data from the functional reach method was collected, but analysis of this data was beyond the scope of this report. For all statistical analyses completed, $p \leq 0.05$ was used as the threshold of statistical significance and for all charts, error bars denote the plus and minus one standard error, unless otherwise stated.

3.4.1 ROM Measurement Results

3.4.1.1 *Trunk Rotation*

A repeated-measures ANOVA was carried out on the trunk rotation measurements for all four methods. The identified significant effects are summarized in Table 44.

Table 44: Summary of Repeated Measures ANOVA for Trunk Rotation

Effect	Significance	P-value
Condition	Significant	0.0000
Iteration	Significant	0.0010
Method	Significant	0.0000
Direction	Significant	0.0047
Trial	Significant	0.0001
Condition x Iteration	Not significant	0.6126[2]
Condition x Method	Significant	0.0106
Iteration x Method	Significant	0.0093
Condition x Direction	Significant	0.0014
Iteration x Direction	Not significant	0.7078
Method x Direction	Not significant	0.5053[2]
Condition x Trial	Not significant	0.084
Iteration x Trial	Not significant	0.2129[2]
Method x Trial	Significant	0.0110
Direction x Trial	Significant	0.0263
Condition x Iteration x Method	Not significant	0.0949
Condition x Iteration x Direction	Not significant	0.9091[2]
Condition x Method x Direction	Significant	0.0014
Iteration x Method x Direction	Not significant	0.6821
Condition x Iteration x Trial	Not significant	0.2904[2]
Condition x Method x Trial	Not significant	0.0996
Iteration x Method x Trial	Not significant	0.7384
Condition x Direction x Trial	Not significant	0.8719[3]
Iteration x Direction x Trial	Not significant	0.0747[3]
Method x Direction x Trial	Not significant	0.0827[3]
Condition x Iteration x Method x Direction	Not significant	0.1674[2]
Condition x Iteration x Method x Trial	Not significant	0.0706
Condition x Iteration x Direction x Trial	Not significant	0.3106[2]
Condition x Method x Direction x Trial	Not significant	0.4316
Iteration x Method x Direction x Trial	Not significant	0.2144
Condition x Iteration x Method x Direction x Trial	Not significant	0.3947[2]

[2] Adjusted using Greenhouse-Geisser (1959) correction.
[3] Adjusted using Hunyh-Feldt (1976) correction.

Figure 48 shows the effect of condition on trunk rotation angle across all methods.

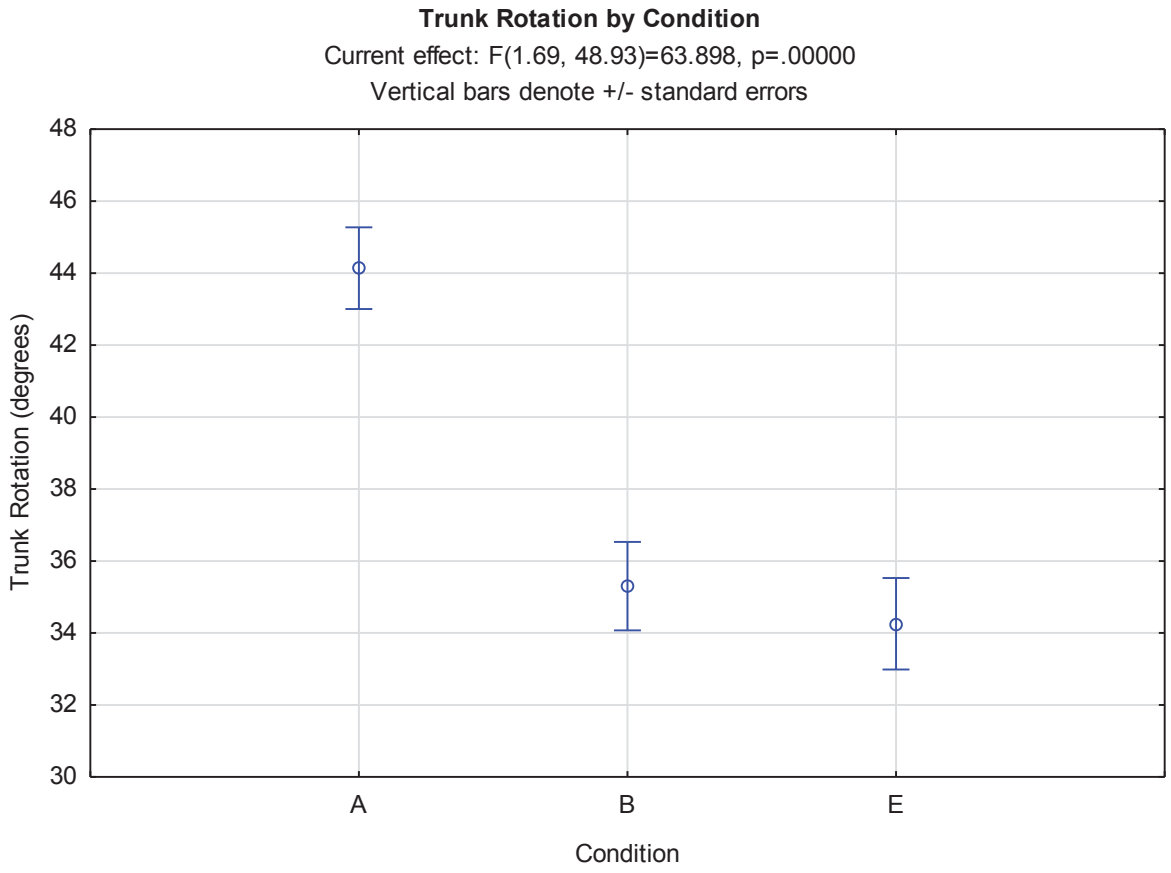

Figure 48: The Effect of Condition on Trunk Rotation Angle

Mauchly's test indicated that the assumption of sphericity had been violated ($\chi^2(2)=7.85$, $p=0.0198$). The degrees of freedom were adjusted using the Huynh-Feldt correction. There was a significant difference observed between conditions ($n=30$, $F(1.69, 48.93)=63.90$, $p=0.0000$). A Tukey HSD post-hoc analysis revealed that Condition A was significantly different than all other conditions but that Condition B and E were not significantly different from each other. There were no other significant effects.

Figure 49 shows the effect of iteration on trunk rotation angle across all methods.

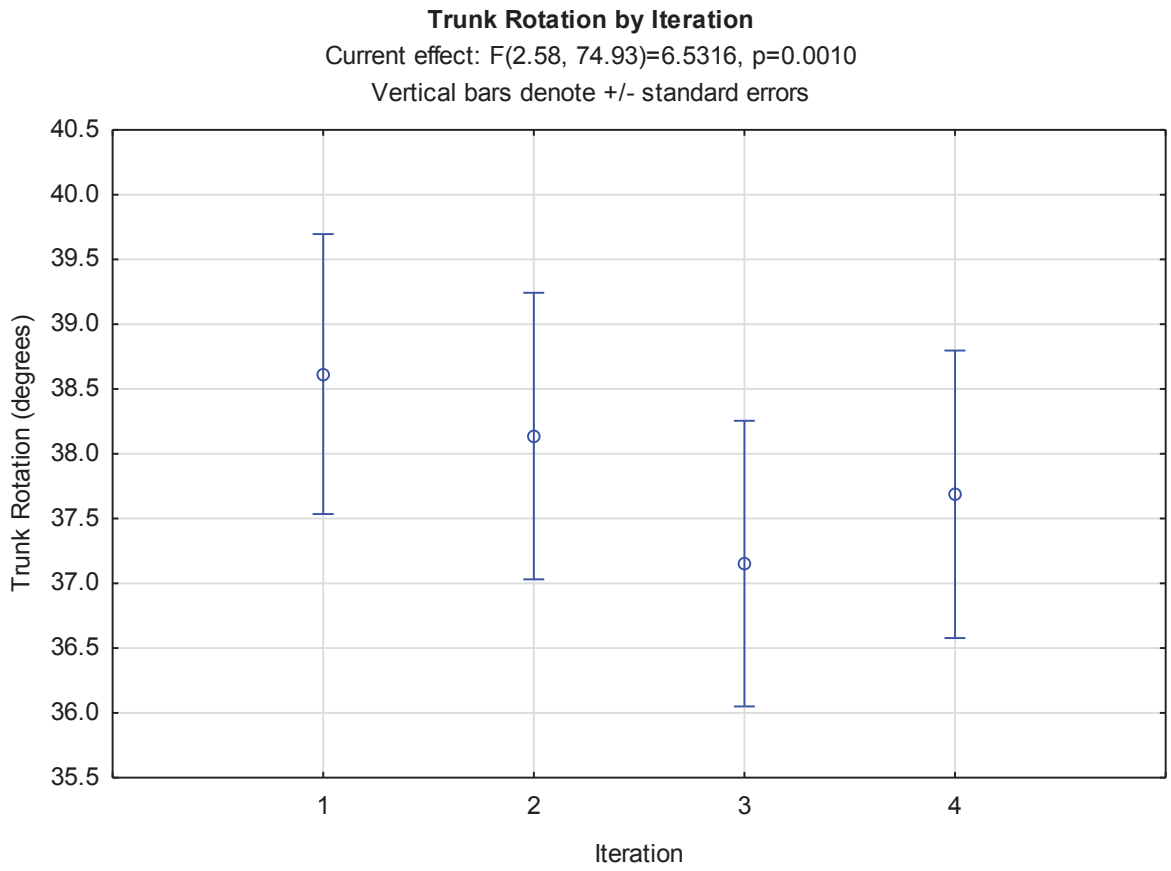

Figure 49: The Effect of Iteration on Trunk Rotation Angle

Mauchly's test indicated that the assumption of sphericity had been violated ($\chi^2(5)=11.73$, $p=0.0387$). The degrees of freedom were adjusted using the Huynh-Feldt correction. There was a significant difference observed between iterations ($n=30$, $F(2.58, 74.93)=6.53$, $p=0.0010$) however the mean difference between iterations was small. A Tukey HSD post-hoc analysis revealed that Iteration 3 was significantly different from Iterations 1 and 2. Iterations 1 and 4 were significantly different from each other. There were no other significant effects.

Figure 50 shows the effect of method on trunk rotation angle.

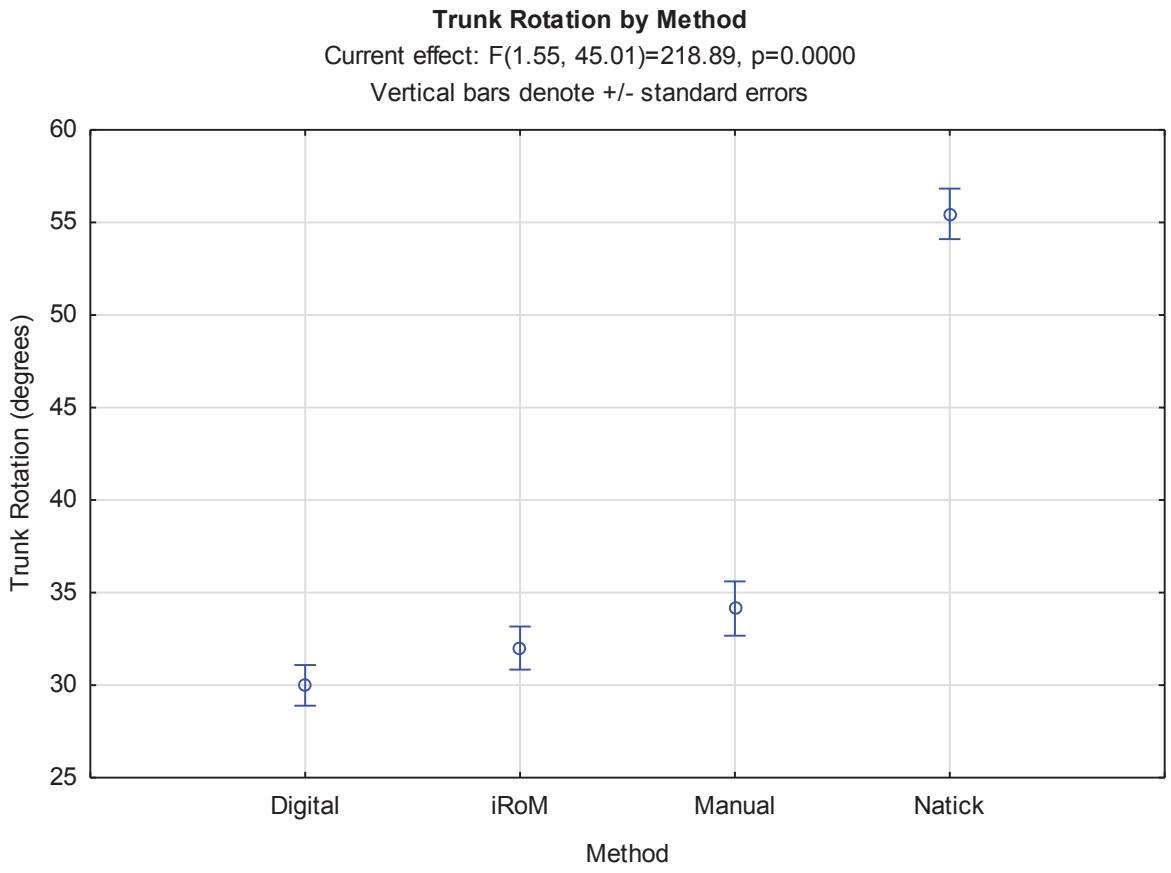

Figure 50: The Effect of Method on Trunk Rotation Angle

Mauchly's test indicated that the assumption of sphericity had been violated ($\chi^2(5)=72.13$, $p=0.0000$). The degrees of freedom were adjusted using the Greenhouse-Geisser correction. There was a significant difference observed between methods ($n=30$, $F(1.55, 45.01)=218.89$, $p=0.0000$). A Tukey HSD post-hoc analysis revealed that Natick was significantly different from all other methods. The Digital method was significantly different from Manual and Natick methods but not significantly different than the iRoM method. The iRoM method was only significantly different from Natick. The Manual method was significantly different than the Digital and Natick methods but not significantly different from the iRoM method.

Figure 51 shows the effect of direction on trunk rotation angle.

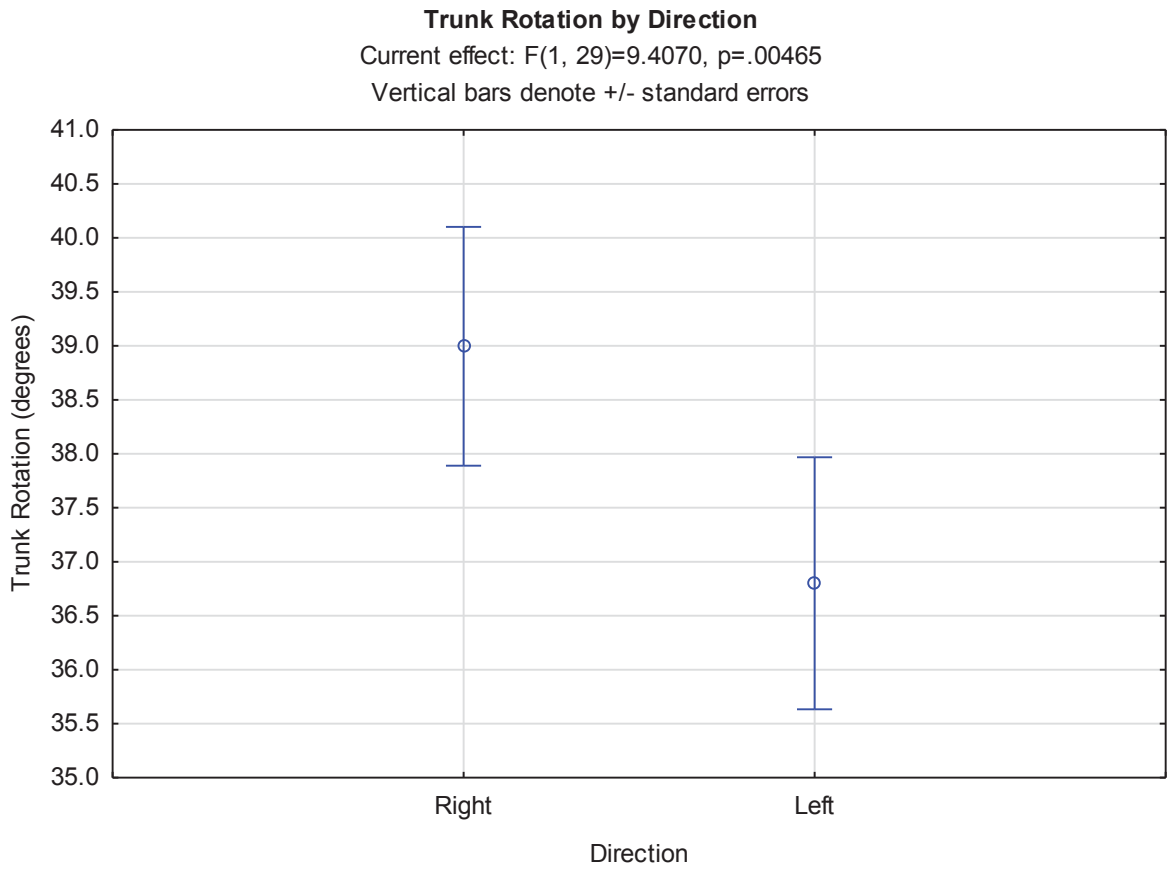

Figure 51: The Effect of Direction on Trunk Rotation Angle

There was a significant difference observed between right and left directions (n=30, F(1, 29)=9.41, p=0.0047) however the mean difference between directions was small.

Figure 52 shows the effect of trial on trunk rotation angle.

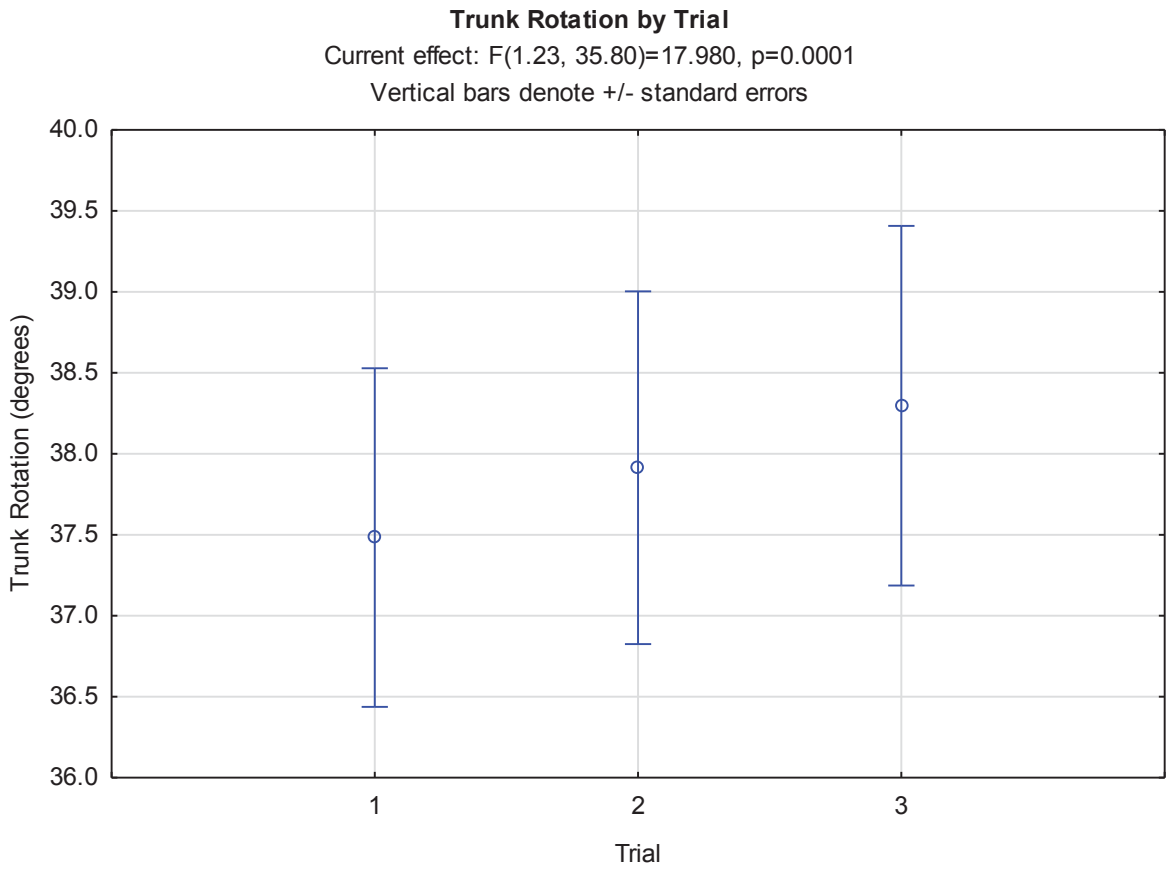

Figure 52: The Effect of Trial on Trunk Rotation Angle

Mauchly's test indicated that the assumption of sphericity had been violated ($\chi^2(2)=27.08$, $p=0.0000$). The degrees of freedom were adjusted using the Greenhouse-Geisser correction. There was a significant difference observed between trials ($n=30$, $F(1.23, 35.80)=17.98$, $p=0.0001$). A Tukey's HSD post-hoc analysis revealed that all three trials were significantly different from each other however the mean difference between trials was small.

Figure 53 shows the effect of Condition x Method on trunk rotation angle.

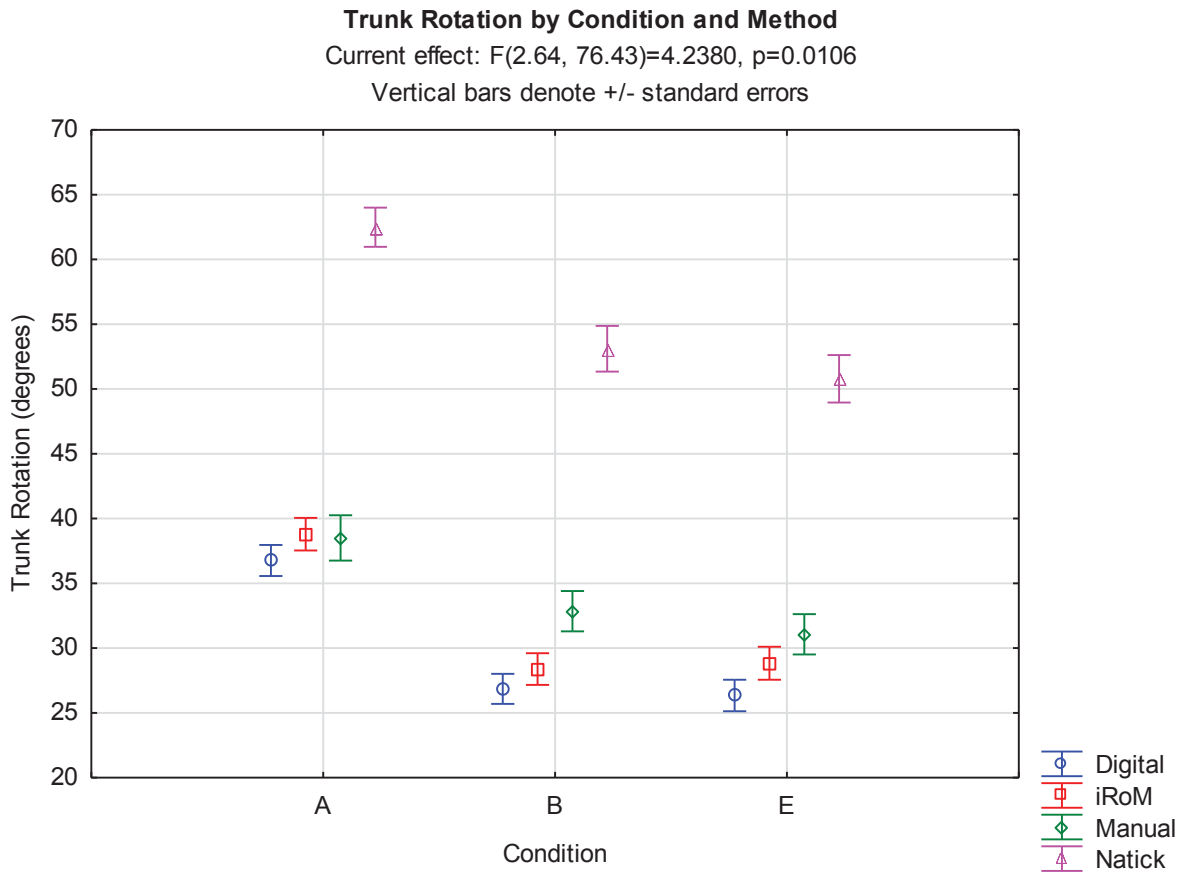

Figure 53: The Effect of Condition x Method on Trunk Rotation Angle

Mauchly's test indicated that the assumption of sphericity had been violated ($\chi^2(20)=118.44$, $p=0.0000$). The degrees of freedom were adjusted using the Greenhouse-Geisser correction. There was a significant difference observed between conditions x methods ($n=30$, $F(2.64, 76.43)=4.24$, $p=0.0106$). A Tukey's HSD post-hoc analysis revealed that for all methods, Condition A was significantly different than Conditions B and E. For all methods, Conditions B and E were not significantly different from one another. All other significant differences can be seen in Annex L: Additional ROM Results.

Figure 54 shows the effect of Iteration x Method on trunk rotation angle.

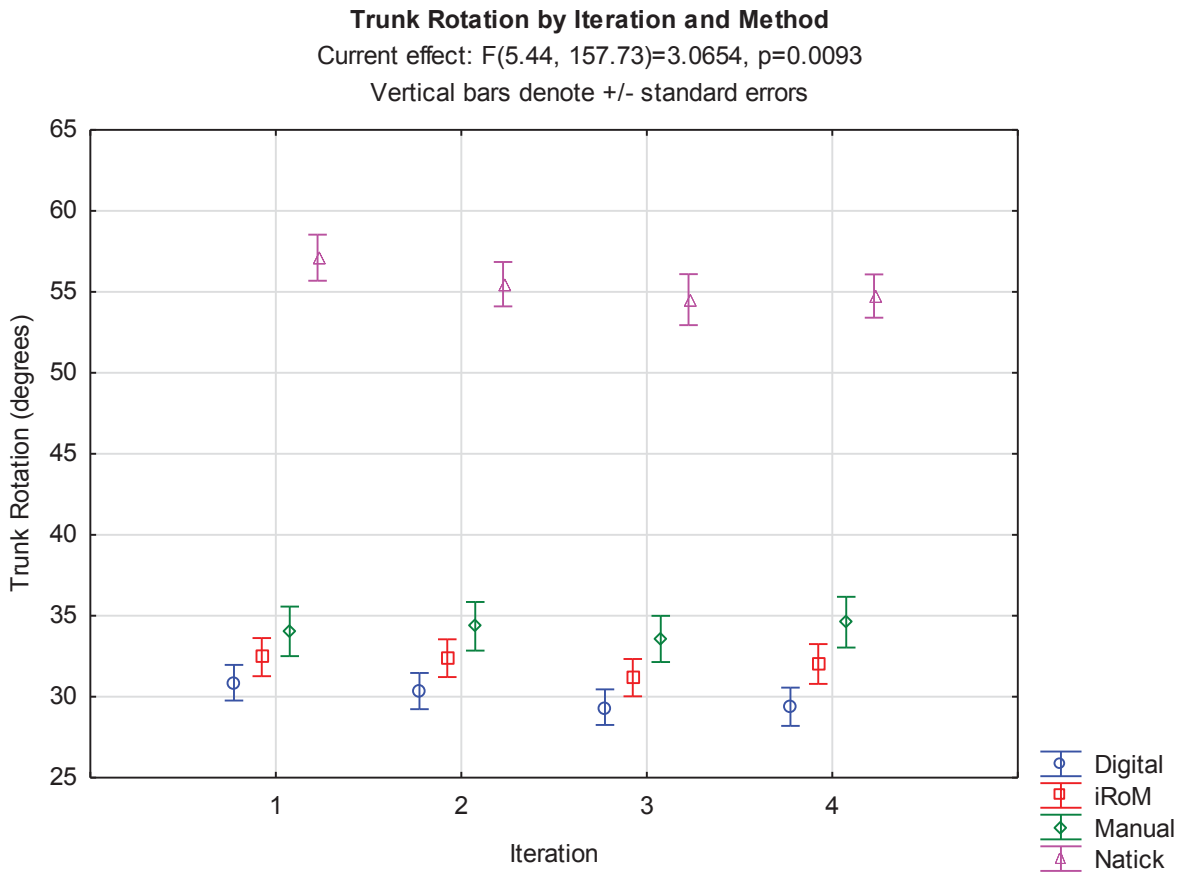

Figure 54: Effect of Iteration x Method on Trunk Rotation Angle

Mauchly's test indicated that the assumption of sphericity had been violated ($\chi^2(44)=112.49$, $p=0.0000$). The degrees of freedom were adjusted using the Greenhouse-Geisser correction. There was a significant difference observed between iterations x methods ($n=30$, $F(5.44, 157.73)=3.07$, $p=0.0093$). A Tukey's HSD post-hoc revealed that Iterations 1, 2, 3, and 4 were not significantly different from each other for Digital, iRoM, and Manual methods. For Natick, Iteration 1 was significantly different than all other iterations; Iterations 2, 3, and 4 were not significantly different from each other. All other significant differences can be seen in Annex L: Additional ROM Results.

Figure 55 shows the effect of condition x direction on trunk rotation angle.

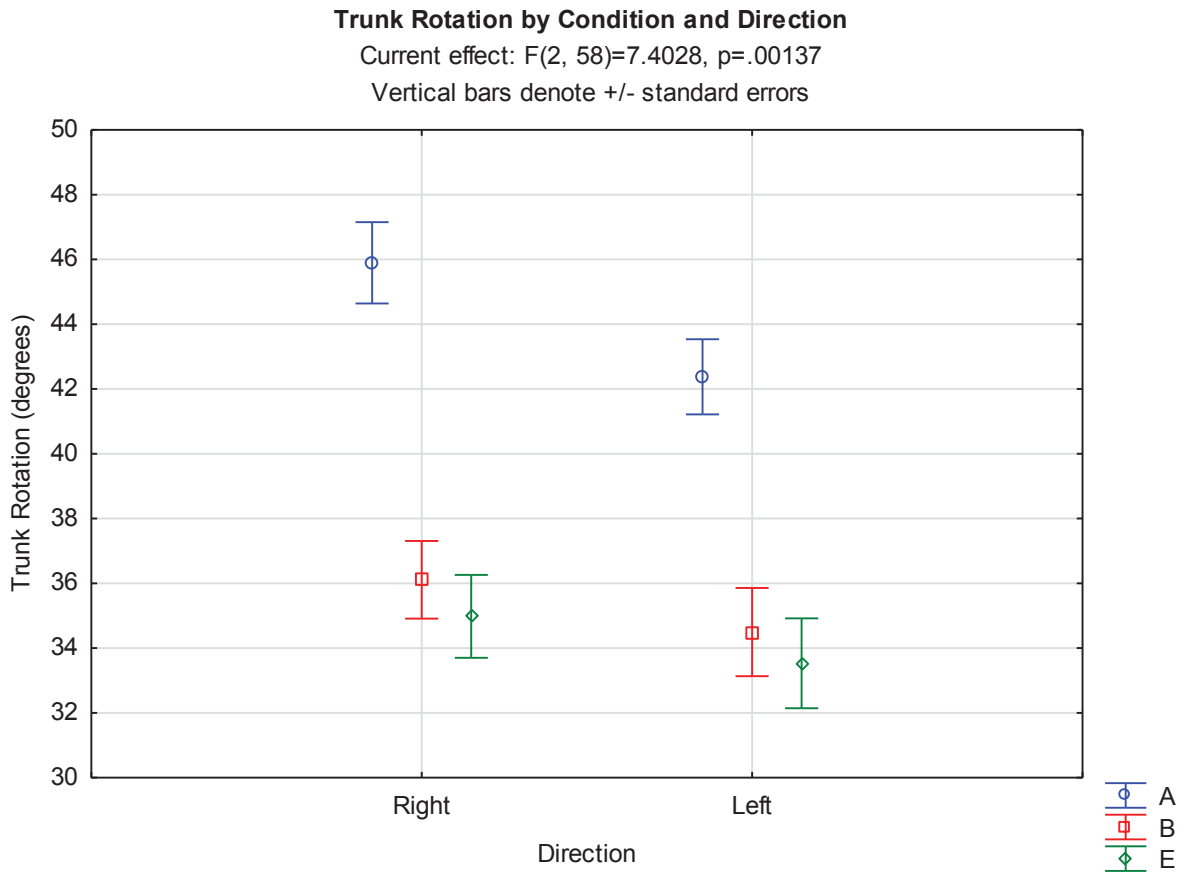

Figure 55: Effect of Condition x Direction on Trunk Rotation Angle

There was a significant difference observed between conditions x directions (n=30, F(2,58)=7.40, p=0.0014). A Tukey's HSD post-hoc analysis revealed that right and left trunk rotations were significantly different for each of Conditions A, B, and E. All other significant differences can be seen in Annex L: Additional ROM Results.

Figure 56 shows the effect of Method x Trial on trunk rotation angle.

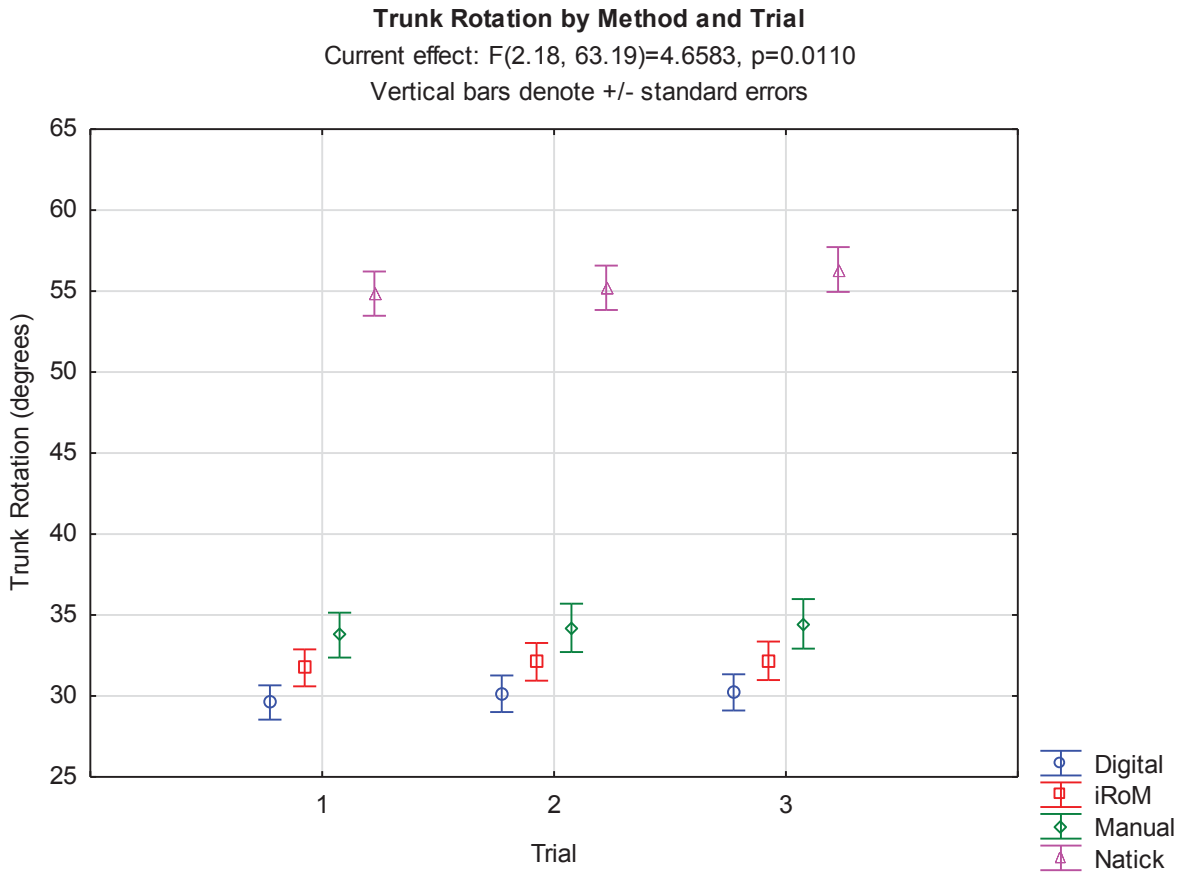

Figure 56: Effect of Method x Trial on Trunk Rotation Angle.

Mauchly's test indicated that the assumption of sphericity had been violated ($\chi^2(20)=123.65$, $p=0.0000$). The degrees of freedom were adjusted using the Greenhouse-Geisser correction. There was a significant difference observed between methods x trials ($n=30$, $F(2.18, 63.19)=4.66$, $p=0.0110$). A Tukey's HSD post-hoc analysis revealed that for Digital, Manual, and Natick methods Trial 1 was significantly different than Trial 3 but not significantly different than Trial 2. For iRoM, none of the trials were significantly different than the other. All other significant differences can be seen in Annex L: Additional ROM Results.

Figure 57 shows the effect of Direction x Trial on trunk rotation angle.

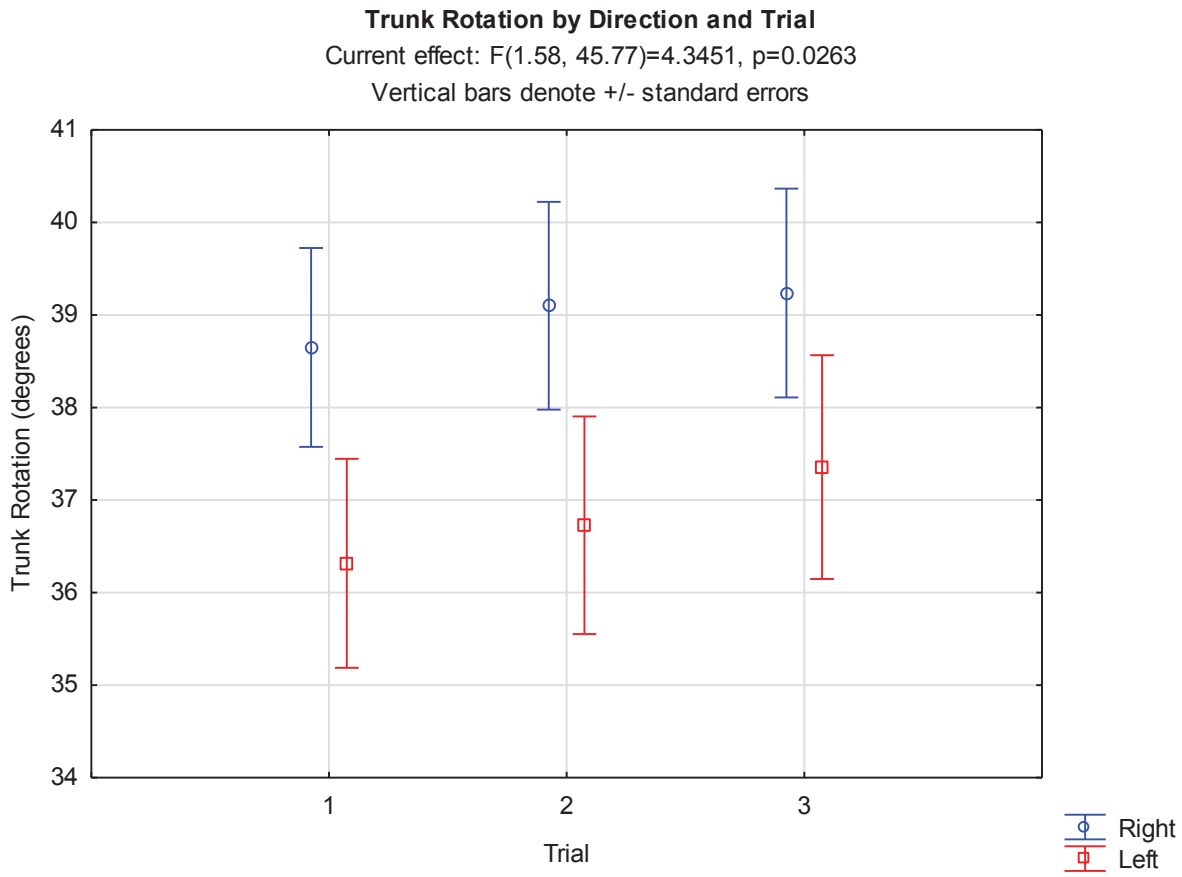

Figure 57: Effect of Direction x Trial on Trunk Rotation Angle

Mauchly's test indicated that the assumption of sphericity had been violated ($\chi^2(2)=10.89$, $p=0.0043$). The degrees of freedom were adjusted using the Huynh-Feldt correction. There was a significant difference observed between directions x trials ($n=30$, $F(1.58, 45.77)=4.35$, $p=0.0263$). A Tukey's HSD post-hoc analysis revealed that most direction-trial pairwise comparisons are significant except for Trial 3 Right side-Trial 2 right side. All other significant differences can be seen in Annex L: Additional ROM Results.

Figure 58 shows the effect of Condition x Method x Direction on trunk rotation angle.

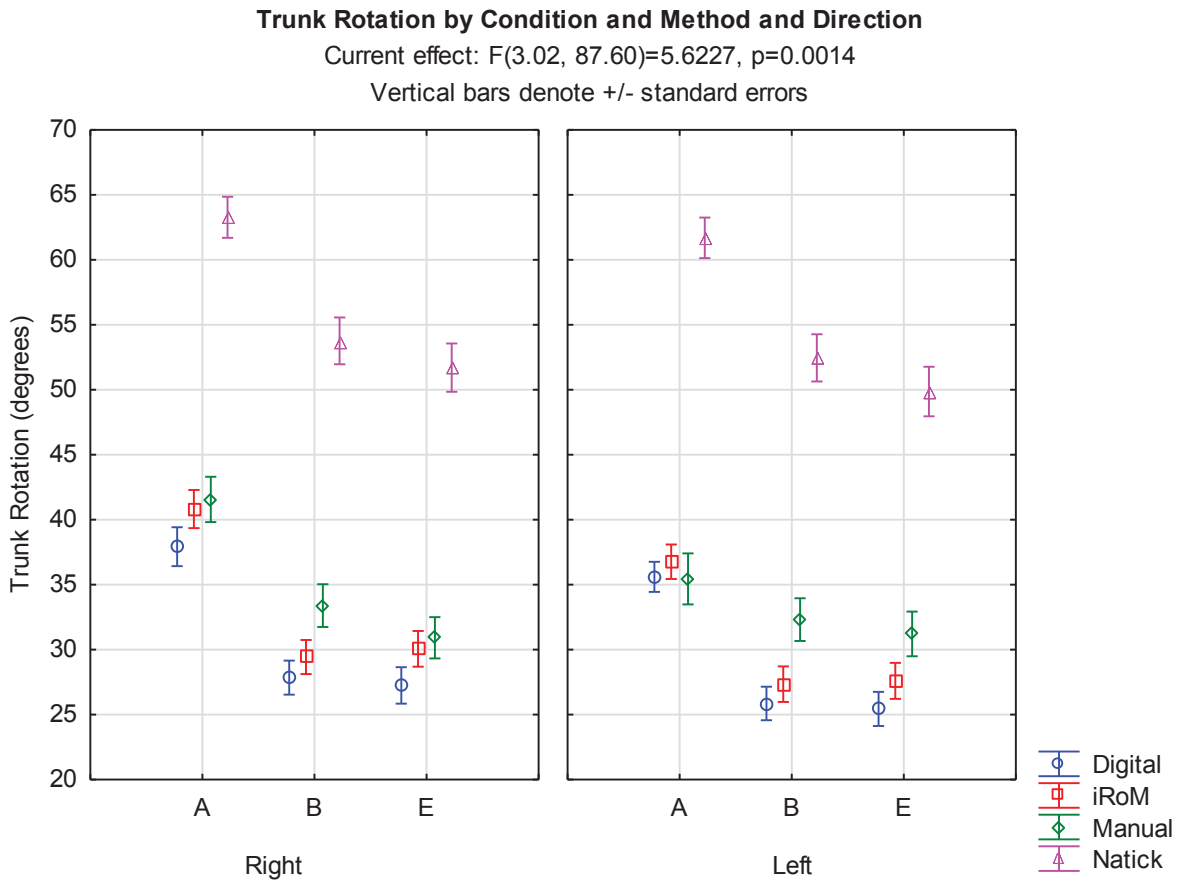

Figure 58: Effect of Condition x Method x Direction on Trunk Rotation Angle

Mauchly's test indicated that the assumption of sphericity had been violated ($\chi^2(20)=89.81$, p=0.0000). The degrees of freedom were adjusted using the Greenhouse-Geisser correction. There was a significant difference observed between condition x method x direction (n=30, F(3.02, 87.60)=5.62, p=0.0014). A Tukey's HSD post-hoc analysis revealed significant differences between many of the condition x method x direction effects. All significant differences can be seen in Annex L: Additional ROM Results.

3.4.1.2 *Lateral Bending*

Digital, iRoM, and Manual methods were analyzed separately from the Natick method for this portion of the results due to differences in measurement units.

3.4.1.2.1 Digital, iRoM, and Manual Methods

A repeated-measures ANOVA was carried out on the lateral bending measurements for all Digital, iRoM, and Manual methods. Table 45 summarizes the significant effects that were identified in this analysis.

Table 45: Summary of Repeated Measures ANOVA Results for Lateral Bending (Digital, iRoM, and Manual Methods)

Effect	Significance	P-value
Condition	Significant	0.0000
Iteration	Not significant	0.04907[5]
Method	Significant	0.0000[4]
Direction	Not significant	0.1265
Trial	Significant	0.0000[4]
Condition x Iteration	Not significant	0.7227[4]
Condition x Method	Significant	0.0000[4]
Iteration x Method	Not significant	0.7468[5]
Condition x Direction	Significant	0.0061[5]
Iteration x Direction	Not significant	0.2877
Method x Direction	Not significant	0.2862[4]
Condition x Trial	Not significant	0.8593[4]
Iteration x Trial	Not significant	0.5729[4]
Method x Trial	Significant	0.0040[4]
Direction x Trial	Not significant	0.8777[5]
Condition x Iteration x Method	Not significant	0.7971[4]
Condition x Iteration x Direction	Not significant	0.8057
Condition x Method x Direction	Not significant	0.3384[4]
Iteration x Method x Direction	Not significant	0.5755[4]
Condition x Iteration x Trial	Not significant	0.5049[4]
Condition x Method x Trial	Not significant	0.5222[4]
Iteration x Method x Trial	Not significant	0.3877[4]
Condition x Direction x Trial	Not significant	0.7430
Iteration x Direction x Trial	Not significant	0.6313
Method x Direction x Trial	Not significant	0.8967[4]
Condition x Iteration x Method x Direction	Not significant	0.3677
Condition x Iteration x Method x Trial	Not significant	0.4793[4]
Condition x Iteration x Direction x Trial	Not significant	0.3224[4]
Condition x Method x Direction x Trial	Not significant	0.4598[4]
Iteration x Method x Direction x Trial	Not significant	0.2174[4]
Condition x Iteration x Method x Direction x Trial	Not significant	0.2124[4]

[4] Adjusted using the Greenhouse-Geisser (1959) correction.
[5] Adjusted using the Huynh-Feldt (1976) correction.

Figure 59 shows the effect of condition on lateral bending angles.

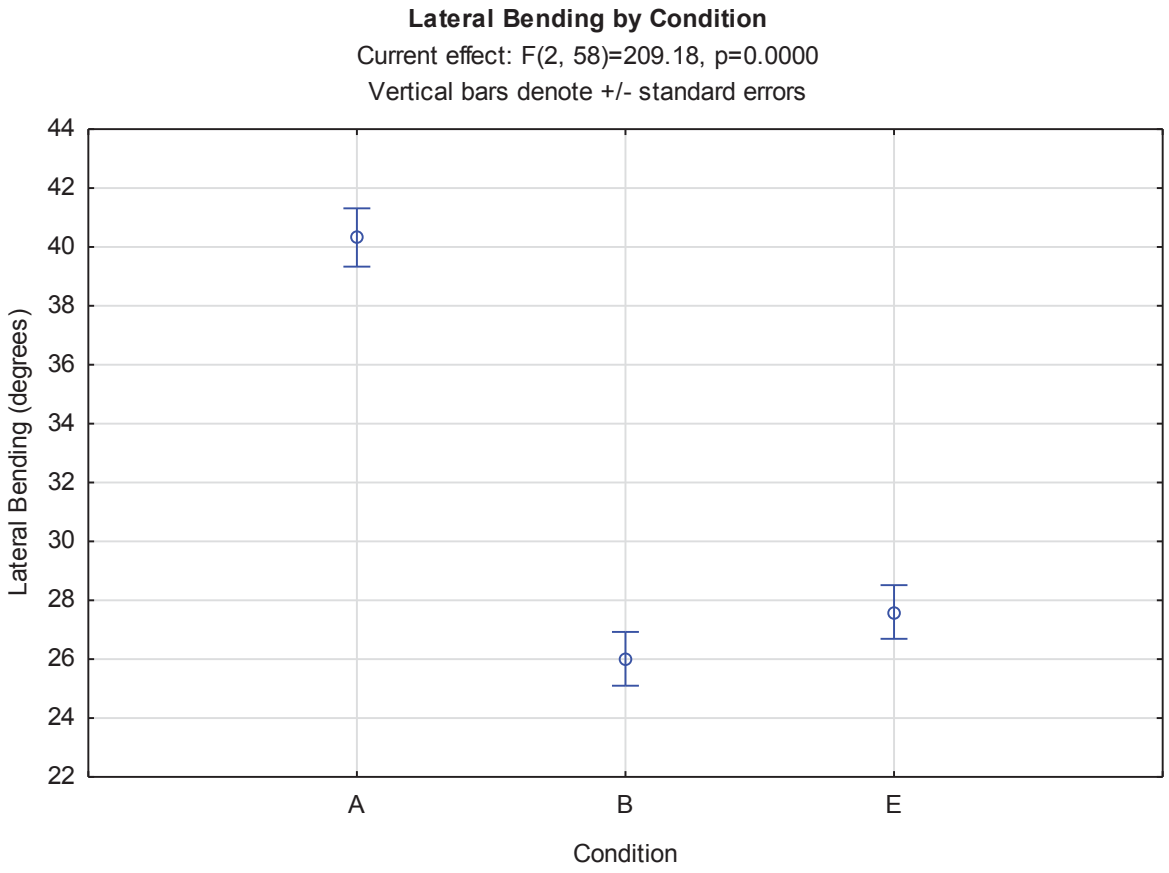

Figure 59: Effect of Condition on Lateral Bending Angle for Digital, iRoM, and Manual Methods

There was a significant difference observed between conditions (n=30, F(2, 58)=209.19, p=0.0000). A Tukey's HSD post-hoc analysis revealed that Condition A was significantly different than Conditions B and E, but Conditions B and E were not significantly different from each other.

Figure 60 shows the effect of method on lateral bending angles.

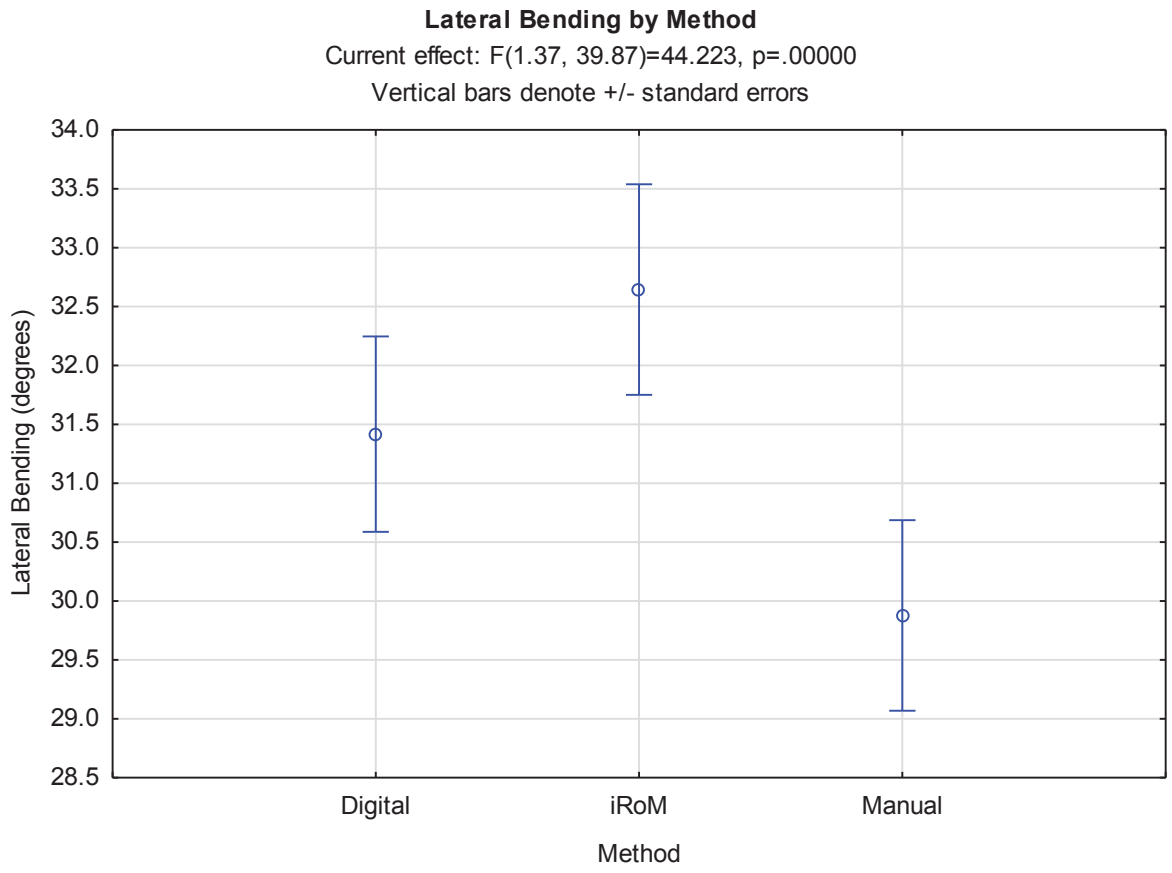

Figure 60: Effect of Method on Lateral Bending Angles for the Digital, iRoM, and Manual Methods

Mauchly's test indicated that the assumption of sphericity had been violated ($\chi^2(2)=16.98$, $p=0.0002$). The degrees of freedom were adjusted using the Greenhouse-Geisser correction. There was a significant difference observed between methods ($n=30$, $F(1.37, 39.87)=44.22$, $p=0.0000$). A Tukey's HSD post-hoc analysis revealed that all methods (digital, iRoM, manual) were significantly different from each other.

Figure 61 shows the effect of trial on lateral bending angle.

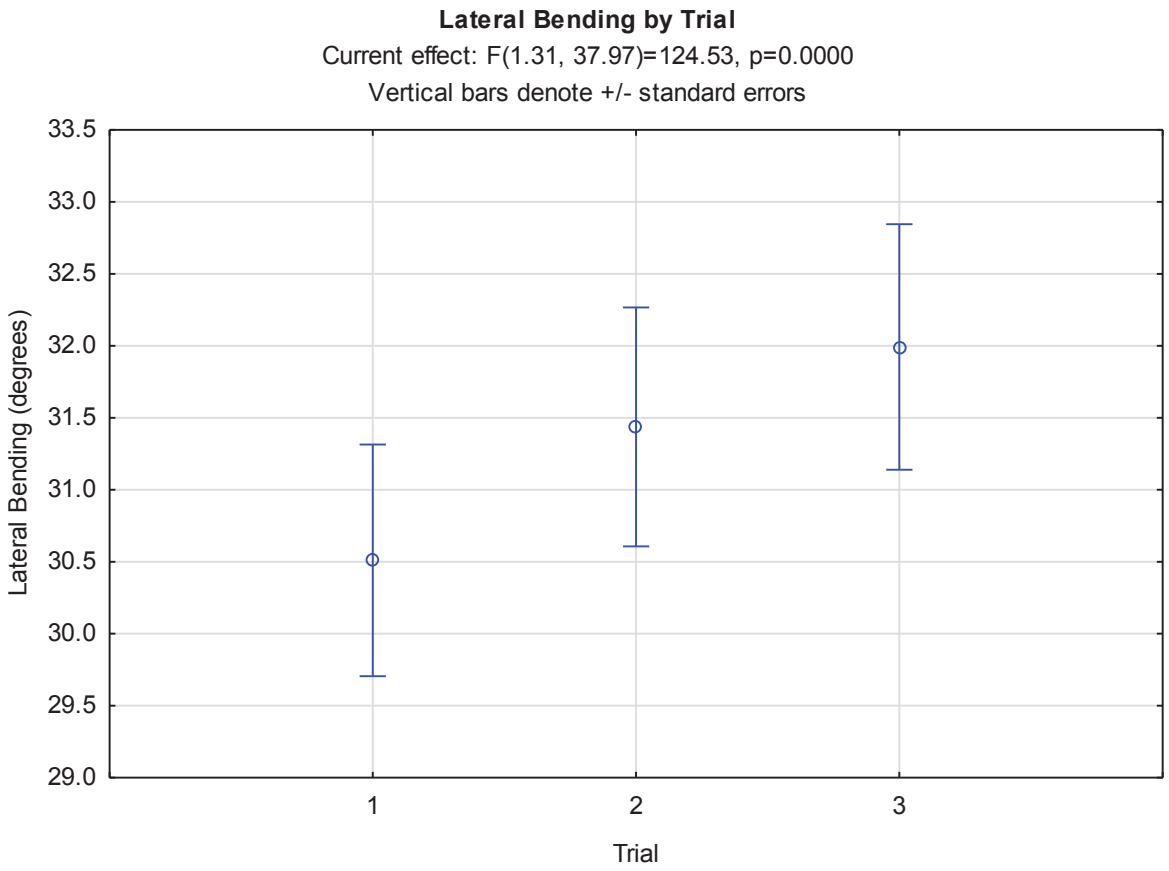

Figure 61: Effect of Trial on Lateral Bending for Digital, iRoM, and Manual Methods

Mauchly's test indicated that the assumption of sphericity had been violated ($\chi^2(2)=21.00$, $p=0.0000$). The degrees of freedom were adjusted using the Greenhouse-Geisser correction. There was a significant difference observed between trials ($n=30$, $F(1.31, 37.97)=124.53$, $p=0.0000$) however the mean difference between trials is very small. A Tukey's HSD post-hoc analysis revealed that all trials were significantly different from each other.

Figure 61 shows the effect of condition x method on lateral bending angle.

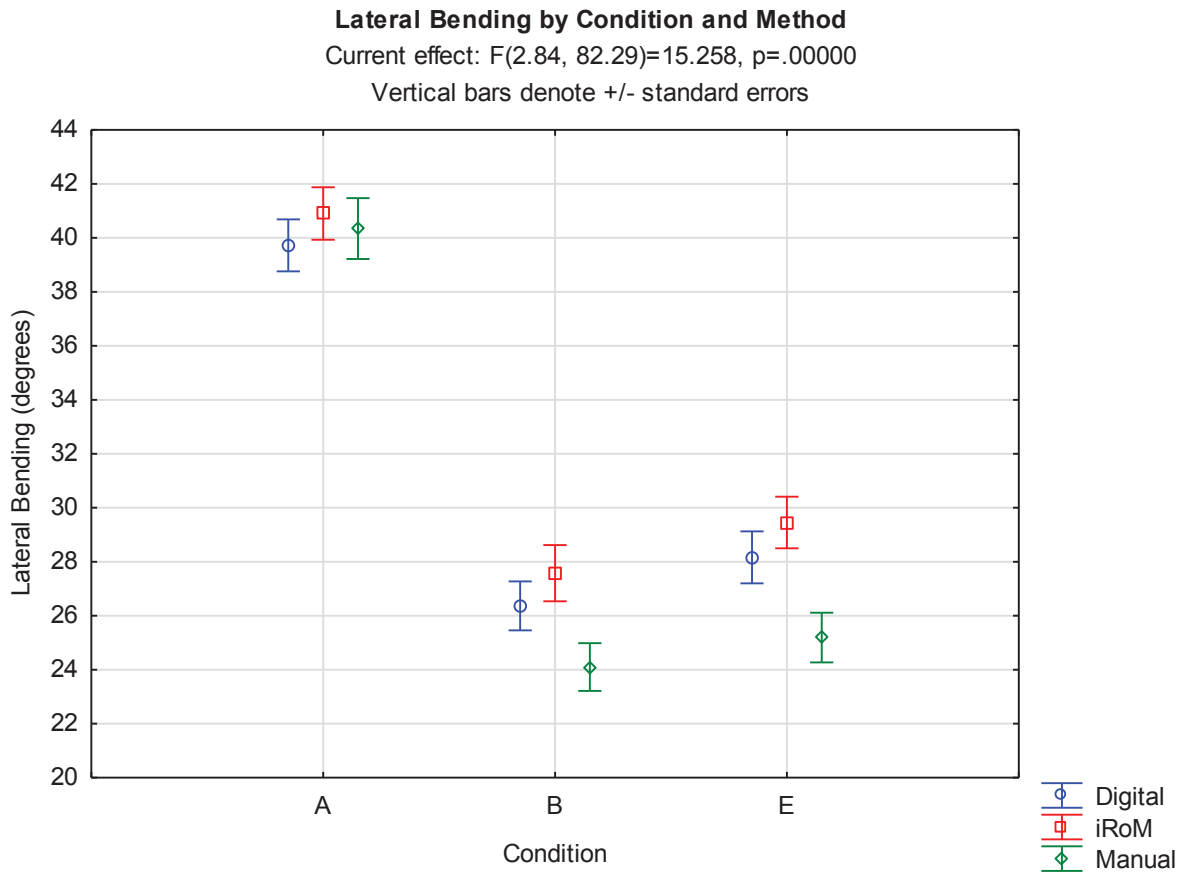

Figure 62: Effect of Condition x Method on Lateral Bending for Digital, iRoM and Manual Methods

Mauchly's test indicated that the assumption of sphericity had been violated ($\chi^2(9)=26.95$, $p=0.0014$). The degrees of freedom were adjusted using the Greenhouse-Geisser correction. There was a significant difference observed between condition x method ($n=30$, $F(2.84, 82.29)=15.26$, $p=0.0000$). A Tukey's HSD post-hoc analysis revealed that for Digital and iRoM methods, all conditions were significantly different than each other. For Manual methods, Condition A was significantly different than all other conditions, but Conditions B and E were not significantly different than each other. All other significant differences can be seen in Annex L: Additional ROM Results.

Figure 63 shows the effect of condition x direction on lateral bending angle.

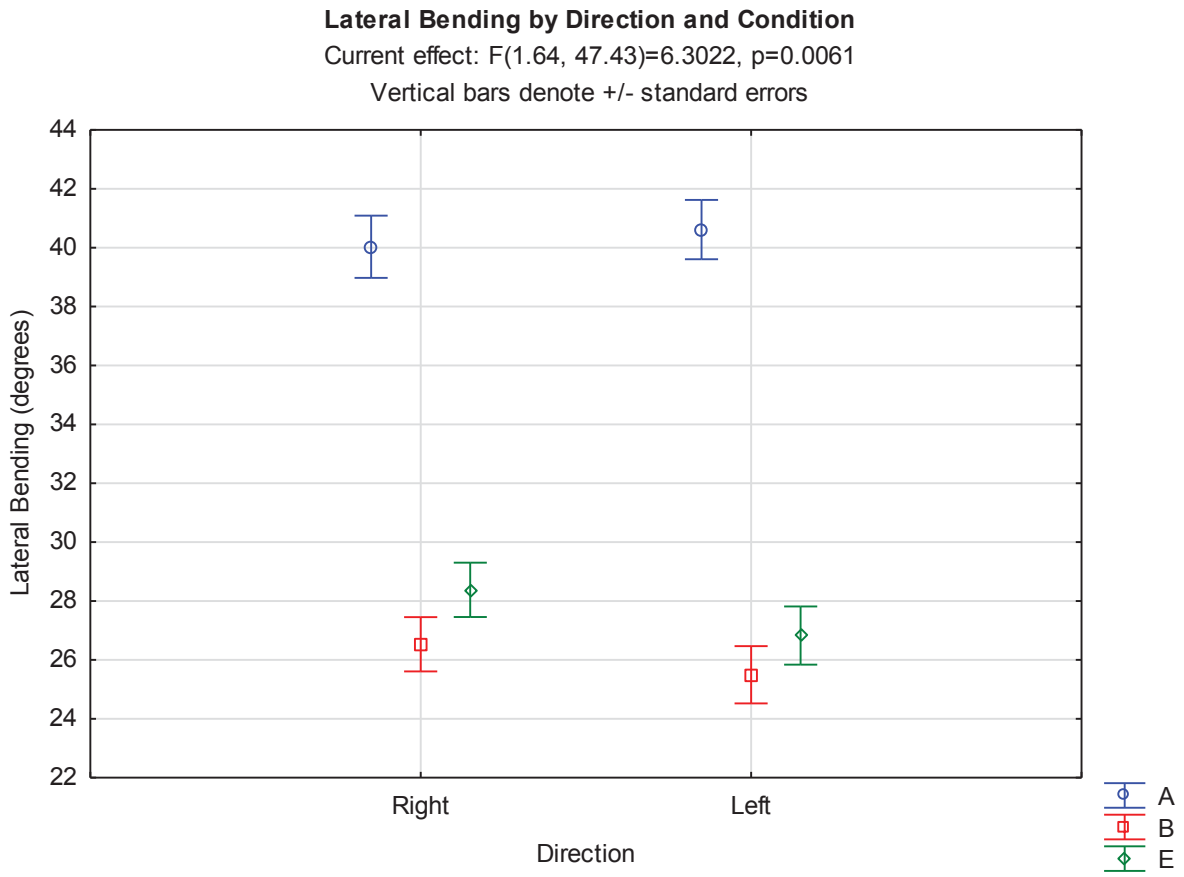

Figure 63: Effect of Condition x Direction on Lateral Bending for Digital, iRoM, and Manual Methods

Mauchly's test indicated that the assumption of sphericity had been violated ($\chi^2(2)=9.20$, $p=0.0101$). The degrees of freedom were adjusted using the Huynh-Feldt correction. There was a significant difference observed between condition x direction ($n=30$, $F(1.64, 47.43)=6.30$, $p=0.0061$). A Tukey's HSD post-hoc analysis revealed that in Conditions A and B there was no significant difference between right and left lateral bends but in Condition E there was a significant difference between right and left lateral bends. All other significant differences can be seen in Annex L: Additional ROM Results.

Figure 64 shows the effect of Method x Trial on lateral bending angle.

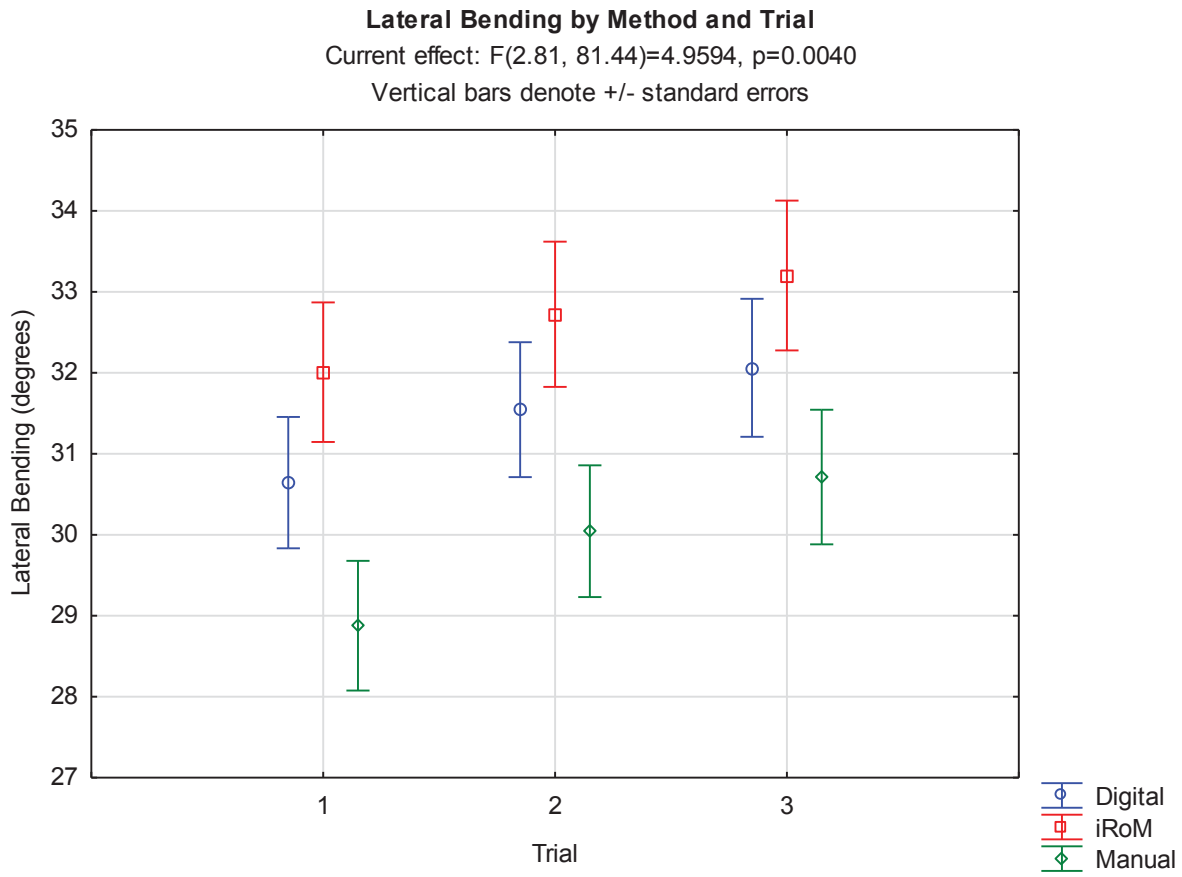

Figure 64: Effect of Method x Trial on Lateral Bending for Digital, iRoM, and Manual Methods

Mauchly's test indicated that the assumption of sphericity had been violated ($\chi^2(9)=30.53$, $p=0.0004$). The degrees of freedom were adjusted using the Greenhouse-Geisser correction. There was a significant difference observed between method x trial ($n=30$, $F(2.81, 81.44)=4.96$, $p=0.0040$). A Tukey's HSD post-hoc analysis revealed that all trials were significantly different from each other for each of the Digital, iRoM, and Manual methods. All other significant differences can be seen in Annex L: Additional ROM Results.

3.4.1.2.2 Natick Method

A repeated-measures ANOVA was carried out on the lateral bending measurements for the Natick method. Table 46 summarizes the significant effects identified.

Table 46: Summary of Repeated Measures ANOVA Results for Lateral Bending (Natick)

Effect	Significance	P-value
Condition	Significant	0.0001
Iteration	Significant	0.0000
Direction	Significant	0.0493
Trial	Significant	0.0000[6]
Condition x Iteration	Not significant	0.5964[6]
Condition x Direction	Significant	0.0095[6]
Iteration x Direction	Not significant	0.0679
Condition x Trial	Not significant	0.5999[6]
Iteration x Trial	Not significant	0.1096[6]
Direction x Trial	Significant	0.0011[7]
Condition x Iteration x Direction	Not significant	0.1306
Condition x Iteration x Trial	Not significant	0.0613[6]
Condition x Direction x Trial	Not significant	0.7258
Iteration x Direction x Trial	Not significant	0.4513
Condition x Iteration x Direction x Trial	Not significant	0.7204

[6] Adjusted using the Greenhouse-Geisser (1959) correction.
[7] Adjusted using the Huynh-Feldt (1976) correction.

Figure 65 shows the effect of condition on lateral bending distance.

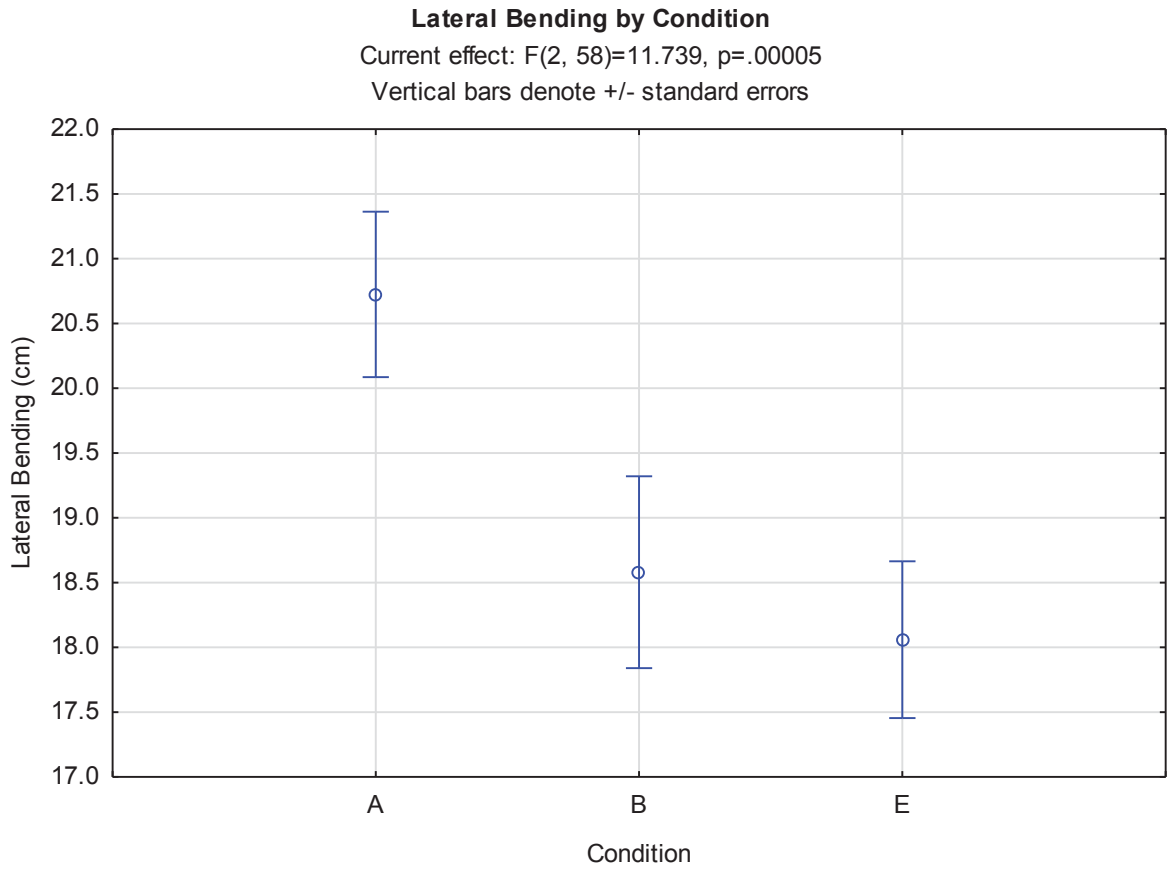

Figure 65: Effect of Condition on Lateral Bending Distance for Natick Method

There was a significant difference observed between conditions (n=30, F(2, 58)=11.74, p=0.0001). A Tukey's HSD post-hoc analysis revealed that Condition A was significantly different than all other conditions, but Condition B and E were not significantly different from each other.

Figure 66 shows the effect of iteration on lateral bending distance.

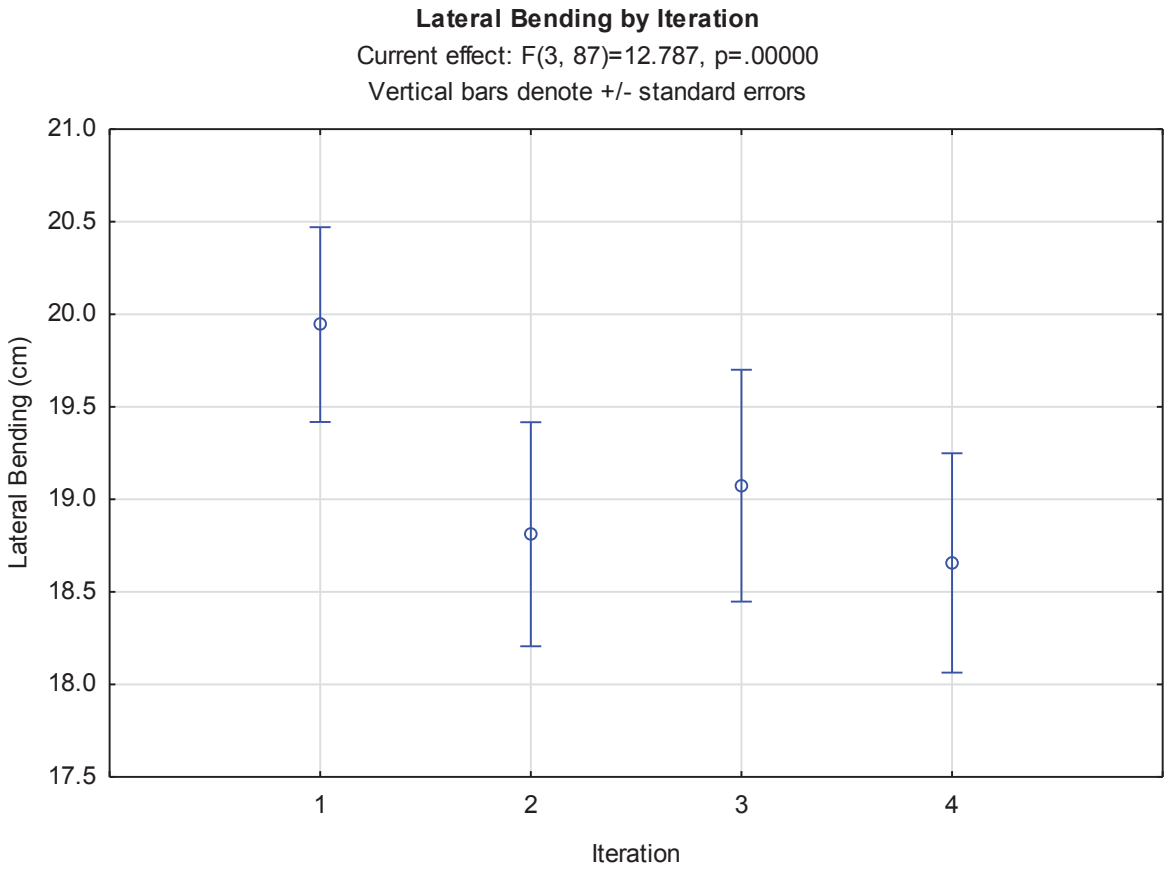

Figure 66: Effect of Iteration on Lateral Bending Distance for Natick Method

There was a significant difference observed between condition (n=30, F(3, 87)=12.79, p=0.0000). A Tukey's HSD post-hoc analysis revealed that Iteration 1 was significantly different than all other iterations, but Iterations 2, 3, and 4 were not significantly different than each other.

Figure 67 shows the effect of direction on lateral bending distance.

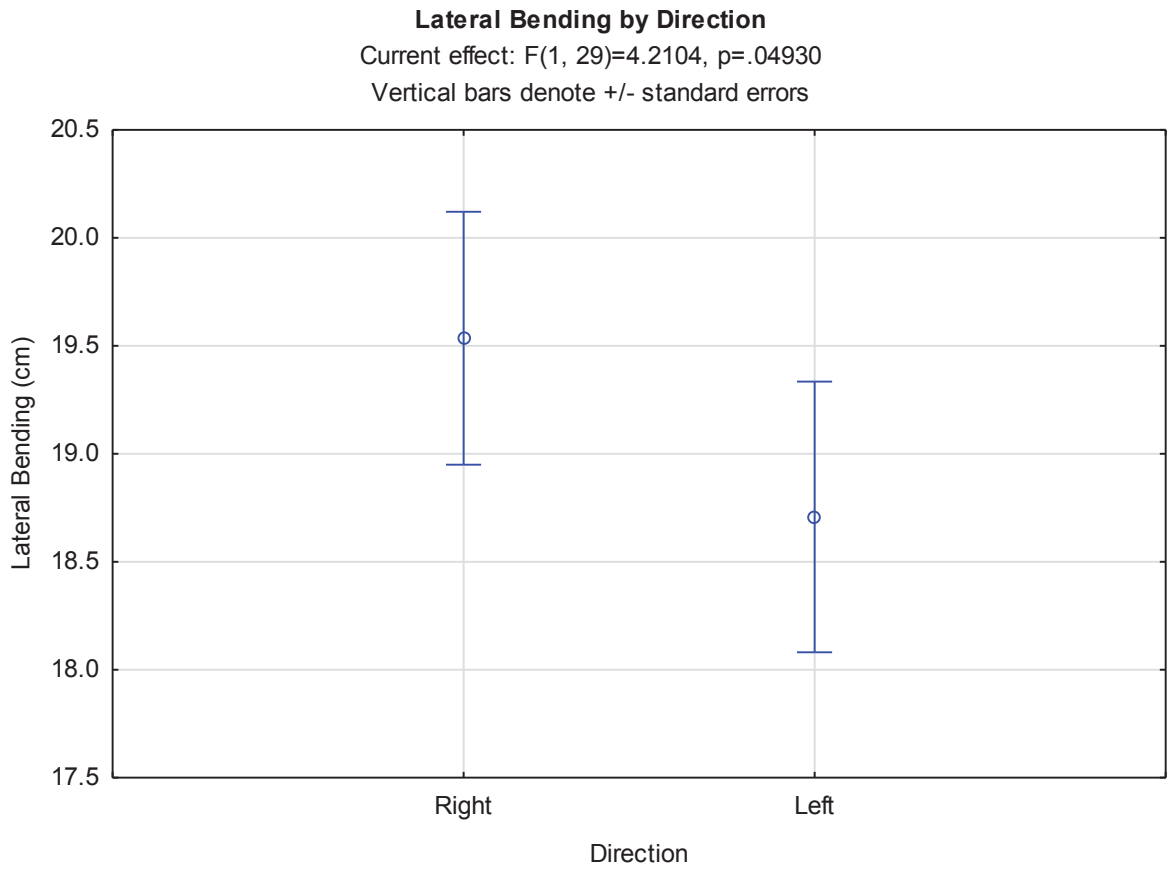

Figure 67: Effect of Direction on Lateral Bending Distance for Natick Method

There was a significant difference observed between right and left directions (n=30, F(1, 29)=4.21, p=0.0493) however the mean difference between directions is small.

Figure 68 shows the effect of trial on lateral bending distance.

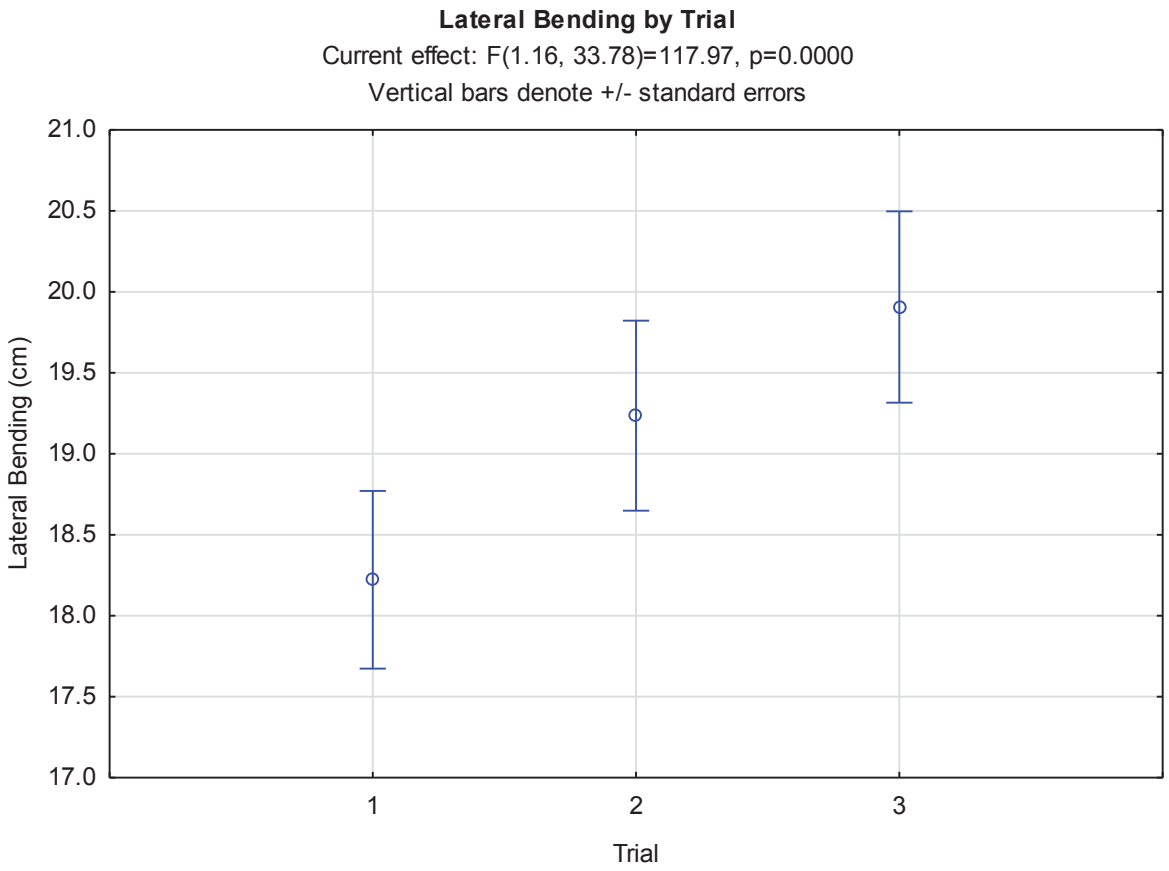

Figure 68: Effect of Trial on Lateral Bending for Natick Method

Mauchly's test indicated that the assumption of sphericity had been violated ($\chi^2(2)=35.35$, $p=0.0000$). The degrees of freedom were adjusted using the Greenhouse-Geisser correction. There was a significant difference observed between trials ($n=30$, $F(1.16, 33.78)=117.97$, $p=0.0000$). A Tukey's HSD post-hoc analysis revealed that all trials were significantly different from one another.

Figure 69 shows the effect of condition x direction on lateral bending distance.

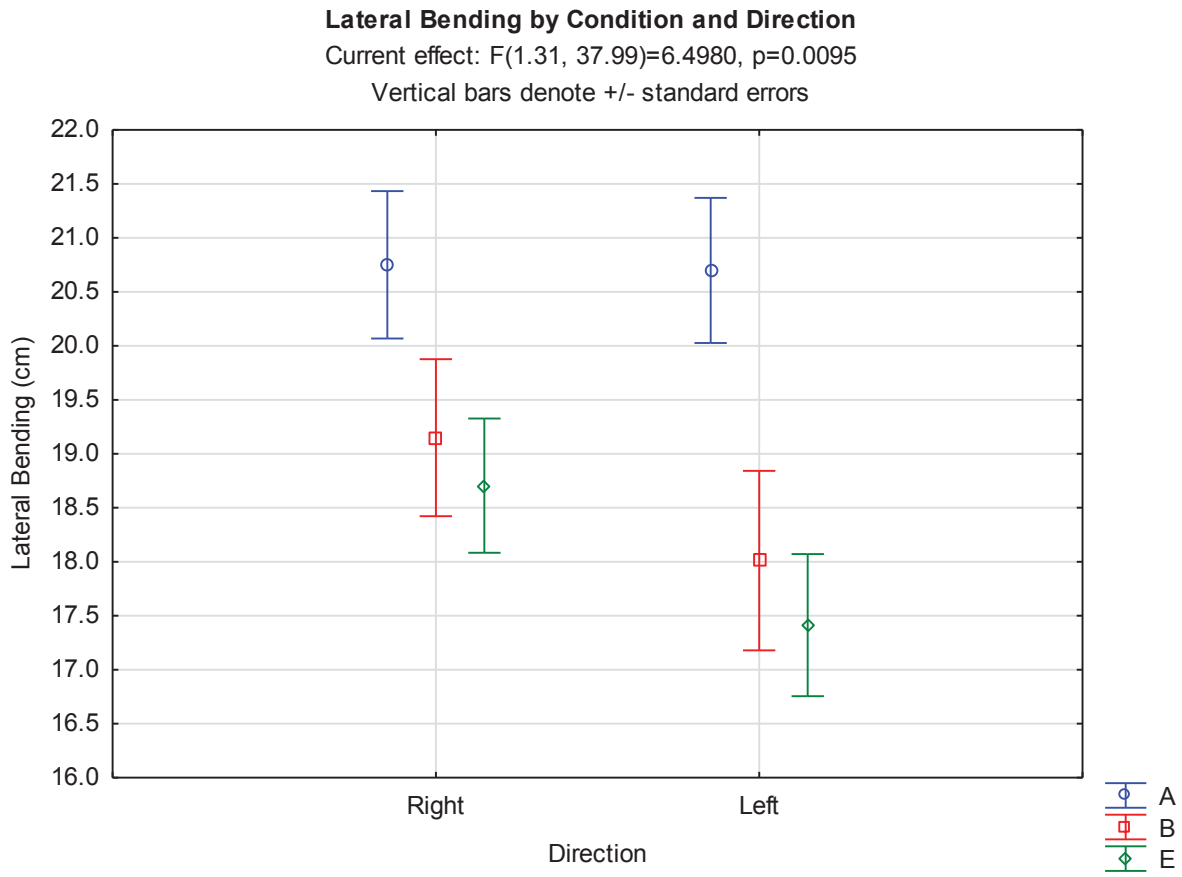

Figure 69: Effect of Condition x Direction on Lateral Bending for Natick Method

Mauchly's test indicated that the assumption of sphericity had been violated ($\chi^2(2)=20.94$, $p=0.0000$). The degrees of freedom were adjusted using the Greenhouse-Geisser correction. There was a significant difference observed between condition x direction ($n=30$, $F(1.31, 37.99)=6.50$, $p=0.0095$). A Tukey's HSD post-hoc analysis revealed that in Conditions B and E, right and left lateral bends were significantly different. In Condition A, right and left lateral bends were not significantly different. All other significant differences can be seen in Annex L: Additional ROM Results.

Figure 70 shows the effect of direction x trial on lateral bending distance.

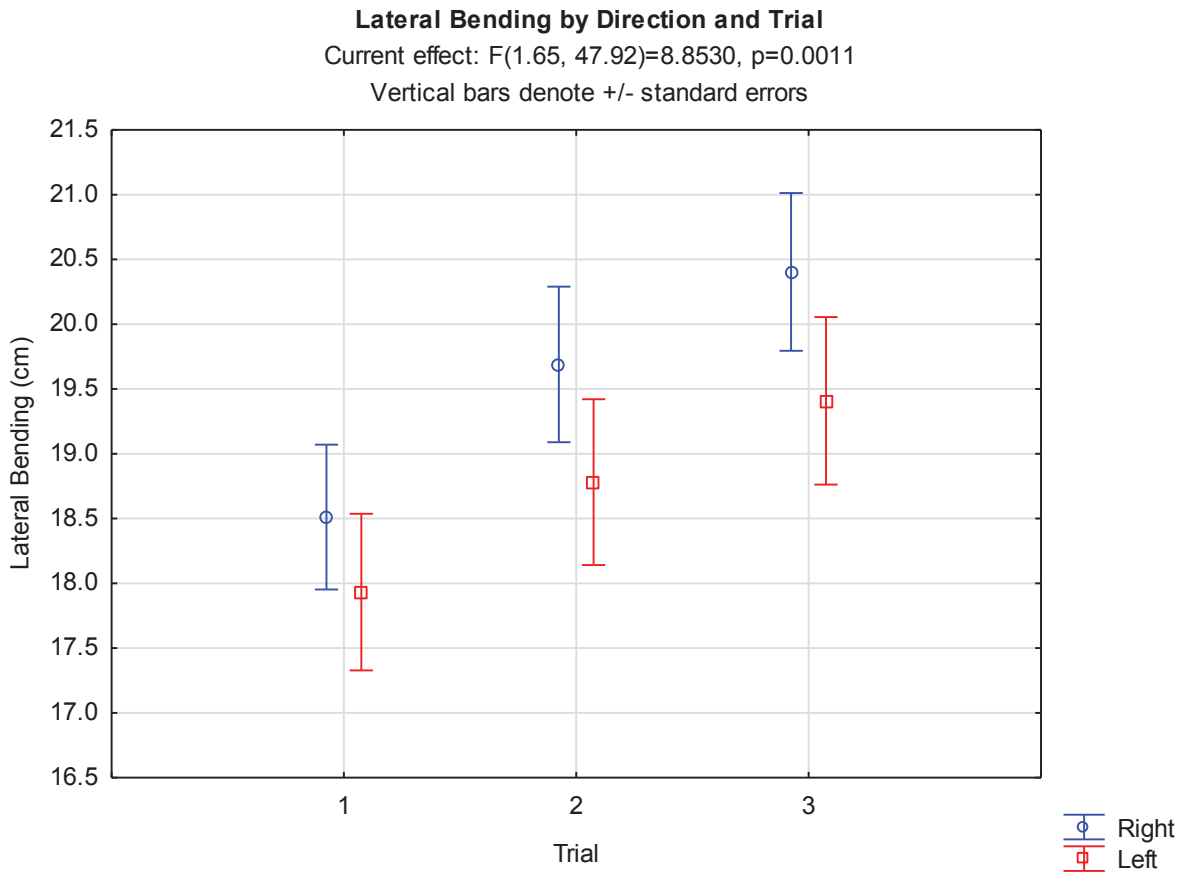

Figure 70: Effect of Direction x Trial on Lateral Bending for Natick Method

Mauchly's test indicated that the assumption of sphericity had been violated ($\chi^2(2)=8.74$, $p=0.0126$). The degrees of freedom were adjusted using the Huynh-Feldt correction. There was a significant difference observed between direction x trial ($n=30$, $F(1.65, 47.92)=8.85$, $p=0.0011$). A Tukey's HSD post-hoc analysis revealed that all trials for the right side were significantly different than each other and all the trials for the left side were significantly different from each other. All other significant differences can be seen in Annex L: Additional ROM Results.

3.4.1.3 *Front Forward Flexion*

Digital and iRoM methods were analyzed separately from the Manual and Natick methods for this portion of the results due to differences in measurement units.

3.4.1.3.1 Digital and iRoM Method

A repeated-measures ANOVA was carried out on the front forward flexion measurements for the digital and iRoM methods. Table 47 summarizes the significant effects identified.

Table 47: Summary of Repeated Measures ANOVA Results for Front Forward Flexion (Digital and iRoM Methods)

Effect	Significance	P-value
Condition	Significant	0.0018[8]
Iteration	Significant	0.0028
Method	Significant	0.0060
Trial	Significant	0.0000[8]
Condition x Iteration	Not significant	0.3100[9]
Condition x Method	Significant	0.0022[9]
Iteration x Method	Not significant	0.3066[9]
Condition x Trial	Not significant	0.2413[9]
Iteration x Trial	Not significant	0.7532[9]
Method x Trial	Not significant	0.1365
Condition x Iteration x Method	Not significant	0.4677[9]
Condition x Iteration x Trial	Not significant	0.1414
Condition x Method x Trial	Not significant	0.6999[9]
Iteration x Method x Trial	Not significant	0.3217
Condition x Iteration x Method x Trial	Not significant	0.9573[9]

[8] Adjusted using the Huynh-Feldt (1976) correction.
[9] Adjusted using the Greenhouse-Geisser (1959) correction.

Figure 71 shows the effect of condition on front forward flexion.

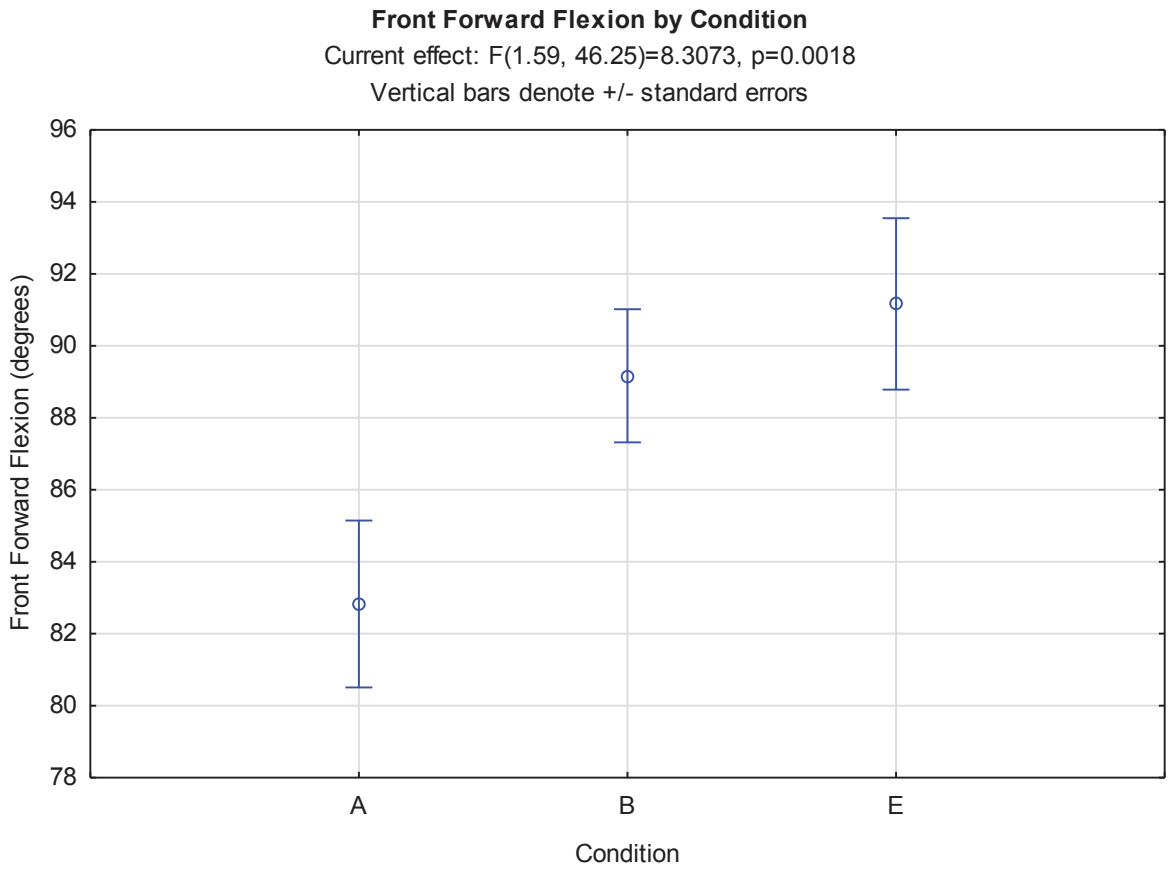

Figure 71: Effect of Condition on Front Forward Flexion for Digital and iRoM Methods

Mauchly's test indicated that the assumption of sphericity had been violated ($\chi^2(2)=10.38$, $p=0.0056$). The degrees of freedom were adjusted using the Huynh-Feldt correction. There was a significant difference observed between conditions ($n=30$, $F(1.59, 46.25)=8.31$, $p=0.0018$). A Tukey's HSD post-hoc analysis revealed that Condition A was significantly different from all other conditions but Conditions B and E were not significantly different than each other.

Figure 72 shows the effect of iteration on front forward flexion.

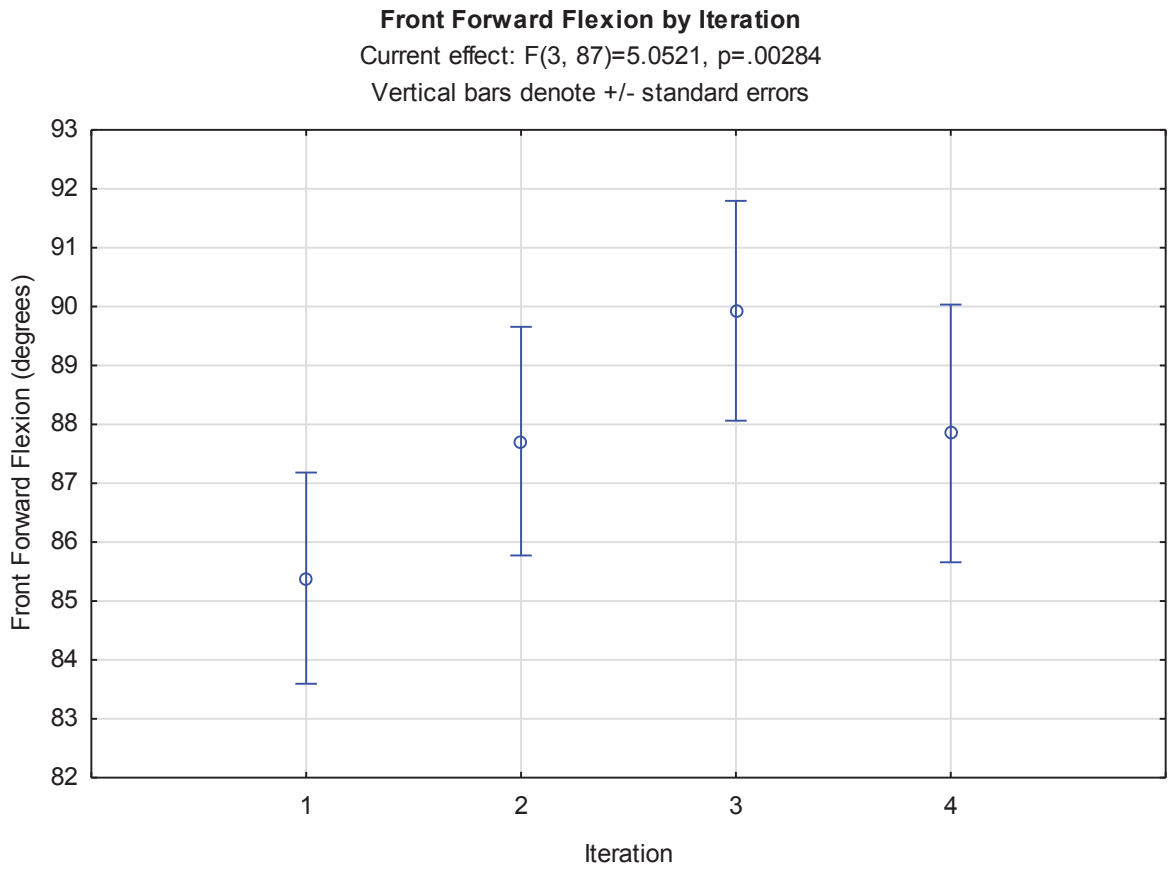

Figure 72: Effect of Iteration on Front Forward Flexion for Digital and iRoM Methods

There was a significant difference observed between iterations (n=30, F(3, 87)=5.05, p=0.0028). A Tukey's HSD post-hoc analysis revealed that Iteration 1 was significantly different than Iteration 3. There were no other significant differences.

Figure 73 shows the effect of method on front forward flexion.

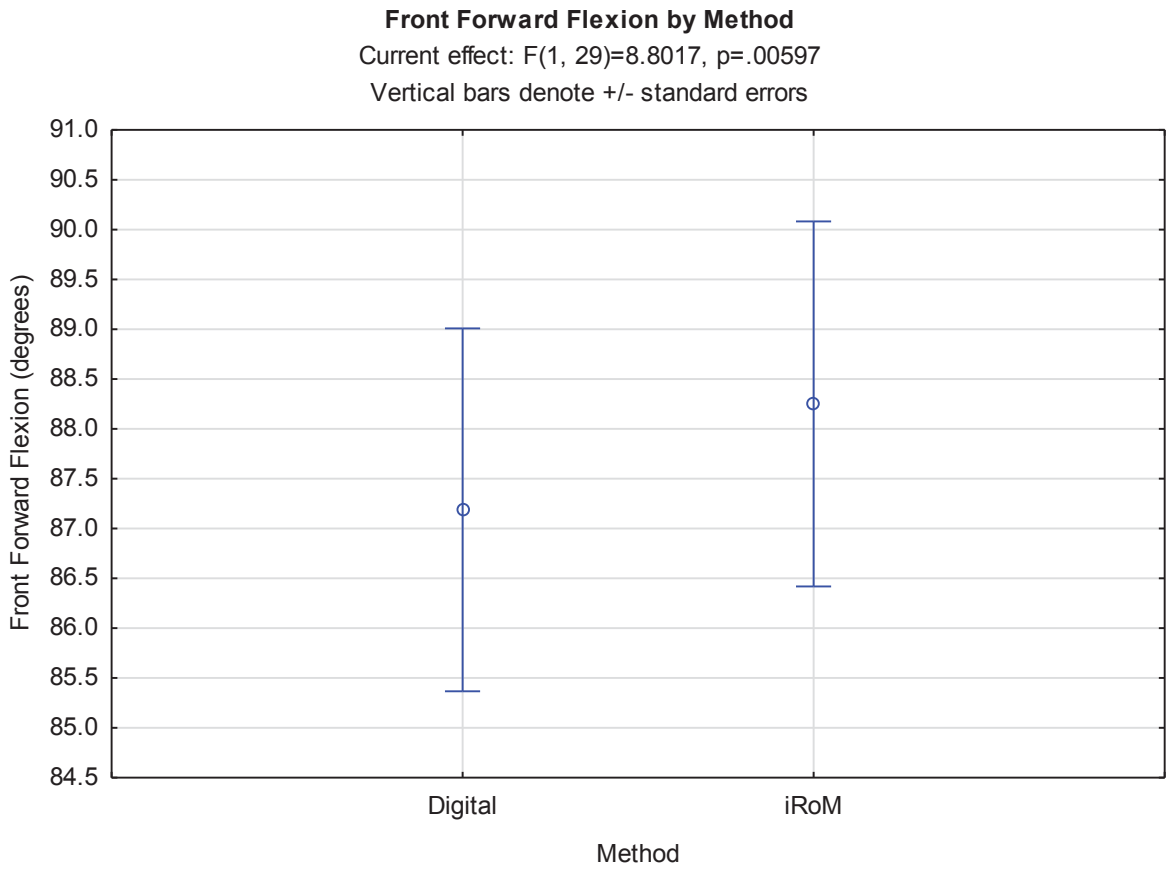

Figure 73: Effect of Method on Front Forward Flexion

There was a significant difference observed between the digital and iRoM methods (n=30, F(1, 29)=8.80, p=0.0060) however the mean differences between methods is very small.

Figure 74 shows the effect of trial on front forward flexion.

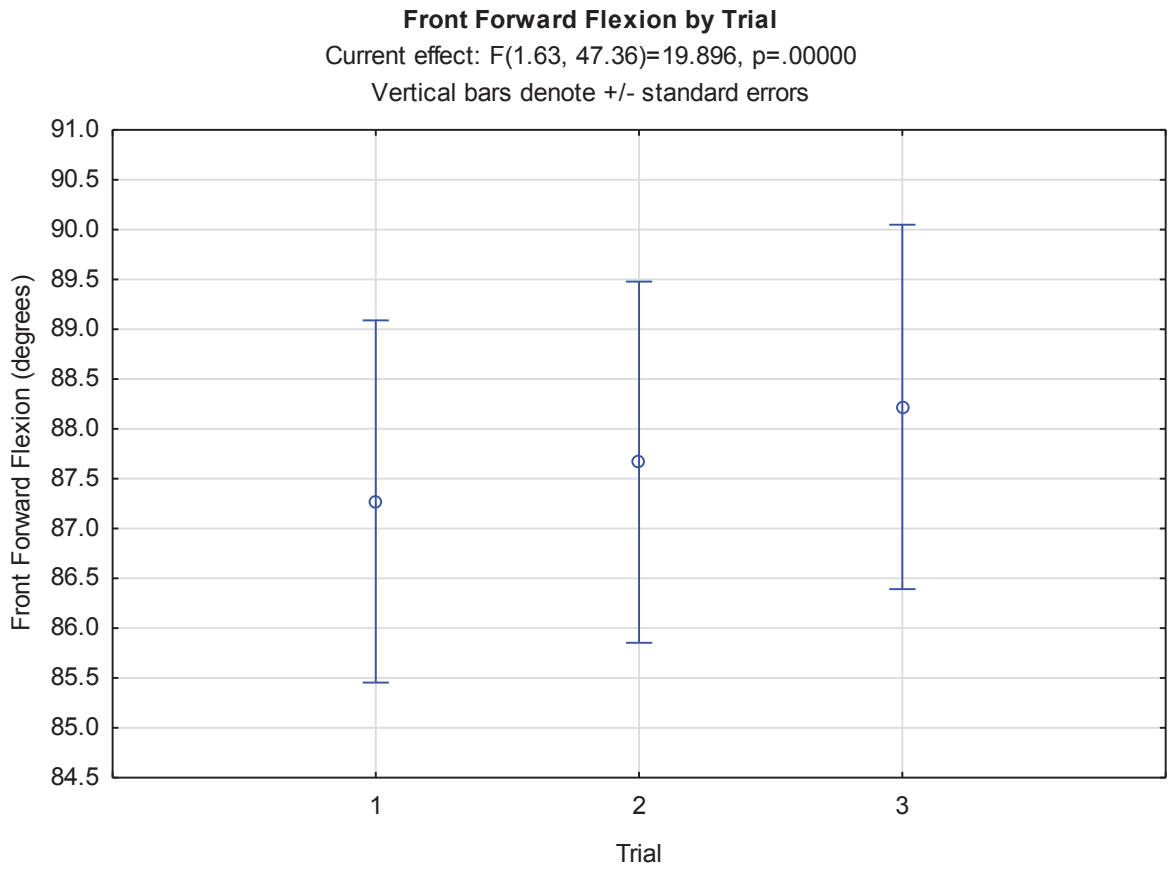

Figure 74: Effect of Trial on Front Forward Flexion for Digital and iRoM Methods

Mauchly's test indicated that the assumption of sphericity had been violated ($\chi^2(2)=9.26$, $p=0.0097$). The degrees of freedom were adjusted using the Huynh-Feldt correction. There was a significant difference observed between trials ($n=30$, $F(1.63, 47.36)=19.90$, $p=0.0000$). A Tukey's HSD post-hoc analysis revealed that all trials were significantly different than each other however the mean differences between trials was small.

Figure 75 shows the effect of condition x method on front forward flexion.

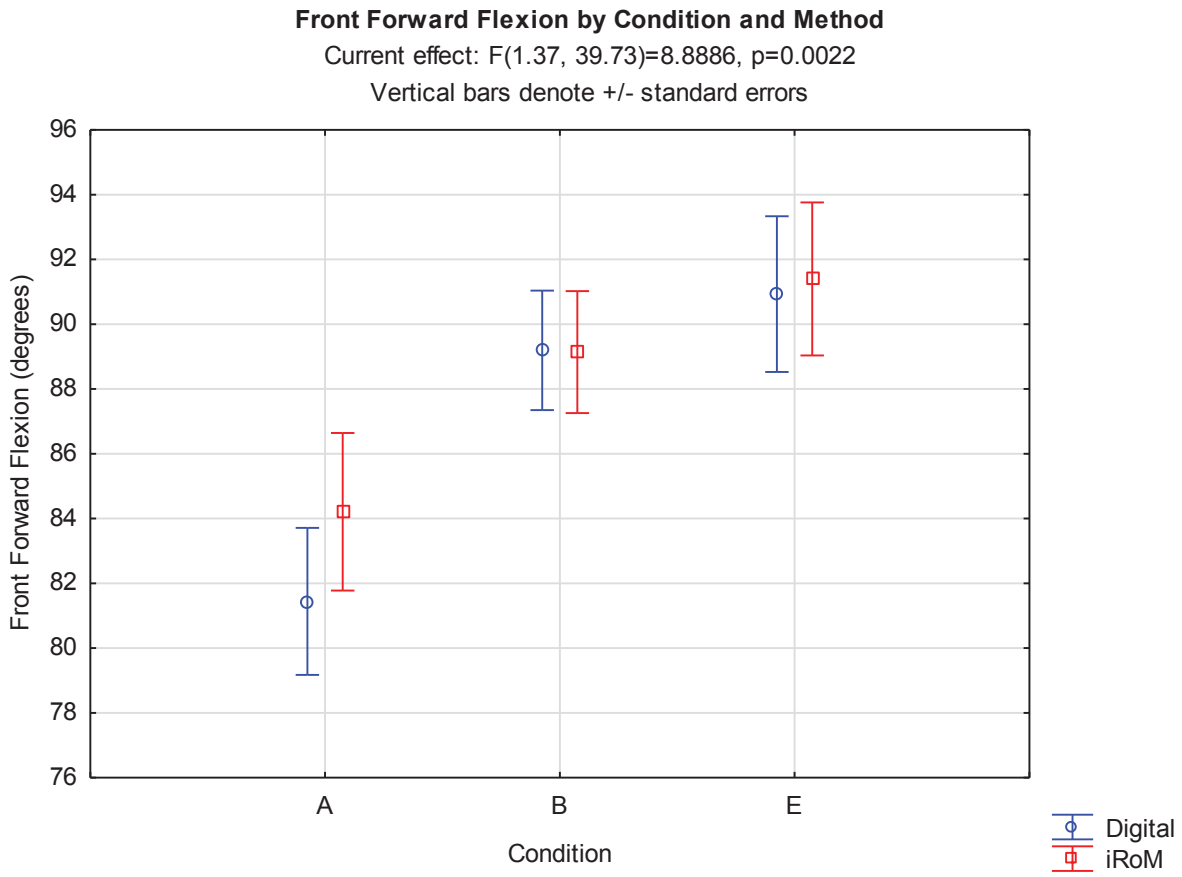

Figure 75: Effect of Condition x Method on Front Forward Flexion for Digital and iRoM Methods

Mauchly's test indicated that the assumption of sphericity had been violated ($\chi^2(2)=17.24$, $p=0.0002$). The degrees of freedom were adjusted using the Greenhouse-Geisser correction. There was a significant difference observed between condition x method ($n=30$, $F(1.37, 39.73)=8.89$, $p=0.0022$). A Tukey's HSD post-hoc analysis revealed that in Condition A, Digital and iRoM methods were significantly different. In Conditions B and E, Digital and iRoM methods were not significantly different than each other. Conditions A, B, and E were all significantly different than each other when using the iRoM measurement method as well as when using the Digital measurement method with Condition A allowing the most front forward flexion. All other significant differences can be seen in Annex L: Additional ROM Results.

3.4.1.3.2 *Manual and Natick Method*

A repeated-measures ANOVA was carried out on the front forward flexion measurements for the manual and Natick methods. Table 48 summarizes the significant effects identified.

Table 48: Summary of Repeated Measures ANOVA Results for Front Forward Flexion (Manual and Natick Methods)

Effect	Significance	P-value
Condition	Significant	0.0000[10]
Iteration	Significant	0.0000[10]
Method	Significant	0.0117
Trial	Significant	0.0000[10]
Condition x Iteration	Not significant	0.4711
Condition x Method	Significant	0.0000
Iteration x Method	Not significant	0.1808
Condition x Trial	Not significant	0.2057[10]
Iteration x Trial	Not significant	0.2871[10]
Method x Trial	Not significant	0.9500[11]
Condition x Iteration x Method	Not significant	0.4647
Condition x Iteration x Trial	Not significant	0.5503[10]
Condition x Method x Trial	Not significant	0.3839[10]
Iteration x Method x Trial	Not significant	0.8131[10]
Condition x Iteration x Method x Trial	Not significant	0.3874[10]

[10] Adjusted using the Greenhouse-Geisser (1959) correction.
[11] Adjusted using the Huynh-Feldt (1976) correction.

Figure 76 shows the effect of condition on front forward flexion.

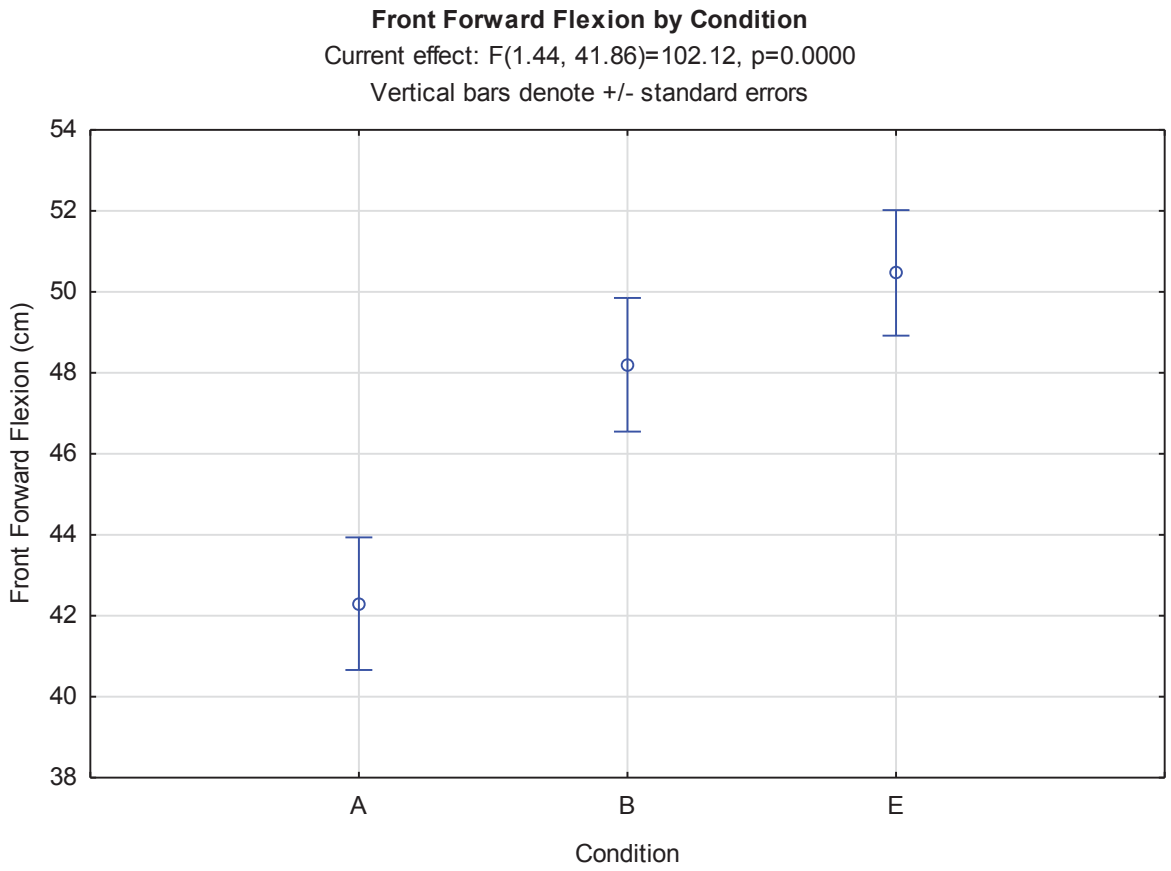

Figure 76: Effect of Condition on Front Forward Flexion for Manual and Natick methods

Mauchly's test indicated that the assumption of sphericity had been violated ($\chi^2(2)=13.64$, $p=0.0011$). The degrees of freedom were adjusted using the Greenhouse-Geisser correction. There was a significant difference observed between conditions ($n=30$, $F(1.44, 41.86)=102.12$, $p=0.0000$). A Tukey's HSD post-hoc analysis revealed that all conditions were significantly different than each other.

Figure 77 shows the effect of iteration on front forward flexion.

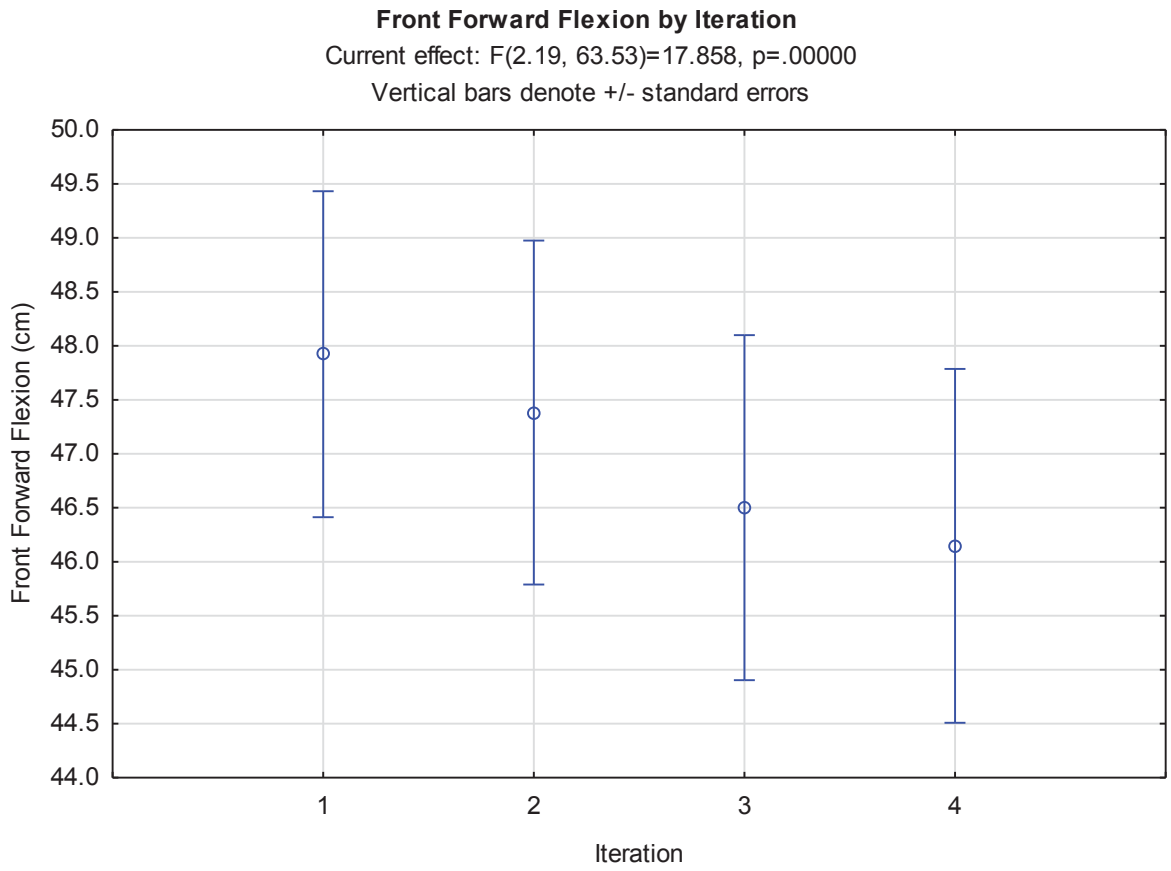

Figure 77: Effect of Iteration on Front Forward Flexion for Manual and Natick Methods

Mauchly's test indicated that the assumption of sphericity had been violated ($\chi^2(5)=14.43$, $p=0.0131$). The degrees of freedom were adjusted using the Greenhouse-Geisser correction. There was a significant difference observed between iterations ($n=30$, $F(2.19, 63.53)=17.86$, $p=0.0000$). A Tukey's HSD post-hoc analysis revealed that Iteration 1 was significantly different than Iterations 3 and 4 but not significantly different than Iteration 2. Iteration 2 was significantly different than Iterations 3 and 4, but Iterations 3 and 4 were not significantly different than each other.

Figure 78 shows the effect of method on front forward flexion.

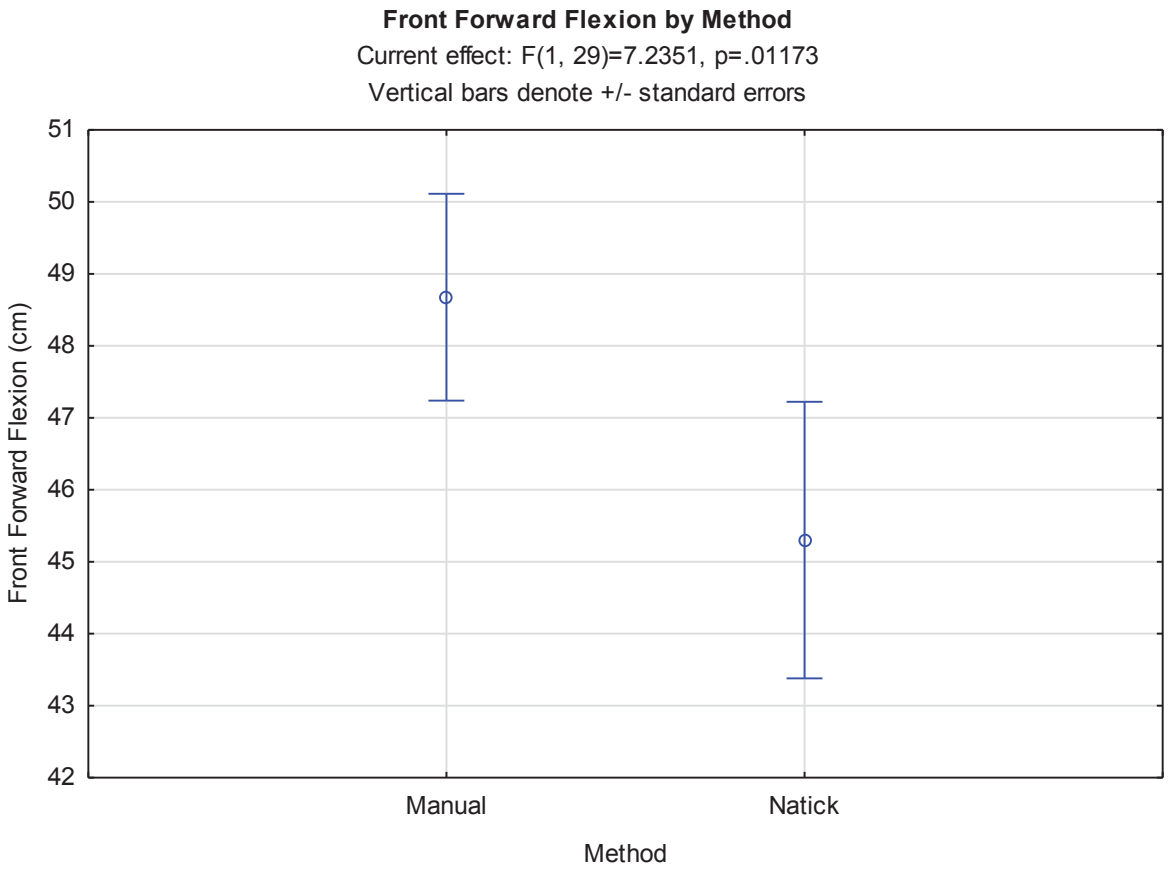

Figure 78: Effect of Method on Front Forward Flexion

There was a significant difference observed between Manual and Natick methods (n=30, F(1, 29)=7.24, p=0.0117).

Figure 79 shows the effect of trial on front forward flexion.

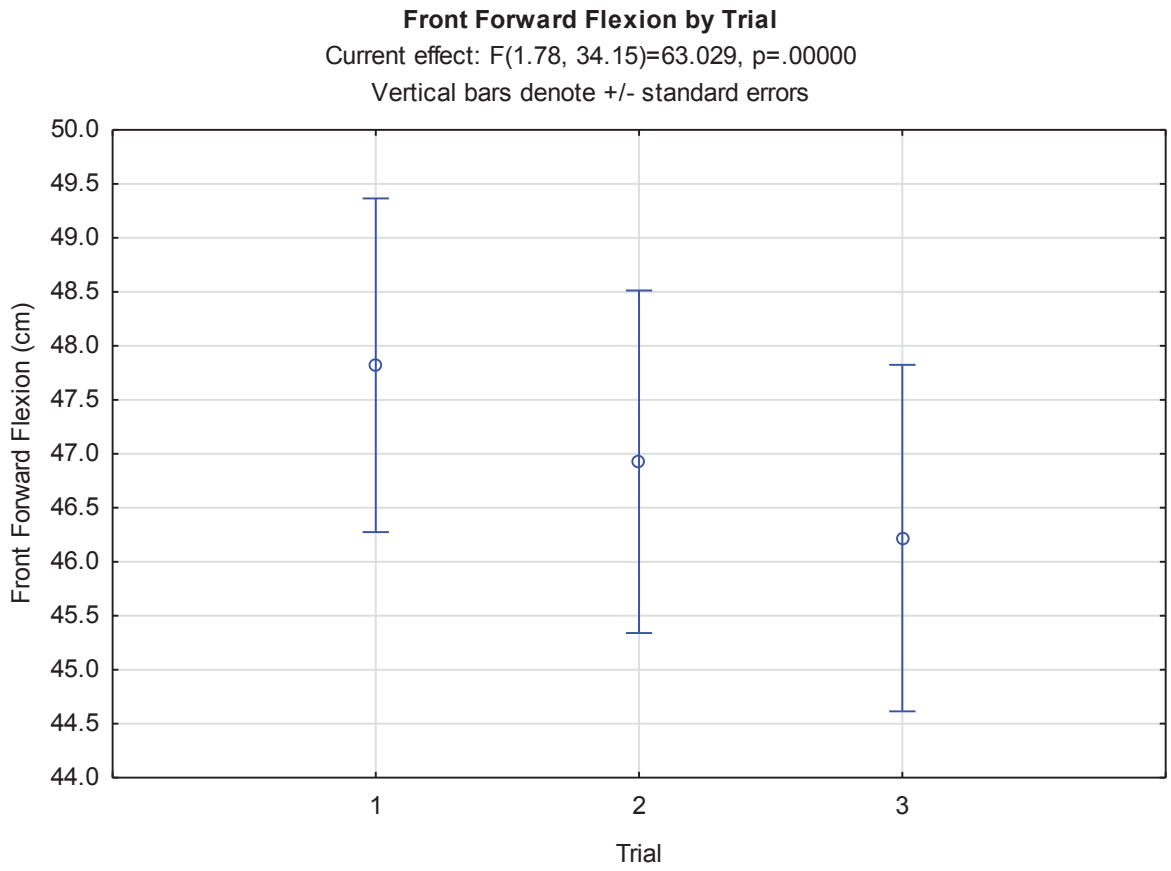

Figure 79: Effect of Trial on Front Forward Flexion for Manual and Natick Methods

Mauchly's test indicated that the assumption of sphericity had been violated ($\chi^2(2)=33.56$, $p=0.0000$). The degrees of freedom were adjusted using the Greenhouse-Geisser correction. There was a significant difference observed between trials ($n=30$, $F(1.78, 34.15)=63.03$, $p=0.0000$). A Tukey's HSD post-hoc analysis revealed that all trials were significantly different than each other however the mean differences between trials was small.

Figure 80 shows the effect of condition x method on front forward flexion.

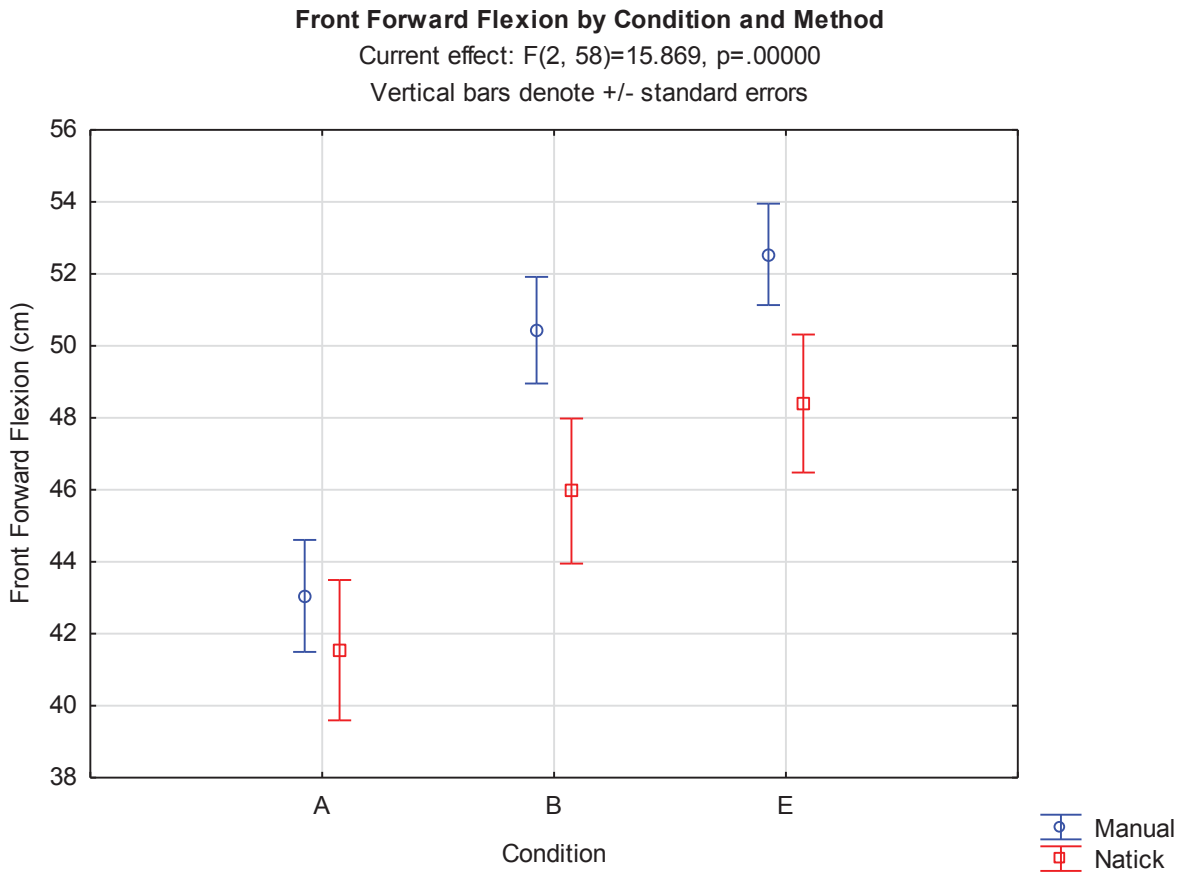

Figure 80: Effect of Condition x Method on Front Forward Flexion for Manual and Natick Methods

There was a significant difference observed between condition x method (n=30, F(2, 58)=15.87, p=0.0000). A Tukey's HSD post-hoc analysis revealed that all conditions were significantly different than each other for both Manual and Natick methods. All other significant differences can be seen in Annex L: Additional ROM Results.

3.4.1.4 *High Knee Lift*

High knee lift was only part of the Natick method, therefore there is no comparison across methods for this portion of the results. A repeated-measures ANOVA was carried out on the high knee lift measurements. Table 49 summarizes the results.

Table 49: Summary of Repeated Measures ANOVA Results for High Knee Lift

Effect	Significance	P-value
Condition	Significant	0.0000[12]
Iteration	Significant	0.0373[12]
Direction	Not significant	0.1987
Trial	Significant	0.0004[13]
Condition x Iteration	Significant	0.0265
Condition x Direction	Not significant	0.3281
Iteration x Direction	Not significant	0.0935
Condition x Trial	Not significant	0.8424
Iteration x Trial	Not significant	0.2477
Direction x Trial	Not significant	0.5508
Condition x Iteration x Direction	Not significant	0.9934
Condition x Iteration x Trial	Not significant	0.5552[13]
Condition x Direction x Trial	Significant	0.0166
Iteration x Direction x Trial	Not significant	0.4960
Condition x Iteration x Direction x Trial	Not significant	0.1312

[12] Adjusted using the Huynh-Feldt (1976) correction.
[13] Adjusted using the Greenhouse-Geisser (1959) correction.

Figure 81 shows the effect of condition on high knee lift.

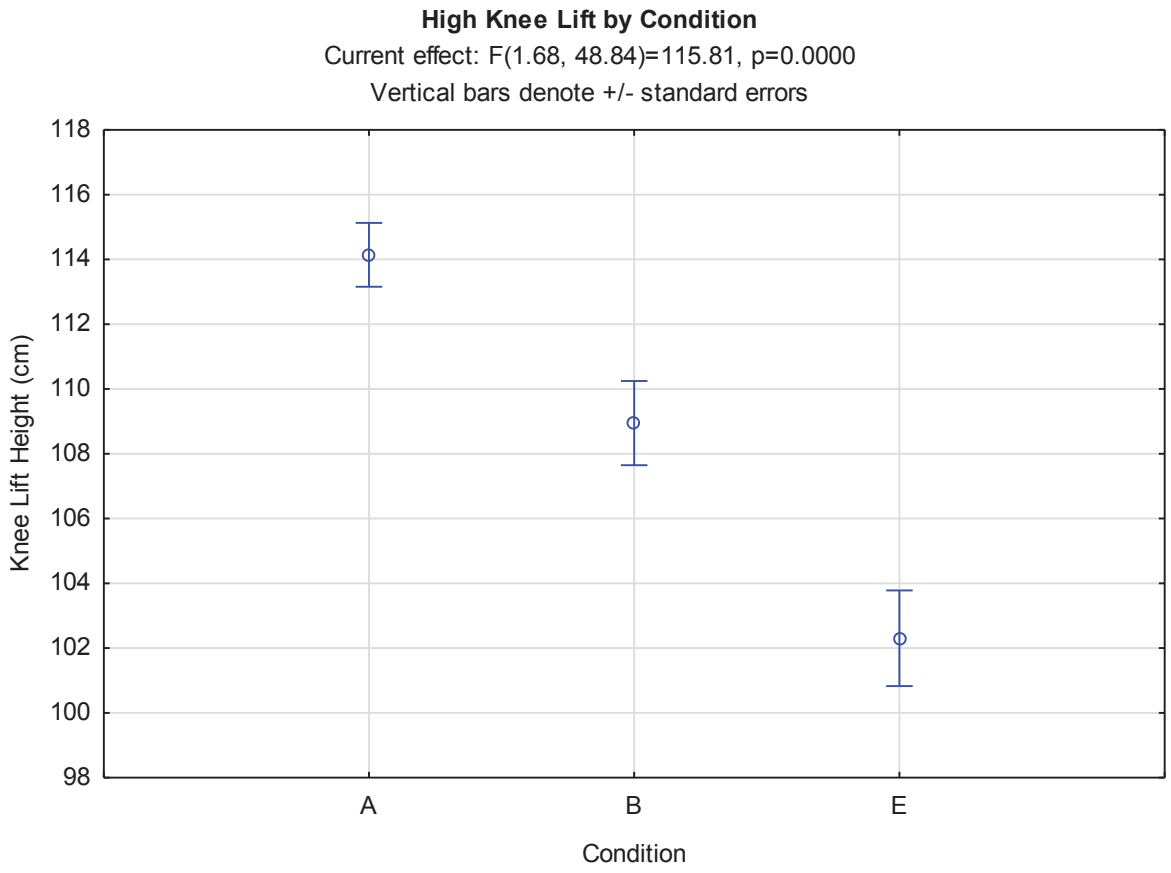

Figure 81: Effect of Condition on High Knee Lift

Mauchly's test indicated that the assumption of sphericity had been violated ($\chi^2(2)=7.92$, $p=0.0190$). The degrees of freedom were adjusted using the Huynh-Feldt correction. There was a significant difference observed between conditions ($n=30$, $F(1.68, 48.84)=115.81$, $p=0.0000$). A Tukey's HSD post-hoc analysis revealed that all conditions were significantly different than each other.

Figure 82 shows the effect of iteration on high knee lift.

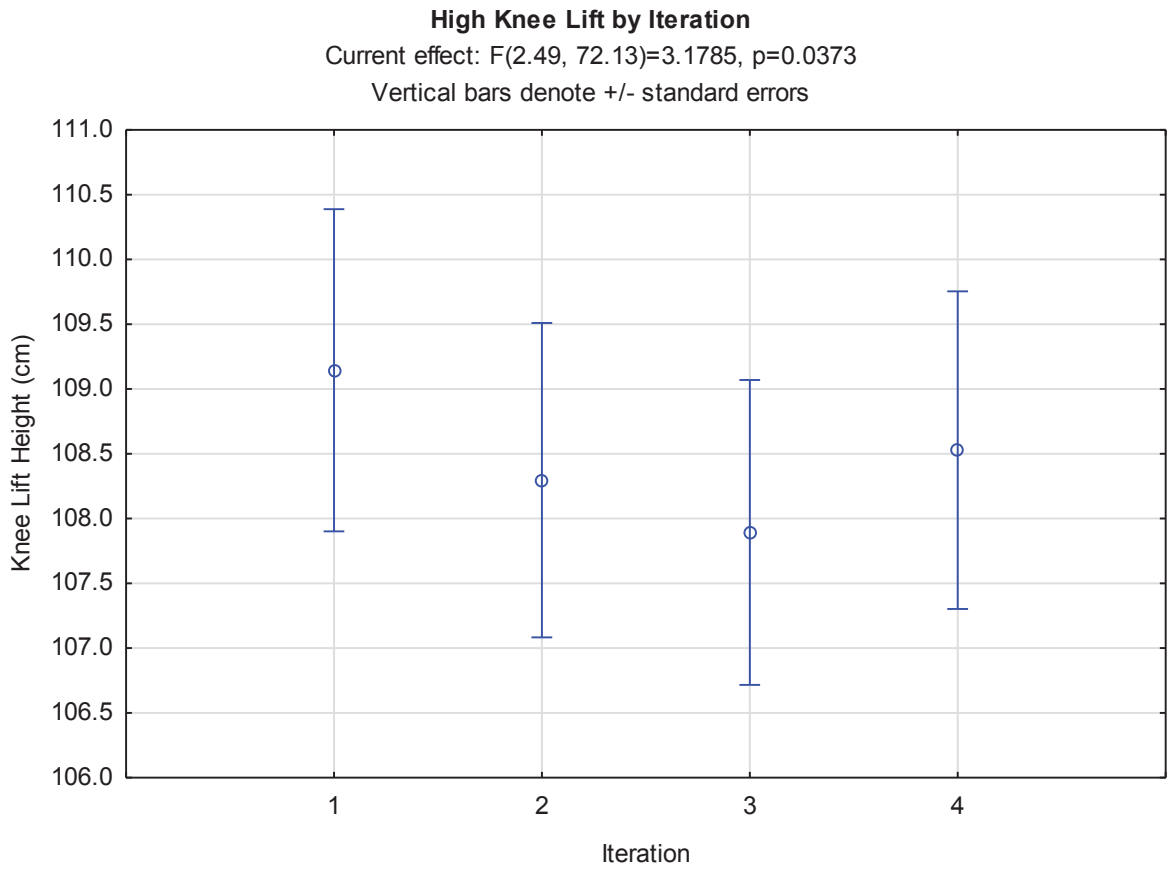

Figure 82: Effect of Iteration on High Knee Lift

Mauchly's test indicated that the assumption of sphericity had been violated ($\chi^2(5)=16.52$, $p=0.0055$). The degrees of freedom were adjusted using the Huynh-Feldt correction. There was a significant difference observed between iterations ($n=30$, $F(2.49, 72.13)=3.18$, $p=0.0373$). A Tukey's HSD post-hoc analysis revealed that Iteration 1 was significantly different than Iteration 3. There were no other significant differences observed between iterations.

Figure 83 shows the effect of trial on high knee lift.

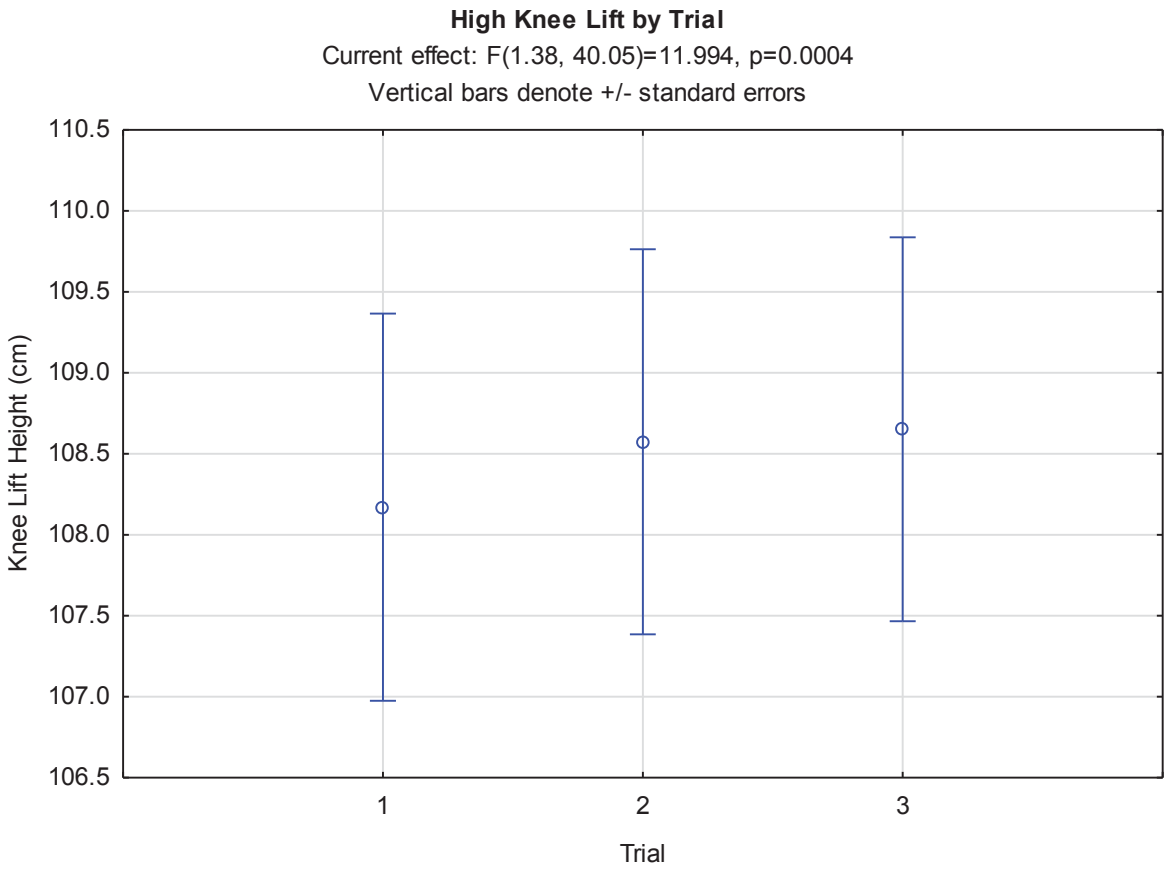

Figure 83: Effect of Trial on High Knee Lift

Mauchly's test indicated that the assumption of sphericity had been violated ($\chi^2(2)=16.65$, $p=0.0002$). The degrees of freedom were adjusted using the Greenhouse-Geisser correction. There was a significant difference observed between trials ($n=30$, $F(1.38, 40.05)=11.99$, $p=0.0004$). A Tukey's HSD post-hoc analysis revealed that Trial 1 was significantly different than Trials 2 and 3, but Trials 2 and 3 were not significantly different than each other.

Figure 84 shows the effect of condition x iteration on high knee lift.

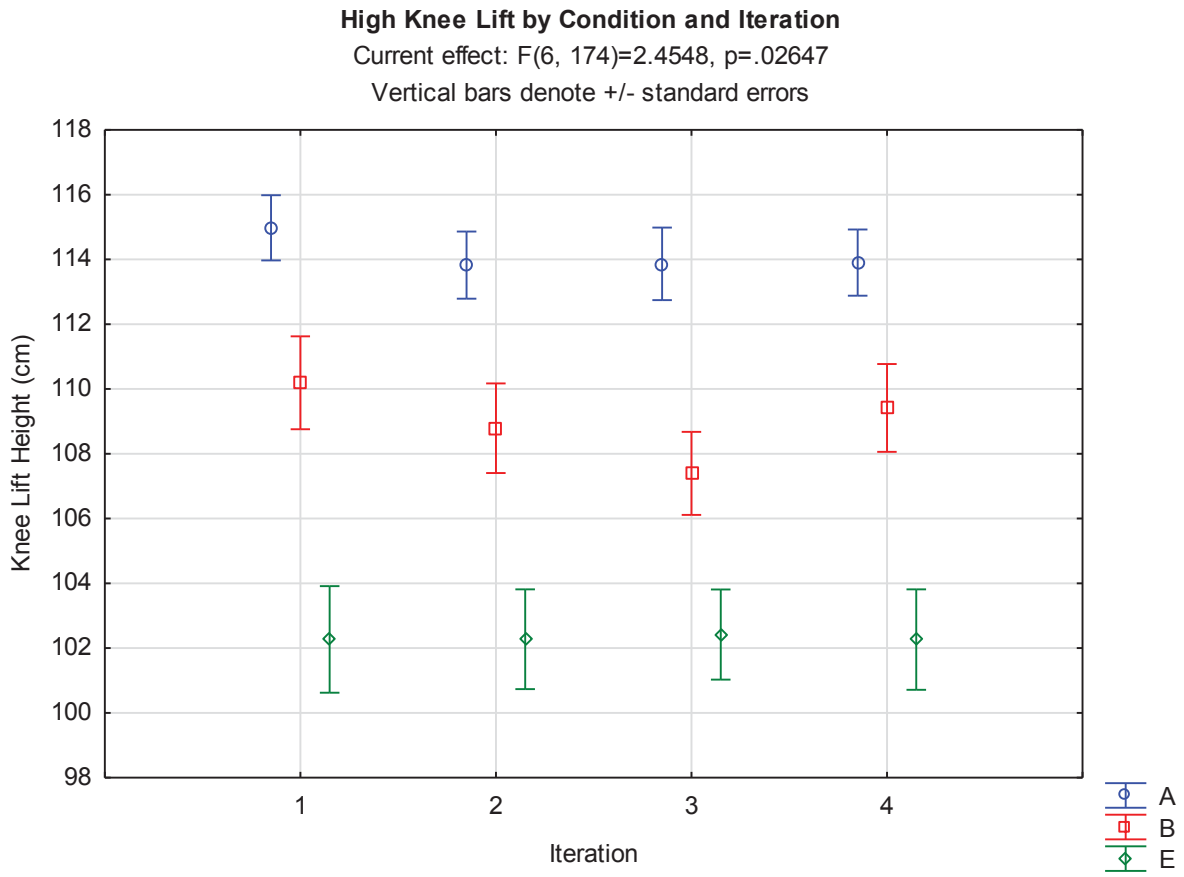

Figure 84: Effect of Condition x Iteration on High Knee Lift

There was a significant difference observed between condition x iteration (n=30, F(6, 174)=2.46, p=0.0265). A Tukey's HSD post-hoc analysis revealed that, for Condition A, iterations were not significantly different. For Condition B, Iteration 1 was significantly different than Iteration 3, and Iteration 3 was significantly different than Iteration 4. For Condition E, iterations were not significantly different. All other significant differences can be seen in Annex L: Additional ROM Results.

Figure 85 shows the effect of condition x side x trial on high knee lift.

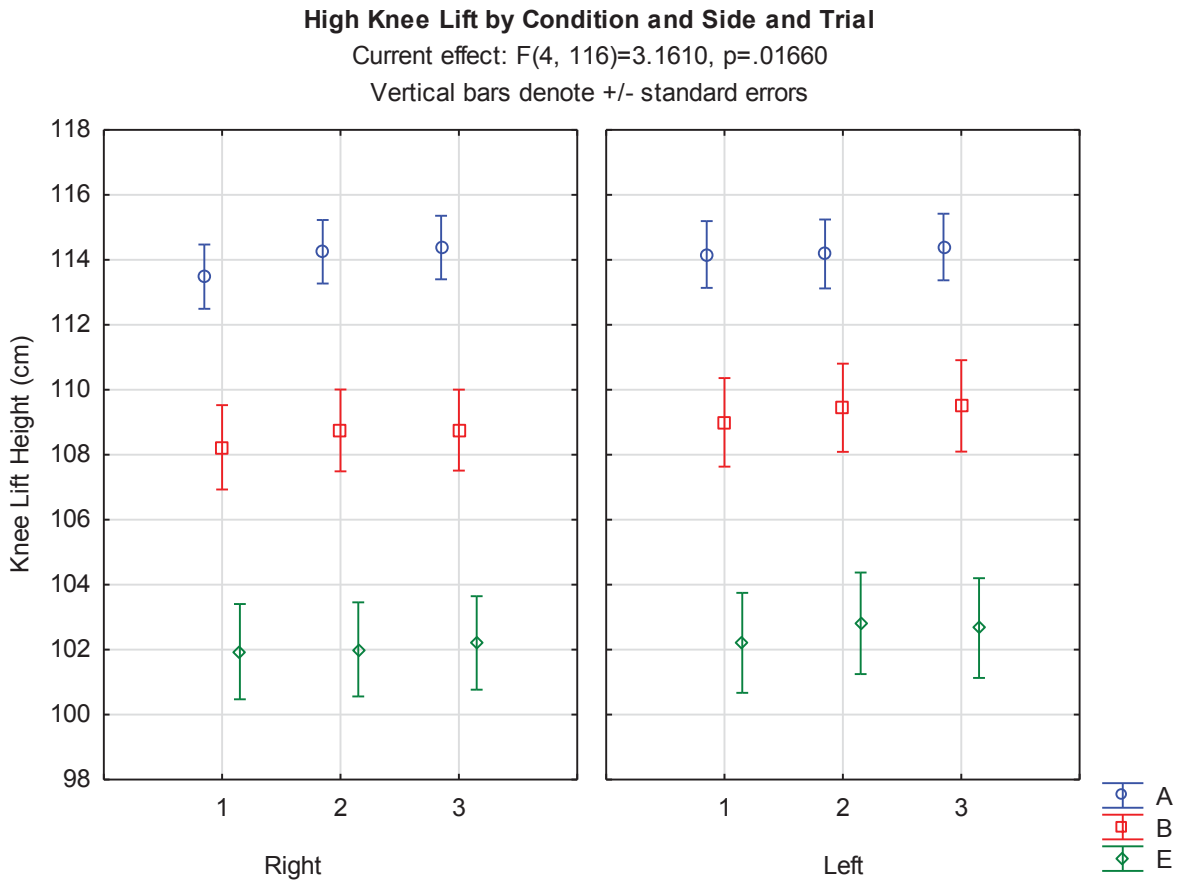

Figure 85: Effect of Condition x Side x Trial on High Knee Lift

There was a significant difference between condition x side x trial (n=30, F(4, 116)=3.16, p=0.0166). A Tukey's HSD post-hoc analysis revealed many significant differences. All significant differences can be seen in Annex L: Additional ROM Results.

3.4.1.5 *Shoulder Abduction*

Shoulder abduction was only part of the Natick method, therefore there is no comparison across methods for this portion of the results. A repeated-measures ANOVA was carried out on the shoulder abduction measurements. Table 50 summarizes the results.

Table 50: Summary of Repeated Measures ANOVA Results for Shoulder Abduction

Effect	Significance	P-value
Condition	Significant	0.0000
Iteration	Not significant	0.1537
Direction	Not significant	0.3246
Trial	Not significant	0.2068[14]
Condition x Iteration	Not significant	0.6356[15]
Condition x Direction	Not significant	0.2369
Iteration x Direction	Not significant	0.9200
Condition x Trial	Not significant	0.1032[15]
Iteration x Trial	Not significant	0.2699
Direction x Trial	Not significant	0.4939[14]
Condition x Iteration x Direction	Not significant	0.9879
Condition x Iteration x Trial	Significant	0.0496
Condition x Direction x Trial	Not significant	0.5284[14]
Iteration x Direction x Trial	Not significant	0.3773
Condition x Iteration x Direction x Trial	Not significant	0.1395

[14] Adjusted using the Huynh-Feldt (1976) correction.
[15] Adjusted using the Greenhouse-Geisser (1959) correction.

Figure 86 shows the effect of condition on shoulder abduction.

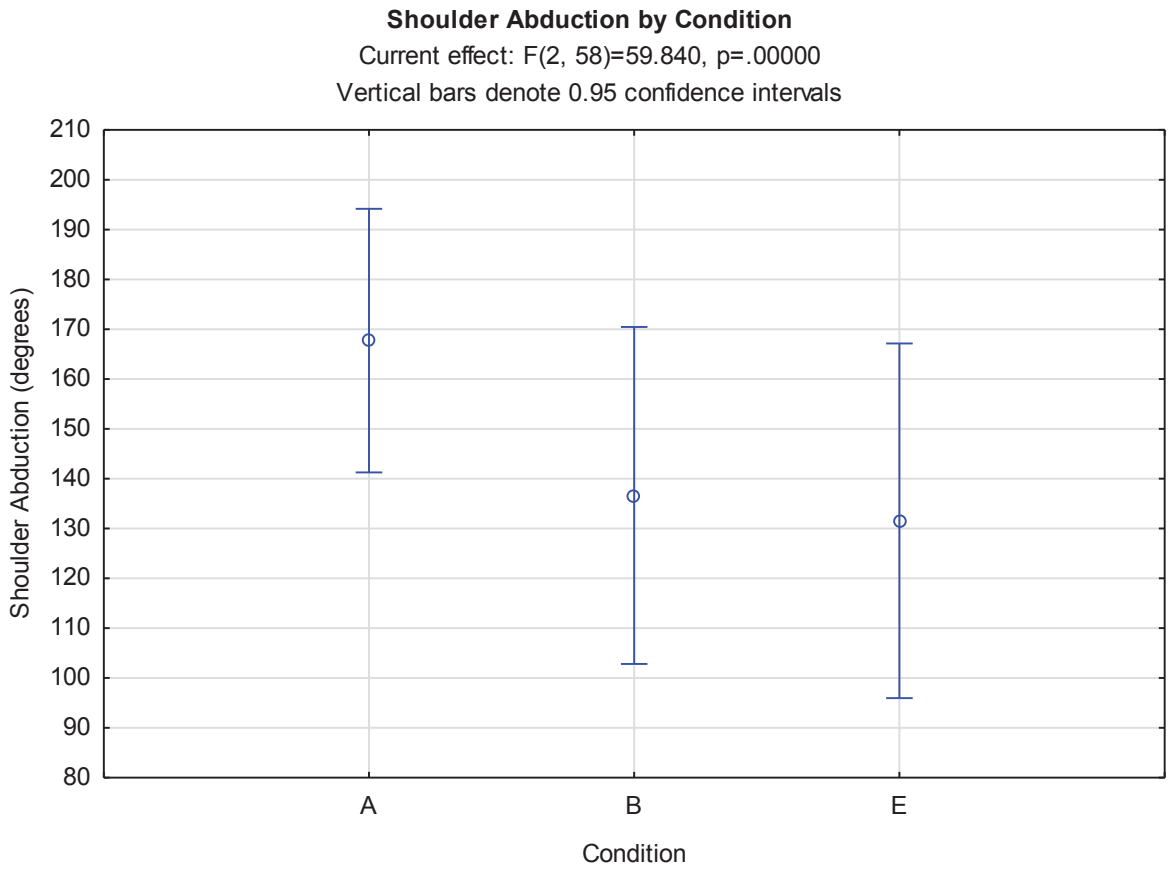

Figure 86: Effect of Condition on Shoulder Abduction

There was a significant difference observed between conditions (n=30, F(2, 58)=59.84, p=0.0000). A Tukey's HSD post-hoc analysis revealed that Condition A was significantly different than Conditions B and E, but Conditions B and E were not significantly different than each other.

Figure 87 shows the effect of condition x iteration x trial on shoulder abduction.

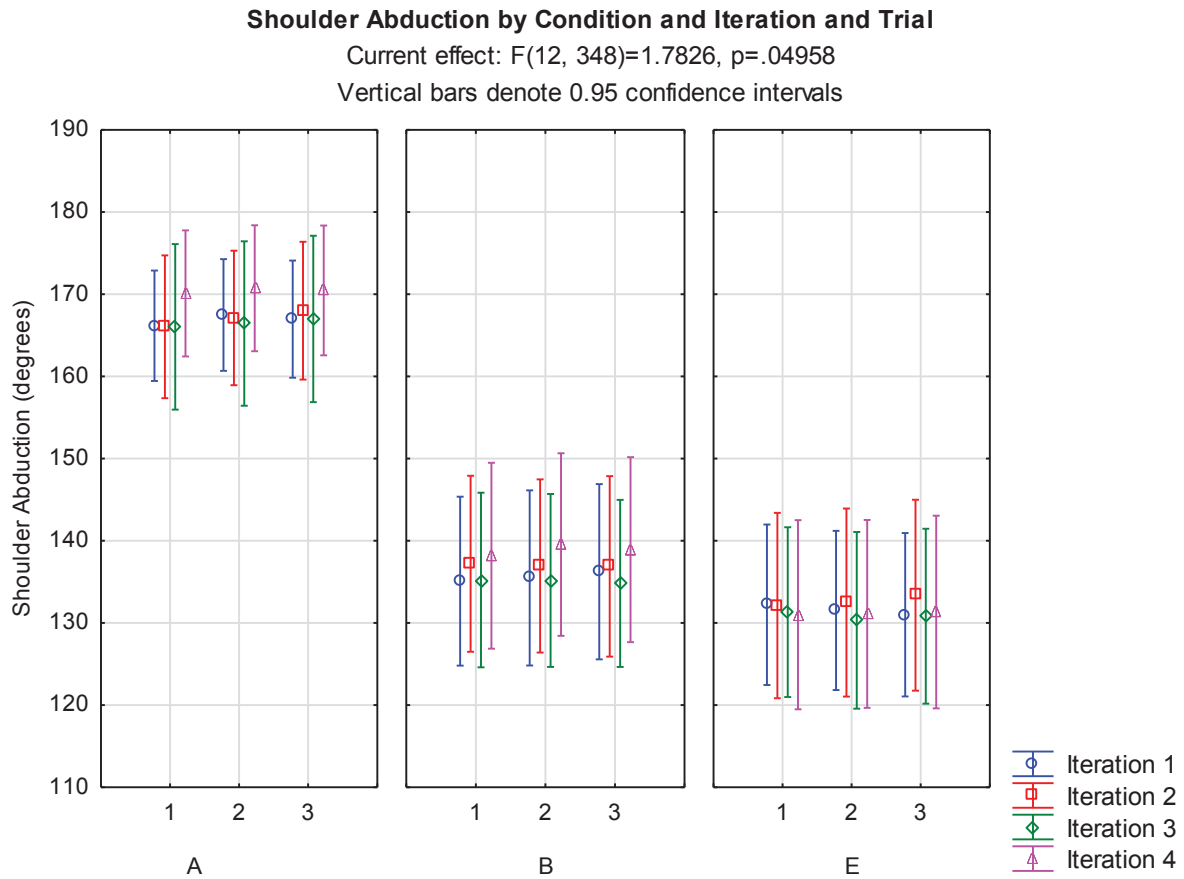

Figure 87: Effect of Condition x Iteration x Trial on Shoulder Abduction

There was a significant difference observed between condition x iteration x trial (n=30, F(21, 348)=1.78, p=0.0496). A Tukey's HSD post-hoc analysis revealed many significant differences. All significant differences can be seen in Annex L: Additional ROM Results.

3.4.2 ROM Reliability Analyses

3.4.2.1 *Repeatability - ICC(A,k)*

Table 51 summarizes the ICC values calculated between Iterations 1 and 2 for each of the ROM measures. The ICCs calculated are presented for each condition since collapsing and averaging across conditions would not be an accurate representation of the repeatability of the method; methods could have better or worse repeatability depending on the condition so all values are presented for completeness. The ICC values were transformed using Fisher's Z-transformation to accommodate for the non-normality of the ICCs as per McGraw and Wong (1996). Figure 88 is a box and whisker plot of the Fisher's z-transformed ICCs calculated between iterations 1 & 2. The box represents the first and third quartile and the whiskers represent the maximum and minimum excluding outliers. The median is also represented by the bar within the box plot.

Table 51: ICC Between Iterations 1 & 2

Measure	Side	Condition	Method			
			Digital	iRoM	Manual	Natick
Trunk Rotation	Right	A	0.9454	0.9381	0.8435	0.8426
		B	0.9080	0.8914	0.8972	0.8968
		E	0.9644	0.9427	0.8928	0.9261
	Left	A	0.9077	0.9243	0.9431	0.8344
		B	0.9027	0.9004	0.8575	0.8921
		E	0.9275	0.9552	0.9155	0.9050
Lateral Bending	Right	A	0.8383	0.8878	0.8019	0.8575
		B	0.8581	0.9256	0.7946	0.9419
		E	0.8138	0.8672	0.8950	0.8778
	Left	A	0.7369	0.8524	0.5634	0.8839
		B	0.8014	0.9642	0.8656	0.9090
		E	0.9205	0.9511	0.8875	0.9059
Front Forward Flexion		A	0.7351	0.7383	0.9578	0.9916
		B	0.4538	0.2995	0.9677	0.9852
		E	0.9056	0.9162	0.9752	0.9875
High Knee Lift	Right	A				0.9333
		B				0.9215
		E				0.9466
	Left	A				0.9517
		B				0.9383
		E				0.9785
Shoulder Abduction	Right	A				0.9194
		B				0.9342
		E				0.9428
	Left	A				0.9321
		B				0.9428
		E				0.9544

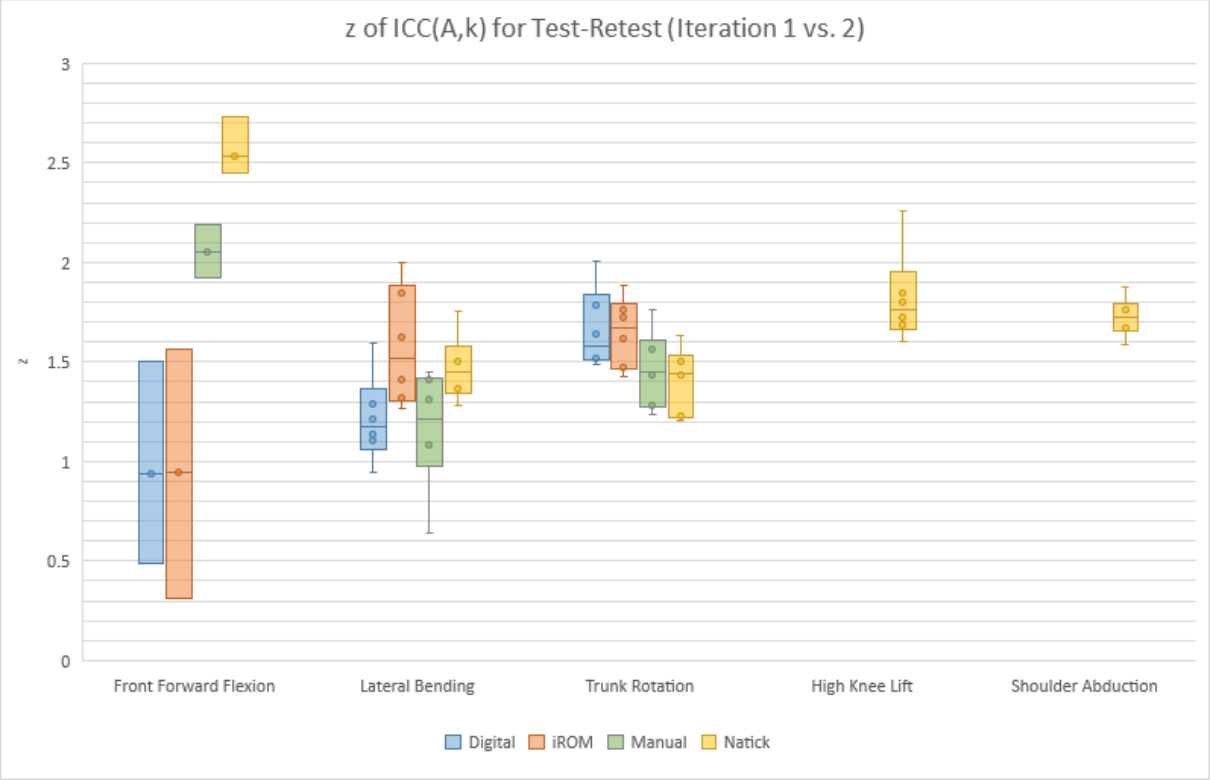

Figure 88: Box and Whisker Plot of Fisher's *z*-transformation of the ICCs (between iterations) for all ROM Measures

3.4.2.2 ***Precision - ICC(A,1)***

Table 52 to Table 55 below summarize the ICC values calculated between trials for each of the ROM measures. The ICCs are presented for each condition and iteration since collapsing and averaging would not be an accurate representation of the precision of the method; methods could have had better or worse precision in different conditions so all values are presented for completeness. The ICC values were transformed using Fisher's Z-transformation to accommodate for the non-normality of the data, as per McGraw and Wong (1996), and plotted in Figure 89. The box represents the first and third quartile and the whiskers represent the maximum and minimum excluding outliers. The median is also represented by the bar within the box plot.

Table 52: ICC Values across Conditions for Right and Left Trunk Rotation

Side	Condition	Iteration	Method			
			Digital	iRoM	Manual	Natick
Right	A	1	0.9733	0.9685	0.9548	0.8512
		2	0.9685	0.9592	0.9586	0.8274
		3	0.9658	0.9567	0.9712	0.9041
		4	0.9671	0.9551	0.9605	0.8535
	B	1	0.9534	0.9538	0.9149	0.9330
		2	0.9516	0.9565	0.9421	0.9075
		3	0.9514	0.9763	0.9398	0.9139
		4	0.9638	0.9636	0.9189	0.9236
	E	1	0.9702	0.9470	0.9492	0.9405
		2	0.9695	0.9673	0.9450	0.9176
		3	0.9584	0.9436	0.9217	0.9528
		4	0.9651	0.9697	0.9121	0.9335
Left	A	1	0.9599	0.9666	0.9596	0.8799
		2	0.9312	0.9496	0.9670	0.8961
		3	0.9236	0.9279	0.9351	0.8958
		4	0.9481	0.9578	0.9530	0.8708
	B	1	0.9746	0.9650	0.9038	0.9420
		2	0.9461	0.9710	0.9456	0.8830
		3	0.9504	0.9768	0.9117	0.8710
		4	0.9628	0.9546	0.9522	0.8889
	E	1	0.9450	0.9593	0.9316	0.9405
		2	0.9660	0.9738	0.9468	0.9262
		3	0.9695	0.9681	0.9290	0.9054
		4	0.9625	0.9609	0.9282	0.8937

Table 53: ICC Values across Conditions for Right and Left Lateral Bending

Side	Condition	Iteration	Method			
			Digital	iRoM	Manual	Natick
Right	A	1	0.9444	0.9367	0.8300	0.8805
		2	0.9293	0.9456	0.9025	0.9381
		3	0.9271	0.9475	0.8759	0.9577
		4	0.9641	0.9185	0.8972	0.8621
	B	1	0.9313	0.9721	0.7154	0.9256
		2	0.9479	0.9453	0.7716	0.8985
		3	0.9439	0.9662	0.7660	0.9064
		4	0.9413	0.9461	0.8535	0.8405
	E	1	0.9481	0.9443	0.8221	0.8788
		2	0.9425	0.9581	0.8924	0.8888
		3	0.9314	0.9548	0.7842	0.9044
		4	0.9475	0.9474	0.7698	0.8815
Left	A	1	0.8974	0.9433	0.7763	0.9306
		2	0.9412	0.9542	0.8630	0.9401
		3	0.9667	0.9656	0.7926	0.9185
		4	0.9494	0.9565	0.8441	0.9220
	B	1	0.9532	0.9677	0.8627	0.9628
		2	0.9575	0.9758	0.8932	0.9518
		3	0.9572	0.9502	0.8848	0.9436
		4	0.9564	0.9747	0.8910	0.9063
	E	1	0.9619	0.9507	0.8505	0.9219
		2	0.9686	0.9534	0.8573	0.9097
		3	0.9451	0.9470	0.7462	0.9227
		4	0.9609	0.9523	0.8792	0.9345

Table 54: ICC Values across Conditions for Front Forward Flexion

Condition	Iteration	Method			
		Digital	iRoM	Manual	Natick
A	1	0.9546	0.9768	0.9670	0.9835
	2	0.9356	0.9626	0.9658	0.9850
	3	0.9335	0.9754	0.9620	0.9643
	4	0.9580	0.9636	0.9595	0.9800
B	1	0.9617	0.9869	0.9581	0.9796
	2	0.9592	0.9817	0.9575	0.9862
	3	0.9700	0.9771	0.9794	0.9837
	4	0.9677	0.9814	0.9775	0.9815
E	1	0.9629	0.9853	0.9123	0.9730
	2	0.9862	0.9920	0.9622	0.9768
	3	0.9636	0.9875	0.9726	0.9854
	4	0.9892	0.9907	0.9764	0.9825

Table 55: ICC Values across Conditions for Right and Left High Knee Lift and Shoulder Abduction

Measure	Condition	Iteration	Side	
			Left	Right
High Knee Lift	A	1	0.9573	0.8941
		2	0.9390	0.9149
		3	0.9331	0.9409
		4	0.9398	0.9291
	B	1	0.9787	0.9639
		2	0.9605	0.9468
		3	0.9606	0.9624
		4	0.9487	0.9573
	E	1	0.9744	0.9676
		2	0.9650	0.9536
		3	0.9595	0.9520
		4	0.9706	0.9670
Shoulder Abduction	A	1	0.9786	0.9596
		2	0.9765	0.9670
		3	0.9834	0.9830
		4	0.9593	0.9660
	B	1	0.9795	0.9724
		2	0.9771	0.9657
		3	0.9784	0.9675
		4	0.9847	0.9720
	E	1	0.9761	0.9356
		2	0.9843	0.9733
		3	0.9805	0.9712
		4	0.9789	0.9706

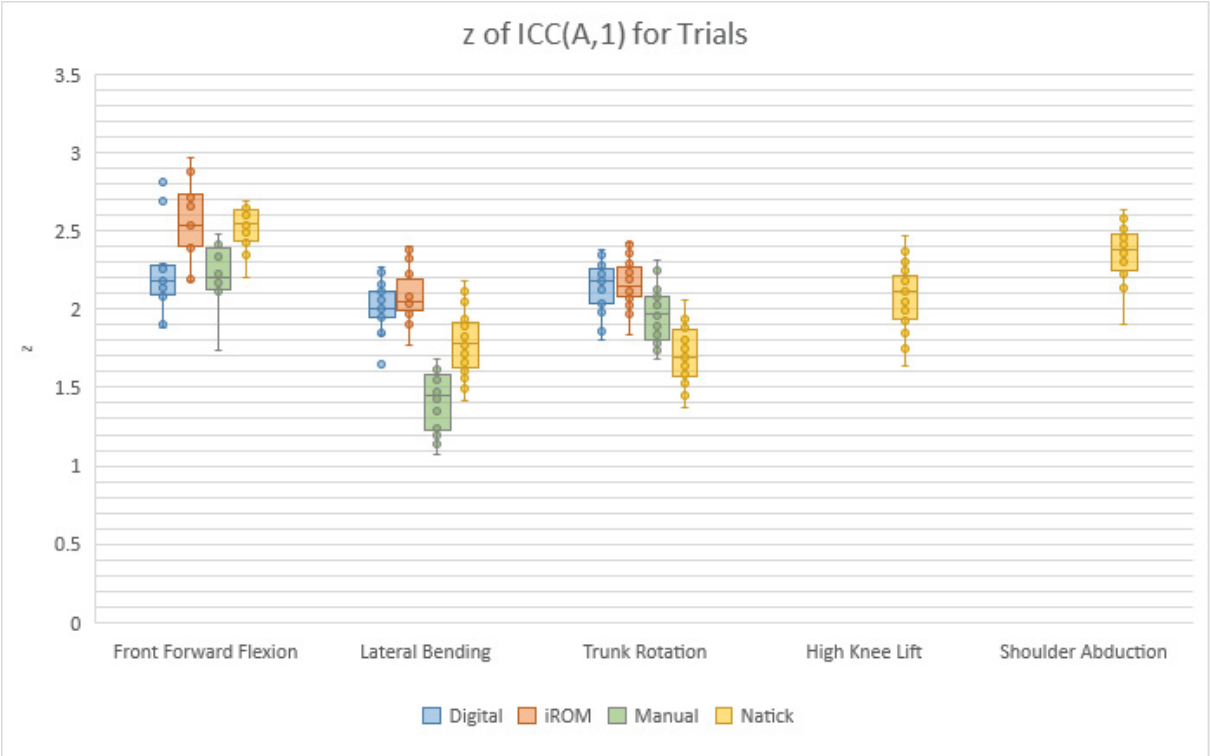

Figure 89: Box and Whisker Plot for z-transformation of the ICCs (between trials) for all ROM measures

3.5 Regression Analysis

The most precise, repeatable, and reliable methods chosen for each ROM measure are summarized in Table 56. These methods were used for the regression analyses completed below. Only 29 participants were used for the regression analyses since one participant was unable to complete the LEAP course in all three conditions.

Table 56: Most Precise, Repeatable, and Reliable Method for Each ROM Measure

ROM Measure	Measurement Method
Trunk Rotation	iRoM
Lateral Bending	iRoM
Front Forward Flexion	Natick
Shoulder Abduction	Natick
High Knee Lift	Natick

3.5.1 ROM Regression with Overall LEAP Times

Table 57 summarizes the ROM correlation with the overall LEAP course times. The regression line coefficients for each correlation as well as their respective 2.5th and 97.5th percentiles for each of the coefficients are summarized in the following tables.

Table 57: Summary of ROM correlation with overall LEAP course time

Range of Motion	Method	Correlation with Overall LEAP Course Time (R^2)
Right Trunk Rotation	iRoM	0.13
Left Trunk Rotation	iRoM	0.06
Right Lateral Bending	iRoM	0.13
Left Lateral Bending	iRoM	0.17
Front Forward Flexion	Natick	0.03
Right Shoulder Abduction	Natick	0.10
Left Shoulder Abduction	Natick	0.09
Right High Knee Lift	Natick	0.30
Left High Knee Lift	Natick	0.30

The associated graphs for each regression line can be seen in Annex M: Additional Regression Results.

Table 58 shows the mean slope, intercept, and R^2 values, the standard error (SE) as well as the 2.5th and 97.5th percentiles computed through the two-stage cluster bootstrap techniques for Right Trunk Rotation vs. Overall LEAP Time.

Table 58: Regression Coefficients for Right Trunk Rotation vs. Overall LEAP Time

Right Trunk Rotation vs. Overall LEAP Time, Regression Coefficients				
	Mean	**2.5th Percentile**	**97.5th Percentile**	**SE**
Slope	-2.46	-4.21	-0.26	1.00
Intercept	394.50	308.94	456.62	37.27
R^2	0.13	-0.05	0.24	0.08

Table 59 shows the regression coefficients and confidence intervals for Left Trunk Rotation vs. Overall LEAP Time.

Table 59: Regression Coefficients for Left Trunk Rotation vs. Overall LEAP Time

Left Trunk Rotation vs. Overall LEAP Time, Regression Coefficients				
	Mean	**2.5th Percentile**	**97.5th Percentile**	**SE**
Slope	-1.46	-3.98	1.13	1.31
Intercept	355.87	271.09	431.78	40.66
R^2	0.06	-0.10	0.12	0.06

Table 60 shows the regression coefficients and confidence intervals for Right Lateral Bending vs. Overall LEAP Time.

Table 60: Regression Coefficients for Right Lateral Bending vs. Overall LEAP Time

Right Lateral Bending vs. Overall LEAP Time, Regression Coefficients				
	Mean	**2.5th Percentile**	**97.5th Percentile**	**SE**
Slope	-2.90	-4.47	-1.02	0.87
Intercept	407.14	335.03	459.93	32.08
R^2	0.13	-0.03	0.23	0.07

Table 61 shows the regression coefficients and confidence intervals for Left Lateral Bending vs. Overall LEAP Time.

Table 61: Regression Coefficients for Left Lateral Bending vs. Overall LEAP Time

Left Lateral Bending vs. Overall LEAP Time, Regression Coefficients				
	Mean	**2.5th Percentile**	**97.5th Percentile**	**SE**
Slope	-3.26	-4.71	-1.40	0.84
Intercept	416.26	342.98	470.16	32.80
R^2	0.17	0.03	0.28	0.06

Table 62 shows the regression coefficients and 2.5th and 97.5th percentiles for each coefficient for Front Forward Flexion vs. Overall LEAP Time.

Table 62: Regression Coefficients for Front Forward Flexion vs. Overall LEAP Time

Front Forward Flexion vs. Overall LEAP Time, Regression Coefficients				
	Mean	**2.5th Percentile**	**97.5th Percentile**	**SE**
Slope	0.74	-1.23	2.23	0.85
Intercept	277.37	196.03	367.29	42.21
R^2	0.03	-0.08	0.06	0.04

Table 63 shows the regression coefficients and 2.5th/97.5th percentiles for the coefficients for Right Shoulder Abduction vs. Overall LEAP Time.

Table 63: Regression Coefficients for Right Shoulder Abduction vs. Overall LEAP Time

Right Shoulder Abduction vs. Overall LEAP Time, Regression Coefficients				
	Mean	**2.5th Percentile**	**97.5th Percentile**	**SE**
Slope	-0.80	-1.54	-0.08	0.37
Intercept	426.80	319.13	527.20	53.27
R^2	0.10	-0.09	0.20	0.08

Table 64 shows the regression coefficients and 2.5th/97.5th percentiles for each coefficient for Left Shoulder Abduction vs. Overall LEAP Time.

Table 64: Regression Coefficients for Left Shoulder Abduction vs. Overall LEAP Time

Left Shoulder Abduction vs. Overall LEAP Time, Regression Coefficients				
	Mean	2.5th Percentile	97.5th Percentile	SE
Slope	-0.66	-1.43	0.09	0.38
Intercept	407.09	295.73	515.51	55.96
R^2	0.09	-0.12	0.17	0.08

Table 65 shows the regression coefficients and 2.5th/97.5th percentiles for each coefficient for Right High Knee Lift vs. Overall LEAP Time.

Table 65: Regression Coefficients for Right High Knee Lift vs. Overall LEAP Time

Right High Knee Lift vs. Overall LEAP Time, Regression Coefficients				
	Mean	2.5th Percentile	97.5th Percentile	SE
Slope	-4.16	-6.38	-1.66	1.20
Intercept	762.66	480.09	1011.93	135.88
R^2	0.30	0.07	0.52	0.11

Table 66 shows the regression coefficients and 2.5th/97.5th percentiles for each coefficient for Left High Knee Lift vs. Overall LEAP Time.

Table 66: Regression Coefficients for Left High Knee Lift vs. Overall LEAP Time

Left High Knee Lift vs. Overall LEAP Time, Regression Coefficients				
	Mean	2.5th Percentile	97.5th Percentile	SE
Slope	-4.02	-6.21	-1.65	1.17
Intercept	748.13	479.66	995.92	133.27
R^2	0.30	0.07	0.52	0.12

3.5.2 ROM Correlation with Subjective Ratings

Table 67 summarizes the ROM correlation with the overall LEAP course subjective ratings. The regression line coefficients for each correlation as well as the respective 2.5th and 97.5th percentiles for each of the coefficients are summarized in the following tables.

Table 67: Summary of ROM correlation with LEAP course subjective ratings

Range of Motion	Method	Correlation with Subjective Ratings (R^2)
Right Trunk Rotation	iRoM	0.22
Left Trunk Rotation	iRoM	0.12
Right Lateral Bending	iRoM	0.30
Left Lateral Bending	iRoM	0.36
Front Forward Flexion	Natick	0.06
Right Shoulder Abduction	Natick	0.28
Left Shoulder Abduction	Natick	0.25
Right High Knee Lift	Natick	0.34
Left High Knee Lift	Natick	0.31

The associated graphs for each regression line can be seen in Annex M: Additional Regression Results.

Table 68 shows the mean slope, intercept, and R^2 values, the standard error (SE) as well as the 2.5th and 97.5th percentiles computed through the two-stage cluster bootstrap techniques for Right Trunk Rotation vs. Subjective Rating.

Table 68: Regression Coefficients for Right Trunk Rotation vs. LEAP Course Subjective Rating

Right Trunk Rotation vs. LEAP Course Subjective Rating, Regression Coefficients				
	Mean	**2.5th Percentile**	**97.5th Percentile**	**SE**
Slope	0.08	0.04	0.12	0.02
Intercept	1.99	0.52	3.53	0.76
R^2	0.22	0.02	0.39	0.10

Table 69 shows the regression coefficients and 2.5th/97.5th percentiles for each coefficient for Left Trunk Rotation vs. Subjective Rating.

Table 69: Regression Coefficients for Left Trunk Rotation vs. LEAP Course Subjective Rating

Left Trunk Rotation vs. LEAP Course Subjective Rating, Regression Coefficients				
	Mean	**2.5th Percentile**	**97.5th Percentile**	**SE**
Slope	0.06	0.00	0.13	0.03
Intercept	2.90	0.91	4.78	0.99
R^2	0.12	-0.09	0.25	0.09

Table 70 shows the regression coefficients and 2.5th/97.5th percentiles for each coefficient for Right Lateral Bending vs. Subjective Rating.

Table 70: Regression Coefficients for Right Lateral Bending vs. LEAP Course Subjective Rating

Right Lateral Bending vs. LEAP Course Subjective Rating, Regression Coefficients				
	Mean	2.5th Percentile	97.5th Percentile	SE
Slope	0.11	0.07	0.16	0.02
Intercept	1.02	-0.52	2.75	0.83
R^2	0.30	0.11	0.46	0.09

Table 71 shows the regression coefficients and 2.5th/97.5th percentiles for each coefficient for Left Lateral Bending vs. Subjective Rating.

Table 71: Regression Coefficients for Left Lateral Bending vs. LEAP Course Subjective Rating

Left Lateral Bending vs. LEAP Course Subjective Rating, Regression Coefficients				
	Mean	2.5th Percentile	97.5th Percentile	SE
Slope	0.12	0.07	0.16	0.02
Intercept	0.93	-0.59	2.58	0.81
R^2	0.36	0.18	0.54	0.09

Table 72 shows the regression coefficients and 2.5th/97.5th percentiles for each coefficient for Front Forward Flexion vs. Subjective Rating.

Table 72: Regression Coefficients for Front Forward Flexion vs. LEAP Course Subjective Rating

Front Forward Flexion vs. LEAP Course Subjective Rating, Regression Coefficients				
	Mean	2.5th Percentile	97.5th Percentile	SE
Slope	-0.03	-0.08	0.01	0.02
Intercept	6.28	4.34	8.36	1.02
R^2	0.06	-0.09	0.12	0.06

Table 73 shows the regression coefficients and 2.5th/97.5th percentiles for each coefficient for Right Shoulder Abduction vs. Subjective Rating.

Table 73: Regression Coefficients for Right Shoulder Abduction vs. LEAP Course Subjective Rating

Right Shoulder Abduction vs. LEAP Course Subjective Rating, Regression Coefficients				
	Mean	2.5th Percentile	97.5th Percentile	SE
Slope	0.04	0.02	0.05	0.01
Intercept	-0.58	-3.09	1.91	1.29
R^2	0.28	0.08	0.46	0.10

Table 74 shows the regression coefficients and 2.5th/97.5th percentiles for each coefficient for Left Shoulder Abduction vs. Subjective Rating.

Table 74: Regression Coefficients for Left Shoulder Abduction vs. LEAP Course Subjective Rating

Left Shoulder Abduction vs. LEAP Course Subjective Rating, Regression Coefficients				
	Mean	2.5th Percentile	97.5th Percentile	SE
Slope	0.03	0.02	0.05	0.01
Intercept	-0.06	-2.66	2.52	1.32
R^2	0.25	0.03	0.44	0.10

Table 75 shows the regression coefficients and 2.5th/97.5th percentiles for each coefficient for Right High Knee Lift vs. Subjective Rating.

Table 75: Regression Coefficients for Right High Knee Lift vs. LEAP Course Subjective Rating

Right High Knee Lift vs. LEAP Course Subjective Rating, Regression Coefficients				
	Mean	2.5th Percentile	97.5th Percentile	SE
Slope	0.11	0.06	0.16	0.02
Intercept	-7.26	-12.60	-1.69	2.79
R^2	0.34	0.13	0.56	0.11

Table 76 shows the regression coefficients and 2.5th/97.5th percentiles for each coefficient for Left High Knee Lift vs. Subjective Rating.

Table 76: Regression Coefficients for Left High Knee Lift vs. LEAP Course Subjective Rating

Left High Knee Lift vs. LEAP Course Subjective Rating, Regression Coefficients				
	Mean	2.5th Percentile	97.5th Percentile	SE
Slope	0.10	0.05	0.15	0.03
Intercept	-6.29	-11.90	-0.71	2.84
R^2	0.31	0.08	0.53	0.12

3.5.3 ROM Correlation with RPE

Table 77 summarizes the ROM correlation with the overall LEAP course RPE. The regression line coefficients for each correlation as well as their respective 2.5th and 97.5th percentiles for each of the coefficients are summarized in the following tables.

Table 77: Summary of ROM correlation with LEAP course RPE

Range of Motion	Method	Correlation with RPE (R^2)
Right Trunk Rotation	iRoM	0.06
Left Trunk Rotation	iRoM	0.04
Right Lateral Bending	iRoM	0.08
Left Lateral Bending	iRoM	0.14
Front Forward Flexion	Natick	0.03
Right Shoulder Abduction	Natick	0.15
Left Shoulder Abduction	Natick	0.17
Right High Knee Lift	Natick	0.20
Left High Knee Lift	Natick	0.14

The associated graphs for each regression line can be seen in Annex M: Additional Regression Results.

Table 78 shows the mean slope, intercept, and R^2 values, the standard error (SE) as well as the 2.5th and 97.5th percentiles computed through the two-stage cluster bootstrap techniques for Right Trunk Rotation vs. RPE.

Table 78: Regression Coefficients for Right Trunk Rotation vs. LEAP Course RPE

Right Trunk Rotation vs. LEAP Course RPE, Regression Coefficients				
	Mean	**2.5th Percentile**	**97.5th Percentile**	**SE**
Slope	-0.06	-0.14	0.02	0.04
Intercept	16.20	12.91	18.78	1.49
R^2	0.06	-0.08	0.12	0.05

Table 79 shows the regression coefficients and 2.5th/97.5th percentiles for each coefficient for Left Trunk Rotation vs. RPE.

Table 79: Regression Coefficients for Left Trunk Rotation vs. LEAP Course RPE

Left Trunk Rotation vs. LEAP Course RPE, Regression Coefficients				
	Mean	**2.5th Percentile**	**97.5th Percentile**	**SE**
Slope	-0.04	-0.12	0.05	0.04
Intercept	15.35	12.44	18.02	1.43
R^2	0.04	-0.08	0.07	0.04

Table 80 shows the regression coefficients and 2.5th/97.5th percentiles for each coefficient for Right Lateral Bending vs. RPE.

Table 80: Regression Coefficients for Right Lateral Bending vs. LEAP Course RPE

Right Lateral Bending vs. LEAP Course RPE, Regression Coefficients				
	Mean	**2.5th Percentile**	**97.5th Percentile**	**SE**
Slope	-0.09	-0.17	0.00	0.04
Intercept	16.89	13.71	19.69	1.51
R^2	0.08	-0.07	0.15	0.06

Table 81 shows the regression coefficients and 2.5th/97.5th percentiles for each coefficient for Left Lateral Bending vs. RPE.

Table 81: Regression Coefficients for Left Lateral Bending vs. LEAP Course RPE

Left Lateral Bending vs. LEAP Course RPE, Regression Coefficients				
	Mean	**2.5th Percentile**	**97.5th Percentile**	**SE**
Slope	-0.12	-0.20	-0.02	0.05
Intercept	17.86	14.69	20.66	1.54
R^2	0.14	-0.05	0.27	0.08

Table 82 shows the regression coefficients and 2.5th/97.5th percentiles for each coefficient for Front Forward Flexion vs. RPE.

Table 82: Regression Coefficients for Front Forward Flexion vs. LEAP Course RPE

Front Forward Flexion vs. LEAP Course RPE, Regression Coefficients				
	Mean	**2.5th Percentile**	**97.5th Percentile**	**SE**
Slope	0.03	-0.07	0.09	0.04
Intercept	12.79	9.74	16.89	1.79
R^2	0.03	-0.08	0.05	0.04

Table 83 shows the regression coefficients and 2.5th/97.5th percentiles for each coefficient for RCA for Right Shoulder Abduction vs. RPE.

Table 83:Regression Coefficients for Right Shoulder Abduction vs. LEAP Course RPE

Right Shoulder Abduction vs. LEAP Course RPE, Regression Coefficients				
	Mean	**2.5th Percentile**	**97.5th Percentile**	**SE**
Slope	-0.04	-0.07	-0.01	0.02
Intercept	20.07	16.01	24.43	2.15
R^2	0.15	-0.06	0.29	0.09

Table 84 shows the regression coefficients and 2.5th/97.5th percentiles for each coefficient for Left Shoulder Abduction vs. RPE.

Table 84: Regression Coefficients for Left Shoulder Abduction vs. LEAP Course RPE

Left Shoulder Abduction vs. LEAP Course RPE, Regression Coefficients				
	Mean	**2.5th Percentile**	**97.5th Percentile**	**SE**
Slope	-0.04	-0.07	-0.02	0.01
Intercept	20.28	16.57	24.53	2.02
R^2	0.17	-0.04	0.33	0.10

Table 85 shows the regression coefficients and 2.5th/97.5th percentiles for each coefficient for Right High Knee Lift vs. RPE.

Table 85: Regression Coefficients for Right High Knee Lift vs. LEAP Course RPE

Right High Knee Lift vs. LEAP Course RPE, Regression Coefficients				
	Mean	**2.5th Percentile**	**97.5th Percentile**	**SE**
Slope	-0.13	-0.23	-0.04	0.05
Intercept	28.46	18.67	38.54	5.17
R^2	0.20	-0.04	0.37	0.11

Table 86 shows the regression coefficients and 2.5th/97.5th percentiles for each coefficient for Left High Knee Lift vs. RPE.

Table 86: Regression Coefficients for Left High Knee Lift vs. LEAP Course RPE

Left High Knee Lift vs. LEAP Course RPE, Regression Coefficients				
	Mean	**2.5th Percentile**	**97.5th Percentile**	**SE**
Slope	-0.11	-0.19	-0.02	0.04
Intercept	25.60	16.42	34.86	4.77
R^2	0.14	-0.07	0.27	0.09

4. Discussion

4.1 Obstacle Course

The analyses for the obstacle course performance were separated into four different sections: total course performance, obstacle performance, transition time performance, and ancillary stand performance. The relevant findings and possible explanations are discussed below.

4.1.1 Total Course Performance

Overall course completion times were significantly different across all analyzed conditions. The soldiers' fastest course times were completed in the baseline condition. It comes as no surprise that this was the fastest time since Condition A was considered the slick condition and consisted of only combat trousers, their t-shit, combat shit, combat boots, in-service helmet, and C7A2 assault rifle with C79 sight and sling. The next slowest course time was completed in Condition B (FFO – FPV and TAV) which, again, is as expected due to the addition of body armour and combat load. The addition of extended body armour (PUG/POG, and shoulder brassards) resulted in the slowest total course completion time. These findings suggest that the addition of extended body armour decreases a soldier's performance on the CAN-LEAP course in a statistically significant way; whether the mean differences observed between baseline (262.19s), Condition B (323.10s) and Condition E (347.91s) are operationally meaningful is another question.

Although no statistical tests of significance were run on Conditions C (FFO + PUG/POG), D (FFO + brassards), and F (FFO + PUG), overall course completion times for Conditions D and F were similar to that of Condition B. This may indicate that the PUG and shoulder brassards, individually, did not appear to be any more of a hindrance to the overall course time than when wearing solely the FPV and TAV. Given this observation, it appears that the addition of the combination of all three pieces of extended body armour (PUG, POG, shoulder brassards) caused a noticeable hindrance resulting in the lowest course completion time, while the addition of only one piece (PUG or brassards) or two pieces (PUG and POG) did not have a noticeable impact on overall course time.

4.1.2 Subjective Ratings for Overall Performance

Subjective ratings for overall performance were significantly different across all analyzed conditions (A, B, E). Self-reported rating of overall performance indicated Condition E (FFO +PUG/POG) as the lowest, which is aligned with the fact that Condition E was the slowest course time. According to the comments made in the focus group, this dissatisfaction with Condition E was likely due soldiers' discomfort and perceived restrictiveness of the PUG and POG. Condition C (FFO + PUG/POG) appears to have a similar overall subjective rating which would back up that theory. It would also appear that Conditions D (FFO + brassards) and F (FFO + PUG) had similar overall subjective ratings to that of Condition B which may suggest that soldiers did not dislike the addition of shoulder brassards or just the PUG any less than wearing just their FPV and TAV; this suggests that the POG is a primary driver of dissatisfaction amongst the additional armour components (brassard, PUG, POG). In contrast, soldiers subjectively rated Condition A (slick) the highest which is consistent with their objective results.

4.1.3 Rating of Perceived Exertion

The two armoured conditions, FFO (B) and FFO extended (E), were given similar perceived ratings of exertion, while the slick condition (A) were rated significantly lower in RPE. It is unsurprising that the addition of body armour led to higher levels of exertion. There was no significant difference in ratings of perceived exertion between the FFO condition and the FFO extended (PUG/POG and brassards) condition which is not consistent with soldiers' subjective ratings given in the questionnaire. This likely shows that, while soldiers did not feel significantly more exerted after completing the obstacle course, the subjective acceptability of their overall performance and completion time was significantly affected by the addition of the shoulder brassards and PUG/POG.

4.1.4 Performance by Obstacle

In addition to total obstacle course time, the results for each individual obstacle were analyzed separately. The general trend observed for most obstacles was different than what was seen for overall course performance. Generally, the obstacle times indicated that the addition of body armour significantly affected obstacle completion times however the addition of extended body armour did not significantly affect obstacle completion time any further. The following obstacles displayed this general trend between conditions:

- Tunnel and Hatch
- Sprint
- Casualty Drag
- Windows
- Balance Beam
- Low Crawl
- Back Crawl
- High Crawl
- Outer Wall

The obstacles that followed the same general trend as the overall obstacle course performance often required more hip and shoulder mobility from the soldier thus more easily differentiating between the FFO and FFO extended condition. These obstacles are discussed in the subsections below.

Stairs and Ladder

The use of the FitLight timing system allowed for certain obstacles, such as the stair and ladder obstacle, to be split up and analyzed into separate component parts. The stair and ladder obstacle was split into four segments:

1) Ascending steep stairs/descending shallow stairs
2) Ascending shallow stairs/descending steep stairs
3) Ascending straight ladder/descending angled ladder
4) Ascending angled ladder/descending straight ladder

For the stair components, the trends mirrored those observed for the overall obstacle course time where obstacle times were significantly slower in Condition E than in Condition B and A. In addition, although no statistical tests of significance were completed on Conditions C, D, and F, the obstacle timings for all three conditions appeared to be similar to the timings of Condition B which may

indicate that the individual equipment components were not slowing the soldiers down, however the combination of all three components significantly hindered soldiers' performance when ascending and descending shallow and steep stairs.

For the ladder components, ascending the straight ladder and descending the angled ladder mirrored the trend observed for the overall obstacle course time but for the ascending the angled ladder and descending straight ladder interval, obstacle timings for Condition E did not differ significantly from obstacle timings for Condition B. This may be attributed to the restrictiveness of the extended body armour when having to reach directly upwards. This type of movement is more challenging than when climbing an angled ladder which may accentuate the restrictiveness of the extended body armour.

Agility Run

All conditions for the agility run obstacle times were significantly different with soldiers completing the obstacle fastest in Condition A and slowest in Condition E. Although no statistical tests of significance were run on Conditions C, D, and F, it appears that the obstacle timings for Conditions D (FFO + brassards) and F (FFO + PUG) were similar to the timings of Condition B while the obstacle timings for Condition C (FFO + PUG/POG) were similar to the timings in Condition E, suggesting that the combination of the PUG/POG hindered the soldiers' ability to complete the agility run.

Bounding Rushes

All conditions for the bounding rushes obstacle times were significantly different with soldiers completing the obstacle fastest in Condition A and slowest in Condition E. Although there were no statistical tests of significance ran on Conditions C, D, and F, it would appear that their obstacle times were similar to the timings for Condition B. This may suggest that the individual addition of the PUG/POG, just the PUG, or the shoulder brassards did not appear to hinder soldier performance on the bounding rushes any more than FFO. The addition of all three equipment components in Condition E, significantly decreased soldier performance suggesting that this combination affects soldiers' ability to go from standing to prone and acquiring a sight picture.

Inner Wall

The obstacle timings for the inner wall mirrored the general trend that was seen for the overall obstacle course time.

4.1.5 Performance by Transition Time

Using the FitLight timing system allowed for discrete transition times within the obstacle course. This allowed for the analysis of completion times not only of the individual obstacle itself, but also of the different transition times between obstacles. The transition times that were deemed to be of relevance were the tunnel to sprint (getting from a prone to standing position), the stair to ladder (sling rifle), the stair and ladder to agility (unsling rifle), agility to casualty drag (some rifle slinging), balance beam to crawl (getting from standing to prone position), and crawl to outer wall (getting from prone to standing posture). Almost all transition times showed no significant difference between wearing body armour (Condition B) and wearing extended body armour (Condition E), suggesting that transition times were not influential in differentiating the two body armour conditions.

The only transition time that suggested a difference in wearing extended body armour in comparison to just FFO, was during the tunnel to sprint transition. During this transition, Condition E was significantly

slower than the other conditions suggesting that soldiers had more difficulty getting from a prone position, at the end of the tunnel, to a standing position, at the beginning of the sprint. As has been noted in some of the obstacle timings, this is likely attributed to the combination of the PUG/POG and shoulder brassards limiting the soldiers' ability to easily get from a prone to standing position.

4.1.6 Ancillary Stands

The goal for including accessory stations in the CAN-LEAP (i.e. those other than the timed obstacle course) was to gather objective combat-related performance metrics and subjective ratings (as in the case of the Questionnaire Kiosk) that could not effectively be captured within the parameters of the timed obstacle course.

4.1.6.1 *Noptel*

For the Noptel Marksmanship station, participants were required to perform three sets of three shots, with each set being performed in a different randomized shooting posture (standing, kneeling, or prone). The shooting task was performed in a rested state prior to the obstacle course being run, and immediately following the completion of the obstacle course in a fatigued state. Daily, participants completed a zeroing process where they each fired five shots from the prone position at the target; the centre of this shot grouping was used as the aiming point for all analyses. The three shots taken in each posture in the rested and fatigued states were analyzed using the aiming point to determine the distance from center.

As hypothesized, there was a significant difference between accuracy results with respect to rest state, where rested shooting resulted in shots landing closer to the aiming point than in fatigued shooting. For both rested and fatigued states, there was a significant difference found between shooting postures, where prone resulted in significantly closer distances to the aiming point than both kneeling and standing. This is expected as the prone position is a more stable shooting posture than kneeling or standing.

With respect to comparisons between conditions, in both the rested and fatigued states shot distances were not found to be any closer to the aiming point in one condition over another; there was no significant difference in shot distances between conditions. This contradicts the LEAP course findings where the overall LEAP time was significantly affected by addition of body armour and extended body armour. This could indicate that although the addition of body armour (and extended body armour) significantly reduced LEAP course performance, the additional equipment did not significantly affect marksmanship.

The lack of difference found between conditions in specifically the fatigued state, but also the rested state, may also suggest that the firing task was not challenging enough to elicit a sufficient level of heterogeneity in the results and tease out the differences between conditions. Suggestions for increasing the difficulty of this task include moving the target further away from the shooter, imposing more strict external time pressure, and/or instituting a friend/foe decision into the firing sequence.

4.1.6.2 *Vertical Weight Transfer*

The vertical weight transfer task was performed twice in each condition; it was performed once in the rested state and once in the fatigued state. Interestingly, the analyses showed that soldiers did not complete the task any faster in the rested state than in the fatigued state. The analysis was completed together for the rested and fatigued data set and showed that soldiers performed the vertical weight transfer task significantly faster in Condition A (slick) than in Conditions B and E. This is expected, since the addition of body armour will traditionally decrease the speed with which soldiers can complete a task. Since the task was not completed significantly faster in Condition B (FFO) than in

Condition E (FFO extended), this may show that the extended body armour did not significantly affect the soldiers' ability to move their upper body in order to complete this type of task.

It was unexpected that there was no significant difference in timings between the rested and fatigued states, however this is likely due to the lack of fatigue caused by the additional body armour used in this study. It is likely that although the addition of the FFO body armour, PUG/POG, and shoulder brassards restricted motion and significantly decreased LEAP course completion time, the overall weight and effect of this additional body armour did not significantly affect the soldiers' fatigue level.

4.1.6.3 *Horizontal Weight Transfer*

The horizontal weight transfer task was performed twice in each condition; it was performed once in the rested state and once in the fatigued state. The trends for timings identified in the horizontal weight transfer stations mirrored those of the vertical weight transfer.

4.1.6.4 *Vertical Jump*

Soldiers performed three repetitions of the vertical jump task in each condition, and the average jump height was calculated and analyzed. For this task, the analysis showed that participants were able to jump significantly higher in the fatigued state than in the rested state. Although this seems unusual, this finding is consistent with past LEAP reports where the general trend of vertical jump height was that the fatigued jump was higher than the rested jump; these findings were typically not significant though. This may be because the individual has warmed up from doing the LEAP run.

Unsurprisingly, significantly higher jump heights were achieved when participants were in Condition A than in Conditions B and E both before running the LEAP course and after running the LEAP course. There was no significant difference in jump height after adding extended body armour in both the fatigued and rested state indicating that although adding body armour decreases jump performance, extended body armour may not have an added significant effect on jump height.

4.1.6.5 *Horizontal Jump*

Soldiers performed one maximal effort leap at the horizontal jump station to simulate leaping over obstacles in their path such as hedges or canals. For this task, the analysis showed that participants were able to jump significantly further in the fatigued state than in the rested state. While this is interesting, it is not overly meaningful and may have been associated with the warm-up effects from running the LEAP course.

Unsurprisingly, significantly further distances were achieved when participants were wearing Condition A than when they were wearing Conditions B and E. In the fatigued state there was no significant difference in the distances achieved with and without extended body armour (Conditions B and E), however in the rested state participants jumped significantly shorter distances when wearing extended body armour than when wearing just their FPV and TAV. This difference in results for the fatigued state and rested state may be attributed to the tightness of the PUG/POG and/or shoulder brassards. The PUG/POG and/or shoulder brassards may have loosened and become more flexible and less restrictive over the duration of the LEAP course allowing the participant to be able to jump further when completing this station after their LEAP run, and restricting the participant's jump distance before the run, resulting in the difference between Condition B and E in the fatigued state to not be significant. This finding could also be a statistical anomaly and not overly meaningful.

4.2 Range of Motion

The analyses for the range of motion measurements were divided into the five main measures: trunk rotation, lateral bending, front forward flexion, high knee lift, and shoulder abduction. Within these

measures all methods were analyzed to determine the effect of condition, iteration, direction, and trials on the overall ROM.

A common theme throughout all of the ROM analyses was the significant differences between methods. While interesting, this finding is not overly important and was expected for most of the methods. Given the different protocols, administrators, reference points, tools, and techniques employed across the methods, it makes sense that the measurement values were not identical. The only methods that should have been similar throughout this study were the iRoM and Digital methods since they both used the same motion capture system with slightly different protocols. Any observed differences in iRoM and Digital results will be discussed in more detail in the subsections below. Since none of the methods could be considered the gold standard for ROM measurements, speculations cannot be made as to which method was most accurate. Instead, general trends and reliability of methods were analyzed. The repeatability of each method (i.e. Were the measurement values similar between Iterations 1 and 2?) and the precision of each method (i.e. Were the three trials similar to each other?) could be calculated and compared using ICCs as a form of reliability. These results are discussed in Section 4.3 Reliability of ROM Methods.

Another important observation to note is the observed reliability of the measurements obtained for the manual method. It was hypothesized that the manual method would obtain the least reliable measurement values due to interference of measurement tools with body armour resulting in inconsistent values between trials. Surprisingly, this lack of repeatability was not as apparent as expected likely due to the design of the study. For data collection, digital and manual methods were administered concurrently. The software used for the digital method constrains the variability between trials by requiring the user to re-do any trials that fall outside the variability parameters set. If this ever occurred during data collection, both digital and manual measurements were retaken meaning that the variability of the manual measurements was also controlled. Due to this oversight, the manual measurements that were collected were more consistent than normally obtained with this method since measurers do not typically accommodate for the variability of this data before moving on.

Unsurprisingly, all ROM measures, regardless of method, showed a significant decrease in ROM from Condition A (slick) to Condition B (FFO) indicating that the addition of body armour does decrease soldier ROM. Of more importance for discussion though were any ROM measures that showed a significant decrease in ROM when shoulder brassards and PUG/POG were added to the body armour. All significant decreases in ROM will be discussed in the sections below with possible reasons for the noticed effect.

Another common theme throughout all of the ROM analyses, regardless of method, was the significant increase in ROM across the three trials. This trend of increasing ROM from trials one to three was expected since the body becomes warmed up and more flexible with repetition. While the increase was statistically significant, the mean differences between trials was small. Any methods or ROM measures that did not follow this general trend are discussed in more detail in the sections below.

4.2.1 Trunk Rotation

Overall, participants' trunk rotation angles were significantly higher when they were in the slick condition than when they were wearing body armour. As hypothesized, adding the PUG/POG and shoulder brassards did not significantly decrease the participant's ROM when compared to just the FPV and TAV since none of these additional equipment components should have affected the trunk rotation measure. This general trend was consistent across all methods for trunk rotation.

An interesting finding was that trunk rotation angles significantly differed between iterations. The mean differences between trunk rotation angles was so small that this result is not overly meaningful

by itself. When looking at the differences in trunk rotation angles over the four iterations for each method, the results explained this overall finding a little better. As expected, for iRoM, Digital, and Manual methods, trunk rotation angles were not significantly different between iterations. The Natick method however produced a significantly higher trunk rotation angle during the first iteration than any of the other iterations which likely caused the small mean differences in the overall analysis of iterations. Trunk rotation angles being significantly higher during Iteration 1 for the Natick method is unusual since they should have been similar to Iteration 2 and likely all other iterations. A potential cause for this anomaly could be due to the measurer getting used to the measurement method during the first iteration since this general trend was also noticed in the lateral bending measure for Natick.

As mentioned previously, although trunk rotation angles were significantly different between most of the ROM methods this is not overly important. Since there was no gold standard to compare measurement values to, conclusions cannot be drawn regarding accuracy and as to which method is the most or least correct. Differences in methods (e.g., protocols, measurement tools, posture, etc.) likely caused each method to produce significantly different ROM values. Differences in protocols may have isolated the joints included in the ROM measurement differently. For example, in the iRoM, manual, and digital methods the participants bent forward at the waist while maintaining straight knees whereas in the Natick method participants were in a seated posture. These types of postural differences may have allowed the participant to involve more joints in the motion or be more willing to rotate further in a more comfortable posture. It is of importance however to note that Digital and iRoM methods did not produce significantly different trunk rotation results. It was hypothesized that this would be the case since both methods were based on the same motion capture system and theoretically should have had the same output. Since sensor placement was not altered between digital and iRoM methods (the ROM was completed one after the other for these methods), it was expected that there would not be any discrepancy between these two results.

Trunk rotation measurements were taken for both right rotation and left rotation. When completing the analysis, it was found that overall right and left directions for trunk rotation were significantly different. Although this was a combined analysis consisting of all conditions, when broken down by condition the results showed that in each of the three conditions right trunk rotation was always significantly higher than left trunk rotation. This makes sense since most participants were right handed, they likely could rotate further towards the right side than the left side and felt more comfortable rotating in that direction.

With regards to trials, the overall effect showed that all trials were significantly different than each other with the smallest trunk rotation angle being the first trial and the largest trunk rotation angle being the third trial. When looking at the differences in trunk rotation angles between trials for each method; digital, manual, and Natick all showed that trunk rotation angles taken during the first trial were significantly lower than trunk rotation angles taken during the third trial. It was expected that trunk rotation would increase as more trials were measured since the body becomes warmed up and more flexible with repetition. While the iRoM shared the same general trend for the trunk rotation angles captured for the three trials, none of the trials differed significantly. This is likely due to the constraint algorithm contained within the iRoM software that ensured the three trials were kept within a specified variability.

4.2.2 Lateral Bending

For lateral bending, the overall general trend was that lateral bend angles were significantly greater when participants were in the slick condition than when they were wearing body armour. As expected, lateral bend angles did not significantly decrease when participants donned the PUG/POG and shoulder brassards since neither of these equipment components affected this specific ROM.

Surprisingly, for iRoM, Digital, and Manual methods, the general trend for lateral bending appeared to show slightly greater angles for Condition E (FFO extended) than Condition B (FFO). The two methods that likely drove this result appear to be iRoM and Digital. For these two methods, lateral bend angles differed significantly for all conditions with lateral bend angles in the most encumbered condition (Condition E) being significantly higher than when participants were just wearing the FPV and TAV. It is possible that the required sensor placement in Condition E caused the illusion of greater lateral bend angles when participants were wearing extended body armour than when just wearing the FPV and TAV. With the addition of the PUG/POG in Condition E, measurers were forced to attach the pelvic sensor to the top of the POG as opposed to what was done in Condition B where the pelvic sensor was attached to the belt. The rigidity of the POG, and the slightly lower placement of the pelvic sensor, may have resulted in slightly higher lateral bend angles being captured than what was actually being achieved. Although not significant, the manual method showed this same general trend which again can possibly be explained by the altered placement of the measurement tools due to the POG. This probable cause is further supported by the Natick results, where a different protocol was used that did not involve measurement tools that were not interfered with by the POG. As was expected for lateral bending, the general trend for this method showed that lateral bend angles decreased as encumbrance increased.

Overall, all methods showed that lateral bend angles significantly increased over the three trials. This was expected since repetition of a movement increases an individual's flexibility and every time they do that movement they should be able to bend a little further. Although statistically the lateral bend angles were all significantly different, the mean differences between trials were all very small.

With respect to lateral bend directions, most of the time the conditions resulted in similar lateral bend angles for both sides however in Condition E (FFO extended) left lateral bend angles were significantly lower than right lateral bend angles. Since right and left lateral bend angles did not differ significantly when participants were just wearing the FPV and TAV, this difference may be attributable to the addition of the shoulder brassards, the PUG/POG, or both; however, why the extended armour may cause a difference between right and left lateral bending is not clear.

4.2.3 Front Forward Flexion

Due to unit inconsistencies, two separate analyses of front forward flexion were completed; iRoM and Digital methods were analyzed together and, in a separate analysis, Manual and Natick methods were analyzed together. Theoretically, since iRoM and Digital methods used the same sensor system, front forward flexion results should not have differed significantly; however, due to sensor movement issues observed in the slick condition it was hypothesized that these two methods may not have been as accurate as was expected. Unsurprisingly, the results showed that in the slick condition, front forward flexion angles captured during the Digital method and the iRoM method were significantly different however in the two encumbered conditions (Conditions B and E), the captured angles were not significantly different. These findings are consistent with the sensor movement issues observed during data collection. In the slick condition, the chest sensor would occasionally lift off of the participant's chest when they reached their arms in front to complete the front forward flexion motion. This sensor movement resulted in an inaccurate representation of the participant's ROM, typically capturing lesser angles in the slick conditions than in the encumbered conditions. In Conditions B and E, the chest sensor was placed under the FPV which helped decrease the effects of this sensor movement issue allowing for more consistent measures to be taken during the two ROM methods; however, it is unknown if there was any sensor movement underneath the FPV. This sensor movement likely also explains the significant difference between iterations as well for the iRoM and Digital method. Due to the suspicion that the results captured for front forward flexion from the iRoM

and Digital methods were inaccurate, conclusions regarding the effect of wearing body armour and extended body armour will not be drawn from these results.

For the other two methods (Natick and Manual), the results found that front forward flexion decreased significantly between conditions with Condition A allowing the greatest front forward flexion and Condition E restricting front forward flexion the most. These findings are consistent with other results that have been found during the LEAP course and range of motion stations where anything involving hip mobility and shoulder movement was significantly affected by the addition of extended body armour. This significant decrease in front forward flexion may be attributed to the addition of both the shoulder brassards and the PUG/POG. At this ROM station, it was noticed that participants had a lot of difficulty reaching their arms out in front of them and transitioning from a standing to seated position when wearing the shoulder brassards and PUG/POG. Both of these movements are important when completing the various ROM protocols for front forward flexion. These results may suggest that the shoulder brassards and PUG/POG significantly restricted the participants' ability to complete this motion in comparison to just wearing their FPV and TAV.

When looking to see if LEAP and/or doffing and donning had a significant effect on front forward flexion angle, there were some interesting findings. As expected, in the test-retest case (Iterations 1 and 2), front forward flexion angles were not significantly different showing that the two methods are reliably measuring this ROM. After the LEAP run, front forward flexion angles significantly increased, meaning that participants were able to reach significantly further. This may have been a result of equipment loosening and moving throughout the LEAP course allowing participants more hip and shoulder mobility for this station during Iteration 3. This increase in front forward flexion seen in Iteration 3 and 4 could have also been a result of participants warming up during the LEAP run and thereby gaining flexibility.

4.2.4 High Knee Lift

For high knee lift, the distance participants could raise their knee significantly decreased as encumbrance increased. As expected, the slick condition allowed participants to raise their knee significantly higher than when wearing FFO and the extended body armour. More importantly, the distance participants could raise their knee significantly decreased when the shoulder brassards and PUG/POG were added to their traditional FFO. The significantly reduced knee height indicates that the PUG/POG limited hip mobility and restricted the participants' typical range of motion when wearing body armour.

When looking at the differences between high knee lift distances over the four iterations the results showed that in the slick condition the high knee lift heights were not significantly different across iterations. This is expected since the soldiers were not wearing any body armour they should have been able to lift their leg to roughly the same height for every iteration. When the participants were wearing their FPV and TAV, their high knee lift height significantly decreased after they had run the LEAP course. Again, this is expected since the added weight of their FFO likely resulted in a higher fatigue level after having completed the LEAP course and as a result, participants did not lift their leg as high. After doffing the equipment, taking a break for lunch, and donning the equipment, participants' knee lift heights significantly increased to similar heights as the first and second iterations of the day. What is interesting to note is that when participants were wearing shoulder brassards and PUG/POG in addition to their FPV and TAV, their knee lift heights were not significantly different across iterations, suggesting that running LEAP and doffing/donning did not influence ROM performance when in Condition E. These findings could be a result of the PUG/POG limiting this knee lift motion. Even in the rested state, before the LEAP course had been run, the PUG/POG may have restricted this motion to such an extent that fatigue level after running the LEAP

course had no significant impact on the ability of the participant to raise their leg. Knowing the knee lift height was significantly lower when in Condition E than in Condition B is consistent with this theory suggesting that an increase in soldier burden (FPV and TAV) causes a significant decrease in ROM following the LEAP run but the addition of the PUG/POG and shoulder brassards causes an even more significant decrease in soldier ROM such that it is below the decreased level of ROM that would be typical of a soldier who was solely feeling the fatigue effects of the LEAP course.

4.2.5 Shoulder Abduction

For shoulder abduction, angles significantly decreased once the FPV and TAV were added to participants' equipment conditions; the ROM did not significantly decrease with the addition of the extended body armour. These findings may indicate that shoulder brassards do not restrict the upwards motion of the arm and shoulder, but given the results found in front forward flexion, were more likely to restrict movement of the arms when reaching in front.

4.3 Reliability of ROM Methods

Reliability of ROM methods was analyzed using an ICC method. As a rule of thumb, anything greater than 0.75 for an ICC is considered "good reliability" (Koo & Li, 2016). Most papers that calculated and used ICCs did not have situations where multiple ICCs had to be compared to draw a conclusion regarding reliability; typically, an ICC was used to inform on the reliability of a single method in a single situation as opposed to a comparison across methods under many different conditions. In the results for this study, many ICCs were calculated for each ROM measures since one method may be most reliable in one situation but not another. The ICCs were converted using Fisher's z-transformation and plotted to visually show the general reliability of each method for every measure.

ICCs were calculated between trials to compare the precision of methods for each ROM measure. For the ICCs calculated between trials, there was not much apparent variability between methods for each of the ROM measures. Most ICCs calculated between trials were greater than 0.75, indicating good reliability. There were two exceptions, both for the manual measurement method, in right and left lateral bending with ICCs slightly below 0.75. For lateral bending and trunk rotation measures, iRoM and Digital methods seemed to be slightly more precise which makes sense given the constraint parameter in the software that required the three trials to not exceed a certain variability. For front forward flexion measurements, iRoM and Natick methods appeared to be slightly more precise than the other two. For Natick, this may be attributed to the difference in protocol methods indicating that the Natick method may have better consistency between measurement trials. It was interesting to find that the iRoM system appeared to be one of the more precise methods for front forward flexion given the issues encountered with sensor movement during data collection. When discussing reliability, this finding is important to note because although the iRoM system was consistently measuring the same value for each of the three trials, when looking at the ICCs calculated between iterations for the iRoM method it appears much lower in reliability than both the Natick method and the Manual method. This finding confirms the theory that the sensor movement was affecting the reliability of the iRoM system by showing that measurements taken between Iterations 1 and 2 were typically not similar. Therefore, although the iRoM was highly precise, it was not repeatable.

When looking at the ICCs calculated between iterations, the only situations where the ICCs consistently fell below 0.75 (indicating poor reliability) were for the iRoM and Digital methods when measuring front forward flexion. This finding is not unexpected given the amount of sensor movement seen in Condition A when measuring front forward flexion. For this measure, Natick appeared to be more reliable, between iterations, when compared to the other methods. Although it

was expected that Manual and Natick would be similar, it makes sense that Natick methods might be slightly more reliable due to issues with the measurement tools for manual methods. Over the course of the six-week data collection period, the numbers on the Sit and Reach Box became more and more faded until they were no longer recognizable. Although alterations were made to get the most accurate readings possible, different measurers could have read slightly different measurements.

For lateral bending, iRoM appeared to have slightly higher ICCs indicating superior repeatability between iterations when compared to the other methods. For trunk rotation, digital and iRoM methods seemed to have slightly higher ICCs than the other two methods indicating better repeatability between iterations. These reliability findings for trunk rotation and lateral bending methods are not surprising since the iRoM system controlled the placement of the measurement tools by using IMUs, avoided body armour interference by placing the IMUs under the body armour, had a parameter set within the software to control variability in measurement trials, and digitally output ROM angles to minimize human error. Sensor movement was also not as much of a concern for lateral bending and trunk rotation as it was for front forward flexion due to the nature of the movement.

While the Natick method was the only method that measured high knee lift and shoulder abduction, ICC values were calculated to ensure that they were reliable methods. Both measures showed ICC values above 0.75 between trials and between iterations which indicates that the method was precise and reliable. This is not unexpected because for both methods, it was possible to place the measurement tools directly against the participant without having body armour interfere. This eliminated a significant potential source of variability and as a result these methods should have produced reliable measurements.

4.4 ROM Correlation with LEAP Performance

The following methods were chosen as the most repeatable and precise methods for each ROM measure based on their ability to differentiate between equipment conditions and relevant ICC values:

- Trunk Rotation: iRoM
- Lateral Bending: iRoM
- Front Forward Flexion: Natick
- High Knee Lift: Natick
- Shoulder Abduction: Natick

It was decided that for each of these ROM measures, a linear regression through two-stage cluster bootstrapping, would be done using overall course performance, subjective ratings of overall performance, and rating of perceived exertion to determine if ROM is predictive of LEAP performance. Since these three metrics summarize LEAP performance both subjectively and objectively, it was decided that they would be the best metrics to correlate with ROM.

The correlations found between ROM and overall course performance were fairly diverse, with the lowest R^2 value being 0.03 (front forward flexion) and the highest R^2 value being 0.30 (right and left high knee lift). While these R^2 values were not as high as expected, they do help to give an idea of which ROMs had a stronger relationship with overall course times. The best R^2 values were obtained through the linear regression with right and left high knee lift with an R^2 value of 0.30 for both. Interestingly, the lowest R^2 value was for the relationship between front forward flexion and overall LEAP course times. Due to the similarities in hip movement for front forward flexion and high knee lift, it was thought that both relationships with overall course time would have been similar however

there appears to have been very little relationship between front forward flexion and course times with the R^2 value only being 0.03.

With regards to the relationship between ROM and soldiers' subjective ratings, right and left lateral bending, right and left shoulder abduction, and right and left high knee lift all had higher R^2 values between 0.25 to 0.36. In contrast, front forward flexion had the lowest R^2 value with a value of 0.06. Although the R^2 values were fairly reasonable, the calculated slopes for each of the regression equations for subjective ratings were very tiny (<0.12). This could be a result of the Likert's Scale being restricted to a seven point scale while ROM values were much larger, or could indicate that although the regression equations may have explained a reasonable amount of the data, the relationships between ROM and subjective ratings was not very strong. An interesting finding was that right and left shoulder abduction were reasonably correlated with subjective ratings (R^2 values of 0.28 and 0.25 respectively) however their slope coefficients were 0.04 and 0.03 respectively. Although the R^2 between right/left shoulder abduction and LEAP course subjective ratings was amongst the highest for these regressions, their small slope coefficients indicate that a large decrease in ROM resulted in a very small decrease in subjective rating.

Overall, all R^2 values and slope coefficients calculated from the regression of ROM with ratings of perceived exertion were all very small. This suggests a very poor relationship between ROM measures and RPEs.

A regression coefficient analysis was also completed on this data set to look at the within subject relationships between ROM and LEAP performance metrics (see Annex J: Regression Coefficient Analysis). All R^2 values calculated for the RCAs were quite high for all combinations of ROM and LEAP performance regressions. These findings indicate that the strength of the relationship of ROM and LEAP performance metrics, within subject, were quite strong. Seeing lower correlations when computing linear regressions for between subjects (utilizing the bootstrapping method) suggests that the between subject differences overwhelmed the relationship of ROM and LEAP performance.

It should also be noted that during this experimentation, only three conditions were tested: A (slick), B (FFO), and E (FFO extended). The range of motion measurements used may not have necessarily been best suited to the equipment conditions tested during this particular trial resulting in little difference between ROM in encumbered conditions.

5. Conclusion

Many conclusions can be drawn from this study regarding the effects of extended body armour on LEAP course performance and ROM, the reliability of individual ROM methods, and the predictability of LEAP performance from ROM.

As expected, the soldiers posted the fastest obstacle course time in the slick condition, and the slowest time in the most encumbered condition. These results were consistent with overall subjective ratings; soldiers rated the slick condition as most acceptable and the most encumbered condition as least acceptable. What was interesting, however, was how both these results compared to the ratings of perceived exertion. The RPEs followed the same general trend where the worst ratings were given in the encumbered conditions, however the most encumbered condition (Condition E) was not rated significantly lower than when wearing just the FPV and TAV. The only obstacles that were able to differentiate between the effects of body armour and extended body armour were the stairs and ladder, agility run, bounding rushes and inner wall suggesting that the addition of the PUG/POG and shoulder brassards significantly restricted these types of movements. The CAN-LEAP course results suggested that the PUG/POG and shoulder brassards seemed to cause performance decrements during tasks that required upward movement of the legs and/or arms (agility run, stairs and ladder, and inner wall) and having to transition between standing and prone postures (bounding rushes).

As expected, all ROM measurements decreased as encumbrance increased. While all ROM measures differentiated between when participants were in the slick condition and when they were wearing FFO, only front forward flexion and high knee lift were able to differentiate between wearing FFO and extended body armour (PUG/POG and shoulder brassards). This finding may have been attributed to the shoulder brassards restriction of forward movement of the arms and the PUG/POG restricting flexion of the hips, both of which are accentuated during these two ROM measures.

With regards to reliability of methods, it was determined that most of the methods were reliable, but depending on the measure of interest, different methods were considered the most reliable. The iRoM method was determined to be most reliable, repeatable, and precise for both trunk rotation and lateral bending while the Natick method was determined to be the most reliable, repeatable, and precise when measuring front forward flexion. Although there were no other methods to compare for high knee lift and shoulder abduction, both measures were determined to be reliably and precisely measured by the Natick method.

Linear regressions on overall LEAP times, overall subjective ratings, and ratings of perceived exertion using the ROM measurements collected from each method deemed to be the most reliable for that measure using a two-stage cluster bootstrapping technique. This method produced regression models that explained only 3% to 36% of the data, depending on the measure. The strongest relationships were right and left high knee lift with LEAP course time (R^2=0.30), and right/left high knee lift (R^2=0.34, 0.31) and right/left lateral bend (R^2=0.30, 0.36) with subjective ratings. All linear regressions computed for ROM vs. RPE were very poorly correlated showing little to no relationship between ROM and ratings of perceived exertion.

This page intentionally left blank.

6. References

Bossi, L., Jones, M., Kelly, A., & Tack, D. (2016, September). A preliminary investigation of the effect of protective clothing weight, bulk and stiffness on combat mobility course performance. *Proceedings of the Human Factors and Ergonomics Society 2016 Annual Meeting*.

Field, C. A., & Welsh, A. H. (2007). Bootstrapping clustered data. *J.R. Statist. Soc. B*, 369-390.

Fisher, R. (1934). *Statistical Methods for Research Workers.* Edinburgh: Oliver and Boyd.

Girden, E. (1992). *ANOVA: Repeated measures.* Newbury Park, CA: Sage.

Greenhouse, S., & Geisser, S. (1959). On methods in the analysis of profile data. *Psychometrika, 24*(2), 95-112.

Huynh, H., & Feldt, L. (1976). Estimation of the Box Correction for Degrees of Freedorm from Sample Data in Randomized Block and Split-Plot Designs. *Journal of Educational Statistics, 1*(1), 69-82.

Koo, T., & Li, M. (2016). A Guideline of Selecting and Reporting Intraclass Correlation Coefficients for Reliability Research. *Journal of Chiropractic Medicine, 15*, 155-163.

Kozey, J., Reilly, T., & Brooks, C. (2005). Personal protective equipment affecting functional anthropometric measurement. *Occupational Ergonomics, 5*, 121-129.

Lorch, R., & Myers, J. (1990). Regression analyses of repeated measures data in cognitive research. *Journal of Experimental Psychology: Learning, Memory, and Cognition, Vol. 16*(1), 149-157.

McGraw, K., & Wong, S. (1996). Forming Inferences About Some Intraclass Correlation Coefficients. *Psychological Methods, 1*(1), 30-46.

Myers, L., & Broyles, S. (2000). Regression coefficient analysis for correlated binomial outcomes. *Journal of Applied Statistics, Vol. 27*(2), 217-234.

Shrout, P., & Fleiss, J. (1979). Intraclass Correlations: Uses in Assessing Rater Reliability. *Psychological Bulletin, 86*(2), 420-428.

Silver, N., & Dunlap, W. (1987). Averaging correlation coefficients: should Fisher's z transformation be used? *Journal of Applied Psychology, Vol. 72*(1), 146-148.

Solow, A. R. (1985). Bootstrapping Correlated Data. *Mathematical Geology, 17*(7).

This page intentionally left blank.

Annex A: Sub-Maximal Fitness Testing

Participants will be assessed for their level of fitness (predicted VO2 max) using the modified Canadian Aerobic Fitness Test (mCAFT) (Weller et al., 1995). The mCAFT is a sub-maximal aerobic fitness test where participants complete one or more sessions of three minutes of stepping at predetermined speeds, based on their age and gender. Everyone begins the stepping sequence on double 20.3 cm steps as shown in Figure 90.

Participants may start with either foot. Assuming they choose the right foot, they will step up onto the first step with their right foot, onto the second step with their left foot, up to the second step with their right foot, then down to the first step with their left, down to the floor with their right, then return to starting position by bringing their left foot down to the ground. They then repeat this sequence for three minutes at each stage.

Figure 90: Set-up for sub-maximal modified Canadian Aerobic Fitness Test (mCAFT)

The mCAFT is structured so that, in most cases, the participant's first three-minute stage is at a cadence intensity of 65 to 70 percent of the average aerobic power expected of a person ten years older. The starting stage (rate of stepping) is based on age and gender as indicated in Table 87 and Table 88 below.

Table 87: mCAFT Initial Starting Stage

Age	Starting stage for Males	Starting stage for Females
60-69	1	1
50-59	2	1
40-49	3	2
30-39	3	3
20-29	4	3
15-19	4	3

Table 88: Correct mCAFT Stepping Cadence (footplants/min)

Stage	Stepping cadence for Males	Stepping cadence for Females
1	66	66
2	84	84
3	102	102
4	114	114
5	132	120
6	144	132
7	118*	144
8	132*	118*

***NOTE:** Stages 1-6 for men and stages 1-7 for women are done using a two-step pattern on the double 20.3 cm steps. Stages 7 and 8 for men and stage 8 for women use a single-step pattern on a step 40.6 cm in height. (You can use the back-or side-of the top step for this)

The participant is informed that the first stepping exercise is three minutes in duration. He/she will cease to step when the music stops. The participant will be asked to stand motionless while the experimenter checks heart rate over a 10 second period. Depending on his/her heart rate response (see Table 89), the participant will be informed if he/she is to stop or continue for another stage of stepping. Instructions and time signals are given on a Compact Disc (CD) as to when to start and stop exercising and for the counting of the ten-second measurement of the post-exercise heart rate. Depending on the exercise heart rate response, the participant will either proceed to the next stepping stage or have the test terminated.

Table 89: Ceiling Post-Exercise Heart Rates

Age	10 Sec. Count	Monitor Reading	Age	10 Sec. Count	Monitor Reading
15	29	174	43	25	150
16	28	173	44	25	150
17	28	173	45	25	149
18	28	172	46	24	148
19	28	171	47	24	147
20	28	170	48	24	146
21	28	169	49	24	145
22	28	168	50	24	145
23	28	167	51	24	144
24	28	167	52	24	143
25	27	166	53	23	142
26	27	165	54	23	141
27	27	164	55	23	140
28	27	163	56	23	139
29	27	162	57	23	139
30	27	162	58	23	138
31	27	161	59	23	137
32	26	160	60	22	136
33	26	159	61	22	135
34	26	158	62	22	134
35	26	157	63	22	133
36	26	156	64	22	133
37	26	156	65	22	132
38	26	155	66	22	131
39	25	154	67	21	130
40	25	153	68	21	129
41	25	152	69	21	128
42	25	151			

Heart rate is recorded and VO2 max is calculated using the formula shown below:

Aerobic Fitness Score = 10 x [17.2 + (1.29 x O2 cost*) – (0.09 x Body mass) – (0.18 x age)]

***Table 90: O2 Cost of the last completed stage completed (in ml-kg-1min-1) for Different Stages of the mCAFT**

Stage	Males O_2 Cost	Females O_2 Cost
1	15.9	15.9
2	18.0	18.0
3	22.0	22.0
4	24.5	24.5
5	29.5	26.3
6	33.6	29.5
7	36.2	33.6
8	40.1	36.2

Annex B: Static Strength Testing

Static strength will be measured using three different protocols: upper limb static strength, shoulder strength, and lower limb static strength.

- *Upper limb static strength*: To measure upper limb static strength, a force gauge is attached to a sturdy steel chain, which is attached to an immoveable fixation point at ground level. The force gauge is attached to a point in the chain which coincides with the participants' elbow being flexed 90 degrees forward. The participant is instructed to stand feet shoulder width apart with the chain attachment point midway between the feet. The participant grasps the force gauge (palms up) and flexes their arms using their maximal strength. Encouragement is given by the researchers to help elicit a maximal effort. The force value (in kilograms) is noted from the force gauge and recorded.

- *Shoulder strength*: To measure shoulder strength, a force guage is attached to a sturdy steel chain, which is attached to an immoveable fixation point at ground level. The participant is instructed to stand erect on the force gauge platform with feet shoulder width apart, knees slightly bent and chain attachment point midway between feet, grasp the handle with a wide grip and elbows out and away from the body. When instructed, the participant begins exertion to maximum capacity and maintains for ~3 seconds. Encouragement is given by the researchers to help elicit a maximal effort. The force value (in kilograms) is noted from the force gauge and recorded.

- *Lower limb static strength*: To measure lower limb static strength, a force gauge is attached to a sturdy steel chain, which is attached to an immoveable fixation point at ground level. The participant is instructed to stand feet shoulder width apart with the chain attachment point midway between the feet, then bend his knees to 90°, and lower his arms down in front of him. The force gauge is attached to a point in the chain which coincides with where the centre of the palms are, with respect to the force gauge handles. With knees bent at 90°, the participant is instructed to grasp the force gauge handle (palms down) and extend at the knees using their maximal leg strength. Encouragement is given by the researchers to help elicit a maximal effort. The force value (in kilograms) is noted from the force gauge and recorded.

This page intentionally left blank.

Annex C: Original LEAP Method

The original LEAP ROM method has been previously described and approved in DRDC HREC protocols 2012-033 and 2013-071 - Effect of Load, Bulk and Stiffness of Soldier Equipment on Physical Performance: Canadian Load Effects Assessment Program (CAN-LEAP).

The participant's range of motion measurements were taken during each test condition, including the unencumbered baseline (boots, t-shirt & combat clothing). Measurements were taken using a combination of a goniometer, a Wells and Dillon Sit and Reach apparatus, an inclinometer and a digital level. The following ranges of motion were measured:

Trunk Forward Flexion (Modified Wells and Dillon Sit and Reach)

- The participant sat with legs fully extended with the soles of the feet placed flat against the horizontal crossboard of the apparatus.
- Both inner edges of the feet were placed 2 cm from the scale.
- Keeping the knees fully extended, arms evenly stretched, palms down, the participant bent and reached forward pushing the sliding marker along the scale with their fingertips as forward as possible.
- The position was held for approximately 2 seconds

Refer to Figure 91.

Figure 91: Modified Wells and Dillon Sit and Reach Test

Trunk Lateral Flexion (Standing)

- A single inclinometer was placed at the mid-level (T6) of the thoracic vertebra using a digital level as a vertical guide
- The level and inclinometer were adjusted until a zero degree reading was observed and centered on the spine
- The participant was instructed to bend the trunk to the side (their right) as far as possible and the inclinometer angle was recorded

Trunk Rotation

- The participant assumed a forward flexed posture, as shown in Figure 92, with the thoracic spine in as horizontal a position as can be achieved
- The inclinometers were positioned on T1 and T12 as shown in Figure 92, and the inclinometers were kept vertical
- The participant was instructed to rotate the trunk maximally to the right, and both inclinometer angles were recorded (Refer to Figure 93)
- The process was repeated three times
- Rotation angle was calculated as the difference between the T12 and T1 inclinometer readings

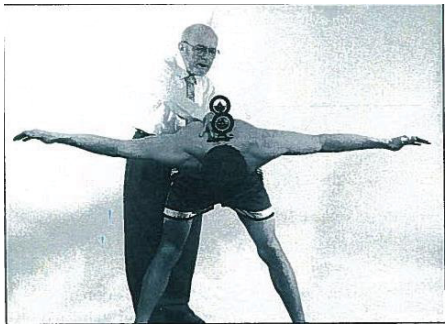

Figure 92: Measuring Trunk Rotation (initial posture)

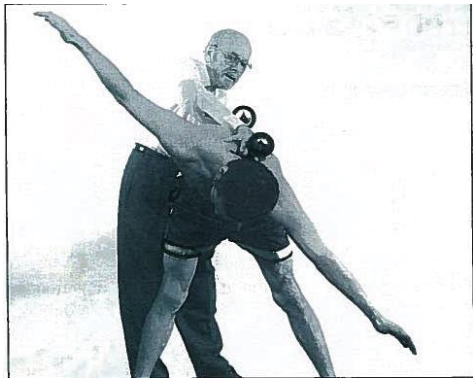

Figure 93: Measuring Trunk Rotation (rotated posture)

Annex D: USMC IMU Method

This method collected the following range of motion movements: trunk rotation, lateral bending, and front forward flexion. The ROM movements were identical to those described in Annex C: Original LEAP Method however, instead of using manual measurement devices the participants were equipped with 6 IMUs (OPAL – APDM Wearable Technologies, Portland, OR). The sensors were placed on the participant's shank (bi-lateral), thigh (bi-lateral), pelvis, and thorax using Velcro straps. The exact placement of the sensors is summarized in Table 91.

Table 91: IMU sensor placement for the iRoM software

Sensor	Placement
Thorax sensor: - Roughly 3 fingers below the suprasternal notch. Pelvic Sensor: - Above the sacrum but no higher than their iliac crests. - Attach to their belt using Velcro straps if possible.	The sensors on the torso, arms, forearms, and pelvis should be placed as illustrated below: 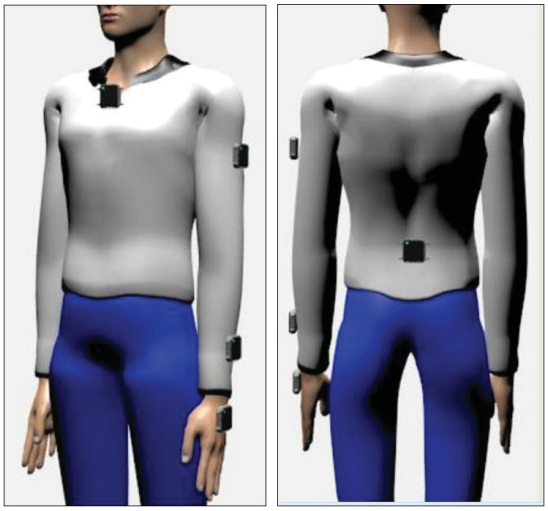
Leg sensor Thigh sensors: - About ¾ of the way up the thigh (on quad muscle) keeping the strap in a spot where it's not likely to slide up/down. Shank sensors: - No higher than the tibial tuberosity. - At top of calf muscle so as not to slip up/down.	The leg sensors should be placed as illustrated below: 

Custom written software (NexGen Ergonomics Inc., Pointe Claire, QC) was used to digitally output the ROM measurement (angle) and to ensure that the participant was not flexing or extending constrained joints (e.g. the software ensured that the knees stayed straight while capturing trunk rotation by providing a warning to the experimenter if either of their knees exceeded the pre-determined threshold for that joint – see Figure 94). The iRoM software also ensured consistency in measures by warning the experimenter if the three trials were not within five degrees of one another or ten percent of the mean (see Figure 95).

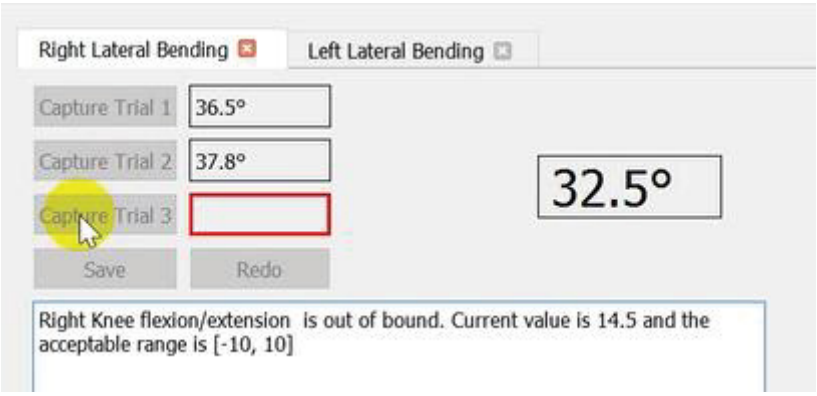

Figure 94: Example of a constraint joint falling outside the specified threshold

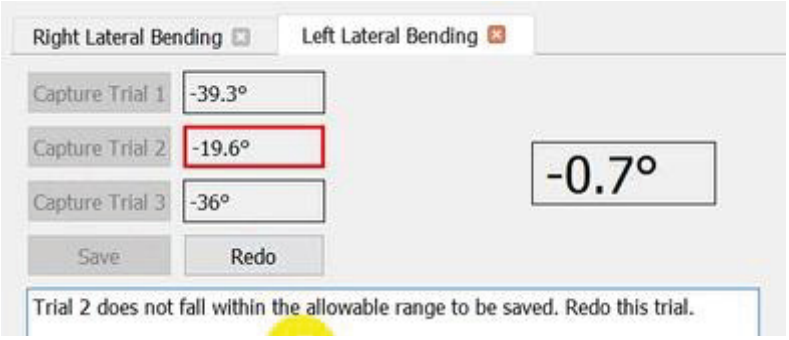

Figure 95: Example of the three trials not falling within the pre-defined specifications

The iRoM software captured each participant's range of motion and once saved, it output the data to a .csv file.

Annex E: Dalhousie Functional Reach Method

For the functional reach method, an electromechanical system called CPSAM (Dalhousie University, Halifax, NS) was used to create a functional reach envelope (Figure 96 and Figure 97). Participants were instructed to comfortably sit in a chair and a stylus was moved into position such that it was in light contact with the participant's skin at the C7 level of their spine. Participants were given a small handle to hold that was attached via four taut strings to four potentiometers. This allowed the experimenter to track the position of the participant's hand in three-dimensional space. Participants were then instructed to 'paint' as much of an imaginary surface as possible without bending their elbow and maintaining contact with the seat pan, seat back, and stylus at all times. Participants repeated the same 'painting' task while standing with their stylus in light contact with the sacrum (S1). This method has been previously described in the literature (Kozey, Reilly, & Brooks, 2005).

Figure 96: CSPAM electromechanical system

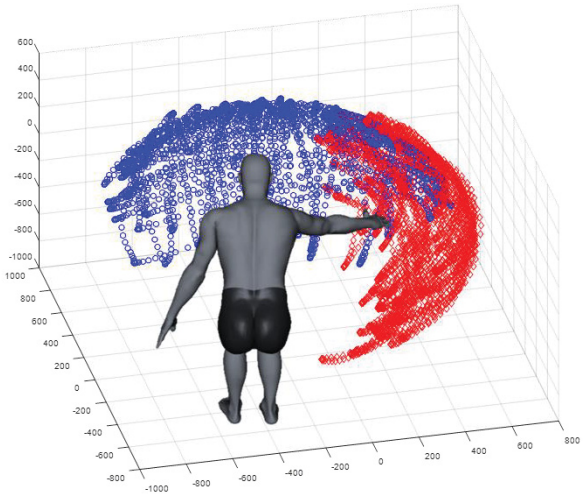

Figure 97: Functional Reach Envelope

Using the functional reach envelope data, functional range of motion measures for arm ab/adduction, flexion/extension, and horizontal flexion/extension (Figure 98) were derived.

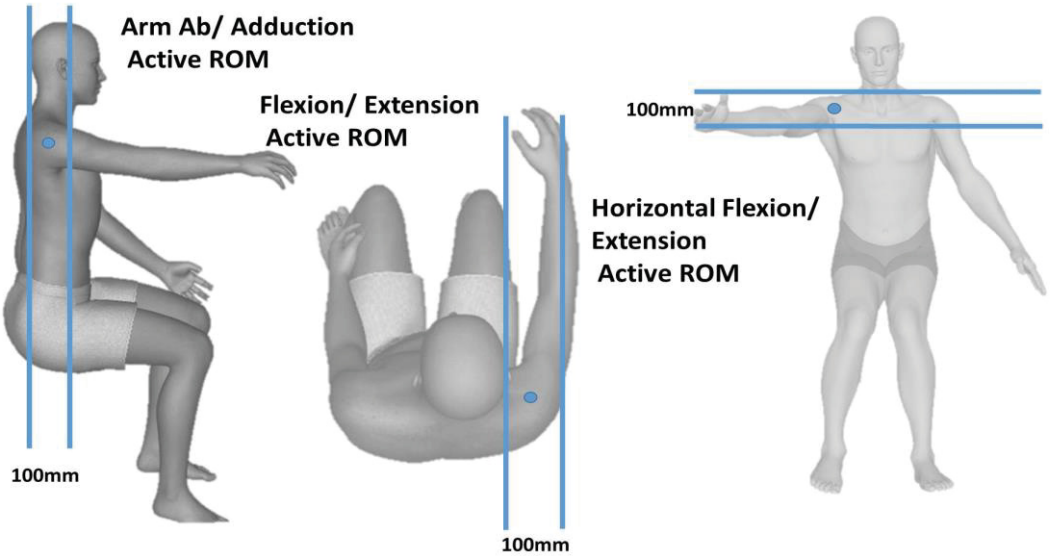

Figure 98: Functional Range of Motion measures

Annex F: Natick Manual Method

Trunk Forward Flexion

The participant was instructed to stand on the platform/box with feet parallel and shoulder width apart. Toes were at the edge of the box facing the upright measurement stick/vertical scale.

The participant attempted to touch their toes by bending at the waist, keeping knees straight. The participant performed two preliminary toe touches prior to starting measurements. Keeping hands together and sliding palms down the outside surface of the board/box, participants were instructed to hold their lowest point of reach for a few seconds before straightening again. The measurement taken was the distance between the longest fingertip and the floor. NOTE: The participant stood on block to allow for flexibility/movement beyond their toes. Participant performed this movement 2-3 times before being measured in order to loosen the muscles.

Trunk Lateral Flexion (Standing)

Participant was instructed to stand with feet shoulder width apart in the anthropometric standing posture. Arms hung freely at the sides of the body with palms facing against thighs. Participant was instructed to bend at waist, leaning as far to the right side of the body as possible, without falling over while keeping their body in the frontal plane. Participant's hand slid down their leg, with their fingertips pointed toward the ground. Both feet remained firmly on the ground, with the test participant's weight evenly distributed. Knees remained straight. Participant held his/her maximum position. Participant did not lean forward or backward. Participant's hand followed the leg so that they did not reach outward with their arm. Participant did not bend their knees or hip. Their fingers were extended, and they looked straight ahead.

Using an anthropometer, the measurer recorded the height from the floor of the longest fingertip on the participant's right hand, usually the middle finger, while the participant stood in the anthropometric posture. The anthropometer remained upright, and perpendicular to the floor. The measurer ensured that the top of the anthropometer did not hit/restrict the participant. After the participant leaned as far to the right as possible, the measurer again recorded the height from the floor of the longest fingertip on the right hand. A delta between the two measurements will be calculated during data analysis.

NOTE: This movement was performed 2 – 3 times before the measurements were started to ensure that the participant was limber. At least 4 measures were recorded to ensure consistency.

Trunk Rotation

Participant was instructed to sit upright on the anthro bench with shoulders back and set. They crossed their arms against their chest and held a rigid body bar at the level of the acromion (in order to visualize the angle of rotation). Participant's feet were flat on the footrest, approximately shoulder width apart, with knees at approximately 90 degrees of flexion. The participant was instructed to turn/twist at the lower back as far to the right as he/she could and hold it. Their head followed their chest, so that they were looking in the direction their chest was facing. Participant was instructed not to turn/twist their knees, hips, upper back, or head. It was ensured that the participant did not slide on their seat as they turned. This was repeated, rotating as far to the left as possible and held at that position.

Measurement used two approaches:

- 1st approach: using go---pro video placed immediately above participant's head; extracted measures from video analysis
- 2nd approach: center joint of goniometer was placed over the test participant's head, but as opposed to being located at the center of the head, it lay above the location where the spine would be if it radiated upward (sticker was used to mark this location and make tracking easier). Sticker or other mark was placed approximately on the participant's acromion

NOTE: This movement was performed 2-3 times before the measurements were started to ensure that the participant was limber. At least 4 measures were recorded to ensure consistency.

Annex G: Demographic Information Questionnaire

PARTICIPANT INFORMATION Participant #:_____

Military Occupation (e.g. infantryman, 0311)		Rank:	
		Age:	
Service	O Regular O Reserve	Indicate your handedness:	O Left handed O Right handed

Marksmanship			
O Shoot from the left O Shoot from the right		O left eye dominant O right eye dominant	
Indicate your Marksmanship level	O PWT 1 O PWT 3 Supplement O PWT 4 Supplement	O PWT 2 O PWT 3 O PWT 4	

Military Experience: Length of Service (Regular and Reserve)			
Years in Regular:		Years in Reserve:	

Operational Experience
Please note operational experience (by theatre) and tour duration (months) (e.g. Afghanistan 12 months)

Experience wearing body Armour	
Estimate number of days soft armour was worn in past 3 years	
In Training	days
On Operations	days
Estimate number of days hard armour was worn in past 3 years:	
In Training	days

On Operations	days
Have you ever worn a hard armour plate alone (in a plate carrier)?	○ Yes ○ No
If yes, estimate the number of days a plate carrier was worn in past 3 years:	
In Training	days
On Operations	days

Annex H: LEAP Station Descriptions

The following Annex describes each of the CAN-LEAP stations (i.e. individual obstacles and ancillary stands), including the proper method of traversing obstacles, how the station is operated, and brief descriptions of station or obstacle assembly if required.

The purpose of the descriptions is to give the reader a broader understanding of the course and its components, not to build and assemble it. In depth details of the CAN-LEAP assembly process can be found in the CAN-LEAP User Manual.

Dynamic warm-up

Prior to completing their run, participants underwent a researcher-led dynamic warm-up to mitigate the risk of injury and prepare for the physical nature of the tasks to follow. The dynamic warm-up consisted of the following components:

i. ***Bent Over Rotations:*** Begin with feet at a comfortable stance wider than shoulder width. Bend over at hips with arms fully extended at sides at 90 degrees from torso. Begin by swinging right arm towards left foot and repeating on opposite side. Continue this motion through comfortable range, but do not strain. Continue this motion for 30 seconds.

ii. ***Arm Circles:*** Stand with feet shoulder width apart and knees slightly bent. Raise arms to a 90 degree from the torso with arms fully extended. Begin by making small circles by bringing arms forward and gradually increase to a full range of shoulder motion. Change direction at 15 seconds. Repeat motion with arms moving in opposite direction for 15 seconds.

iii. ***High Knee Hold Walking while raising knees to chest***: Once knee has reached highest point of ROM, pull knee till a slight stretch is felt, continue with movement. Continue motion for 30 seconds alternating legs during walking.

iv. ***Lunge walk and trunk rotation:*** Begin by taking a large step in a forward direction and lowering body until the forward knee is at 90 degrees. While at lowest position rotate upper body towards forward leg through full ROM until slight stretch is felt. Bring other leg forward and repeat on other side. Continue lunge walk for 30 seconds.

v. ***Leg swings (forward/backward):*** Subjects stands with side to wall, arm length away with hand placed on wall for support. Raising leg closest to wall off of ground and begin by swinging through full ROM. Subject is instructed to swing through full ROM without straining self. 15 seconds on one leg and repeat on opposite leg for 15 seconds.

CAN-LEAP course and Fitlight

The obstacle course section was a series of ten mobility test stands (1-10) with the objective of determining when a soldier's performance is degraded due to various donned or carried equipment sets or configurations relative to a baseline. Of the ten segments, six contained semi-transportable obstacles, which have been constructed specifically for the CAN-LEAP project.

The sections below outline the physical specifications and the method of traversing each of the ten obstacles (segments) within the Fitlight-instrumented CAN-LEAP course. Participants completed all obstacles, in sequence, with no rest breaks. Total course completion time, time for each obstacle, and transition time between obstacles was recorded.

Fitlight Timing Mechanism

Fitlight is a wireless timing system consisting of a series of light-emitting diodes (LED) and a hand-held personal digital assistant (PDA) controller. This system captured time between de-activation of each light in order as the soldier passed by. The dimly lit Fitlight sensors sent out an invisible beam of 80 cm (distance is adjustable). Breaking this beam triggered the light to illuminate brightly and marked the start/end of a split time.

Figure 99: Fitlight Sensors

Tunnel and Hatch

The tunnel and hatch obstacle consisted of a four-step riser with a hatch located in the floor on the top of the stairs. Attached to this was a 'C' shaped tunnel (of varying diameters) that participants traversed through in a crawl position (refer to Figure 100).

Figure 100: Tunnel and Hatch Obstacle

The tunnel and hatch obstacle was comprised of the stair portion and nine separate tunnel segments as shown in Figure 101. The beginning of the tunnel was attached to the opening of the stair platform via screws and a connector ring. The lengths of each tunnel segment are outlined in Figure 101. The diameter of the tunnel segments varied between segments, with the smaller diameter measuring 24" and the larger diameter measuring 30" across.

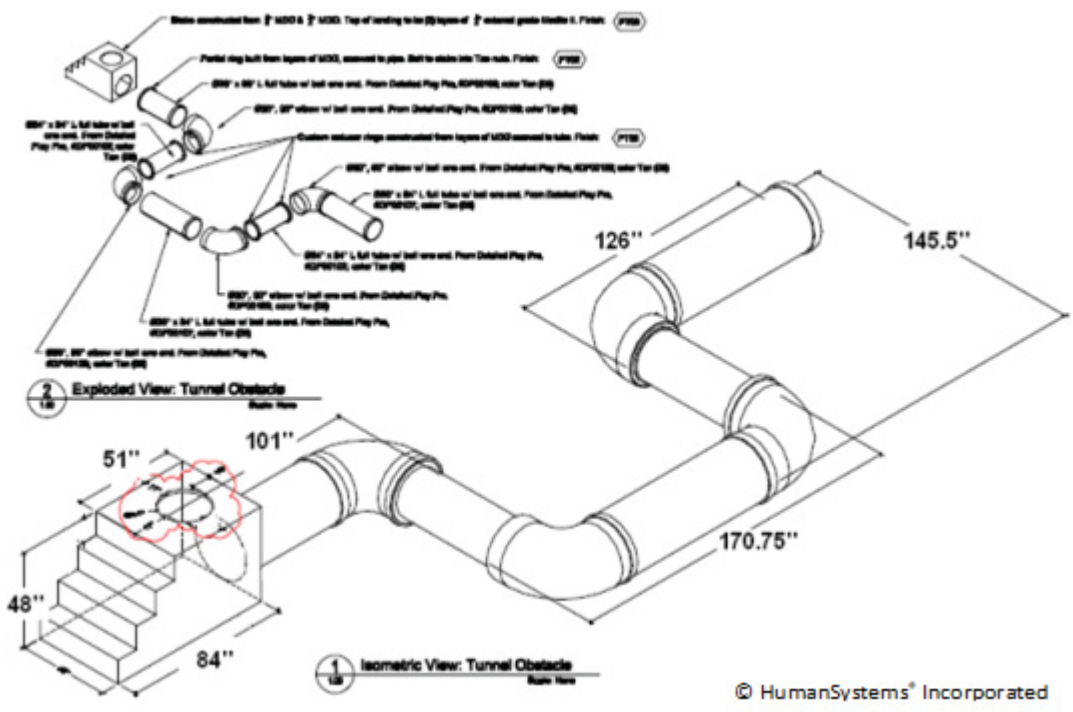

Figure 101: Dimensions of the Tunnel and Hatch Obstacle

To traverse the obstacle, the participant approached the stair portion of the tunnel and hatch and climbed up the stairs one step at a time. The participant then lowered himself (feet first) into the hatch opening, lowered himself into a crouch position, and entered the opening of the tunnel on all fours. The participant continued traversing through the tunnel until he emerged out the other end. Upon completing the length of the tunnel, the participant returned to a standing position while passing by the Fitlight at the end of the tunnel.

Sprint

After emerging from the tunnel obstacle, the participant then passed by the Fitlight which signified the start of the sprint segment (refer to Figure 102). The participant sprinted at his fastest capable running speed for 60 feet (18.3 m), and the sprint ended when the Fitlight at the end of the 60 feet was crossed.

Figure 102: Sprint Segment

Stair and Ladder

The stair and ladder obstacle consisted of two sets of stairs (one with a short run and high rise, the other with a low rise and long run), a platform at the top, and a ladder on each side (one angled, and one vertical) (refer to Figure 103). The stair and ladder obstacle was comprised of five separate segments that were connected with “roto-lock” connectors. The dimensions of the segments are shown in Figure 104.

Figure 103: Stair (steep and shallow rises) and Ladder (straight and angled)

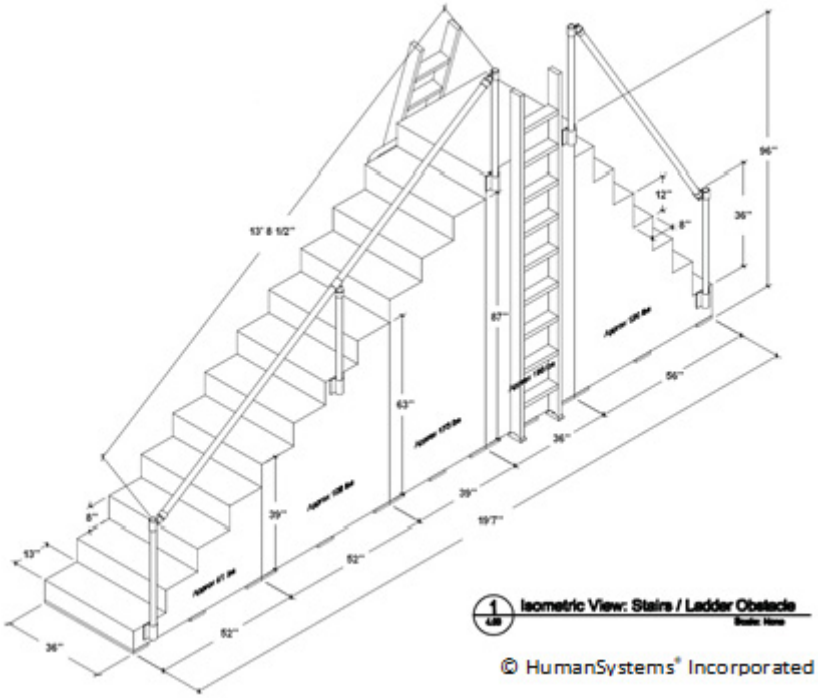

Figure 104: Dimensions of the Stair and Ladder Obstacle

Upon crossing the Fitlight at the start of the stair and ladder obstacle, the participant progressed through this obstacle in the following order:

1) climb up the short run/high rise stairs
2) climb down the long run/low rise stairs
3) pass the Fitlight and place two feet on the ground
4) climb up the long run/low rise stairs
5) climb down the short run/high rise stairs and pass the Fitlight
6) climb up the straight ladder
7) climb down the angled ladder
8) pass the Fitlight and place two feet on the ground
9) climb up the angled ladder
10) climb down the straight ladder

The participant finished this segment by passing the Fitlight at the end of the stair/ladder obstacle.

Agility Run

The agility run obstacle was a sprint around five poles set in a weaving pattern, with a step-over obstacle placed between each pole (refer to Figure 105). A Fitlight was placed at the beginning and end of the agility run. There was a distance of 21’ (6.4 m) between each pole, and a step-over obstacle (hurdle) was placed halfway between each set of poles, requiring the participant to jump or stride over it (see Figure 105).

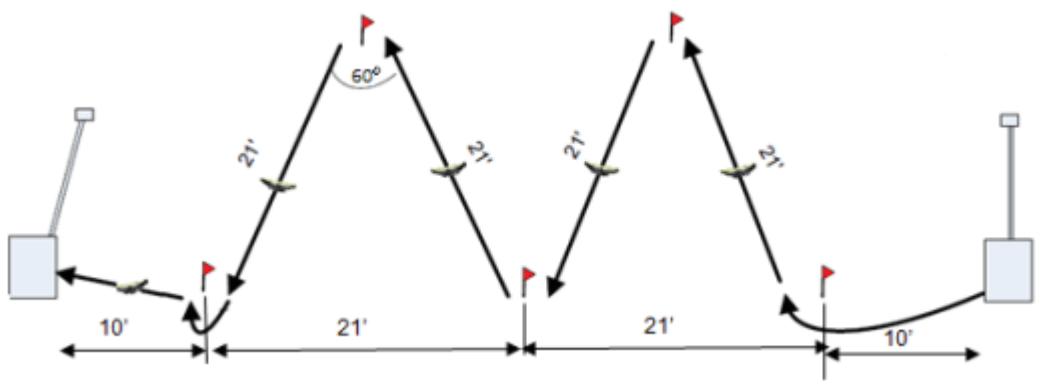

Figure 105: Agility Run Layout

This segment was completed when the participant passed the Fitlight after the fifth hurdle (refer to Figure 106).

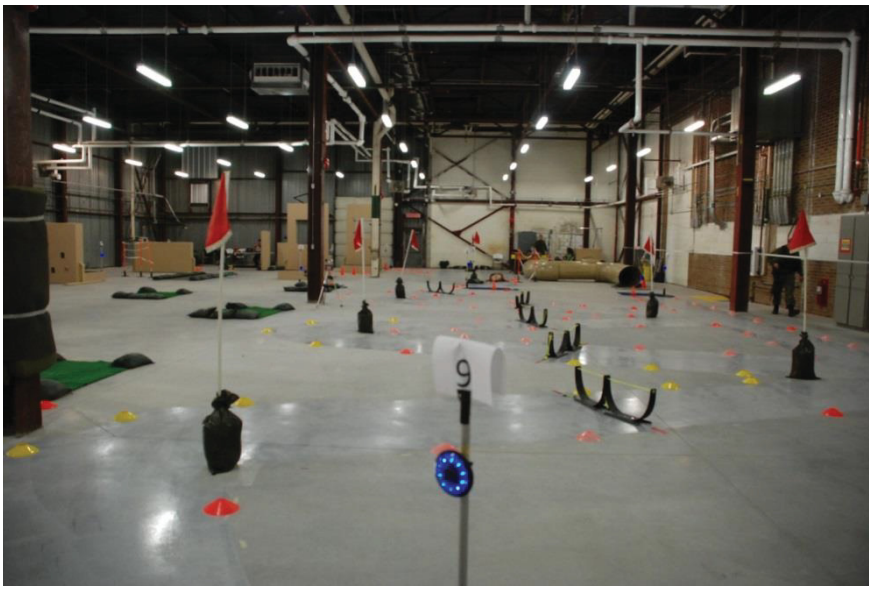

Figure 106: Agility Run Set Up

Casualty Drag

For the casualty drag portion of the obstacle course, the participant dragged a "Rescue Randy" mannequin out to a turn-around point 10 yards (9.1 m) away and back to the original position in which the mannequin was located (refer to Figure 107).

Figure 107: Casualty Drag Set Up

The participant used either the casualty extraction strap on the tactical vest or the shoulder straps to drag the mannequin. The start/finish position of the mannequin was set up by a tape box bounded by small cones. The mannequin weighed 180 lbs (81.8 kg) and was clad in a tactical vest.

Windows

The window component was comprised of two different obstacles, Window #1 and Window #2 (refer to Figure 108). Window #1 consisted of a 5'(w) × 10'(h) × 8"(d) (1.5 m (w) x 3 m (h) x 0.2 m(d)) obstacle with a 36"×36" (0.9 m x 0.9 m) window cut-out, with its bottom ledge situated 5' (1.5 m) (h) from the ground. There was a 4'1½"(d) × 5'(w) (11cm x 1.5m) landing platform on the opposite side. The surface of Window #1 was covered with a textured resin and three toe holds (all protruding) were placed on the approach side to aid in mounting the obstacle. Window #2 consisted of a 5'(w) × 10'(h) × 8"(d) (1.5 m (w) x 3 m (h) x 0.2 m(d)) obstacle with a 36" × 36" (0.9 m x 0.9 m) window cut-out, with its bottom ledge situated 4' (1.2 m) (h) from the ground. The surface of the wall was smooth and there were no toe holds present. The windows were supported by two metal stanchions, each attached with two fasteners.

Figure 108: Window #1 and Window #2

To complete the window obstacles, the participant first went through the opening of Window #1; the participant was free to choose whether or not he wanted to use the toe holds to assist him in climbing up the wall. After landing on the platform, the participant ran to Window #2, climbed through the window opening, and landed on the lightly padded platform on the opposite side. For safety purposes, the participant was required to land on his feet on the landing platform (as opposed to diving or rolling through the window opening). This segment of the obstacle course was completed when the participant passed by the Fitlight after the second window.

Bounding Rushes

The Bounding Rushes segment of the obstacle course consisted of five rushes to staggered prone firing positions, as displayed in Figure 109. Each firing position was marked with a sandbag, and the segment started and ended with a Fitlight. The sandbags were placed in a staggered pattern with the first one 7 feet (2.1 m) away from the Fitlight in front of it. The second sandbag was placed 15 feet (4.6 m) from the first on an angle 45 degrees to the right.

Figure 109: Bounding Rushes

The participant began the bounding rushes segment by passing the first Fitlight and running to the first pile of sandbags. Upon arriving at the first set of sandbags, the participant assumed a prone position, acquired a sight picture utilizing a Figure 11 target affixed to the far wall, and then leapt up to a running position. The participant then sprinted to the next (staggered) pile of sandbags, assumed the prone position, and acquired a sight picture. This cycle was repeated for the remaining sandbag locations, and the segment ended when the participant crossed the Fitlight at the end.

Balance Beam

The balance beam obstacle consisted of a series of four sloped metal 'plank' segments connected together at right angles. Four box-shaped obstacles were located on top of the planks (one on each segment) to provide an additional challenge for the participant as they traversed the beam. Refer to Figure 110.

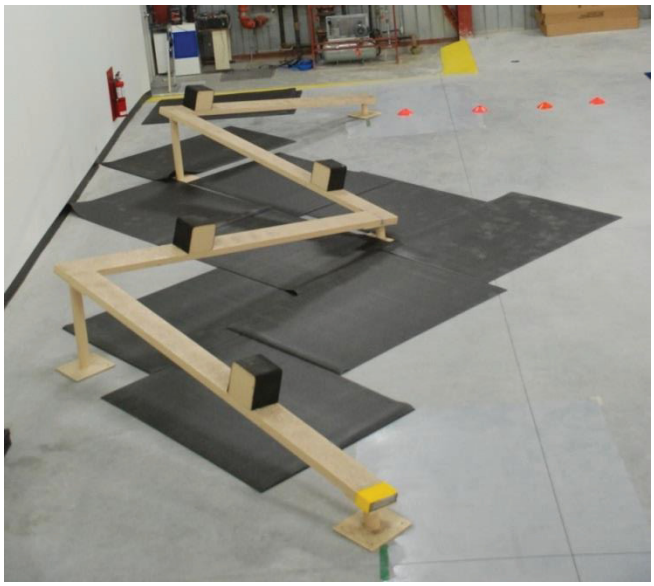

Figure 110: Balance Beam

The first segment started at a height of 6” (15 cm) off the ground and sloped upwards at approximately 15°, reaching a maximum height of approximately 2’7” (0.79 m). The second segment sloped downwards, reaching a height of 6” (15cm) from the ground at the end. The third segment sloped upwards and the fourth downwards, to the same specifications as the first two planks. Each of the ‘plank’ segments was 10’ (3 m) long. The box-shaped obstacles, measuring 8” × 8” × 8” (20 × 20 × 20 cm) were permanently affixed to the plank segments at locations of 41” (104 cm), 40” (101 cm), 28” (71cm), and 12” (30 cm) in from the edge of the first, second, third, and fourth segment respectively.

To traverse this obstacle, the participant kept to the outside of the line of cones and stepped up on to the beam from the end. Jumping up onto the beam from the side was not permitted. The participant walked across the balance beam while stepping over the box-shaped obstacles; stepping on top of the box obstacles was not permitted. The participant exited the balance beam by stepping off the end (not the side) then kept to the outside of the line of cones, and ran towards the next Fitlight.

Crawl

The low crawl obstacle consisted of 14 poles that supported a length of nylon fabric to create an obstacle under which participants were required to crawl (refer to Figure 111).

Figure 111: Crawl (with participant on course)

The height of the low level support poles was 20” (50 cm). The transition pole was a double-supported pole, with the first half reaching 20” (50 cm) and the second half 26” (66 cm). The high level support poles were 26” (66 cm). The low crawl obstacle was 4’ (1.2 m) wide and 30’ (9.1 m) long. Two rows of sandbags were located on the ground at the 10’ (3 m) mark, and 20’ (6 m) mark.

To complete the low crawl obstacle, the participant began by passing by the Fitlight, and crawling underneath the canvas as fast as he could. For the first 10’ (3 m), the participant performed a low crawl. At the 10’ (3 m) sandbag line, the participant passed the next Fitlight, and crawled over the sandbags, turned on his back, and performed a back-crawl to the 20’ (6 m) sandbag line. He then turned onto his front, passed the next Fitlight, and traversed over the sandbags and performed a high crawl to the end where the final Fitlight was passed.

Courtyard Walls

The wall component of CAN-LEAP consisted of two different wall obstacles; an outer and an inner courtyard wall (refer to Figure 112).

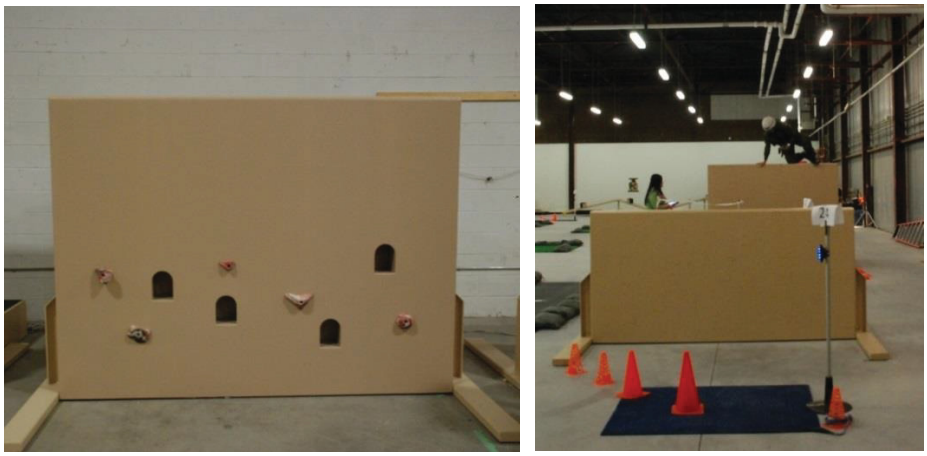

Figure 112: Inner and Outer Courtyard Walls

The outer courtyard wall consisted of an 8’(w) × 6’(h) × 1.5’(d) (2.4 m (w) × 1.8 m (h) × 0.45 m (d)) obstacle with a 4’1½”(d) × 8’(w) (1.3 m (d) × 2.4 m (w)) landing platform on the opposite side. The textured wall surface contained 9 toe holds (5 protruding, 4 receding) on the approach side to aid in mounting the obstacle. The inner courtyard wall consisted of an 8’(w) × 4’(h) ×6”(d) (2.4 m (w) × 1.2

m (h) × 0.15 m (d)) obstacle, with a smooth surface, and no toe holds. The walls were set up in a staggered formation, with 15 feet (4.6 m) between the edge of the landing platform of the outer courtyard wall and the inner courtyard wall. The walls were supported by two metal stanchions, attached to the wall with two fasteners each.

The participant began by traversing over the outer courtyard wall as quickly as possible and landing on the padded platform on the opposite side. Any manner of traversing was permitted, and the participant was able to use the foot holds to assist him if he wished. After traversing the outer courtyard wall, the participant sprinted to the inner courtyard and crossed over it as fast as possible. To complete this segment (and the timed course), the participant ran past the final Fitlight.

Noptel marksmanship stand

Marksmanship performance was recorded using the Noptel ST-2000 Expert Marksmanship System, an integrated rifle marksmanship training and data collection device that attached on to either the barrel or picatinny rail of the rifle.

The Noptel System consisted of an optical unit (Figure 113) that was connected to a laptop computer (containing the Noptel Software) via a USB cable, a Noptel target equipped with reflective prisms, and proprietary software.

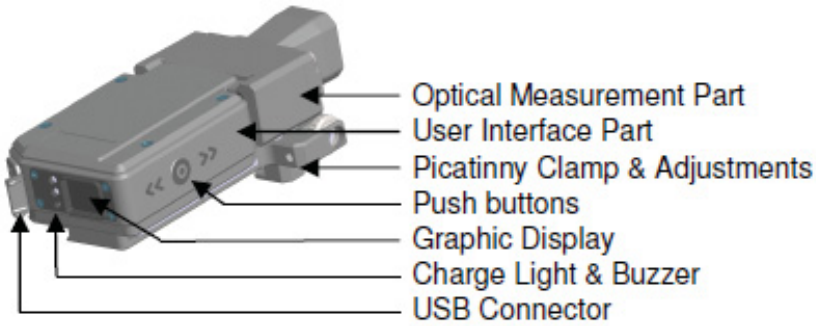

Figure 113: Noptel Optical Unit

The system worked by emitting an infra-red LED light towards the target upon the rifle being fired. The light was then reflected back to the optical receiver by prisms mounted on the target and the software converted this to a target score. The targets were mounted 150 feet (45.7m) away from the firing line.

At the beginning of each testing session (or each time the optical unit gets mounted onto the rifle) the optical unit was zeroed. Zeroing was a daily process that consisted of each participant firing five shots from the prone position at the given target. The aiming point used for each participant's marksmanship analysis was the centre of the shot grouping obtained from this zeroing process.

The participant was instructed to pick up the rifle and approach the firing line in a tactical kneeling, standing or prone position, depending on the randomized order. The researcher then issued a "Threat" command, to which the participant reacted by aiming for the centre of the target and taking one shot as quickly as possible. The "Threat" command and shot response was completed a total of three times for every firing posture. After each shot, but before the next "Threat" command was issued, the participant was required to lower the weapon to 45-degrees (in standing and kneeling; in prone the participant moved his head away from the optical sight) as well as put on the safety. Lowering the

weapon and putting the safety on maintained the safety protocol of the study while also providing the researcher with a cue to issue the next “Threat” command.

Weight transfer

The weight transfer station was used to measure the participant’s ability to quickly transfer a weight from one platform to another while wearing each of the test conditions. There were two components to the weight transfer station: horizontal transfer and vertical transfer.

The horizontal transfer platforms were both 48” (122 cm) from the ground. The first vertical platform sat just above ground height, and the second platform was 68” (173 cm) from the ground.

A 30 lb (or 13.6 kg) ammunition can was used as the lifting load for both the vertical transfer and the horizontal transfer. For both types of transfers, six lifts (with back and forth being considered one lift) were performed, and the time it took to complete this set of six lifts was recorded.

Vertical jump

The vertical jump station consisted of a rubberized mat with an embedded sensor, a hand-held display unit, and a connector cable (refer to Figure 114).

Figure 114: ‘Just Jump’ Equipment

When the participant jumped, the sensor measured the time off the mat, and the software on the handheld unit converted that time to a jump height.

In order to increase the participant’s motivation, a vertical jump target (refer to Figure 115) was fabricated out of a set of 6 balls hanging vertically on a rope. The idea was to have the participant jump and reach as high as possible, using the target to facilitate goal setting for a maximal jump.

Figure 115: Vertical Jump Target

The participant completed a series of three maximal-effort jumps at this station. The database software identified the maximum jump height and calculated the average jump height. The participant was instructed to step on the mat and then make one maximal vertical jump. They then were required to step off the mat, then back on, and take another maximal jump. This was repeated for a third (final) jump.

Horizontal jump

The long jump station was used to measure the participant's ability to jump horizontally, as though they were leaping over an obstacle in their path, such as a hedge or canal. The participant was allowed to take a short run up to the take-off line, where they performed a maximal effort leap. Demarcations from the participant's foot were used to measure the distance covered by their leap. They landed on a rubberized mat that was soft enough to ease the impact of landing, yet firm enough to avoid injury (refer to Figure 116).

Figure 116: Long (Horizontal) Jump

Rating of perceived exertion (RPE)

Immediately after completing the obstacle course, the participants were presented with a scale known as the Borg Scale, which ranges from 6 to 20 and measures perceived exertion (6 being completely relaxed and 20 at maximum possible exertion). The participants were asked to choose their rating, from 6 to 20, based on how they felt at that exact moment of finishing the course. It is important that the rating be chosen immediately after completing the task being rated so that there is no second-guessing or misinterpretation of exertion level if the participant was asked after cardiovascular and thermoregulatory recovery had already begun. The Borg scale can be seen in Figure 117.

rating	description
6	NO EXERTION AT ALL
7	
8	EXTREMELY LIGHT
9	VERY LIGHT
10	
11	LIGHT
12	
13	SOMEWHAT HARD
14	
15	HARD (HEAVY)
16	
17	VERY HARD
18	
19	EXTREMELY HARD
20	MAXIMAL EXERTION

Figure 117: Borg Scale

Questionnaire and RPE

The questionnaire kiosk consisted of a stand-alone computer terminal that ran a program containing a two-page questionnaire. The questionnaire collected subjective data regarding the participant's acceptability rating of various parameters of their test condition and their RPE upon completion of the course. The rating scale ranged from 1 (completely unacceptable) to 7 (completely acceptable) and is shown in Figure 118.

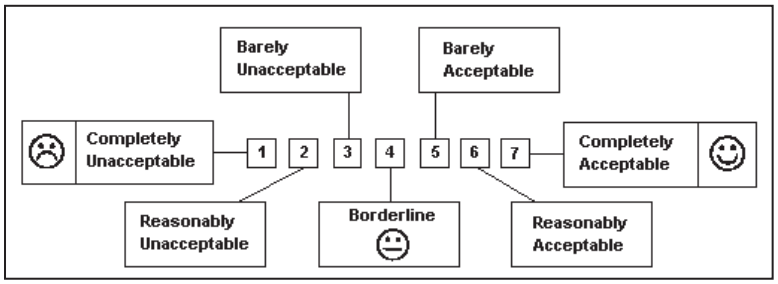

Figure 118. Acceptability Rating Scale

The participant was presented with the two screens as shown in Figure 119 and Figure 120. He was required to fill in his participant number and test condition, as well as an answer for each of the seven questions before the "Next" button became active.

Figure 119: Questionnaire Kiosk – First Screen

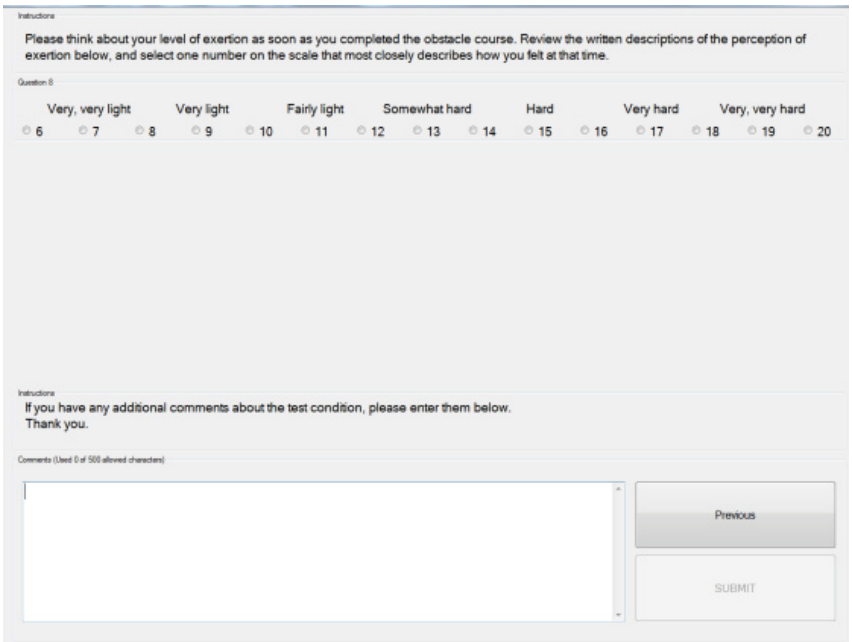

Figure 120: Questionnaire Kiosk - Second Screen

Entry of the RPE was required before the “SUBMIT” button became active. The participant was able to click the “Previous” button if he wished to return to the previous page at any time.

This page intentionally left blank.

Annex I: Intra-Class Correlation Method

An intra-class correlation (ICC) coefficient was computed for each method to determine the reliability in comparison to one another for specific ROM measurements. An ICC is a widely used reliability index in test-retest, intrarater, and interrater reliability analysis (Koo & Li, 2016). An ICC is beneficial for the purposes of this report because it is unit-less and therefore allows for direct comparison across different measurement methods. There are multiple versions of the ICC that give very different results when applied to the same data due to the assumptions they are based on (Shrout & Fleiss, 1979). As a result, the appropriate form of ICC must be chosen carefully.

Figure 121 shows a flow chart adapted from McGraw & Wong (1996) and Koo & Li (2016) that depicts the reasoning behind choosing each ICC form. The yellow path shows the theory behind the two ICC forms that were chosen for this analysis.

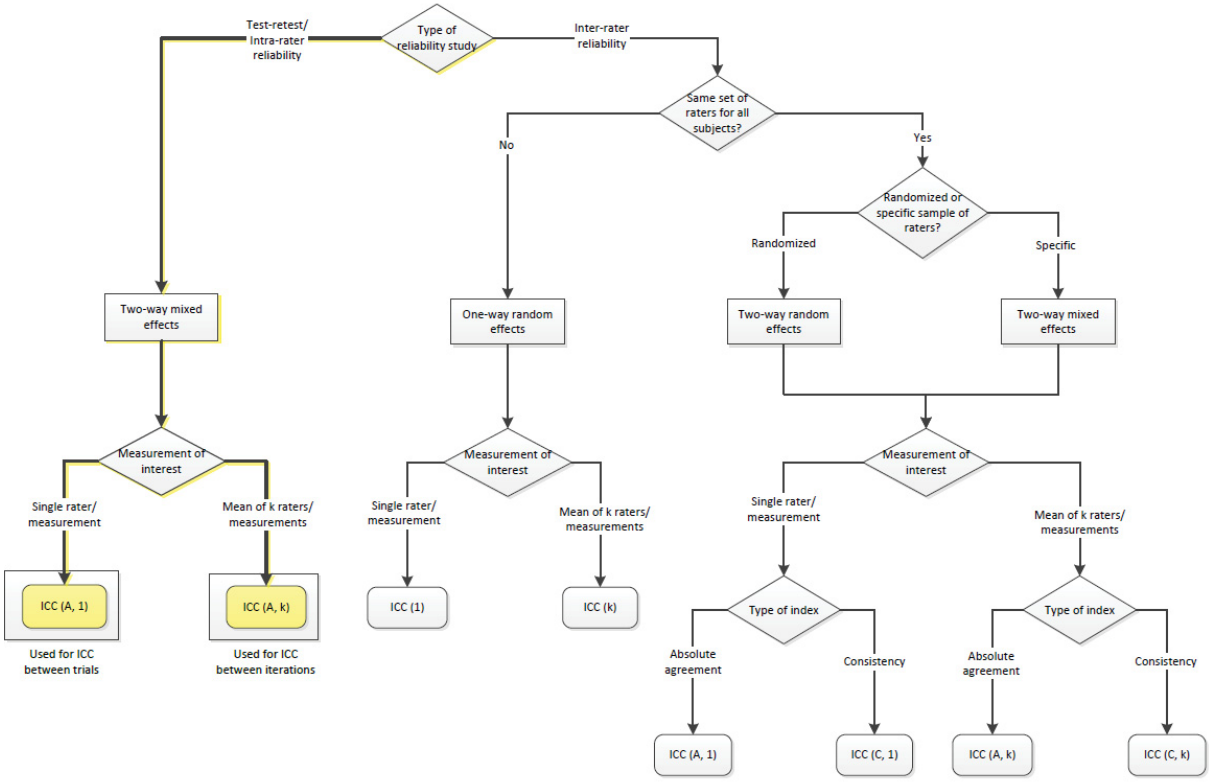

Figure 121: Flow Chart Depicting Path of Chosen ICC Forms for the Reliability Analysis (adapted from McGraw & Wong (1996) and Koo & Li (2016))

An appropriate model (i.e., 1-way random effects, 2-way random effects, or 2-way fixed effects), type (i.e., single measurement or the mean of *k* measurements), and the relationship of importance (i.e., consistency or absolute agreement) had to be chosen. For this experimental design, when calculating the ICC between iterations, a two-way mixed effects model was used based on a mean-rating and absolute agreement (ICC (A,*k)*). When calculating the ICC between trials, a two-way mixed effects model was used but this one was based on a single rater/measurement and absolute agreement

(ICC(A,1)). The ICC was calculated in Excel using the two equations shown in Table 92 (McGraw & Wong, 1996):

Table 92: Equations Used to Calculated ICCs

ICC (A, *k*)	ICC (A, 1)
$= \dfrac{MS_{Rows} - MS_{Error}}{MS_{Rows} + \dfrac{(MS_{Columns} - MS_{Error})}{n}}$	$= \dfrac{MS_{Rows} - MS_{Error}}{MS_{Rows} + (k-1) \cdot MS_{Error} + \frac{k}{n} \cdot (MS_{Columns} - MS_{Error})}$

where,

$$MS = \frac{SS}{df}$$

and,

$$SS_{Total} = \sum_{i=1}^{a} \sum_{j=1}^{b} X_{ij}^2 - C$$

$$SS_{Columns} = \frac{\sum_{i=1}^{a} G_i^2}{b} - C, \quad SS_{Rows} = \frac{\sum_{j=1}^{b} B_j^2}{a} - C$$

$$SS_{Error} = SS_{Total} - SS_{Columns} - SS_{Rows}$$

$$C = \frac{\left(\sum_{i=1}^{a} \sum_{j=1}^{b} X_{ij}\right)^2}{N}$$

Where,

- *a* is the columns (i.e., either iterations or trials),
- *b* is the rows (i.e., participants),
- *n* is the number of objects of measurement,
- *k* is the number of observations made on each object of measurement, and
- *N* is the total number of data points.

Once computed, the ICCs were transformed using the Fisher's *z*-transformation in order to plot and compare across methods. The following equation was used to transform the ICCs (Fisher, 1934):

$$z = 0.5 * ln \frac{1 + (k-1) * r}{1 - r}$$

where,

- *r* is the computed ICC, and
- *k* is the number of observations made on each object of measurement.

Annex J: Regression Coefficient Analysis

In a regression coefficient analysis, a regression equation is estimated for each individual participant giving a slope, intercept, and correlation factor (Myers & Broyles, 2000).The computed coefficients are then averaged across the participant sample to produce a regression equation that predicts marginal probabilities and can be used to test for significance (Myers & Broyles, 2000). Using this statistical method, continuous predictors can be incorporated, and each subject can be used as his/her own control, reducing within subject variability and between subject differences, and increasing statistical power (Myers & Broyles, 2000).

Firstly, a simple linear regression individually on each participant estimated their respective regression coefficients. The linear regression coefficients for each participant were derived in Excel using the following equation:

$$y = a + bx$$

where,

- y is the dependent variable (i.e., VAS Score or 5-point rating),
- x is the independent variable (i.e., plate width relative to chest breadth),
- b is the slope of the line, and
- a is the y-intercept.

Once computed, the slope coefficients were tested for significance. A one-sample t-test was used to determine whether the slope coefficients differed significantly from zero (Lorch & Myers, 1990). Following this analysis, the slope and intercept coefficients were averaged across the entire population to model the probable relationship between the dependent variables and the independent variables.

The correlation coefficients, r, were not computed in the same way since this approach would yield a distorted picture of the correlation factor (Lorch & Myers, 1990). Instead, a Fisher's z-transformation was used to transform the correlation coefficients to a Fisher's z prior to averaging using the following equation (Silver & Dunlap, 1987):

$$z = 0.5log_e\left(\frac{1+r}{1-r}\right)$$

where,

- z is Fisher's z transformation coefficient, and
- r is the correlation coefficient obtained during the linear regression analysis.

The Fisher's z from each participant was then averaged and back-transformed to a single correlation coefficient using the following equation (Silver & Dunlap, 1987):

$$r = \frac{e^{2z} - 1}{e^{2z} + 1}$$

where,

- z is the averaged Fisher's z, and

- r is the back-transformed, median correlation coefficient.

Due to the small sample size, this transformation more appropriately summarizes the amount of variability in the ROM and LEAP measurements that is being explained per soldier (Silver & Dunlap, 1987). A 95% confidence interval was determined for the summary coefficients using the following equation:

$$\bar{x} \pm 1.96\left(\frac{\sigma}{\sqrt{n}}\right)$$

where,

- 1.96 is the z-value for a 95% confidence interval,
- $\bar{x}$ is the mean of the population (i.e., averaged slope),
- σ is the standard deviation of the population (i.e., summary slopes), and
- n is the sample size (i.e., number of participants).

For the correlation coefficient, the upper and lower bounds for the confidence interval were determined from the z values and then back-transformed.

RCA Results

ROM Correlation with Overall LEAP Times

Table 58 shows the mean slope and intercept, and the median R^2 values as well as the upper and lower bounds of their 95% confidence interval and the standard deviation calculated from the RCA for Right Trunk Rotation vs. Overall LEAP Time. A one sample t-test revealed that the slope was significantly different than zero (t(28)=-7.89, p=0.0000).

Table 93: Regression Coefficients for Right Trunk Rotation vs. Overall LEAP Time

Right Trunk Rotation vs. Overall LEAP Time, RCA Coefficients				
	Mean	**95% Confidence Interval – Upper Bound**	**95% Confidence Interval – Lower Bound**	**Standard Deviation**
Slope	-7.23	-9.03	-5.43	4.94
Intercept	545.34	619.19	390.37	202.91
R^2	0.84*	0.92*	0.71*	N/A

*The median R^2 value and its associated confidence interval was calculated using Fisher's z-transformation.

Table 59 shows the mean slope and intercept, and the median R^2 values as well as the upper and lower bounds of their 95% confidence interval and the standard deviation calculated from the RCA for Left Trunk Rotation vs. Overall LEAP Time. A one sample t-test revealed that the slope was significantly different than zero (t(28)=-3.58, p=0.0013).

Table 94: Regression Coefficients for Left Trunk Rotation vs. Overall LEAP Time

Left Trunk Rotation vs. Overall LEAP Time, RCA Coefficients				
	Mean	**95% Confidence Interval – Upper Bound**	**95% Confidence Interval – Lower Bound**	**Standard Deviation**
Slope	-9.13	-14.13	-4.13	13.73
Intercept	585.28	740.58	338.38	426.71
R^2	0.81*	0.91*	0.62*	N/A

*The median R^2 value and its associated confidence interval was calculated using Fisher's *z*-transformation.

Table 60 shows the mean slope and intercept, and the median R^2 values as well as the upper and lower bounds of their 95% confidence interval and the standard deviation calculated from the RCA for Right Lateral Bending vs. Overall LEAP Time. A one sample t-test revealed that the slope was significantly different than zero (t(28)=-9.72, p=0.0000).

Table 95: Regression Coefficients for Right Lateral Bending vs. Overall LEAP Time

Right Lateral Bending vs. Overall LEAP Time, RCA Coefficients				
	Mean	**95% Confidence Interval – Upper Bound**	**95% Confidence Interval – Lower Bound**	**Standard Deviation**
Slope	-5.10	-6.13	-4.07	2.83
Intercept	480.41	526.94	402.52	127.83
R^2	0.72*	0.83*	0.58*	N/A

*The median R^2 value and its associated confidence interval was calculated using Fisher's *z*-transformation.

Table 61 shows the mean slope and intercept, and the median R^2 values as well as the upper and lower bounds of their 95% confidence interval and the standard deviation calculated from the RCA for Left Lateral Bending vs. Overall LEAP Time. A one sample t-test revealed that the slope was significantly different than zero (t(28)=-11.04, p=0.0000).

Table 96: Regression Coefficients for Left Lateral Bending vs. Overall LEAP Time

Left Lateral Bending vs. Overall LEAP Time, RCA Coefficients				
	Mean	**95% Confidence Interval – Upper Bound**	**95% Confidence Interval – Lower Bound**	**Standard Deviation**
Slope	-5.68	-6.69	-4.68	2.77
Intercept	493.54	539.82	410.00	127.17
R^2	0.84*	0.91*	0.71*	N/A

*The median R^2 value and its associated confidence interval was calculated using Fisher's *z*-transformation.

Table 62 shows the mean slope and intercept, and the median R^2 values as well as the upper and lower bounds of their 95% confidence interval and the standard deviation calculated from the RCA for Front Forward Flexion vs. Overall LEAP Time. A one sample t-test revealed that the slope was significantly different than zero (t(28)=3.84, p=0.0006).

Table 97: Regression Coefficients for Front Forward Flexion vs. Overall LEAP Time

Front Forward Flexion vs. Overall LEAP Time, RCA Coefficients				
	Mean	95% Confidence Interval – Upper Bound	95% Confidence Interval – Lower Bound	Standard Deviation
Slope	12.53	18.92	6.14	17.56
Intercept	-223.55	41.72	-358.09	728.85
R^2	0.79*	0.90*	0.59*	N/A

*The median R^2 value and its associated confidence interval was calculated using Fisher's *z*-transformation.

Table 63 shows the mean slope and intercept, and the median R^2 values as well as the upper and lower bounds of their 95% confidence interval and the standard deviation calculated from the RCA for Right Shoulder Abduction vs. Overall LEAP Time. A one sample t-test revealed that the slope was significantly different than zero (t(28)=-5.84, p=0.0000).

Table 98: Regression Coefficients for Right Shoulder Abduction vs. Overall LEAP Time

Right Shoulder Abduction vs. Overall LEAP Time, RCA Coefficients				
	Mean	95% Confidence Interval – Upper Bound	95% Confidence Interval – Lower Bound	Standard Deviation
Slope	-2.57	-3.43	-1.71	2.37
Intercept	693.29	838.10	448.13	397.86
R^2	0.87*	0.93*	0.75*	N/A

*The median R^2 value and its associated confidence interval was calculated using Fisher's *z*-transformation.

Table 64 shows the mean slope and intercept, and the median R^2 values as well as the upper and lower bounds of their 95% confidence interval and the standard deviation calculated from the RCA for Left Shoulder Abduction vs. Overall LEAP Time. A one sample t-test revealed that the slope was not significantly different than zero (t(28)=-1.61, p=0.1192).

Table 99: Regression Coefficients for Left Shoulder Abduction vs. Overall LEAP Time

Left Shoulder Abduction vs. Overall LEAP Time, RCA Coefficients				
	Mean	95% Confidence Interval – Upper Bound	95% Confidence Interval – Lower Bound	Standard Deviation
Slope	-5.56	-12.34	1.22	18.63
Intercept	1117.95	2086.20	-380.08	2660.33
R^2	0.85*	0.92*	0.73*	N/A

*The median R^2 value and its associated confidence interval was calculated using Fisher's *z*-transformation.

Table 65 shows the mean slope and intercept, and the median R^2 values as well as the upper and lower bounds of their 95% confidence interval and the standard deviation calculated from the RCA for Right High Knee Lift vs. Overall LEAP Time. A one sample t-test revealed that the slope was significantly different than zero (t(28)=-9.21, p=0.0000).

Table 100: Regression Coefficients for Right High Knee Lift vs. Overall LEAP Time

Right High Knee Lift vs. Overall LEAP Time, RCA Coefficients				
	Mean	95% Confidence Interval – Upper Bound	95% Confidence Interval – Lower Bound	Standard Deviation
Slope	-7.22	-8.76	-5.69	4.22
Intercept	1102.00	1283.06	835.32	497.50
R^2	0.89*	0.94*	0.80*	N/A

*The median R^2 value and its associated confidence interval was calculated using Fisher's *z*-transformation.

Table 66 shows the mean slope and intercept, and the median R^2 values as well as the upper and lower bounds of their 95% confidence interval and the standard deviation calculated from the RCA for Left High Knee Lift vs. Overall LEAP Time. A one sample t-test revealed that the slope was significantly different than zero (t(28)=-6.26, p=0.0000).

Table 101: Regression Coefficients for Left High Knee Lift vs. Overall LEAP Time

Left High Knee Lift vs. Overall LEAP Time, RCA Coefficients				
	Mean	95% Confidence Interval – Upper Bound	95% Confidence Interval – Lower Bound	Standard Deviation
Slope	-8.32	-10.92	-5.72	7.16
Intercept	1230.72	1533.53	782.29	831.99
R^2	0.87*	0.94*	0.74*	N/A

*The median R^2 value and its associated confidence interval was calculated using Fisher's *z*-transformation.

ROM Correlation with Subjective Ratings

Table 68 shows the mean slope and intercept, and the median R^2 values as well as the upper and lower bounds of their 95% confidence interval and the standard deviation calculated from the RCA for Right Trunk Rotation vs. Subjective Rating. A one sample t-test revealed that the slope was significantly different than zero (t(28)=4.94, p=0.0000).

Table 102: Regression Coefficients for Right Trunk Rotation vs. LEAP Course Subjective Rating

Right Trunk Rotation vs. LEAP Course Subjective Rating, RCA Coefficients				
	Mean	95% Confidence Interval – Upper Bound	95% Confidence Interval – Lower Bound	Standard Deviation
Slope	0.27	0.38	0.16	0.30
Intercept	-3.26	-0.80	-3.89	6.75
R^2	0.93*	0.99*	0.44*	N/A

*The median R^2 value and its associated confidence interval was calculated using Fisher's *z*-transformation.

Table 69 shows the mean slope and intercept, and the median R^2 values as well as the upper and lower bounds of their 95% confidence interval and the standard deviation calculated from the RCA for Left Trunk Rotation vs. Subjective Rating. A one sample t-test revealed that the slope was significantly different than zero (t(28)=3.68, p=0.0001).

Table 103: Regression Coefficients for Left Trunk Rotation vs. LEAP Course Subjective Rating

Left Trunk Rotation vs. LEAP Course Subjective Rating, RCA Coefficients				
	Mean	95% Confidence Interval – Upper Bound	95% Confidence Interval – Lower Bound	Standard Deviation
Slope	0.32	0.49	0.15	0.46
Intercept	-4.02	0.42	-5.03	12.20
R^2	0.82*	0.92*	0.64*	N/A

*The median R^2 value and its associated confidence interval was calculated using Fisher's *z*-transformation.

Table 70 shows the mean slope and intercept, and the median R^2 values as well as the upper and lower bounds of their 95% confidence interval and the standard deviation calculated from the RCA for Right Lateral Bending vs. Subjective Rating. A one sample t-test revealed that the slope was significantly different than zero (t(28)=6.14, p=0.0000).

Table 104: Regression Coefficients for Right Lateral Bending vs. LEAP Course Subjective Rating

Right Lateral Bending vs. LEAP Course Subjective Rating, RCA Coefficients				
	Mean	95% Confidence Interval – Upper Bound	95% Confidence Interval – Lower Bound	Standard Deviation
Slope	0.18	0.24	0.12	0.16
Intercept	-1.02	0.93	-2.17	5.35
R^2	0.74*	0.87*	0.53*	N/A

*The median R^2 value and its associated confidence interval was calculated using Fisher's *z*-transformation.

Table 71 shows the mean slope and intercept, and the median R^2 values as well as the upper and lower bounds of their 95% confidence interval and the standard deviation calculated from the RCA for Left Lateral Bending vs. Subjective Rating. A one sample t-test revealed that the slope was significantly different than zero (t(28)=10.68, p=0.0000).

Table 105: Regression Coefficients for Left Lateral Bending vs. LEAP Course Subjective Rating

Left Lateral Bending vs. LEAP Course Subjective Rating, RCA Coefficients				
	Mean	95% Confidence Interval – Upper Bound	95% Confidence Interval – Lower Bound	Standard Deviation
Slope	0.18	0.22	0.15	0.09
Intercept	-0.97	0.21	-2.67	3.23
R^2	0.77*	0.86*	0.62*	N/A

*The median R^2 value and its associated confidence interval was calculated using Fisher's *z*-transformation.

Table 72 shows the mean slope and intercept, and the median R^2 values as well as the upper and lower bounds of their 95% confidence interval and the standard deviation calculated from the RCA for Front Forward Flexion vs. Subjective Rating. A one sample t-test revealed that the slope was significantly different than zero (t(28)=-4.35, p=0.0002).

Table 106: Regression Coefficients for Front Forward Flexion vs. LEAP Course Subjective Rating

Front Forward Flexion vs. LEAP Course Subjective Rating, RCA Coefficients				
	Mean	95% Confidence Interval – Upper Bound	95% Confidence Interval – Lower Bound	Standard Deviation
Slope	-0.42	-0.62	-0.23	0.53
Intercept	23.29	31.17	11.18	21.63
R^2	0.81*	0.92*	0.58*	N/A

*The median R^2 value and its associated confidence interval was calculated using Fisher's *z*-transformation.

Table 73 shows the mean slope and intercept, and the median R^2 values as well as the upper and lower bounds of their 95% confidence interval and the standard deviation calculated from the RCA for Right Shoulder Abduction vs. Subjective Rating. A one sample t-test revealed that the slope was significantly different than zero (t(28)=8.32, p=0.0000).

Table 107: Regression Coefficients for Right Shoulder Abduction vs. LEAP Course Subjective Rating

Right Shoulder Abduction vs. LEAP Course Subjective Rating, RCA Coefficients				
	Mean	95% Confidence Interval – Upper Bound	95% Confidence Interval – Lower Bound	Standard Deviation
Slope	0.08	0.09	0.06	0.05
Intercept	-6.53	-3.52	-7.03	8.25
R^2	0.88*	0.95*	0.75*	N/A

*The median R^2 value and its associated confidence interval was calculated using Fisher's *z*-transformation.

Table 74 shows the mean slope and intercept, and the median R^2 values as well as the upper and lower bounds of their 95% confidence interval and the standard deviation calculated from the RCA for Left Shoulder Abduction vs. Subjective Rating. A one sample t-test revealed that the slope was significantly different than zero (t(28)=2.17, p=0.0388).

Table 108: Regression Coefficients for Left Shoulder Abduction vs. LEAP Course Subjective Rating

Left Shoulder Abduction vs. LEAP Course Subjective Rating, RCA Coefficients				
	Mean	95% Confidence Interval – Upper Bound	95% Confidence Interval – Lower Bound	Standard Deviation
Slope	0.13	0.25	0.01	0.33
Intercept	-14.47	2.50	-21.52	46.63
R^2	0.85*	0.92*	0.73*	N/A

*The median R^2 value and its associated confidence interval was calculated using Fisher's *z*-transformation.

Table 75 shows the mean slope and intercept, and the median R^2 values as well as the upper and lower bounds of their 95% confidence interval and the standard deviation calculated from the RCA for Right High Knee Lift vs. Subjective Rating. A one sample t-test revealed that the slope was significantly different than zero (t(28)=10.06, p=0.0000).

Table 109: Regression Coefficients for Right High Knee Lift vs. LEAP Course Subjective Rating

Right High Knee Lift vs. LEAP Course Subjective Rating, RCA Coefficients				
	Mean	95% Confidence Interval – Upper Bound	95% Confidence Interval – Lower Bound	Standard Deviation
Slope	0.23	0.27	0.18	0.12
Intercept	-19.77	-25.96	-14.83	13.58
R^2	0.94*	0.98*	0.85*	N/A

*The median R^2 value and its associated confidence interval was calculated using Fisher's *z*-transformation.

Table 76 shows the mean slope and intercept, and the median R^2 values as well as the upper and lower bounds of their 95% confidence interval and the standard deviation calculated from the RCA for Left High Knee Lift vs. Subjective Rating. A one sample t-test revealed that the slope was significantly different than zero (t(28)=7.21, p=0.0000).

Table 110: Regression Coefficients for Left High Knee Lift vs. LEAP Course Subjective Rating

Left High Knee Lift vs. LEAP Course Subjective Rating, RCA Coefficients				
	Mean	95% Confidence Interval – Upper Bound	95% Confidence Interval – Lower Bound	Standard Deviation
Slope	0.24	0.30	0.17	0.18
Intercept	-21.03	-13.72	-26.86	20.09
R^2	0.95*	0.99*	0.82*	N/A

*The median R^2 value and its associated confidence interval was calculated using Fisher's *z*-transformation.

ROM Correlation with RPE

Table 78 shows the mean slope and intercept, and the median R^2 values as well as the upper and lower bounds of their 95% confidence interval and the standard deviation calculated from the RCA for Right Trunk Rotation vs. RPE. A one sample t-test revealed that the slope was significantly different than zero (t(28)=-3.42, p=0.0019).

Table 111: Regression Coefficients for Right Trunk Rotation vs. LEAP Course RPE

Right Trunk Rotation vs. LEAP Course RPE, RCA Coefficients				
	Mean	95% Confidence Interval – Upper Bound	95% Confidence Interval – Lower Bound	Standard Deviation
Slope	-0.29	-0.45	-0.12	0.45
Intercept	23.78	28.40	16.68	12.68
R^2	0.81*	0.92*	0.62*	N/A

*The median R^2 value and its associated confidence interval was calculated using Fisher's *z*-transformation.

Table 79 shows the mean slope and intercept, and the median R^2 values as well as the upper and lower bounds of their 95% confidence interval and the standard deviation calculated from the RCA for Left Trunk Rotation vs. RPE. A one sample t-test revealed that the slope was significantly different than zero (t(28)=-3.27, p=0.0028).

Table 112: Regression Coefficients for Left Trunk Rotation vs. LEAP Course RPE

Left Trunk Rotation vs. LEAP Course RPE, RCA Coefficients				
	Mean	**95% Confidence Interval – Upper Bound**	**95% Confidence Interval – Lower Bound**	**Standard Deviation**
Slope	-0.36	-0.58	-0.15	0.59
Intercept	24.06	30.39	13.42	17.39
R^2	0.89*	0.97*	0.65*	N/A

*The median R^2 value and its associated confidence interval was calculated using Fisher's *z*-transformation.

Table 80 shows the mean slope and intercept, and the median R^2 values as well as the upper and lower bounds of their 95% confidence interval and the standard deviation calculated from the RCA for Right Lateral Bending vs. RPE. A one sample t-test revealed that the slope was significantly different than zero (t(28)=-3.67, p=0.0010).

Table 113: Regression Coefficients for Right Lateral Bending vs. LEAP Course RPE

Right Lateral Bending vs. LEAP Course RPE, RCA Coefficients				
	Mean	**95% Confidence Interval – Upper Bound**	**95% Confidence Interval – Lower Bound**	**Standard Deviation**
Slope	-0.20	-0.31	-0.09	0.29
Intercept	20.87	24.11	17.00	8.90
R^2	0.73*	0.88*	0.45*	N/A

*The median R^2 value and its associated confidence interval was calculated using Fisher's *z*-transformation.

Table 81 shows the mean slope and intercept, and the median R^2 values as well as the upper and lower bounds of their 95% confidence interval and the standard deviation calculated from the RCA for Left Lateral Bending vs. RPE. A one sample t-test revealed that the slope was significantly different than zero (t(28)=-3.67, p=0.0010).

Table 114: Regression Coefficients for Left Lateral Bending vs. LEAP Course RPE

Left Lateral Bending vs. LEAP Course RPE, RCA Coefficients				
	Mean	**95% Confidence Interval – Upper Bound**	**95% Confidence Interval – Lower Bound**	**Standard Deviation**
Slope	-0.18	-0.28	-0.09	0.27
Intercept	20.43	23.00	17.45	7.05
R^2	0.84*	0.94*	0.59*	N/A

*The median R^2 value and its associated confidence interval was calculated using Fisher's *z*-transformation.

Table 82 shows the mean slope and intercept, and the median R^2 values as well as the upper and lower bounds of their 95% confidence interval and the standard deviation calculated from the RCA for Front Forward Flexion vs. RPE. A one sample t-test revealed that the slope was significantly different than zero (t(28)=2.84, p=0.0083).

Table 115: Regression Coefficients for Front Forward Flexion vs. LEAP Course RPE

Front Forward Flexion vs. LEAP Course RPE, RCA Coefficients				
	Mean	95% Confidence Interval – Upper Bound	95% Confidence Interval – Lower Bound	Standard Deviation
Slope	0.67	1.14	0.21	1.28
Intercept	-14.83	4.65	-25.26	53.51
R^2	0.74*	0.88*	0.50*	N/A

*The median R^2 value and its associated confidence interval was calculated using Fisher's *z*-transformation.

Table 83 shows the mean slope and intercept, and the median R^2 values as well as the upper and lower bounds of their 95% confidence interval and the standard deviation calculated from the RCA for Right Shoulder Abduction vs. RPE. A one sample t-test revealed that the slope was significantly different than zero (t(28)=-4.25, p=0.0002).

Table 116:Regression Coefficients for Right Shoulder Abduction vs. LEAP Course RPE

Right Shoulder Abduction vs. LEAP Course RPE, RCA Coefficients				
	Mean	95% Confidence Interval – Upper Bound	95% Confidence Interval – Lower Bound	Standard Deviation
Slope	-0.09	-0.13	-0.05	0.12
Intercept	27.64	34.34	17.00	18.39
R^2	0.67*	0.87*	0.32*	N/A

*The median R^2 value and its associated confidence interval was calculated using Fisher's *z*-transformation.

Table 84 shows the mean slope and intercept, and the median R^2 values as well as the upper and lower bounds of their 95% confidence interval and the standard deviation calculated from the RCA for Left Shoulder Abduction vs. RPE. A one sample t-test revealed that the slope was not significantly different than zero (t(28)=-1.39, p=0.1761).

Table 117: Regression Coefficients for Left Shoulder Abduction vs. LEAP Course RPE

Left Shoulder Abduction vs. LEAP Course RPE, RCA Coefficients				
	Mean	95% Confidence Interval – Upper Bound	95% Confidence Interval – Lower Bound	Standard Deviation
Slope	-0.25	-0.61	0.10	0.97
Intercept	50.15	100.67	-26.76	138.81
R^2	0.78*	0.92*	0.48*	N/A

*The median R^2 value and its associated confidence interval was calculated using Fisher's *z*-transformation.

Table 85 shows the mean slope and intercept, and the median R^2 values as well as the upper and lower bounds of their 95% confidence interval and the standard deviation calculated from the RCA for Right High Knee Lift vs. RPE. A one sample t-test revealed that the slope was significantly different than zero (t(28)=-4.58, p=0.0001).

Table 118: Regression Coefficients for Right High Knee Lift vs. LEAP Course RPE

Right High Knee Lift vs. LEAP Course RPE, RCA Coefficients				
	Mean	**95% Confidence Interval – Upper Bound**	**95% Confidence Interval – Lower Bound**	**Standard Deviation**
Slope	-0.29	-0.41	-0.17	0.34
Intercept	46.42	59.58	28.18	36.15
R^2	0.81*	0.92*	0.59*	N/A

*The median R^2 value and its associated confidence interval was calculated using Fisher's *z*-transformation.

Table 86 shows the mean slope and intercept, and the median R^2 values as well as the upper and lower bounds of their 95% confidence interval and the standard deviation calculated from the RCA for Left High Knee Lift vs. RPE. A one sample t-test revealed that the slope was significantly different than zero ($t(28)=-3.94$, $p=0.0005$).

Table 119: Regression Coefficients for Left High Knee Lift vs. LEAP Course RPE

Left High Knee Lift vs. LEAP Course RPE, RCA Coefficients				
	Mean	**95% Confidence Interval – Upper Bound**	**95% Confidence Interval – Lower Bound**	**Standard Deviation**
Slope	-0.33	-0.49	-0.17	0.45
Intercept	51.24	69.25	25.07	49.50
R^2	0.83*	0.96*	0.48*	N/A

*The median R^2 value and its associated confidence interval was calculated using Fisher's *z*-transformation.

This page intentionally left blank.

Annex K: Additional LEAP Results

Post-hoc Tables for LEAP Course Obstacles

Table 120 summarizes the post-hoc analysis for total obstacle course time.

Table 120: Summary of Post-Hoc Analysis: Total Course Time

Tukey HSD test; **Total course time**			
COND	A	B	E
A		0.000120	0.000120
B	0.000120		0.001277
E	0.000120	0.001277	

Table 121 summarizes the post-hoc analysis for subjective rating of overall performance.

Table 121: Summary of Post-Hoc Analysis: Subjective Rating of Overall Performance

Tukey HSD test; **Subjective Rating of Overall Performance**			
COND	A	B	E
A		0.000120	0.000120
B	0.000120		0.003584
E	0.000120	0.003584	

Table 122 summarizes the post-hoc analysis for RPE.

Table 122: Summary of Post-Hoc Analysis: RPE

Tukey HSD test; **RPE Borg Scale**			
COND	A	B	E
A		0.000405	0.000120
B	0.000405		0.210639
E	0.000120	0.210639	

Table 123 summarizes the post-hoc analysis results for the tunnel and hatch.

Table 123: Summary of Post-Hoc Analysis: Tunnel and Hatch

Tukey HSD test; **Tunnel and Hatch**			
COND	A	B	E
A		0.000148	0.000120
B	0.000148		0.061019
E	0.000120	0.061019	

Table 124 summarizes the post-hoc analysis results for the sprint interval.

Table 124: Summary of Post-Hoc Analysis: Sprint

Tukey HSD test; **Sprint**			
COND	A	B	E
A		0.000120	0.000120
B	0.000120		0.433444
E	0.000120	0.433444	

Table 125 summarizes the post-hoc analysis results for stair steep to stair shallow.

Table 125: Summary of Post-Hoc Analysis: Stair Steep to Stair Shallow

Tukey HSD test; **Stair Steep to Stair Shallow**			
COND	A	B	E
A		0.000120	0.000120
B	0.000120		0.003503
E	0.000120	0.003503	

Table 126 summarizes the post-hoc analysis results for stair shallow to stair steep.

Table 126: Summary of Post-Hoc Analysis: Stair Shallow to Stair Steep

Tukey HSD test; **Stair Shallow to Stair Steep**			
COND	A	B	E
A		0.000120	0.000120
B	0.000120		0.026077
E	0.000120	0.026077	

Table 127 summarizes the post-hoc analysis results for up straight ladder/down angled ladder.

Table 127: Summary of Post-Hoc Analysis: Up Straight Ladder/Down Angled

Tukey HSD test; **Up Straight Ladder/Down Angled Ladder**			
COND	A	B	E
A		0.000123	0.000120
B	0.000123		0.002365
E	0.000120	0.002365	

Table 128 summarizes the post-hoc results for up angled and down straight ladder.

Table 128: Summary of Post-Hoc Analysis: Up Angled Ladder/Down Straight

Tukey HSD test; **Up Angled Ladder/Down Straight Ladder**			
COND	A	B	E
A		0.000243	0.000120
B	0.000243		0.081212
E	0.000120	0.081212	

Table 129 summarizes the post-hoc results for the agility interval.

Table 129: Summary of Post-Hoc Analysis: Agility

Tukey HSD test; **Agility**			
COND	A	B	E
A		0.000120	0.000120
B	0.000120		0.035430
E	0.000120	0.035430	

Table 130 summarizes the port-hoc results for the casualty drag.

Table 130: Summary of Post-Hoc Analysis: Casualty Drag

Tukey HSD test; **Casualty Drag**			
COND	A	B	E
A		0.000845	0.000125
B	0.000845		0.372471
E	0.000125	0.372471	

Table 131 summarizes thepost-hoc results for the first window interval.

Table 131: Summary of Post-Hoc Analysis: Window #1

Tukey HSD test; **Window 1**			
COND	A	B	E
A		0.000429	0.000120
B	0.000429		0.103743
E	0.000120	0.103743	

Table 132 summarizes the post-hoc results for the second window interval.

Table 132: Summary of Post-Hoc Analysis: Window #2

Tukey HSD test; **Window #2**			
COND	A	B	E
A		0.000205	0.000121
B	0.000205		0.585477
E	0.000121	0.585477	

Table 133 summarizes the post-hoc results for the bounding rushes.

Table 133: Summary of Post-Hoc Analysis: Bounding Rush

Tukey HSD test; **Window #2**			
COND	A	B	E
A		0.000120	0.000120
B	0.000120		0.007931
E	0.000120	0.007931	

Table 134 summarizes the post-hoc analysis for the balance beam.

Table 134: Summary of Post-Hoc Analysis: Balance Beam

Tukey HSD test; **Balance Beam**			
COND	A	B	E
A		0.000120	0.000120
B	0.000120		0.173239
E	0.000120	0.173239	

Table 135 summarizes the post-hoc analysis for the low crawl.

Table 135: Summary of Post-Hoc Analysis: Low Crawl

Tukey HSD test; **Low Crawl**			
COND	A	B	E
A		0.000120	0.000120
B	0.000120		0.167433
E	0.000120	0.167433	

Table 136 summarizes the post-hoc analysis for the back crawl.

Table 136: Summary of Post-Hoc Analysis: Back Crawl

Tukey HSD test; **Back Crawl**			
COND	A	B	E
A		0.000137	0.000120
B	0.000137		0.264519
E	0.000120	0.264519	

Table 137 summarizes the post-hoc analysis for the high crawl.

Table 137: Summary of Post-Hoc Analysis: High Crawl

Tukey HSD test; **High Crawl**			
COND	A	B	E
A		0.000384	0.000121
B	0.000384		0.386214
E	0.000121	0.386214	

Table 138 summarizes the post-hoc analysis for the outer wall.

Table 138: Summary of Post-Hoc Analysis: Outer Wall

Tukey HSD test; **Outer wall**			
COND	A	B	E
A		0.002124	0.000120
B	0.002124		0.072588
E	0.000120	0.072588	

Table 139 summarizes the post-hoc analysis for the inner wall.

Table 139: Summary of Post-Hoc Analysis: Inner Wall

Tukey HSD test; **Inner Wall**			
COND	A	B	E
A		0.033538	0.000120
B	0.033538		0.008141
E	0.000120	0.008141	

Post-hoc Tables for Ancillary Stations

Table 140 summarizes the post-hoc analysis for average shot distance by posture in the rested state.

Table 140: Summary of Post-Hoc Analysis: Average Shot Distance by Posture in the Rested State

Tukey HSD test; **Average Shot Distance by Posture in the Rested State**			
POSTURE	Standing	Prone	Kneeling
Standing		0.000120	0.008893
Prone	0.000120		0.000120
Kneeling	0.008893	0.000120	

Table 141 summarizes the post-hoc analysis for average shot distance by posture in the fatigued state.

Table 141: Summary of Post-Hoc Analysis: Average Shot Distance by Postures (Fatigued State)

Tukey HSD test; **Average Shot Distance by Posture in the Fatigued State**			
POSTURE	Standing	Prone	Kneeling
Standing		0.000120	0.187127
Prone	0.000120		0.000120
Kneeling	0.187127	0.000120	

Table 142 summarizes the post-hoc analysis for vertical weight transfer times by condition.

Table 142: Summary Post-Hoc Analysis: Vertical Weight Transfer Times by Condition

Tukey HSD test; **Vertical Weight Transfer Times by Condition**			
CONDITION	A	B	E
A		0.000129	0.000120
B	0.000129		0.258906
E	0.000120	0.258906	

Table 143 summarizes the post-hoc analysis for horizontal weight transfer times by condition.

Table 143: Summary Post-Hoc Analysis: Horizontal Weight Transfer Times by Condition

Tukey HSD test; **Horizontal Weight Transfer Times by Condition**			
CONDITION	A	B	E
A		0.005860	0.000168
B	0.005860		0.323587
E	0.000168	0.323587	

Table 144 summarizes the post-hoc analysis for vertical jump height by condition in the rested state.

Table 144: Summary Post-Hoc Analysis: Vertical Jump Height by Condition (Rested State)

Tukey HSD test; **Vertical Jump Height by Condition (Rested State)**			
CONDITION	A	B	E
A		0.000120	0.000120
B	0.000120		0.646291
E	0.000120	0.646291	

Table 145 summarizes the post-hoc results for vertical jump height by condition in the fatigued state.

Table 145: Summary Post-Hoc Analysis: Vertical Jump Height by Condition (Fatigued State)

Tukey HSD test; **Vertical Jump Height by Condition (Fatigued State)**			
CONDITION	A	B	E
A		0.000120	0.000120
B	0.000120		0.333130
E	0.000120	0.333130	

Table 146 summarizes the post-hoc analysis for horizontal jump distance by condition in the rested state.

Table 146: Summary of Post-Hoc Analysis: Horizontal Jump Distance by Condition (Rested State)

Tukey HSD test; **Horizontal Jump Distance by Condition (Rested State)**			
CONDITION	A	B	E
A		0.000120	0.000120
B	0.000120		0.030458
E	0.000120	0.030458	

Table 147 summarizes the post-hoc analysis for horizontal jump distance by condition in the fatigued state.

Table 147: Summary of Post-Hoc Analysis: Horizontal Jump Distance by Condition (Fatigued State)

Tukey HSD test; **Horizontal Jump Distance by Condition (Fatigued State)**			
CONDITION	A	B	E
A		0.000120	0.000120
B	0.000120		0.253684
E	0.000120	0.253684	

Post-hoc Tables for LEAP Course Transition Times

Table 148 summarizes the post-hoc analysis for the tunnel to sprint transition times.

Table 148: Summary of Post-Hoc Analysis: Hatch to Sprint

Tukey HSD test; **Hatch to Sprint**			
COND	A	B	E
A		0.000120	0.000120
B	0.000120		0.013345
E	0.000120	0.013345	

Table 149 summarizes the post-hoc analysis for the sprint to stairs transition times.

Table 149: Summary of Post-Hoc Analysis: Sprint to Stairs

Tukey HSD test; **Sprint to Stairs**			
COND	A	B	E
A		0.007513	0.000142
B	0.007513		0.200974
E	0.000142	0.200974	

Table 150 summarizes the post-hoc analysis for the stairs to agility transition times.

Table 150: Summary of Post-Hoc Analysis: Stairs to Agility

Tukey HSD test; **Stairs to Agility**			
COND	A	B	E
A		0.000120	0.000120
B	0.000120		0.998380
E	0.000120	0.998380	

Table 151 summarizes the post-hoc analysis for the casualty drag to windows transition times.

Table 151: Summary of Post-Hoc Analysis: Drag to Window

Tukey HSD test; **Drag to Window**			
COND	A	B	E
A		0.000687	0.000134
B	0.000687		0.565288
E	0.000134	0.565288	

Table 152 summarizes the post-hoc analysis for the balance beam to low crawl transition times.

Table 152: Summary of Post-Hoc Analysis: Beam to Crawl Transition Time

Tukey HSD test; **Beam to Crawl**			
COND	A	B	E
A		0.002781	0.000258
B	0.002781		0.643956
E	0.000258	0.643956	

Table 153 summarizes the post-hoc analysis for the crawl to wall transition times.

Table 153: Summary of Post-Hoc Analysis: Crawl to Wall

Tukey HSD test; **Crawl to Wall**			
COND	A	B	E
A		0.000129	0.000120
B	0.000129		0.794390
E	0.000120	0.794390	

Descriptive Plots for the Second LEAP Run

The mean performance metrics (timings, distance, and marksmanship) across all conditions ran in the 2017 Winter Experimentation Campaign are summarized in descriptive plots within this Annex. The error bars in each plot depict the 95% confidence interval, unless otherwise stated.

Total Course Performance

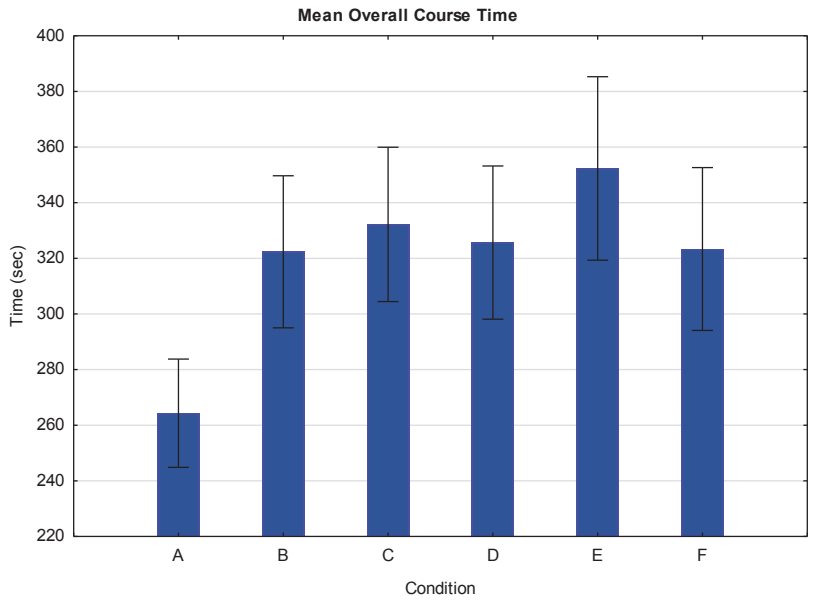

Figure 122: Mean Obstacle Course Time by Condition

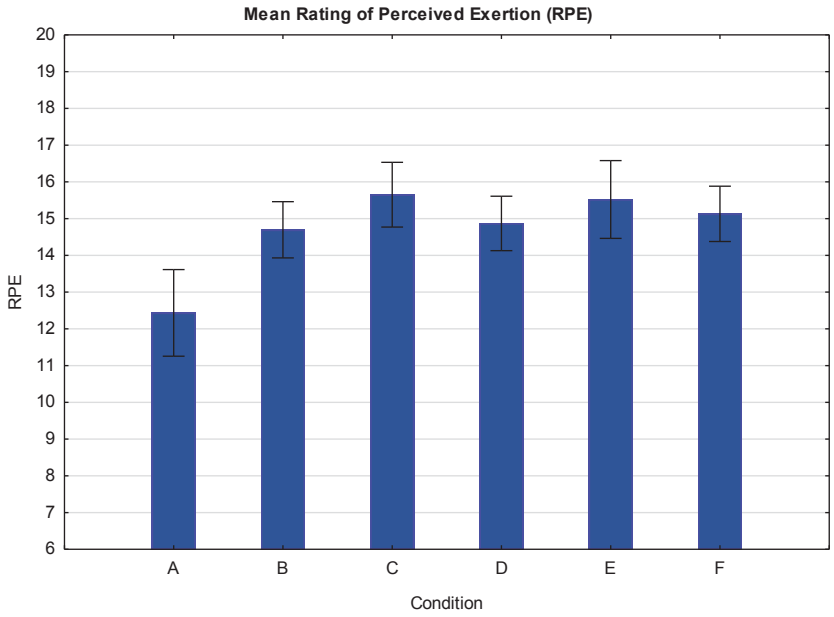

Figure 123: Mean RPE Rating by Condition

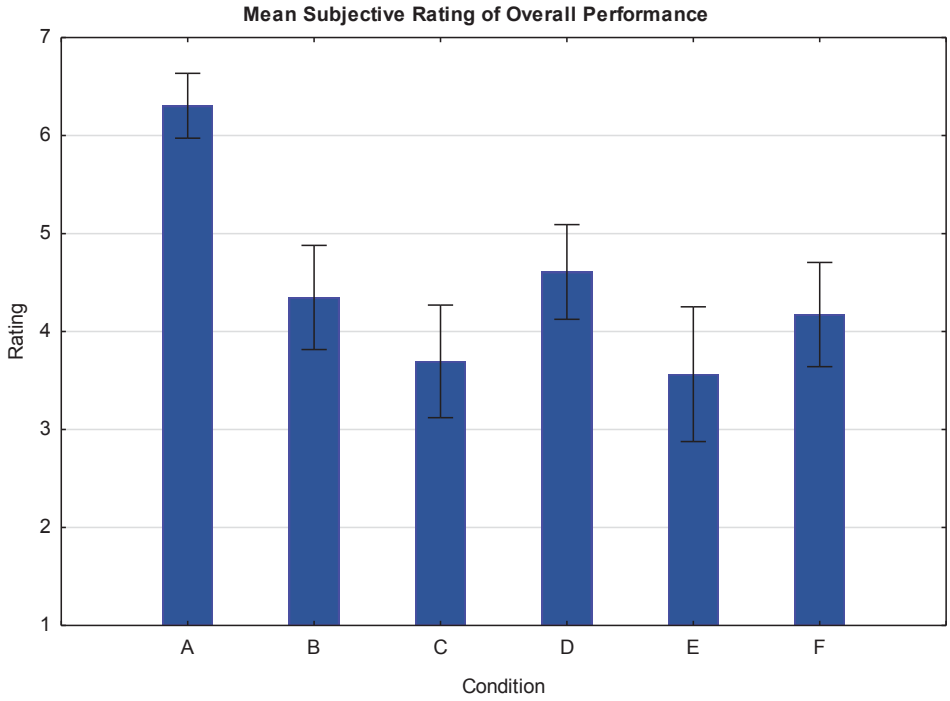

Figure 124: Mean Subjective Rating of Overall Performance by Condition

Individual Obstacle Times

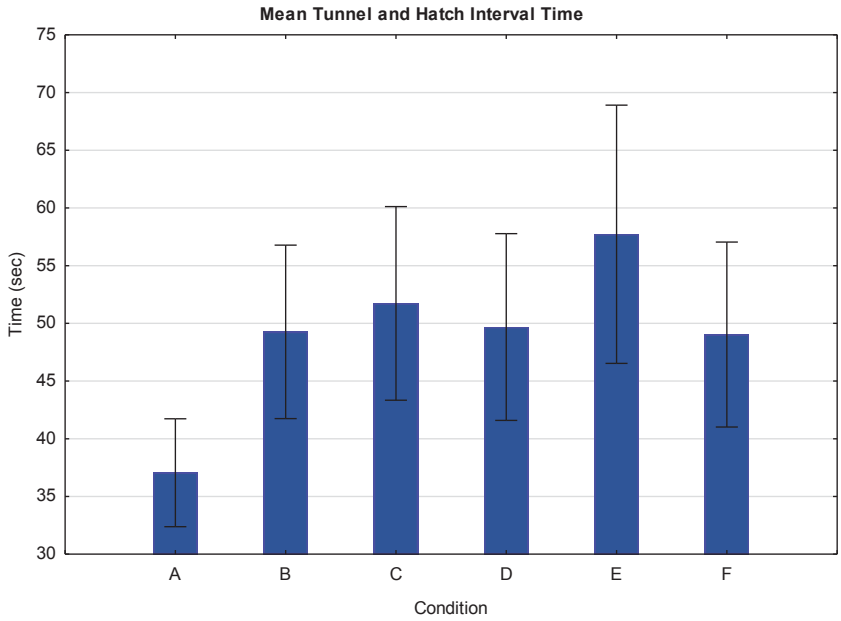

Figure 125: Mean Tunnel and Hatch Interval Time by Condition

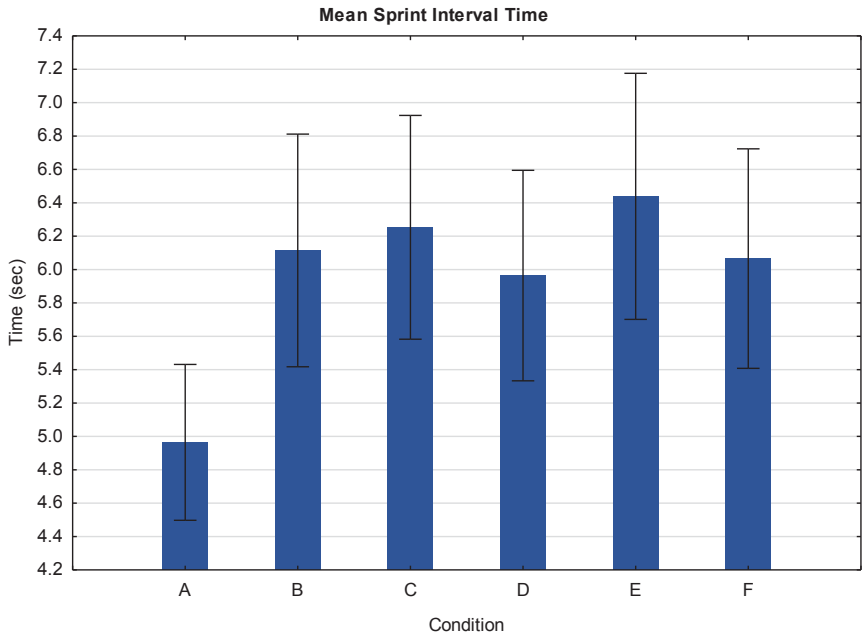

Figure 126: Mean Sprint Interval Time by Condition

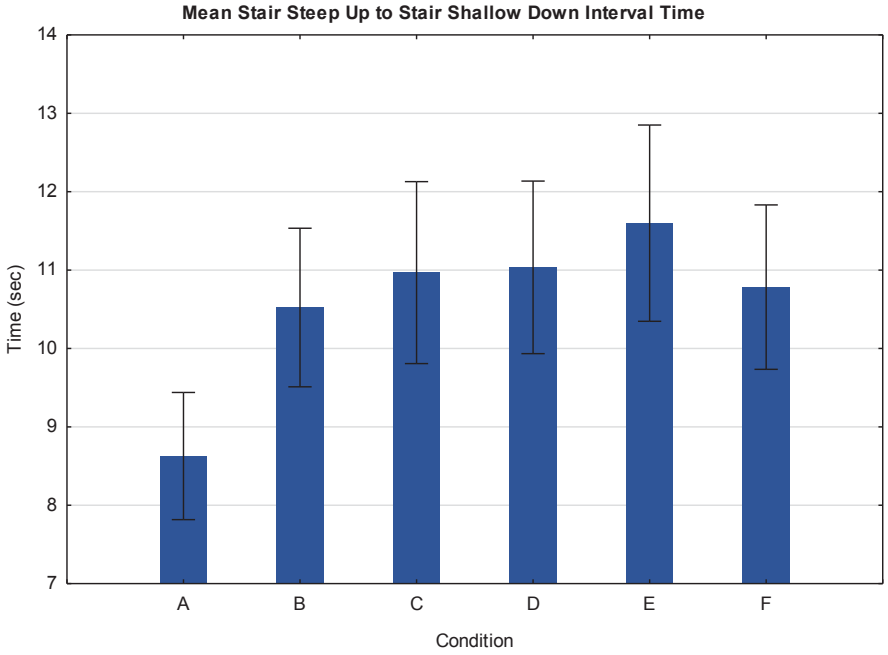

Figure 127: Mean Up Steep Stair/Down Shallow Stair Interval Time by Condition

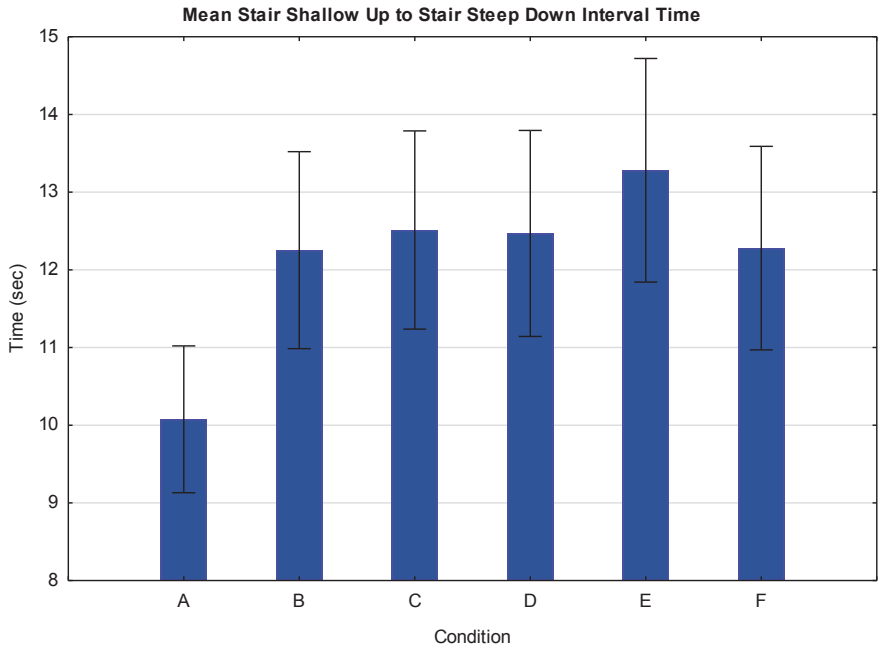

Figure 128: Mean Up Shallow Stair/Down Steep Stair Interval Time by Condition

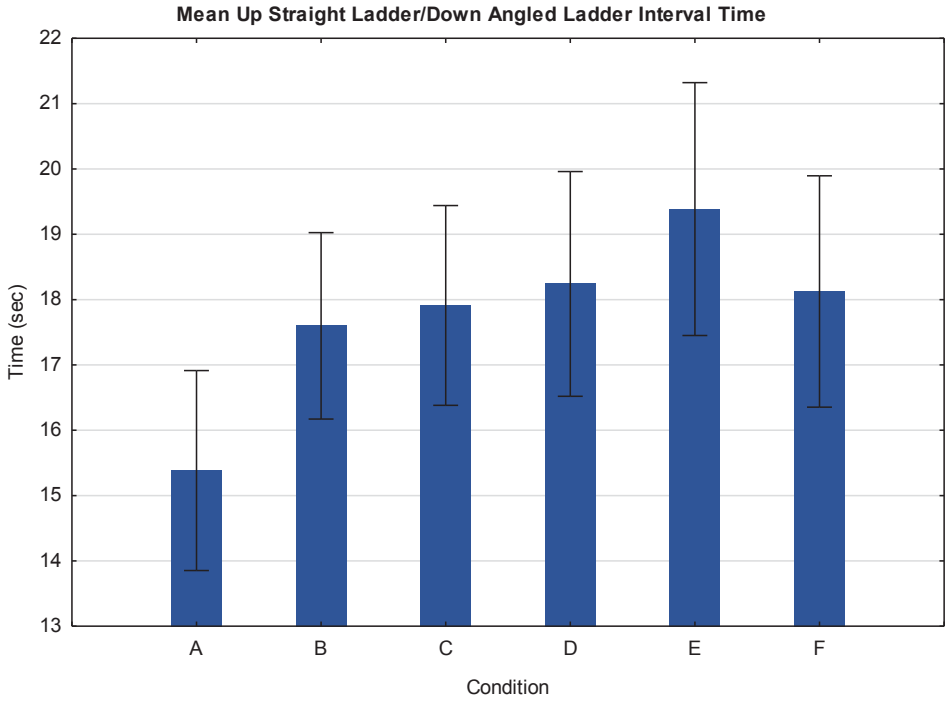

Figure 129: Mean Up Angled Ladder/Down Straight Ladder Interval Time by Condition

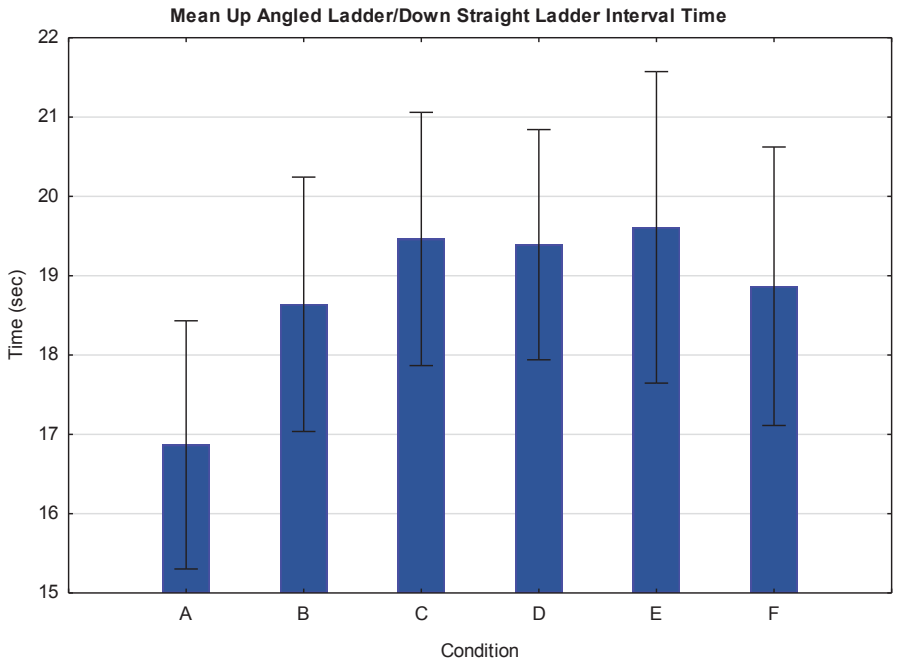

Figure 130: Mean Up Straight Ladder/Down Angled Ladder Interval Time by Condition

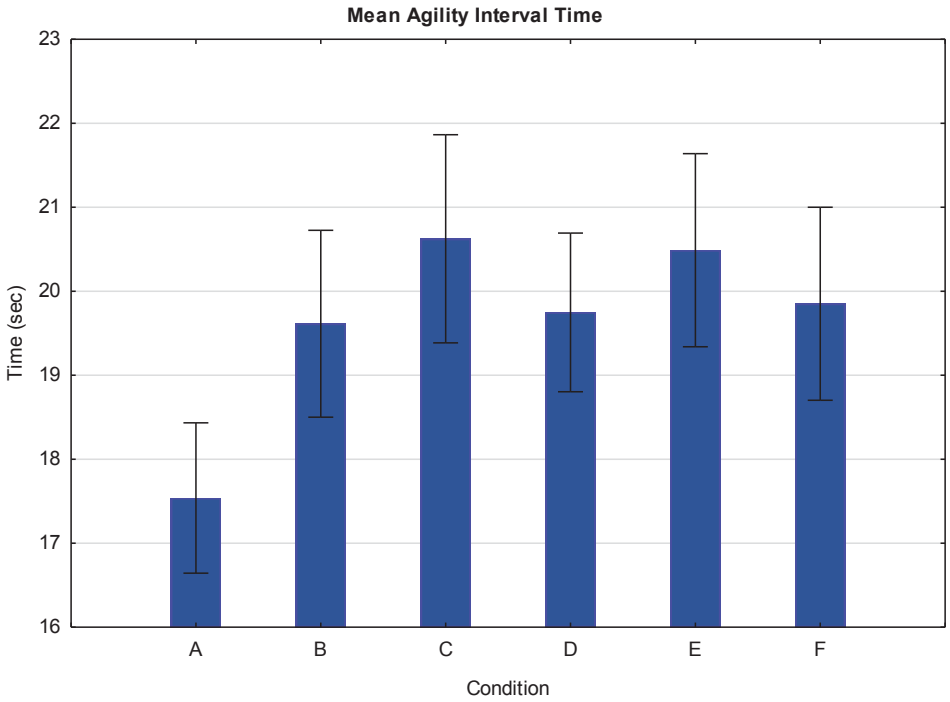

Figure 131: Mean Agility Interval Time by Condition

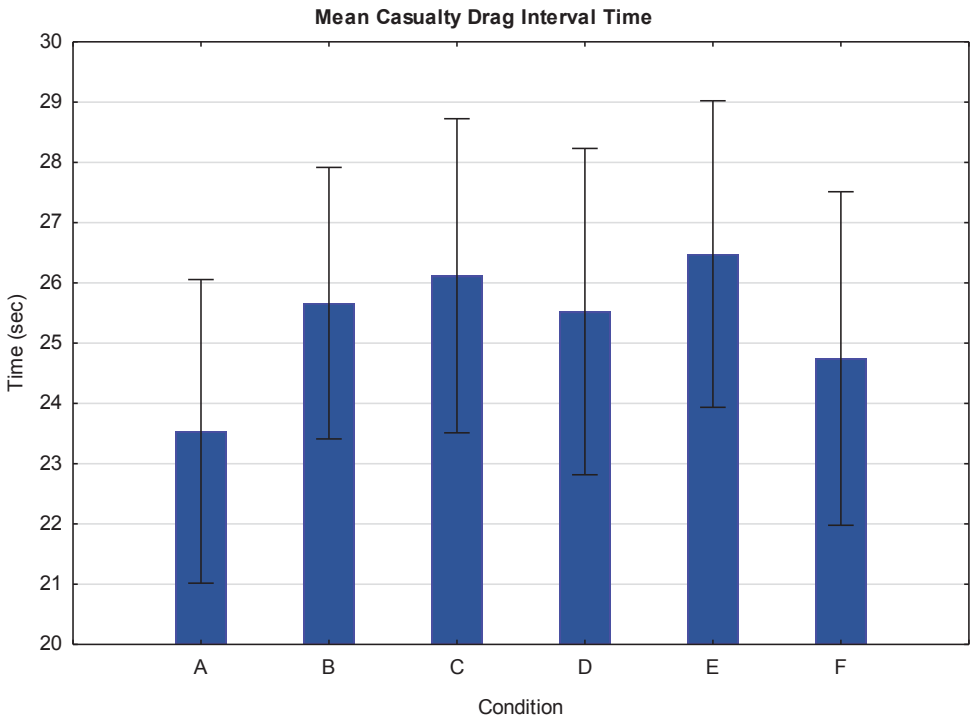

Figure 132: Mean Casualty Drag Interval Time by Condition

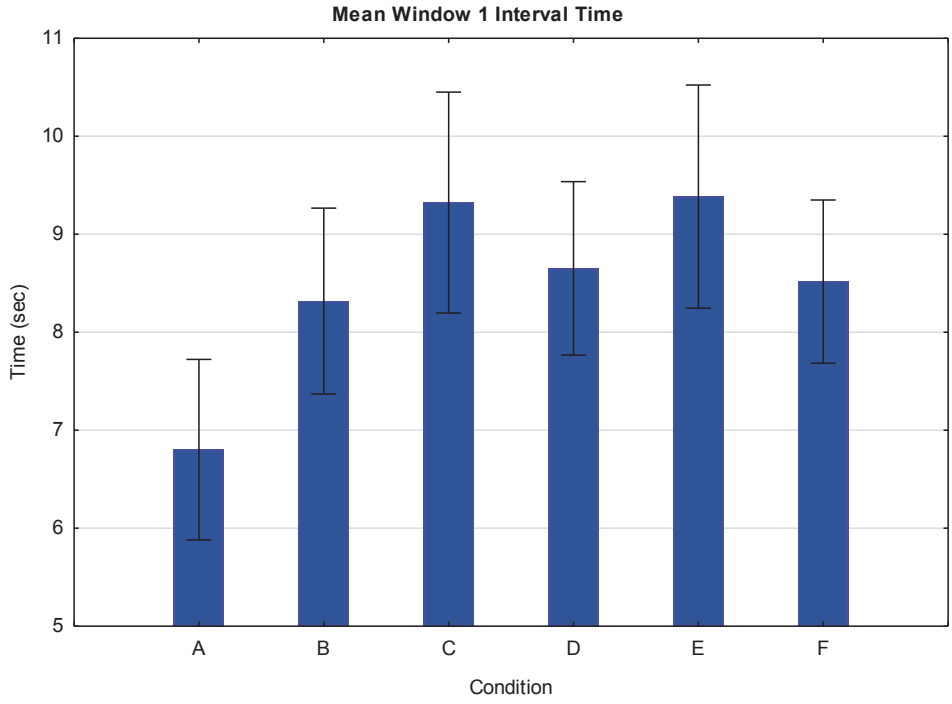

Figure 133: Mean Window 1 Interval Time by Condition

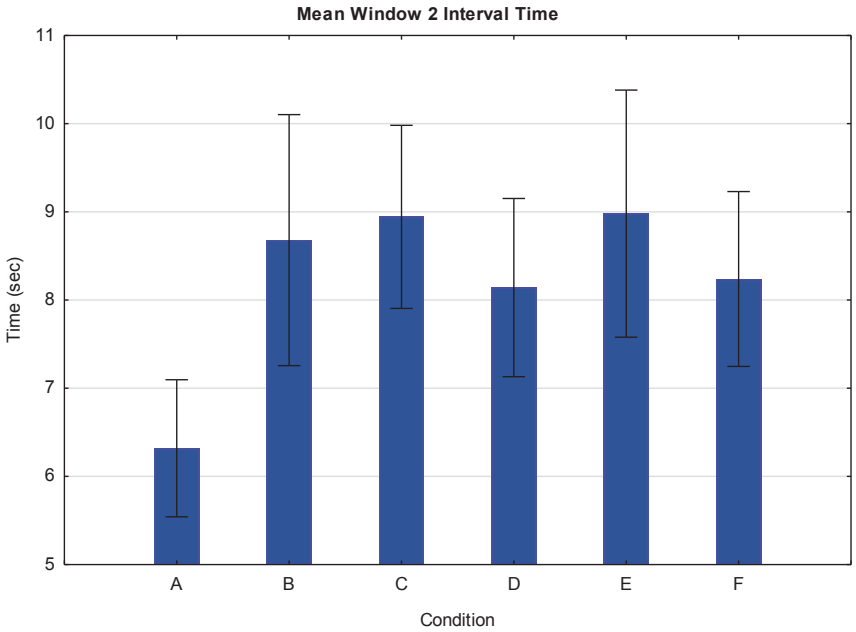

Figure 134: Mean Window 2 Interval Time by Condition

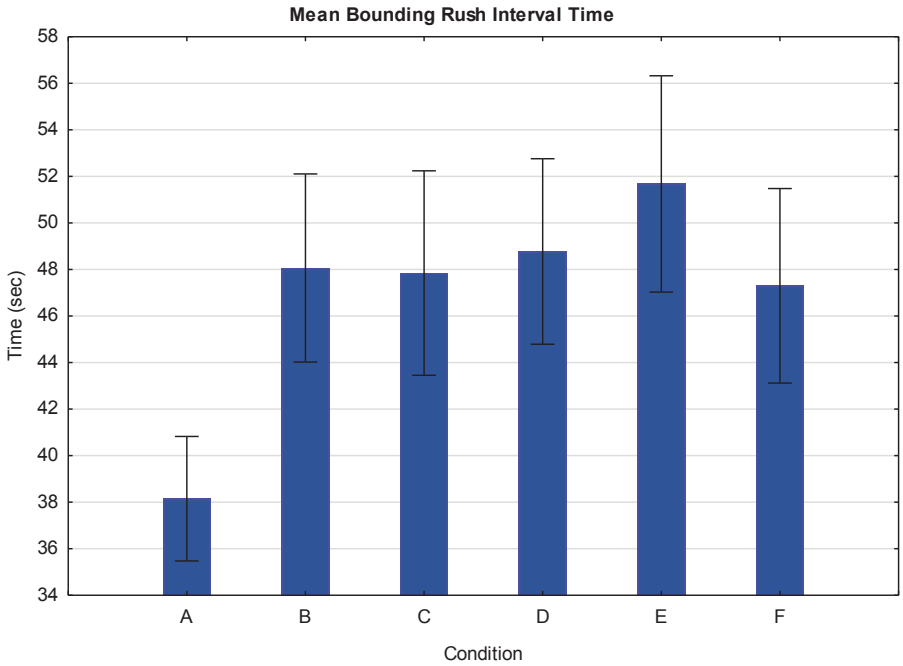

Figure 135: Mean Bounding Rush Interval Time by Condition

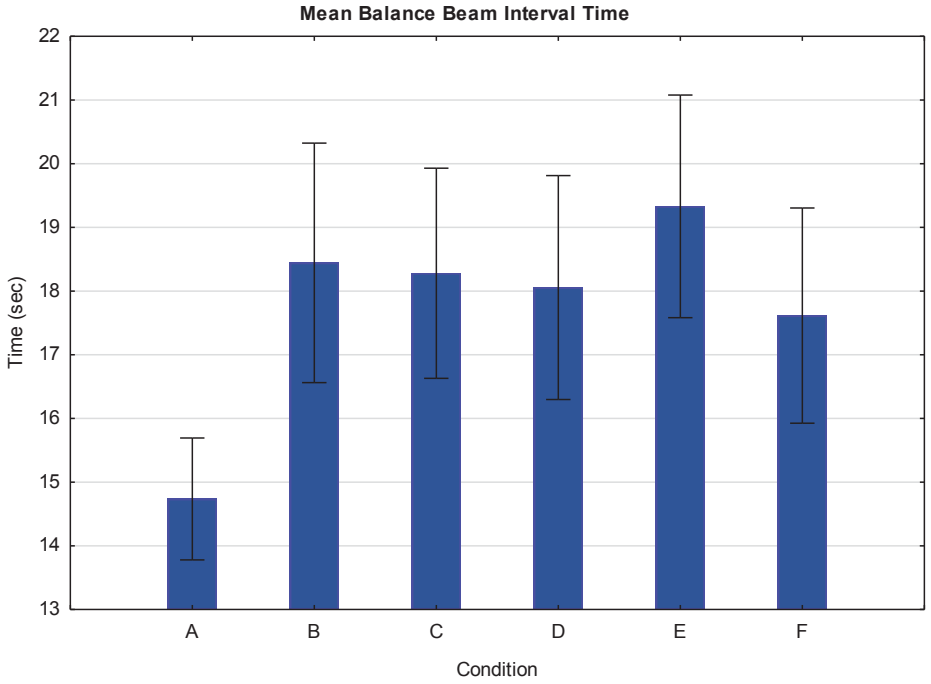

Figure 136: Mean Balance Beam Interval Time by Condition

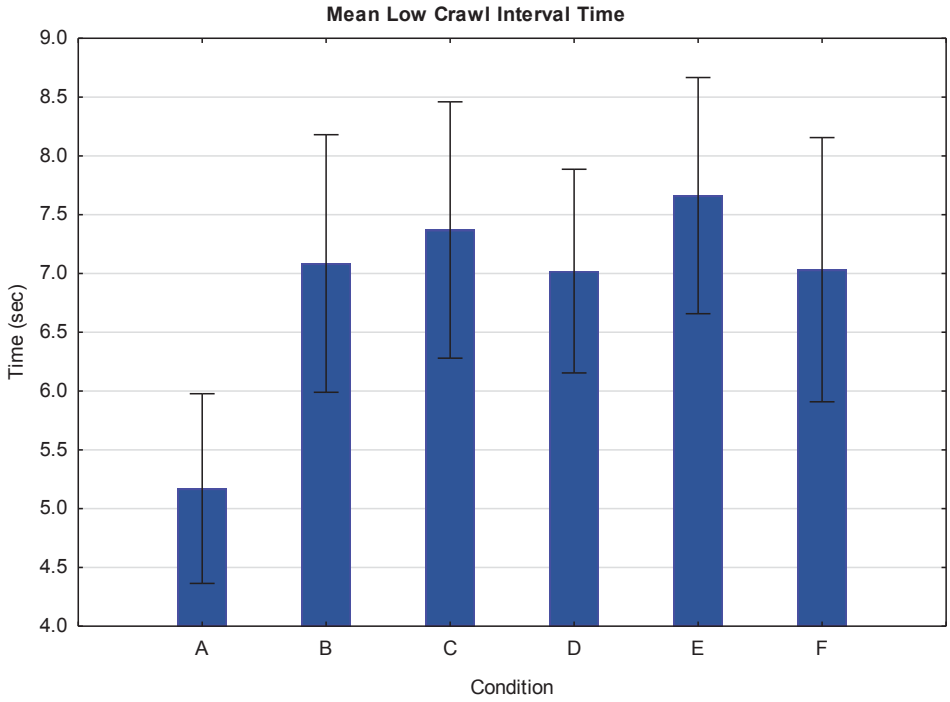

Figure 137: Mean Low Crawl Interval Time by Condition

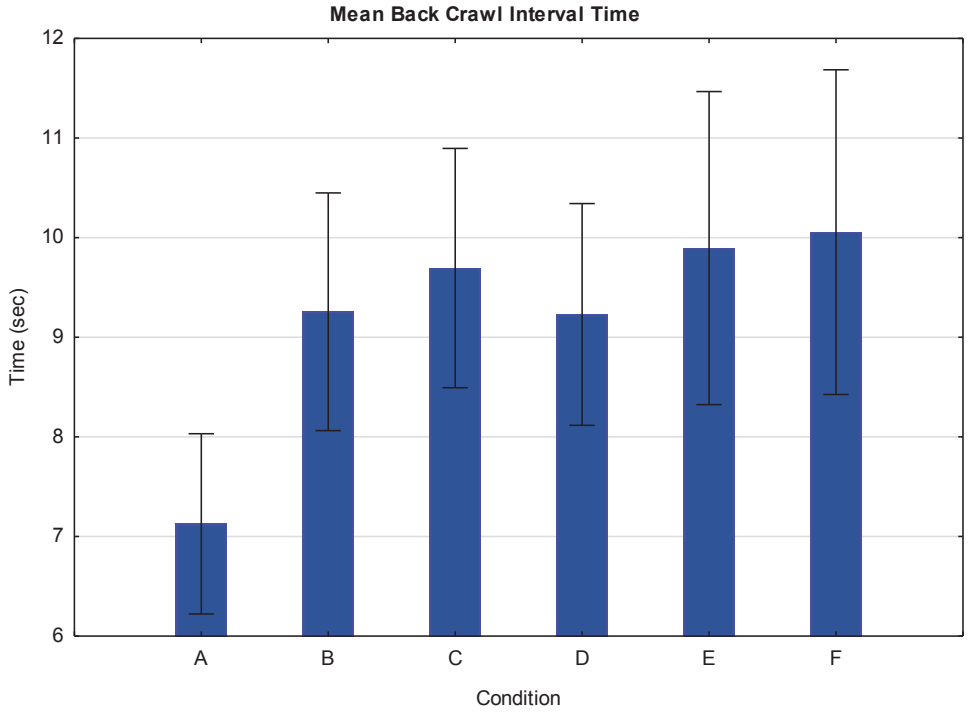

Figure 138: Mean Back Crawl Interval Time by Condition

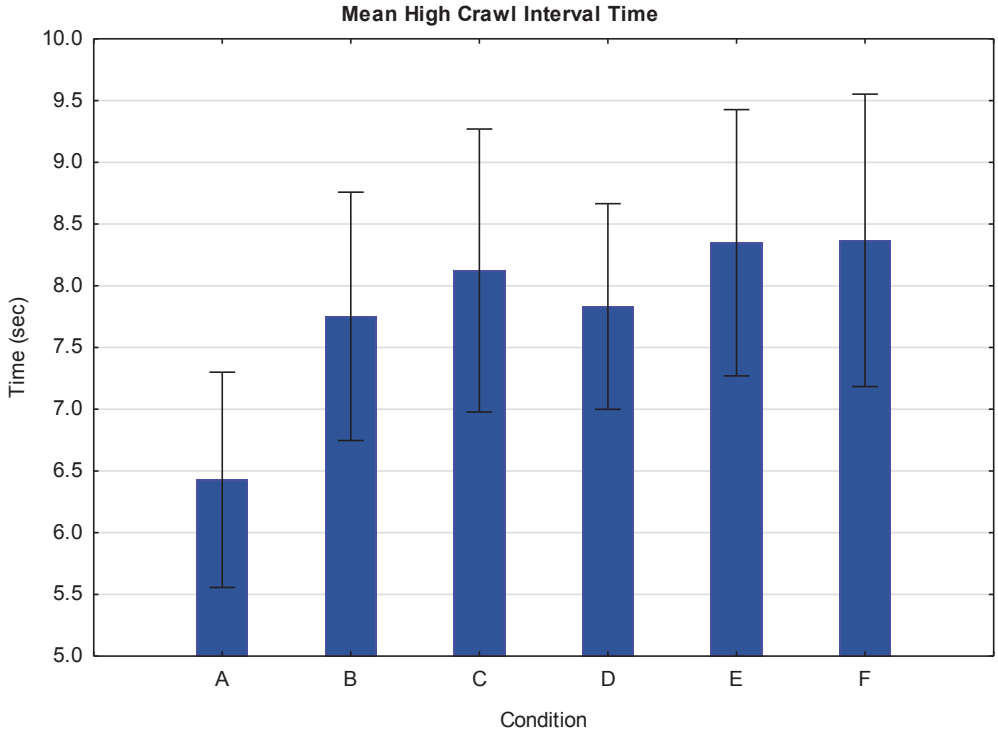

Figure 139: Mean High Crawl Interval Time by Condition

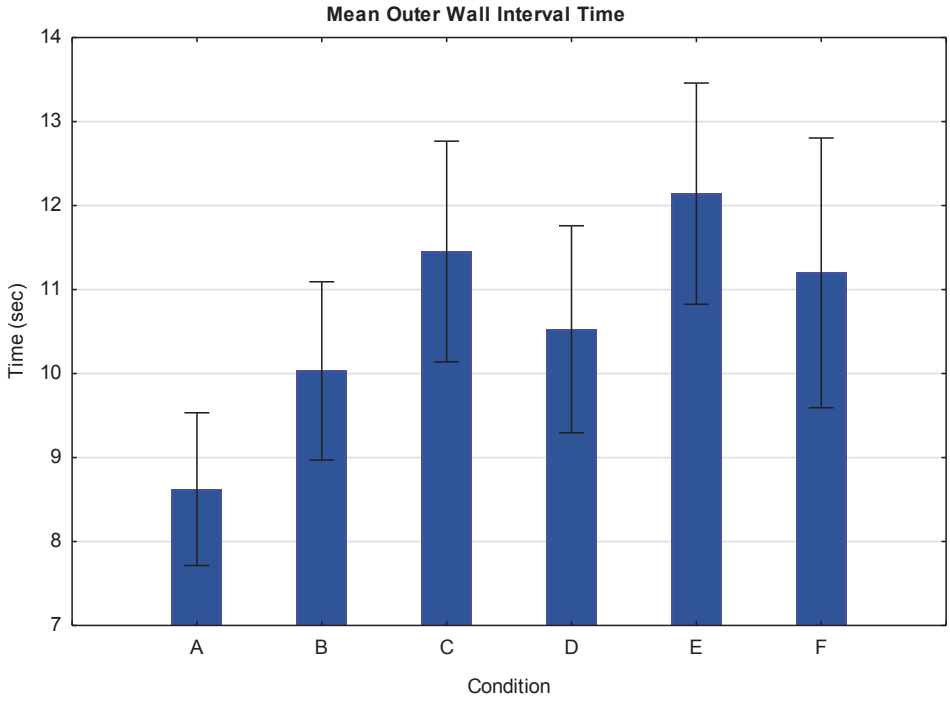

Figure 140: Mean Outer Wall Interval Time by Condition

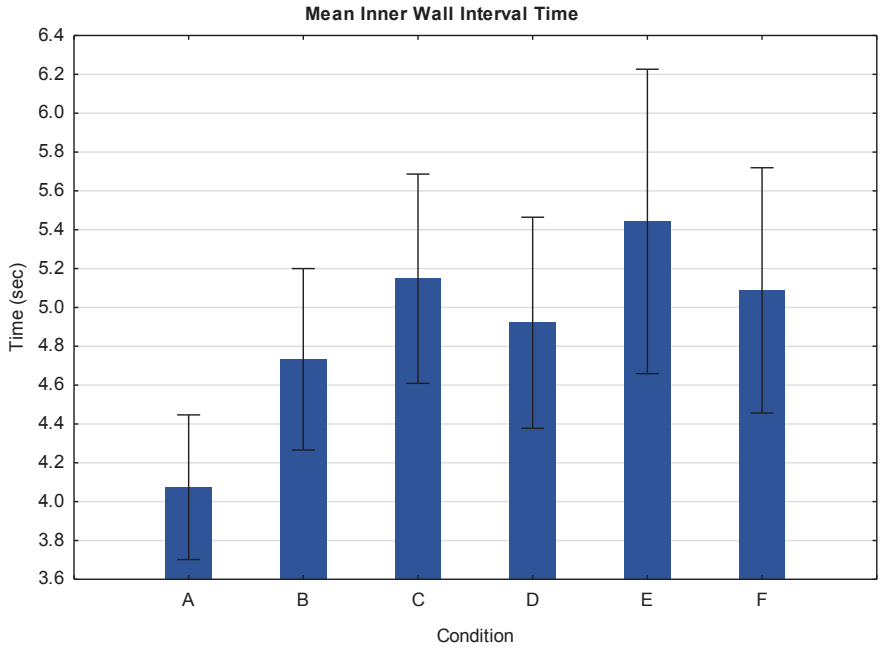

Figure 141: Mean Inner Wall Interval Time by Condition

Ancillary Stands

Noptel Marksmanship

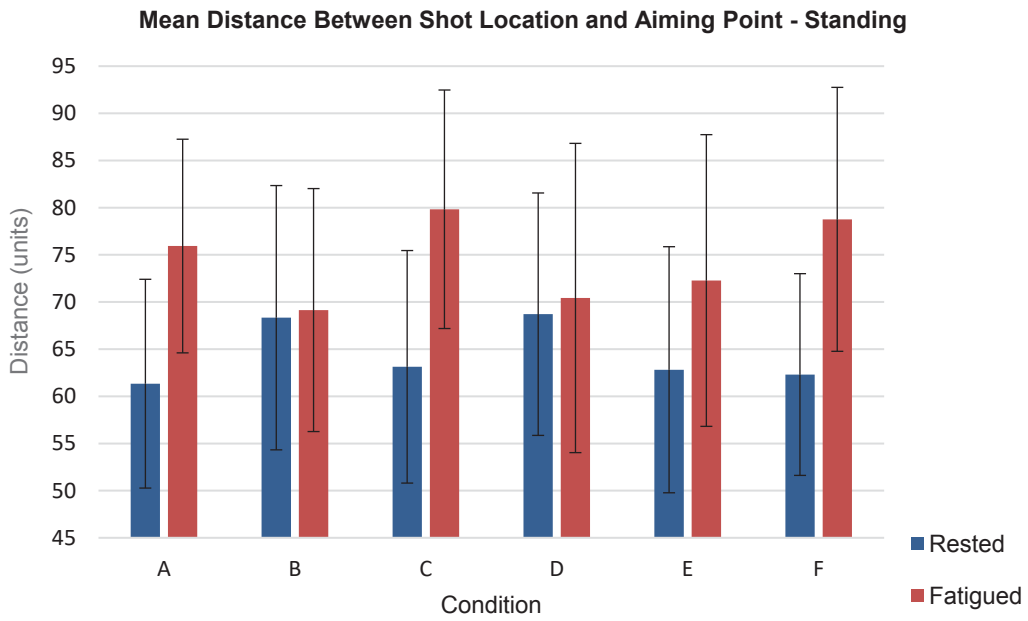

Figure 142: Mean Distance Between Shot Location and Aiming Point in the Standing Posture

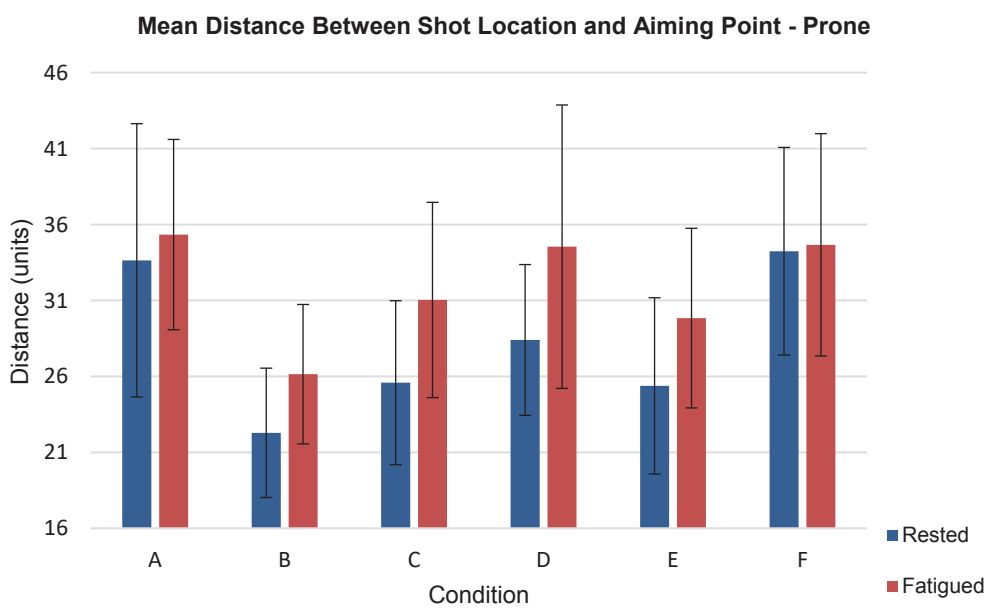

Figure 143: Mean Distance Between Shot Location and Aiming Point in the Prone Posture

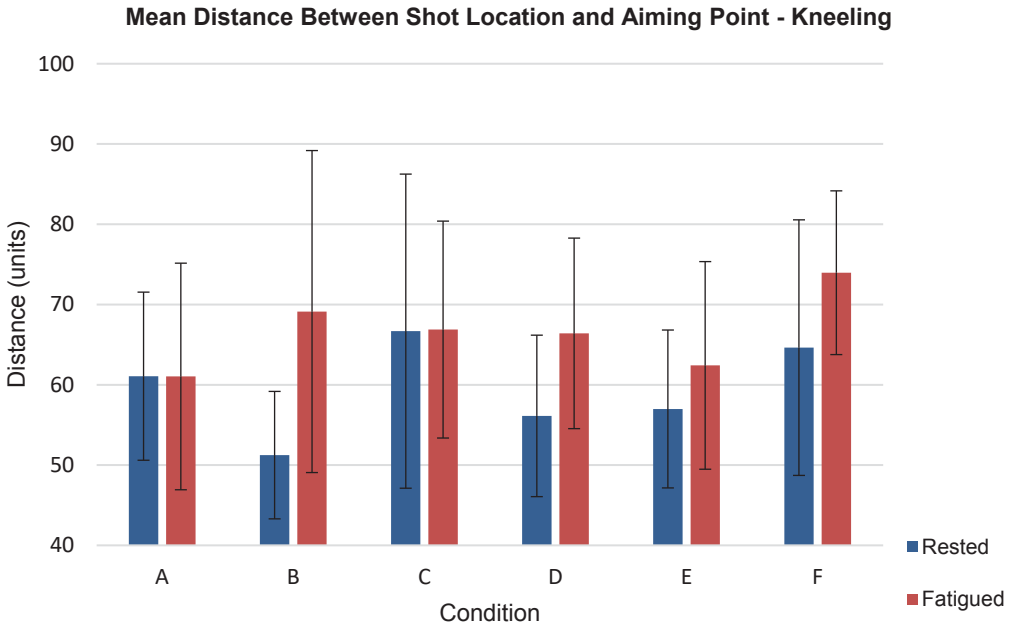

Figure 144: Mean Distance Between Shot Location and Aiming Point in the Kneeling Posture

Weight Transfer

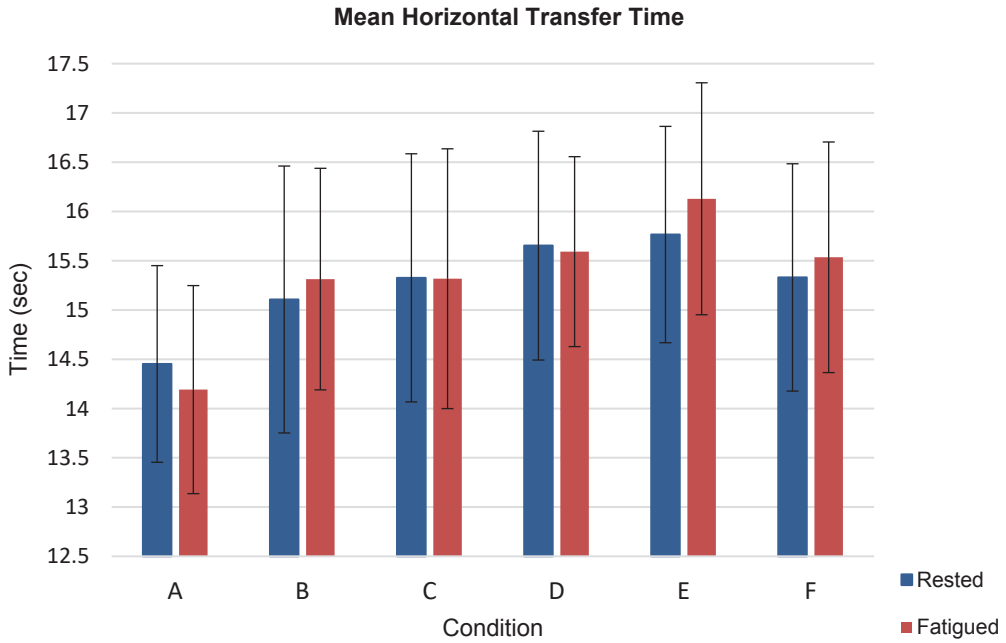

Figure 145: Mean Horizontal Weight Transfer Time by Condition

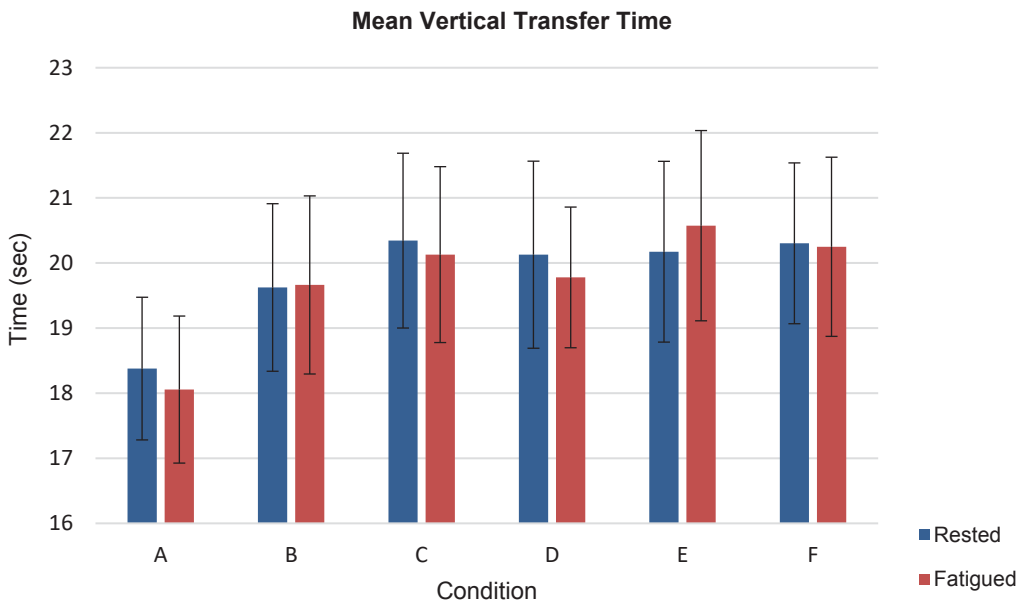

Figure 146: Mean Vertical Weight Transfer Time by Condition

Vertical Jump

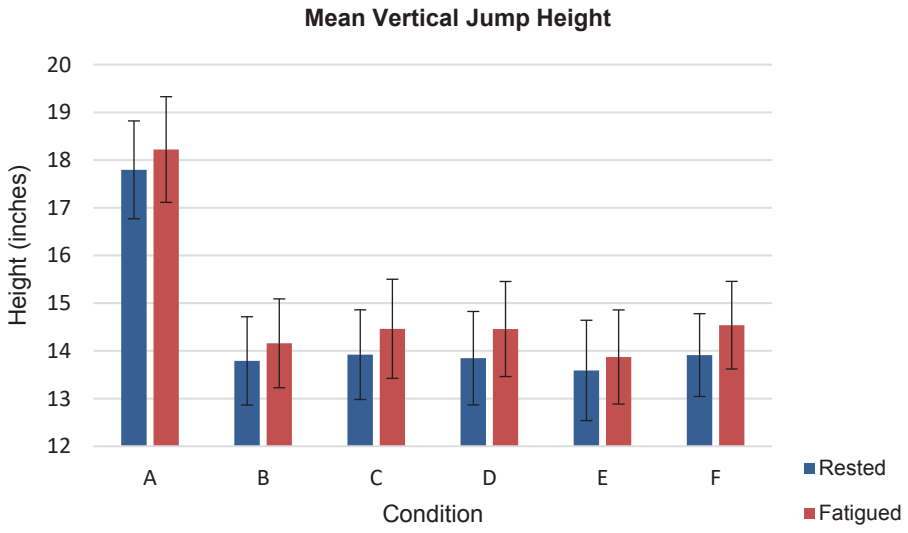

Figure 147: Mean Vertical Jump Height by Condition

Horizontal Jump

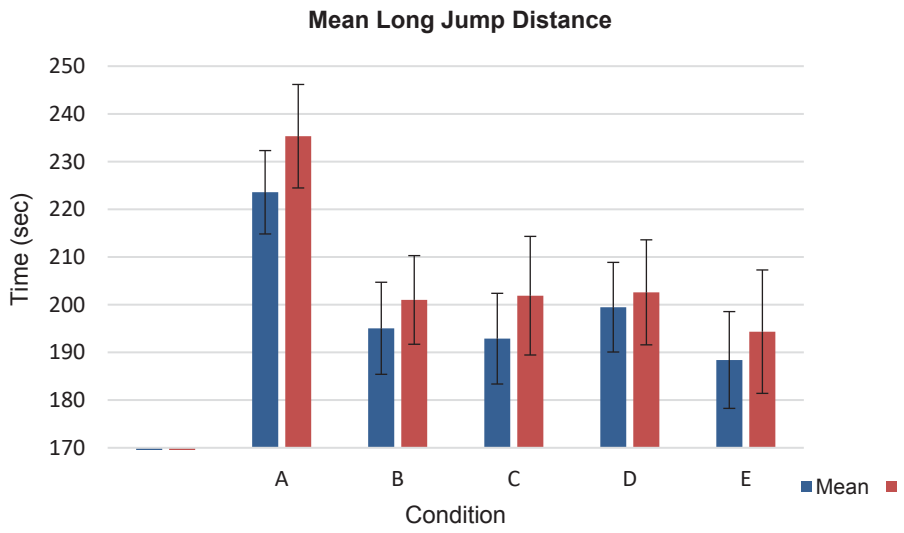

Figure 148: Mean Long Jump Distance by Condition

Annex L: Additional ROM Results

Trunk Rotation

Within this section are all graphs and Tukey HSD post-hoc analyses for the two way and three way interactions that led to significant effects on trunk rotation angles. Note that all red boxes in the Tukey's HSD post-hoc significance charts denote a significant difference.

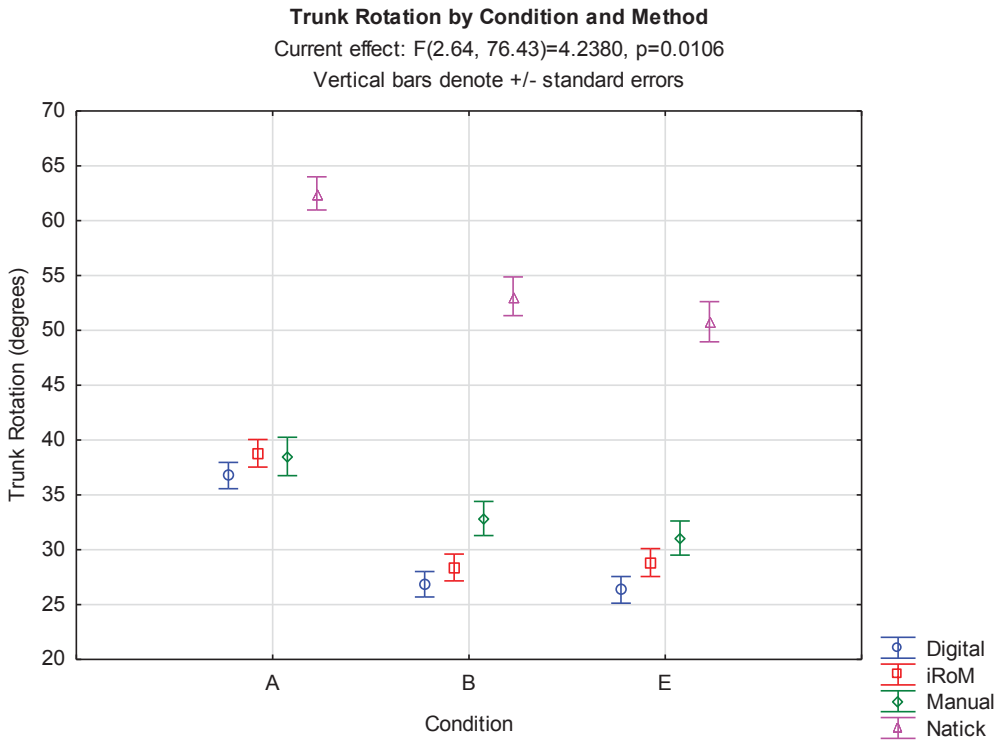

Figure 149: Effect of Condition x Method Interaction on Trunk Rotation for all Methods

		A				B				E			
		Digital	iRoM	Manual	Natick	Digital	iRoM	Manual	Natick	Digital	iRoM	Manual	Natick
A	Digital				X	X	X	X	X	X	X	X	X
	iRoM				X	X	X	X	X	X	X	X	X
	Manual				X	X	X	X	X	X	X	X	X
	Natick	X	X	X		X	X	X	X	X	X	X	X
B	Digital	X	X	X	X			X	X			X	X
	iRoM	X	X	X	X			X	X				X
	Manual	X	X	X	X	X	X		X	X	X		X
	Natick	X	X	X	X	X	X	X		X	X	X	
E	Digital	X	X	X	X			X	X			X	X
	iRoM	X	X	X	X			X	X				X
	Manual	X	X	X	X	X			X	X			X
	Natick	X	X	X	X	X	X	X		X	X	X	

Figure 150: Tukey HSD post-hoc summary of significant differences for Condition x Method Interaction

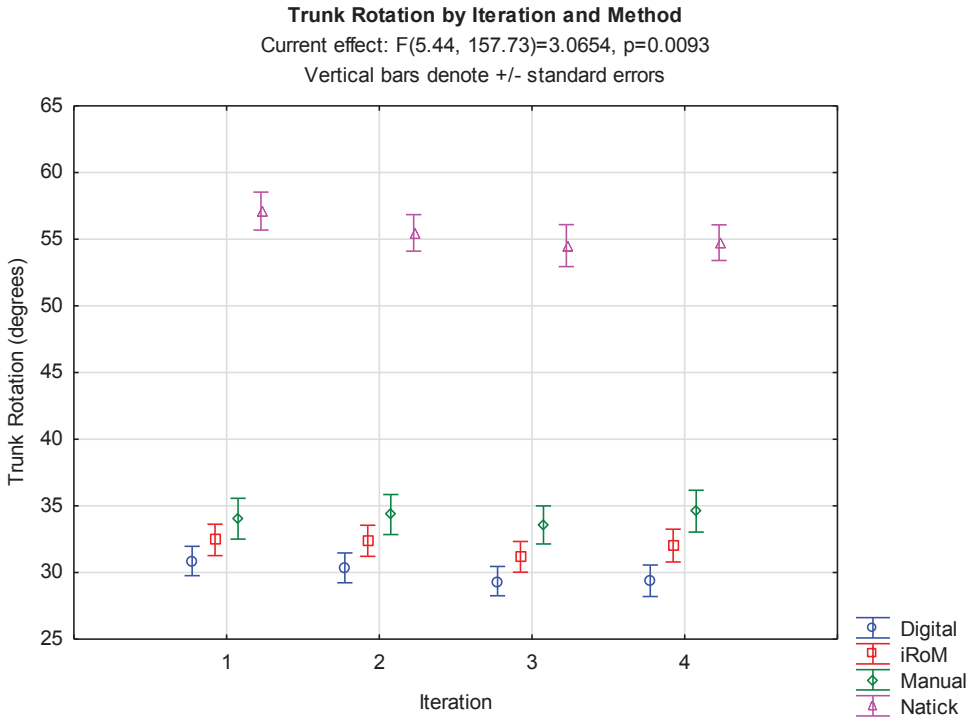

Figure 151: Effect of Iteration x Method Interaction on Trunk Rotation for all Methods

		1				2				3				4			
		Digital	iRoM	Manual	Natick	Digital	iRoM	Manual	Natick	Digital	iRoM	Manual	Natick	Digital	iRoM	Manual	Natick
1	Digital		X	X	X			X	X			X	X			X	X
	iRoM	X		X	X	X		X	X	X			X	X		X	X
	Manual	X	X		X	X	X		X	X	X		X	X	X		X
	Natick	X	X	X		X	X	X	X	X	X	X	X	X	X	X	X
2	Digital		X	X	X		X	X	X			X	X		X	X	X
	iRoM			X	X	X		X	X	X			X	X		X	X
	Manual	X	X		X	X	X		X	X	X		X	X	X		X
	Natick	X	X	X	X	X	X	X		X	X	X		X	X	X	
3	Digital		X	X	X		X	X	X		X	X	X		X	X	X
	iRoM			X	X			X	X	X		X	X	X		X	X
	Manual	X			X	X			X	X	X		X	X	X		X
	Natick	X	X	X	X	X	X	X		X	X	X		X	X	X	
4	Digital		X	X	X		X	X	X		X	X	X		X	X	X
	iRoM			X	X	X		X	X	X		X	X	X		X	X
	Manual	X	X		X	X	X		X	X	X		X	X	X		X
	Natick	X	X	X	X	X	X	X		X	X	X		X	X	X	

Figure 152: Tukey HSD post-hoc summary of significant differences for Iteration x Method Interaction

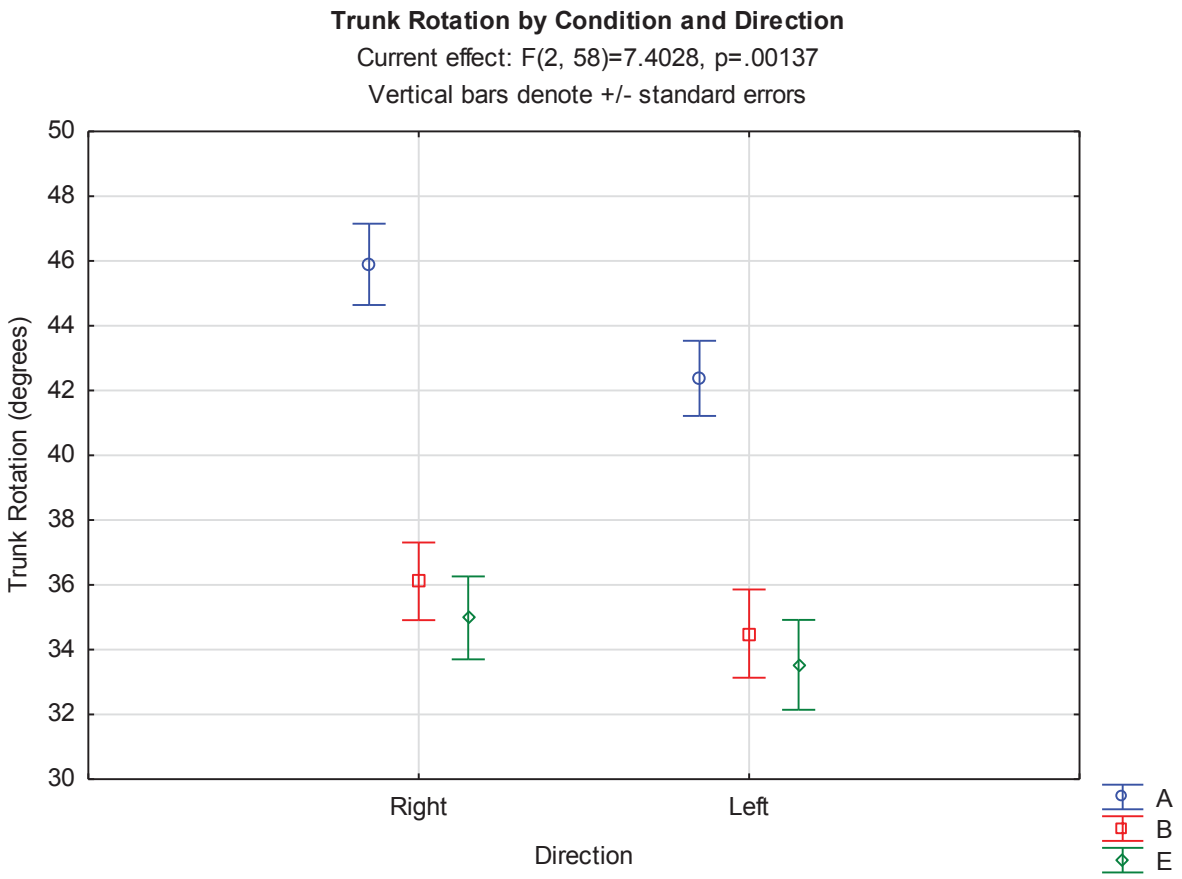

Figure 153: Effect of Condition x Direction Interaction on Trunk Rotation for all Methods

		A		B		E	
		Right	Left	Right	Left	Right	Left
A	Right		X	X	X	X	X
	Left	X		X	X	X	X
B	Right	X	X		X		X
	Left	X	X	X			
E	Right	X	X				X
	Left	X	X	X		X	

Figure 154: Tukey HSD post-hoc summary of significant differences for Condition x Direction Interaction

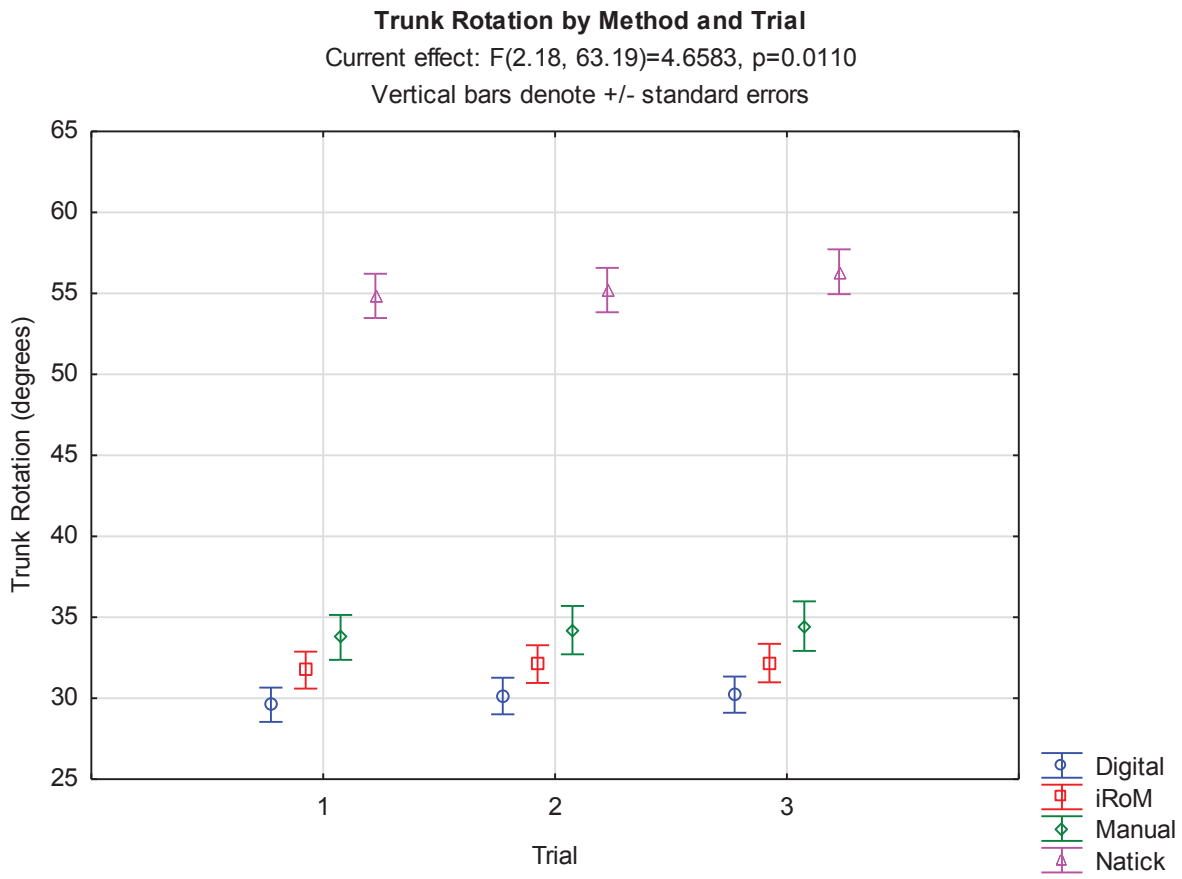

Figure 155: Effect of Method x Trial Interaction on Trunk Rotation for all Methods

		Digital			iRoM			Manual			Natick		
		1	2	3	1	2	3	1	2	3	1	2	3
Digital	1			X	X	X	X	X	X	X	X	X	X
	2				X	X	X	X	X	X	X	X	X
	3	X			X	X	X	X	X	X	X	X	X
iRoM	1	X	X	X				X	X	X	X	X	X
	2	X	X	X				X	X	X	X	X	X
	3	X	X	X				X	X	X	X	X	X
Manual	1	X	X	X	X	X	X			X	X	X	X
	2	X	X	X	X	X	X				X	X	X
	3	X	X	X	X	X	X	X			X	X	X
Natick	1	X	X	X	X	X	X	X	X	X			X
	2	X	X	X	X	X	X	X	X	X			X
	3	X	X	X	X	X	X	X	X	X	X	X	

Figure 156: Tukey HSD post-hoc summary of significant differences for Method x Trial Interaction

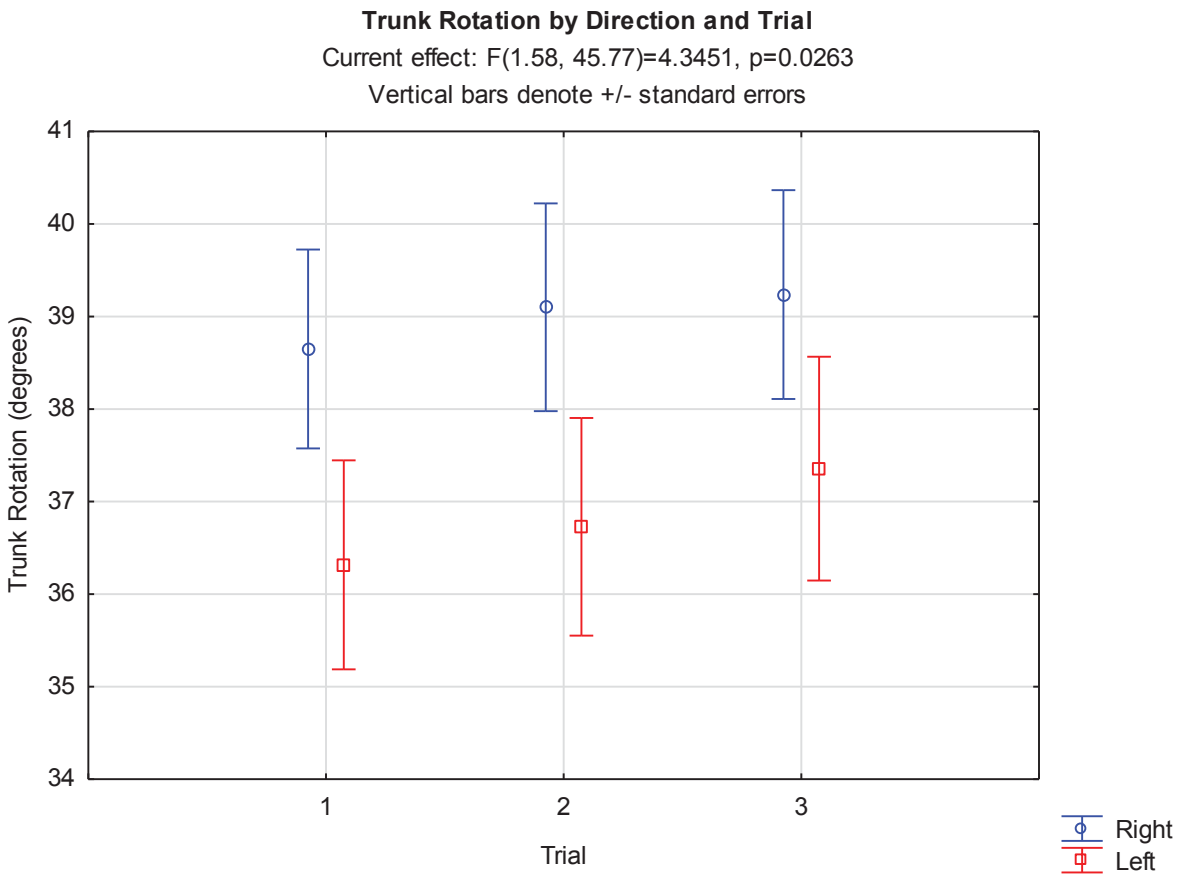

Figure 157: Effect of Direction x Trial on Trunk Rotation Angle for all Methods

		Right			Left		
		1	2	3	1	2	3
Right	1		X	X	X	X	X
	2	X			X	X	X
	3	X			X	X	X
Left	1	X	X	X		X	X
	2	X	X	X	X		X
	3	X	X	X	X	X	

Figure 158: Tukey HSD post-hoc summary of significant differences for Direction x Trial Interaction

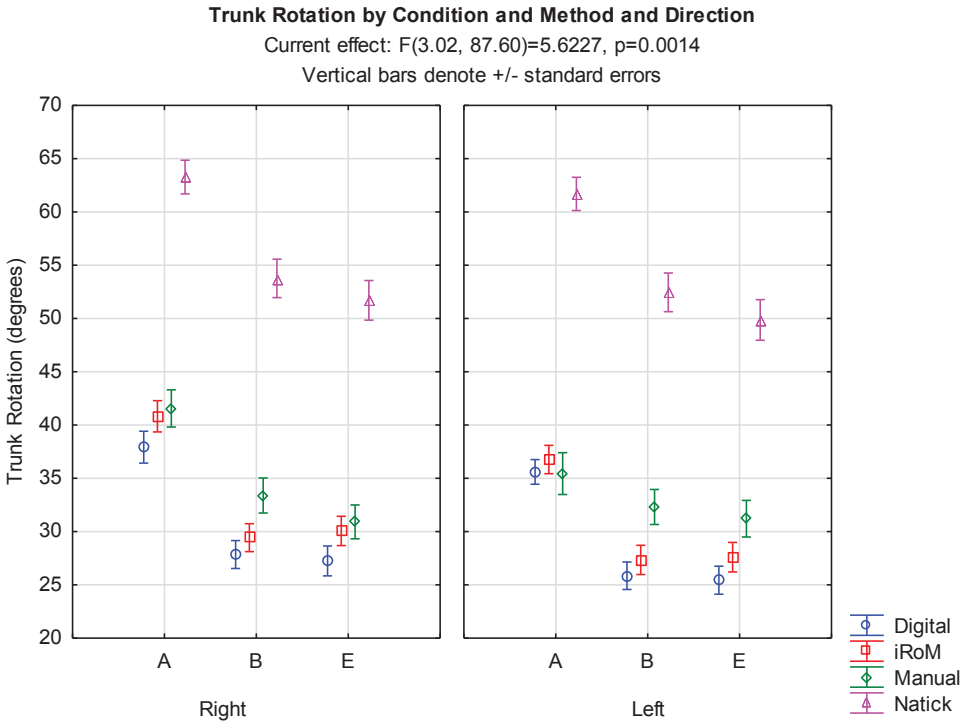

Figure 159: Effect of Condition x Method x Direction on Trunk Rotation Angle

			A								B								E							
			Digital		iRoM		Manual		Natick		Digital		iRoM		Manual		Natick		Digital		iRoM		Manual		Natick	
			Right	Left	Right	Left	Right	Left	Right	Left	Right	Left	Right	Left	Right	Left	Right	Left	Right	Left	Right	Left	Right	Left	Right	Left
A	Digital	Right			X		X	X	X	X	X	X	X	X	X	X	X	X	X	X	X	X	X	X	X	X
		Left			X		X		X	X	X	X	X	X		X	X	X	X	X	X	X	X	X	X	X
	iRoM	Right	X	X		X		X	X	X	X	X	X	X	X	X	X	X	X	X	X	X	X	X	X	X
		Left			X		X		X	X	X	X	X	X	X	X	X	X	X	X	X	X	X	X	X	X
	Manual	Right	X	X		X		X	X	X	X	X	X	X	X	X	X	X	X	X	X	X	X	X	X	X
		Left	X		X		X		X	X	X	X	X	X		X	X	X	X	X	X	X	X	X	X	X
	Natick	Right	X	X	X	X	X	X			X	X	X	X	X	X	X	X	X	X	X	X	X	X	X	X
		Left	X	X	X	X	X	X			X	X	X	X	X	X	X	X	X	X	X	X	X	X	X	X
B	Digital	Right	X	X	X	X	X	X	X	X					X	X	X	X		X			X	X	X	X
		Left	X	X	X	X	X	X	X	X			X		X	X	X	X			X		X	X	X	X
	iRoM	Right	X	X	X	X	X	X	X	X		X			X	X	X	X		X					X	X
		Left	X	X	X	X	X	X	X	X					X	X	X	X			X		X	X	X	X
	Manual	Right	X		X	X	X		X	X	X	X	X	X			X	X	X	X	X	X	X		X	X
		Left	X	X	X	X	X	X	X	X	X	X	X	X			X	X	X	X		X			X	X
	Natick	Right	X	X	X	X	X	X	X	X	X	X	X	X	X	X			X	X	X	X	X	X		X
		Left	X	X	X	X	X	X	X	X	X	X	X	X	X	X			X	X	X	X	X	X		X
E	Digital	Right	X	X	X	X	X	X	X	X					X	X	X	X			X		X	X	X	X
		Left	X	X	X	X	X	X	X	X	X		X		X	X	X	X			X		X	X	X	X
	iRoM	Right	X	X	X	X	X	X	X	X		X		X	X		X	X	X	X		X			X	X
		Left	X	X	X	X	X	X	X	X					X	X	X	X			X		X	X	X	X
	Manual	Right	X	X	X	X	X	X	X	X	X	X		X	X		X	X	X	X		X			X	X
		Left	X	X	X	X	X	X	X	X	X	X		X			X	X	X	X		X			X	X
	Natick	Right	X	X	X	X	X	X	X	X	X	X	X	X	X	X			X	X	X	X	X	X		
		Left	X	X	X	X	X	X	X	X	X	X	X	X	X	X	X	X	X	X	X	X	X	X		

Figure 160: Tukey HSD post-hoc summary of significant differences for Condition x Method x Direction Interaction

Lateral Bending

Within this section are all graphs and Tukey HSD post-hoc analyses for the two way and three way interactions that led to significant effects on lateral bending angles. Note that all red boxes in the Tukey's HSD post-hoc significance charts denote a significant difference.

Digital, iRoM and Manual Methods

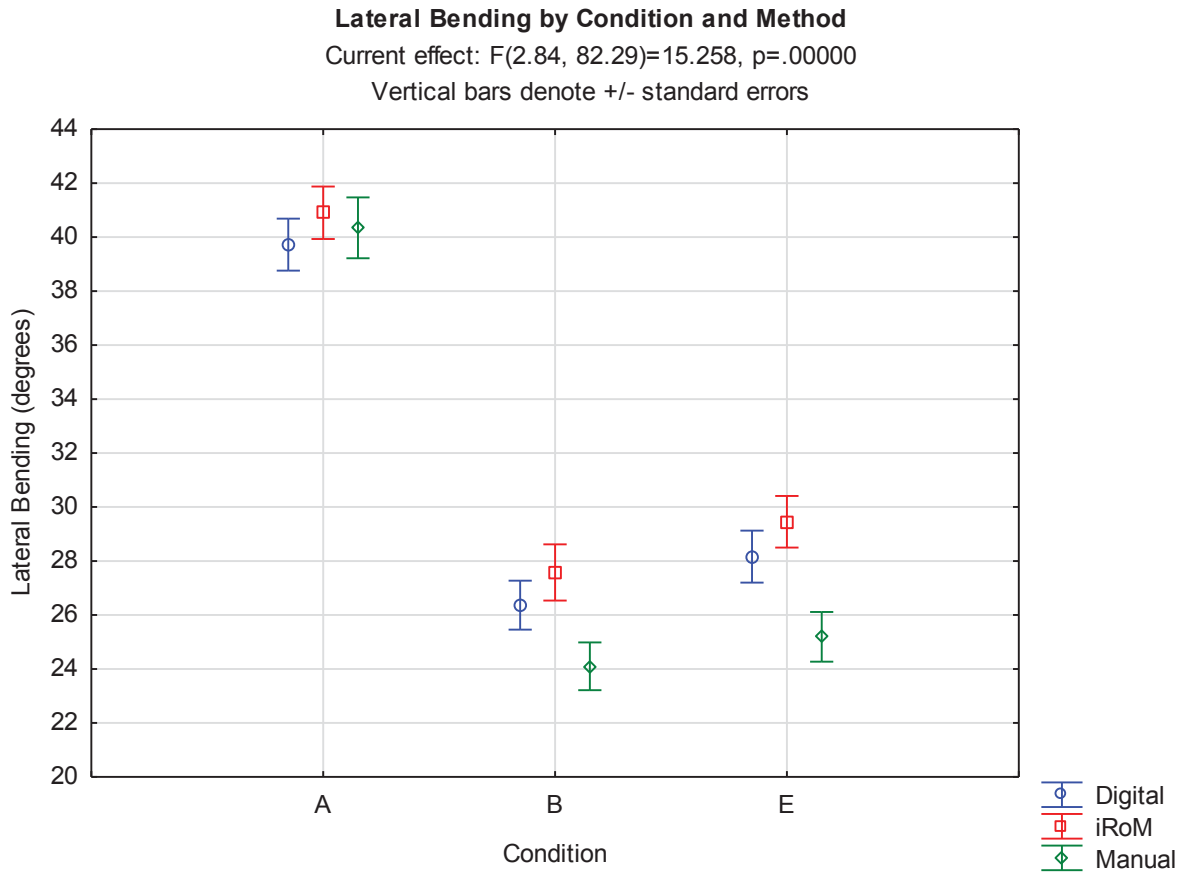

Figure 161: Effect of Condition x Method on Lateral Bending Angle for Digital, iRoM, and Manual Methods

		A			B			E		
		Digital	iRoM	Manual	Digital	iRoM	Manual	Digital	iRoM	Manual
A	Digital				X	X	X	X	X	X
	iRoM				X	X	X	X	X	X
	Manual				X	X	X	X	X	X
B	Digital	X	X	X			X	X	X	
	iRoM	X	X	X			X		X	X
	Manual	X	X	X	X	X		X	X	
E	Digital	X	X	X	X		X		X	X
	iRoM	X	X	X	X	X	X	X		X
	Manual	X	X	X		X		X	X	

Figure 162: Tukey HSD Post-hoc Summary of Significant Differences for Condition x Method Interaction

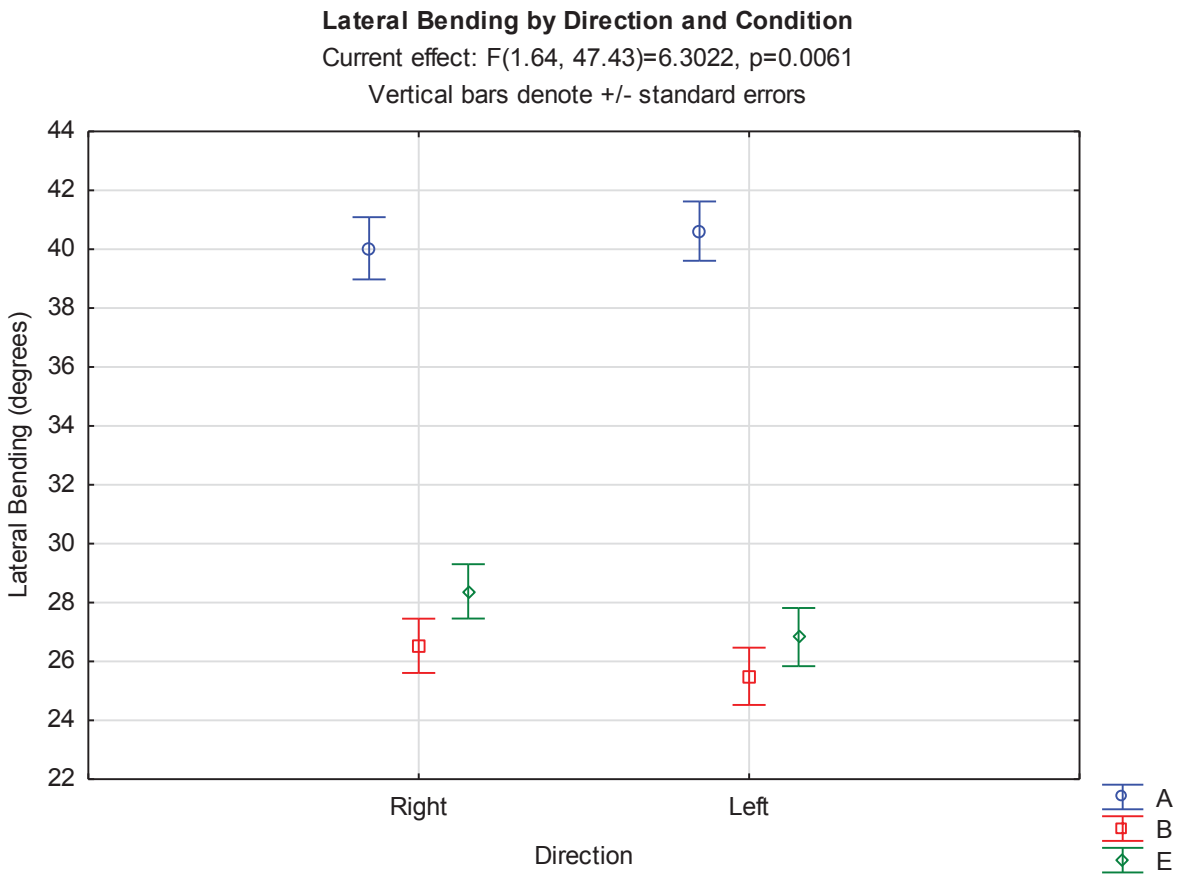

Figure 163: Effect of Condition x Direction on Lateral Bending for Digital, iRoM, and Manual Methods

		A		B		E	
		Right	Left	Right	Left	Right	Left
A	Right			X	X	X	X
	Left			X	X	X	X
B	Right	X	X			X	
	Left	X	X			X	X
E	Right	X	X	X	X		X
	Left	X	X		X	X	

Figure 164: Tukey HSD Post-hoc Summary of Significant Differences for Condition x Direction Interaction

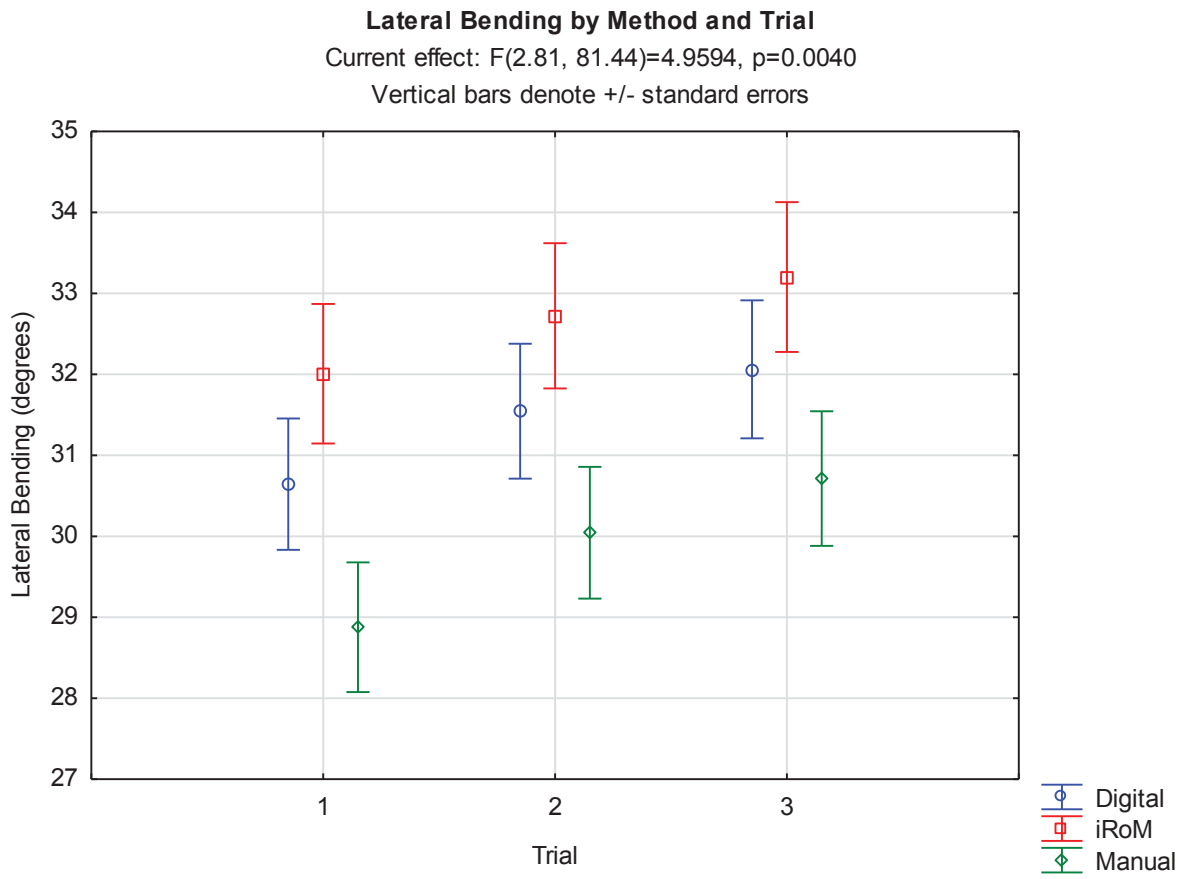

Figure 165: Effect of Method x Trial on Lateral Bending for Digital, iRoM, and Manual Methods

		Digital			iRoM			Manual		
		1	2	3	1	2	3	1	2	3
Digital	1		X	X	X	X	X	X	X	
	2	X		X	X	X	X	X	X	X
	3	X	X			X	X	X	X	X
iRoM	1	X	X			X	X	X	X	X
	2	X	X	X	X		X	X	X	X
	3	X	X	X	X	X		X	X	X
Manual	1	X	X	X	X	X	X		X	X
	2	X	X	X	X	X	X	X		X
	3		X	X	X	X	X	X	X	

Figure 166: Tukey HSD Post-hoc Summary of Significant Differences for Method x Trial Interaction

Natick Method

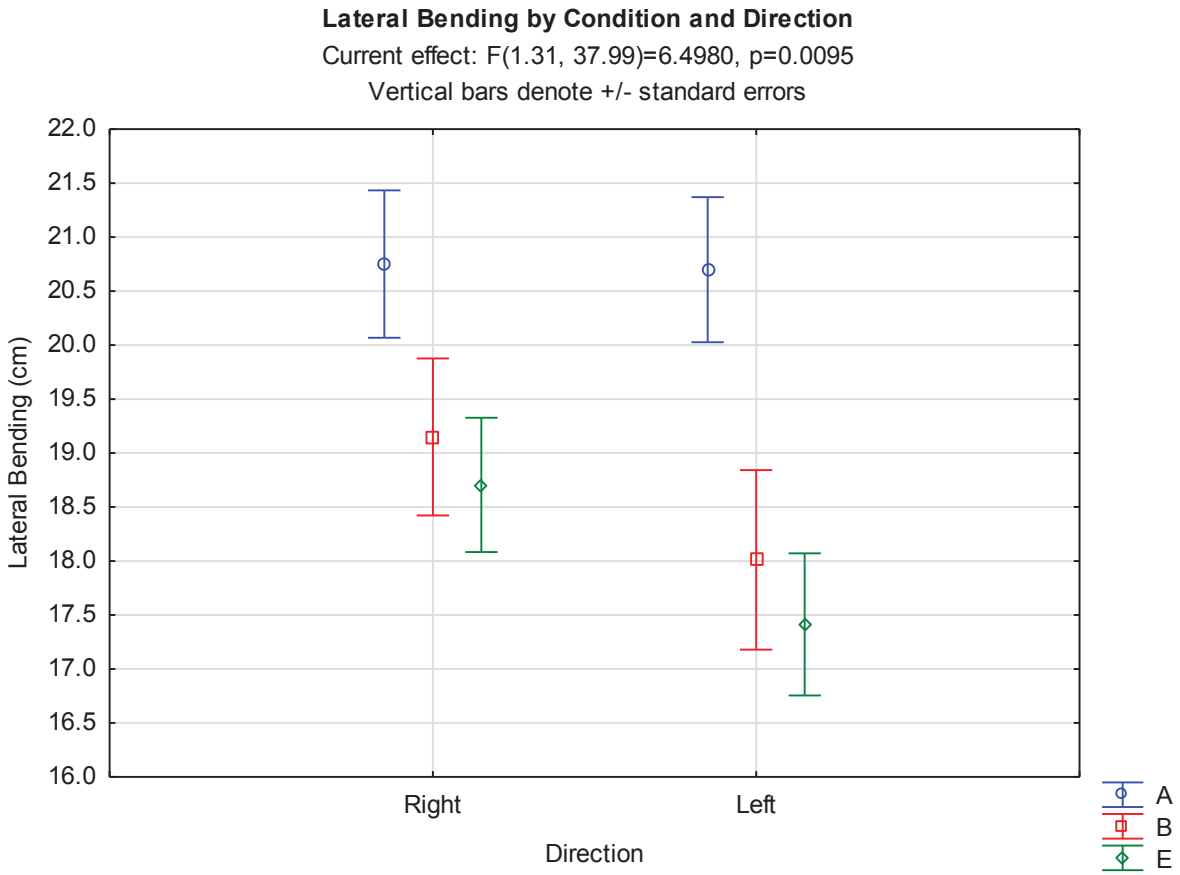

Figure 167: Effect of Condition x Direction on Lateral Bending for Natick Method

		A		B		E	
		Right	Left	Right	Left	Right	Left
A	Right			X	X	X	X
	Left			X	X	X	X
B	Right	X	X		X		X
	Left	X	X	X			
E	Right	X	X				X
	Left	X	X	X		X	

Figure 168: Tukey HSD Post-hoc Summary of Significant Differences for Condition x Direction Interaction

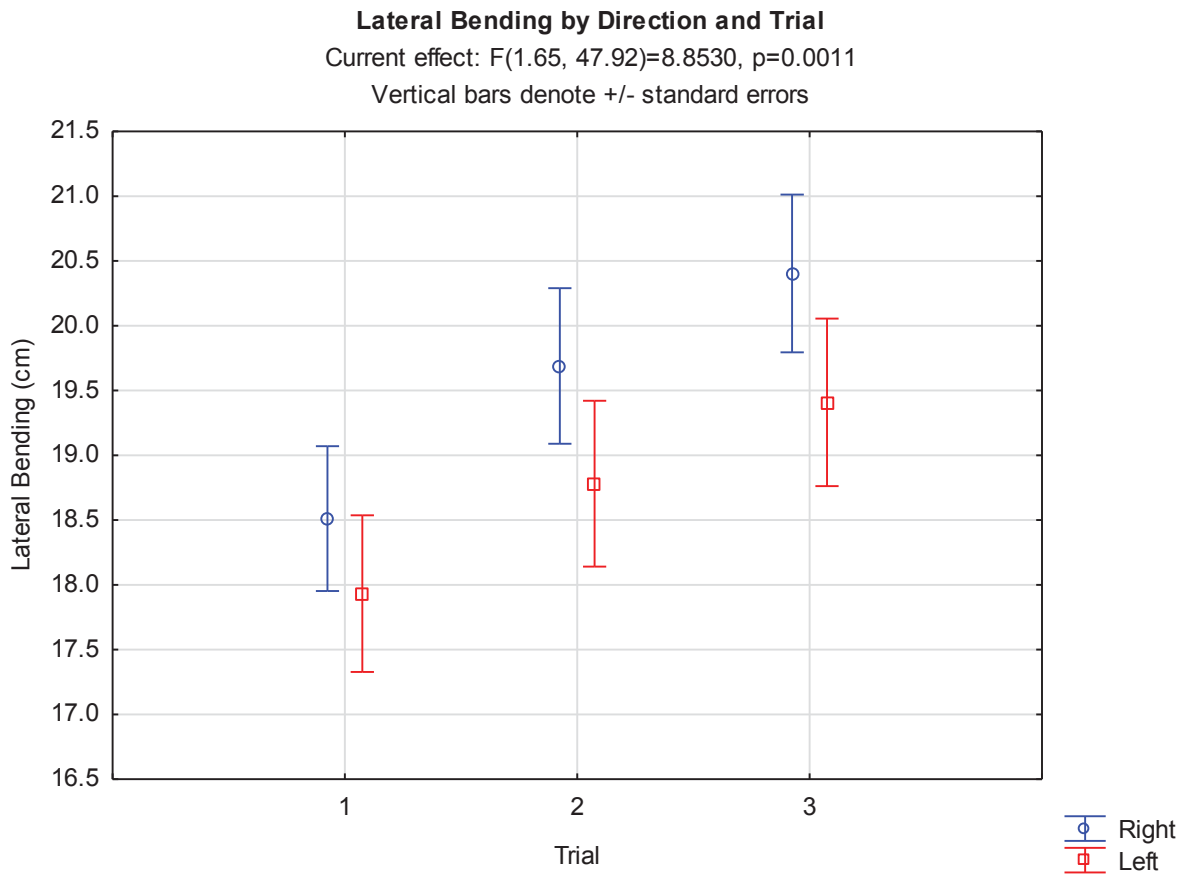

Figure 169: Effect of Direction x Trial on Lateral Bending for Natick Method

		Right			Left		
		1	2	3	1	2	3
Right	1		X	X	X	X	X
	2	X		X	X	X	X
	3	X	X		X	X	X
Left	1	X	X	X		X	X
	2	X	X	X	X		X
	3	X	X	X	X	X	

Figure 170: Tukey HSD Post-hoc Summary of Significant Differences for Direction x Trial Interaction

Front Forward Flexion

Within this section are all graphs and Tukey HSD post-hoc analyses for the two way and three way interactions that led to significant effects on lateral bending angles. Note that all red boxes in the Tukey's HSD post-hoc significance charts denote a significant difference.

Digital and iRoM Methods

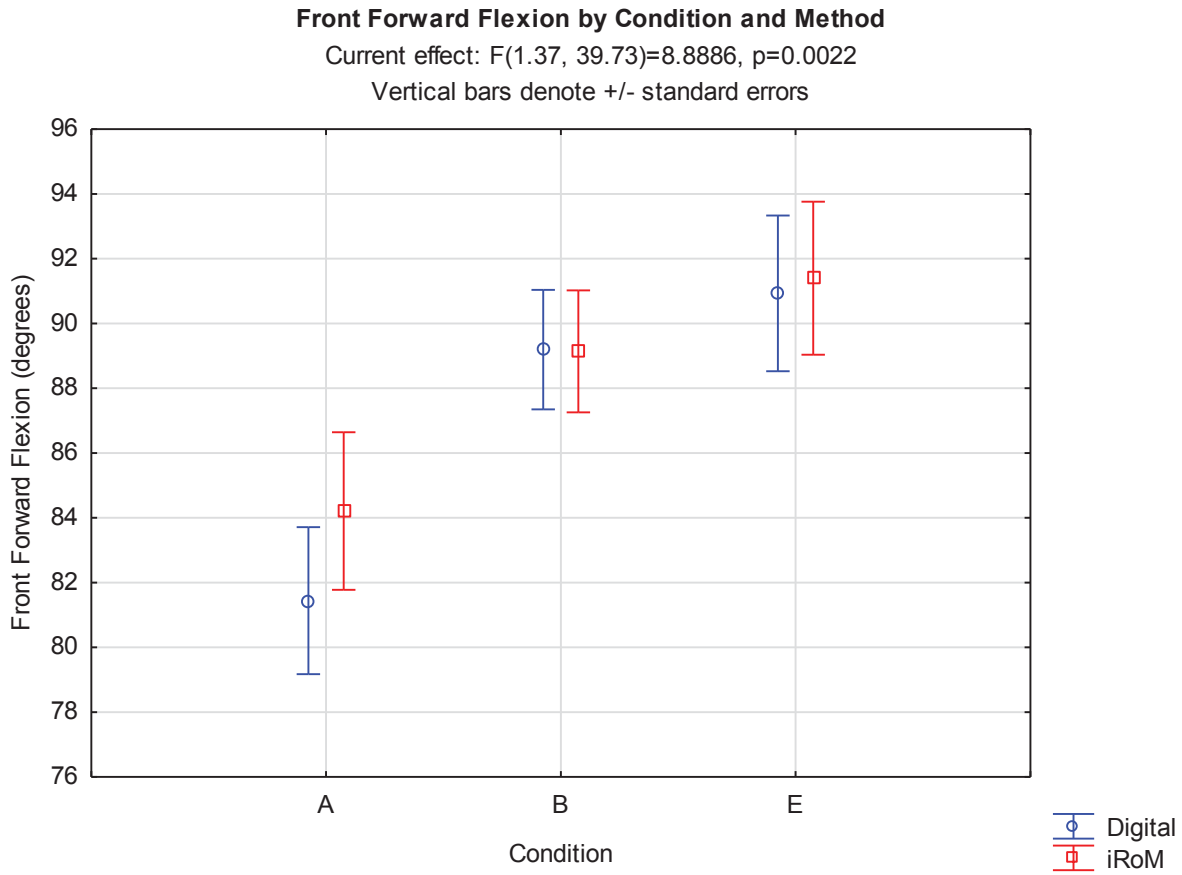

Figure 171: Effect of Condition x Method on Front Forward Flexion for Digital and iRoM Methods

		A		B		E	
		Digital	iRoM	Digital	iRoM	Digital	iRoM
A	Digital		X	X	X	X	X
	iRoM	X		X	X	X	X
B	Digital	X	X			X	X
	iRoM	X	X			X	X
E	Digital	X	X	X	X		
	iRoM	X	X	X	X		

Figure 172: Tukey HSD Post-hoc Summary of Significant Differences for Condition x Method Interaction

Manual and Natick Methods

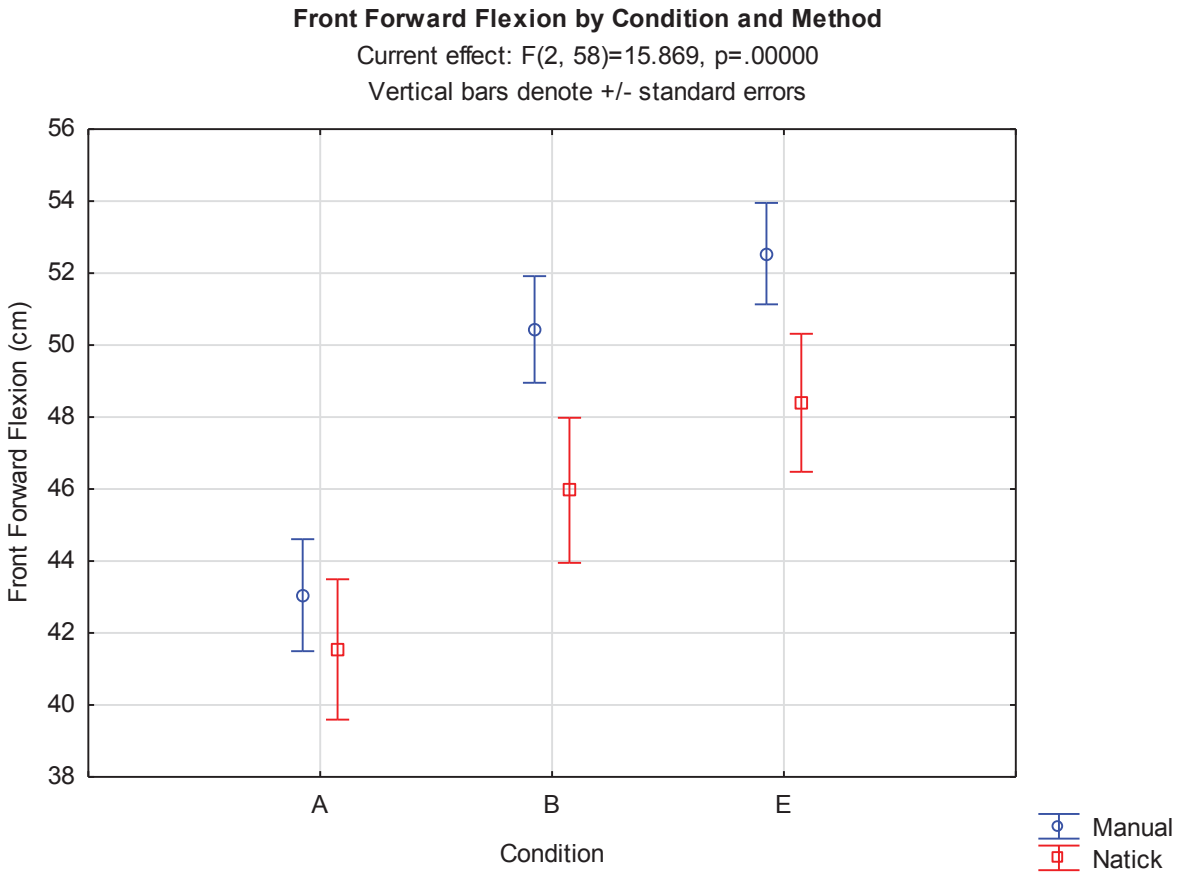

Figure 173: Effect of Condition x Method on Front Forward Flexion for Manual and Natick Methods

		A		B		E	
		Manual	Natick	Manual	Natick	Manual	Natick
A	Manual		X	X	X	X	X
	Natick	X		X	X	X	X
B	Manual	X	X		X	X	X
	Natick	X	X	X		X	X
E	Manual	X	X	X	X		X
	Natick	X	X	X	X	X	

Figure 174: Tukey HSD Post-hoc Summary of Significant Differences for Condition x Method Interaction

High Knee Lift

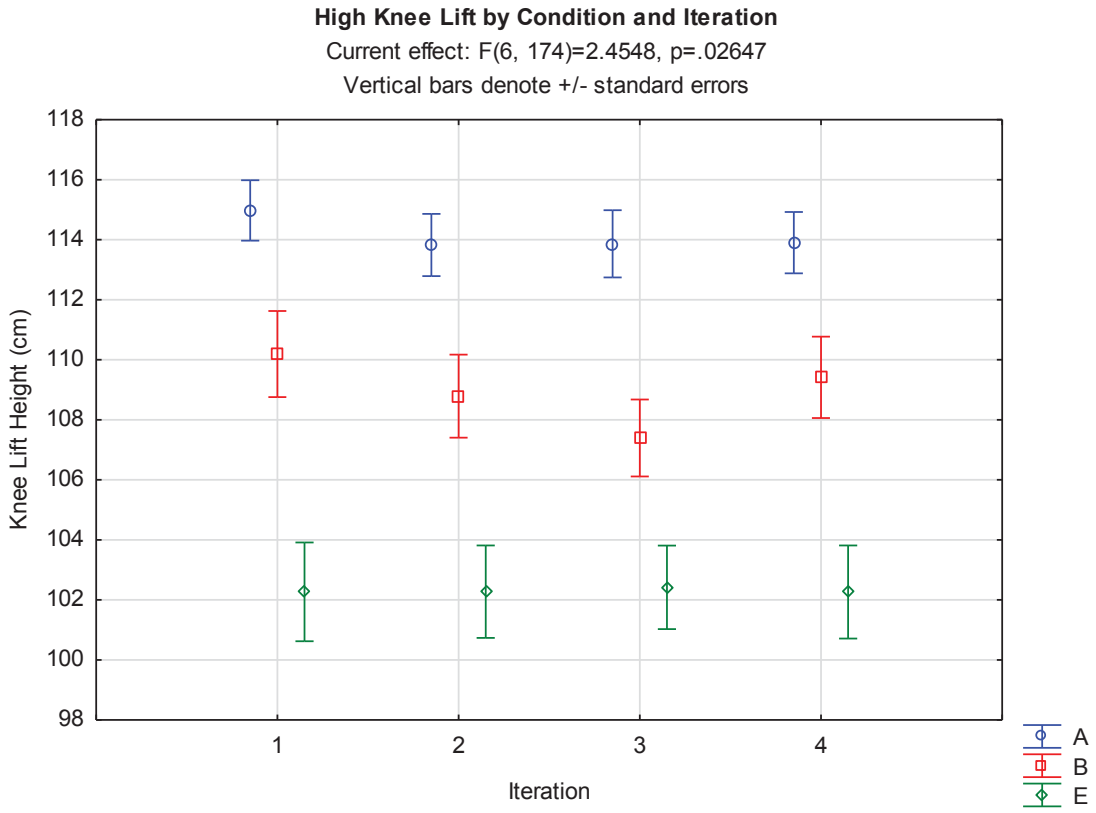

Figure 175: Effect of Condition x Iteration on High Knee Lift

		A				B				E			
		1	2	3	4	1	2	3	4	1	2	3	4
A	1					X	X	X	X	X	X	X	X
	2					X	X	X	X	X	X	X	X
	3					X	X	X	X	X	X	X	X
	4					X	X	X	X	X	X	X	X
B	1	X	X	X	X			X		X	X	X	X
	2	X	X	X	X					X	X	X	X
	3	X	X	X	X	X			X	X	X	X	X
	4	X	X	X	X			X		X	X	X	X
E	1	X	X	X	X	X	X	X	X				
	2	X	X	X	X	X	X	X	X				
	3	X	X	X	X	X	X	X	X				
	4	X	X	X	X	X	X	X	X				

Figure 176: Tukey HSD Post-hoc Summary of Significant Differences for Condition x Iteration Interaction

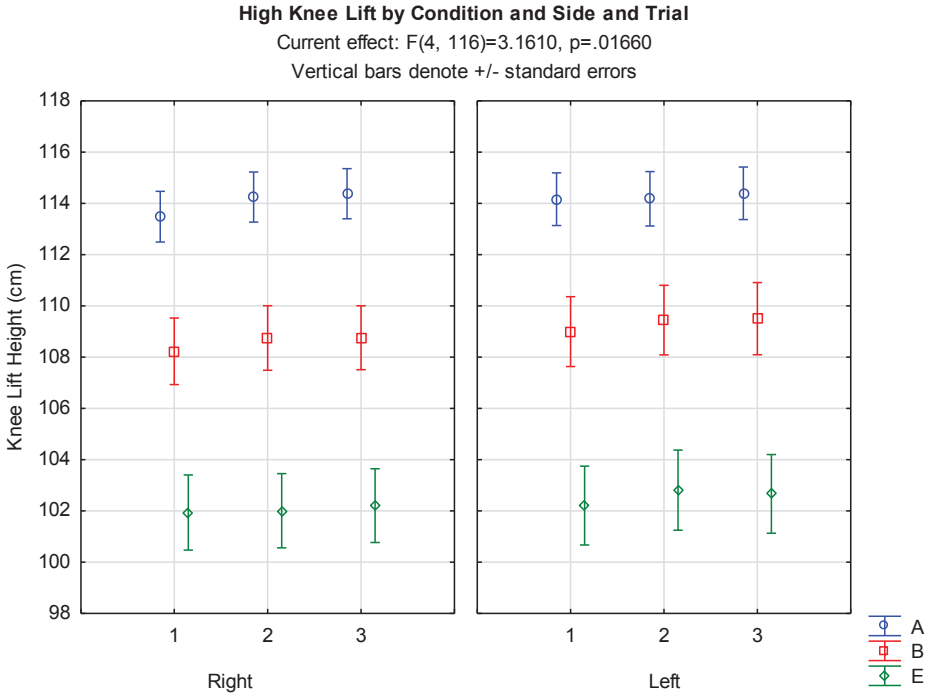

Figure 177: Effect of Condition x Side x Trial on High Knee Lift

			A						B						E					
			Right			Left			Right			Left			Right			Left		
			1	2	3	1	2	3	1	2	3	1	2	3	1	2	3	1	2	3
A	Right	1		X	X	X	X	X	X	X	X	X	X	X	X	X	X	X	X	X
		2	X						X	X	X	X	X	X	X	X	X	X	X	X
		3	X						X	X	X	X	X	X	X	X	X	X	X	X
	Left	1	X						X	X	X	X	X	X	X	X	X	X	X	X
		2	X						X	X	X	X	X	X	X	X	X	X	X	X
		3	X						X	X	X	X	X	X	X	X	X	X	X	X
B	Right	1	X	X	X	X	X	X				X	X	X	X	X	X	X	X	X
		2	X	X	X	X	X	X					X	X	X	X	X	X	X	X
		3	X	X	X	X	X	X					X	X	X	X	X	X	X	X
	Left	1	X	X	X	X	X	X	X						X	X	X	X	X	X
		2	X	X	X	X	X	X	X	X	X				X	X	X	X	X	X
		3	X	X	X	X	X	X	X	X	X				X	X	X	X	X	X
E	Right	1	X	X	X	X	X	X	X	X	X	X	X	X					X	X
		2	X	X	X	X	X	X	X	X	X	X	X	X					X	
		3	X	X	X	X	X	X	X	X	X	X	X	X						
	Left	1	X	X	X	X	X	X	X	X	X	X	X	X						
		2	X	X	X	X	X	X	X	X	X	X	X	X	X	X				
		3	X	X	X	X	X	X	X	X	X	X	X	X	X					

Figure 178: Tukey HSD Post-hoc Summary of Significant Differences for Condition x Side x Trial Interaction

Shoulder Abduction

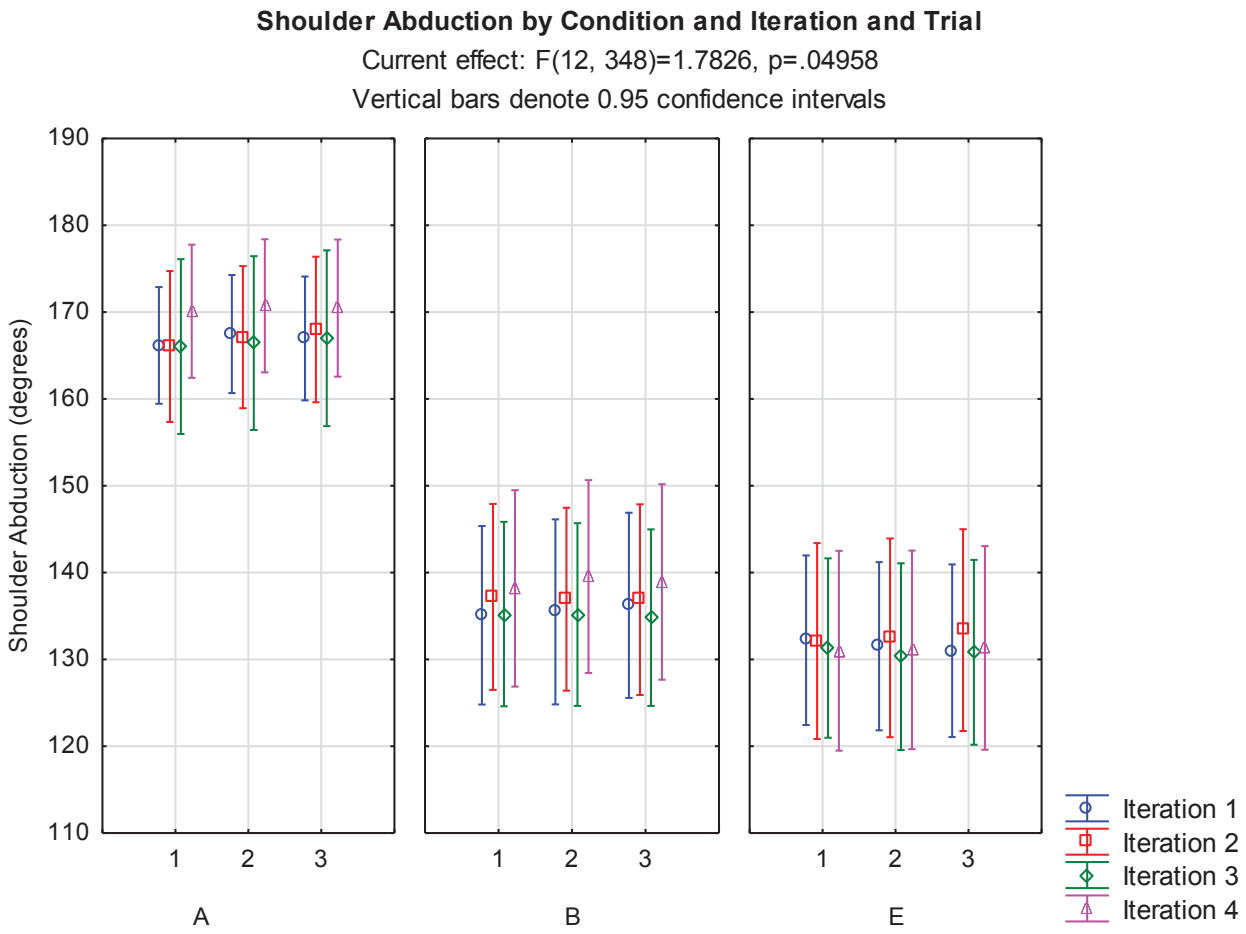

Figure 179: Effect of Condition x Iteration x Trial on Shoulder Abduction

			A												B												E											
			1			2			3			4			1			2			3			4			1			2			3			4		
			1	2	3	1	2	3	1	2	3	1	2	3	1	2	3	1	2	3	1	2	3	1	2	3	1	2	3	1	2	3	1	2	3	1	2	3
A	1	1										X	X	X	X	X	X	X	X	X	X	X	X	X	X	X	X	X	X	X	X	X	X	X	X	X	X	X
		2										X	X	X	X	X	X	X	X	X	X	X	X	X	X	X	X	X	X	X	X	X	X	X	X	X	X	X
		3										X	X	X	X	X	X	X	X	X	X	X	X	X	X	X	X	X	X	X	X	X	X	X	X	X	X	X
	2	1										X	X	X	X	X	X	X	X	X	X	X	X	X	X	X	X	X	X	X	X	X	X	X	X	X	X	X
		2										X	X	X	X	X	X	X	X	X	X	X	X	X	X	X	X	X	X	X	X	X	X	X	X	X	X	X
		3										X	X	X	X	X	X	X	X	X	X	X	X	X	X	X	X	X	X	X	X	X	X	X	X	X	X	X
	3	1										X	X	X	X	X	X	X	X	X	X	X	X	X	X	X	X	X	X	X	X	X	X	X	X	X	X	X
		2										X	X	X	X	X	X	X	X	X	X	X	X	X	X	X	X	X	X	X	X	X	X	X	X	X	X	X
		3										X	X	X	X	X	X	X	X	X	X	X	X	X	X	X	X	X	X	X	X	X	X	X	X	X	X	X
	4	1	X	X	X	X	X	X	X	X	X				X	X	X	X	X	X	X	X	X	X	X	X	X	X	X	X	X	X	X	X	X	X	X	X
		2	X	X	X	X	X	X	X	X	X				X	X	X	X	X	X	X	X	X	X	X	X	X	X	X	X	X	X	X	X	X	X	X	X
		3	X	X	X	X	X	X	X	X	X				X	X	X	X	X	X	X	X	X	X	X	X	X	X	X	X	X	X	X	X	X	X	X	X
B	1	1	X	X	X	X	X	X	X	X	X	X	X	X				X						X	X	X	X	X	X	X	X		X	X	X	X	X	X
		2	X	X	X	X	X	X	X	X	X	X	X	X										X	X	X	X	X	X	X	X	X	X	X	X	X	X	X
		3	X	X	X	X	X	X	X	X	X	X	X	X											X		X	X	X	X	X	X	X	X	X	X	X	X
	2	1	X	X	X	X	X	X	X	X	X	X	X	X	X								X		X		X	X	X	X	X	X	X	X	X	X	X	X
		2	X	X	X	X	X	X	X	X	X	X	X	X									X		X		X	X	X	X	X	X	X	X	X	X	X	X
		3	X	X	X	X	X	X	X	X	X	X	X	X											X		X	X	X	X	X	X	X	X	X	X	X	X
	3	1	X	X	X	X	X	X	X	X	X	X	X	X										X	X	X	X	X	X	X	X		X	X	X	X	X	X
		2	X	X	X	X	X	X	X	X	X	X	X	X										X	X	X	X	X	X	X	X		X	X	X	X	X	X
		3	X	X	X	X	X	X	X	X	X	X	X	X				X	X					X	X	X	X	X	X	X	X		X	X	X	X	X	X
	4	1	X	X	X	X	X	X	X	X	X	X	X	X	X	X					X	X	X				X	X	X	X	X	X	X	X	X	X	X	X
		2	X	X	X	X	X	X	X	X	X	X	X	X	X	X	X	X	X	X	X	X	X				X	X	X	X	X	X	X	X	X	X	X	X
		3	X	X	X	X	X	X	X	X	X	X	X	X	X	X	X				X	X	X				X	X	X	X	X	X	X	X	X	X	X	X
E	1	1	X	X	X	X	X	X	X	X	X	X	X	X	X	X	X	X	X	X	X	X	X	X	X	X												
		2	X	X	X	X	X	X	X	X	X	X	X	X	X	X	X	X	X	X	X	X	X	X	X	X												
		3	X	X	X	X	X	X	X	X	X	X	X	X	X	X	X	X	X	X	X	X	X	X	X	X						X						
	2	1	X	X	X	X	X	X	X	X	X	X	X	X	X	X	X	X	X	X	X	X	X	X	X	X												
		2	X	X	X	X	X	X	X	X	X	X	X	X	X	X	X	X	X	X	X	X	X	X	X	X												
		3	X	X	X	X	X	X	X	X	X	X	X	X		X	X	X	X	X				X	X	X			X						X	X	X	X	
	3	1	X	X	X	X	X	X	X	X	X	X	X	X	X	X	X	X	X	X	X	X	X	X	X	X												
		2	X	X	X	X	X	X	X	X	X	X	X	X	X	X	X	X	X	X	X	X	X	X	X	X					X	X						
		3	X	X	X	X	X	X	X	X	X	X	X	X	X	X	X	X	X	X	X	X	X	X	X	X						X						
	4	1	X	X	X	X	X	X	X	X	X	X	X	X	X	X	X	X	X	X	X	X	X	X	X	X						X						
		2	X	X	X	X	X	X	X	X	X	X	X	X	X	X	X	X	X	X	X	X	X	X	X	X						X						
		3	X	X	X	X	X	X	X	X	X	X	X	X	X	X	X	X	X	X	X	X	X	X	X	X												

Figure 180: Tukey HSD Post-hoc Summary of Significant Differences for Condition x Iteration x Trial Interaction

Annex M: Additional Regression Results

ROM Measure vs. Overall LEAP time

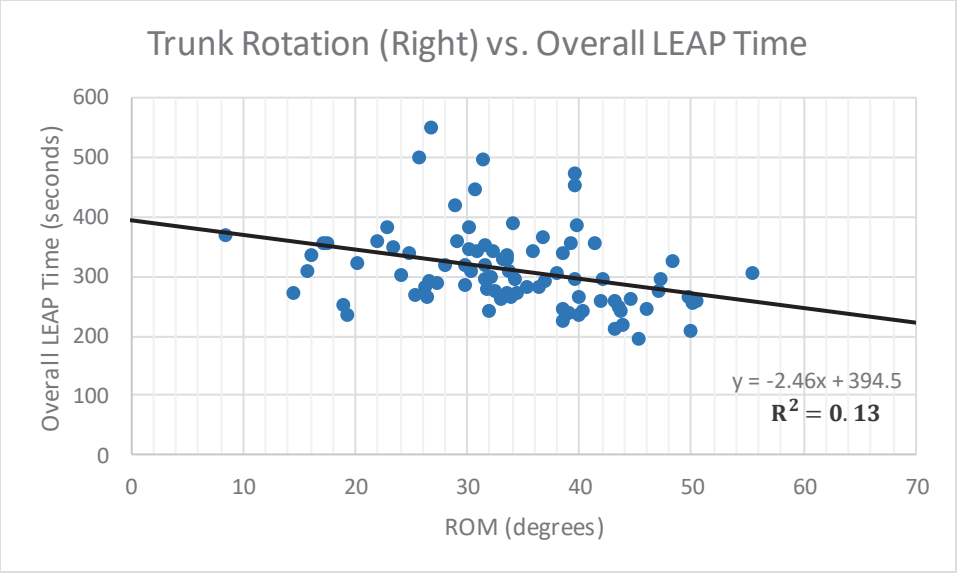

Figure 181: Regression line for Right Trunk Rotation vs. Overall LEAP Time

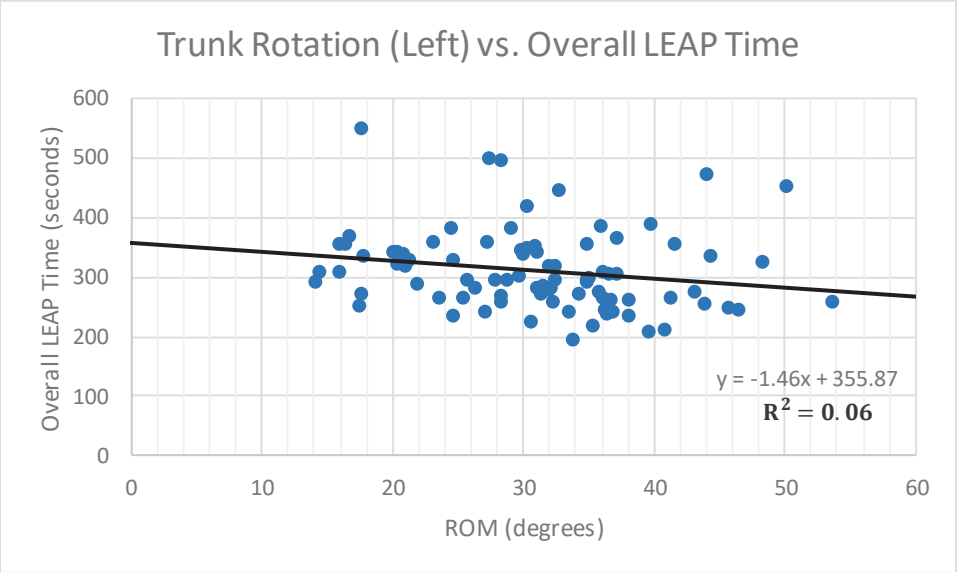

Figure 182: Regression line for Left Trunk Rotation vs. Overall LEAP Time

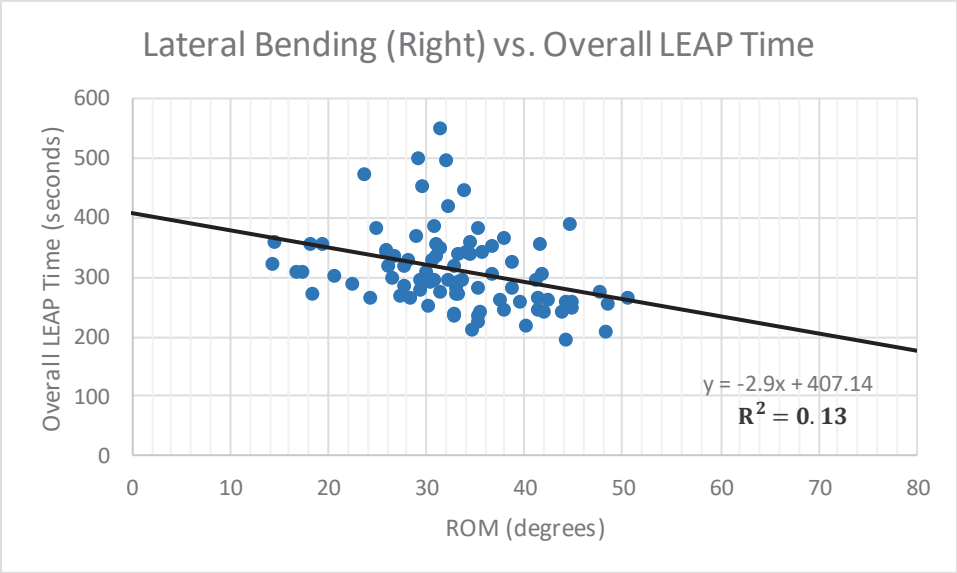

Figure 183: Regression line for Right Lateral Bending vs. Overall LEAP Time

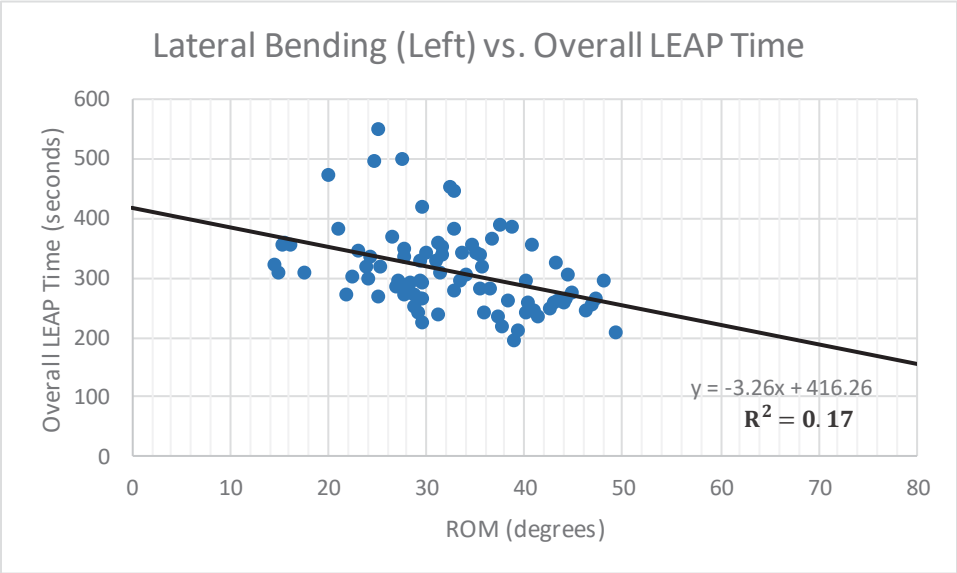

Figure 184: Regression line for Left Lateral Bending vs. Overall LEAP Time

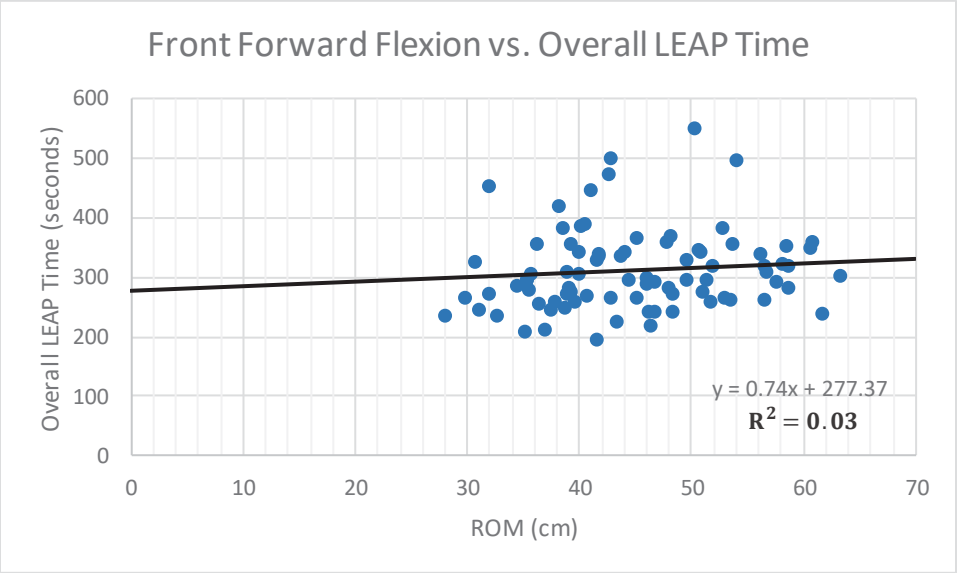

Figure 185: Regression line for Front Forward Flexion vs. Overall LEAP Time

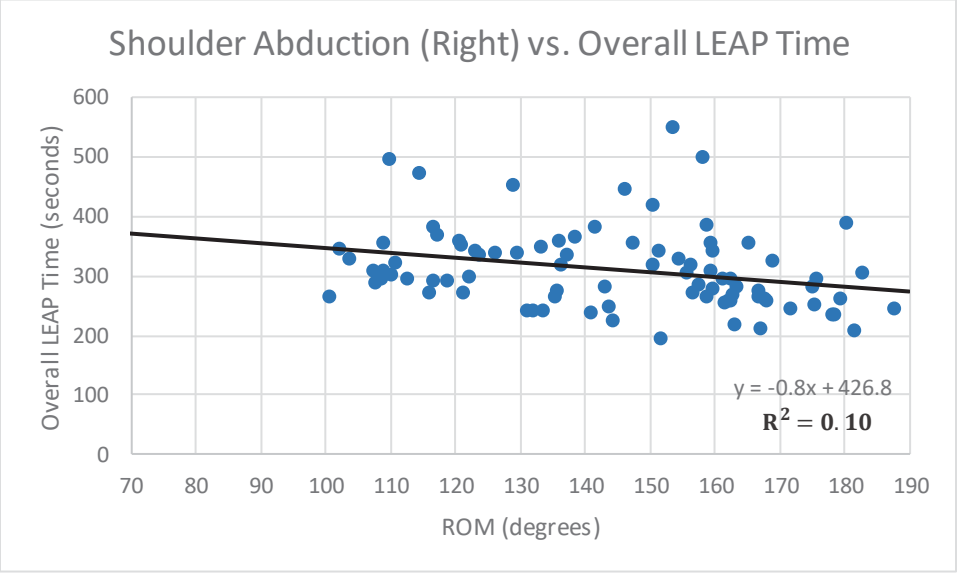

Figure 186: Regression line for Right Shoulder Abduction vs. Overall LEAP Time

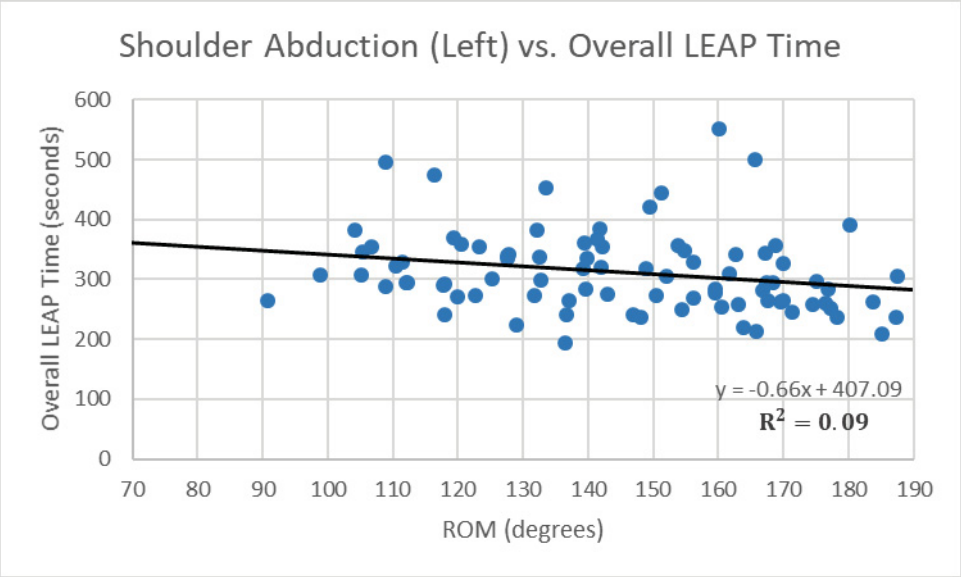

Figure 187: Regression line for Left Shoulder Abduction vs. Overall LEAP Time

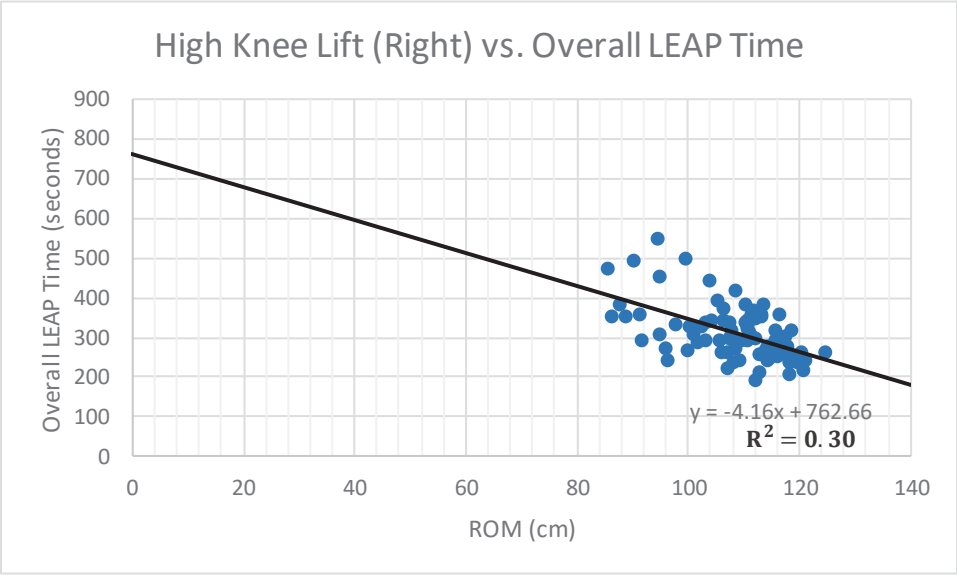

Figure 188: Regression line for Right High Knee Lift vs. Overall LEAP Time

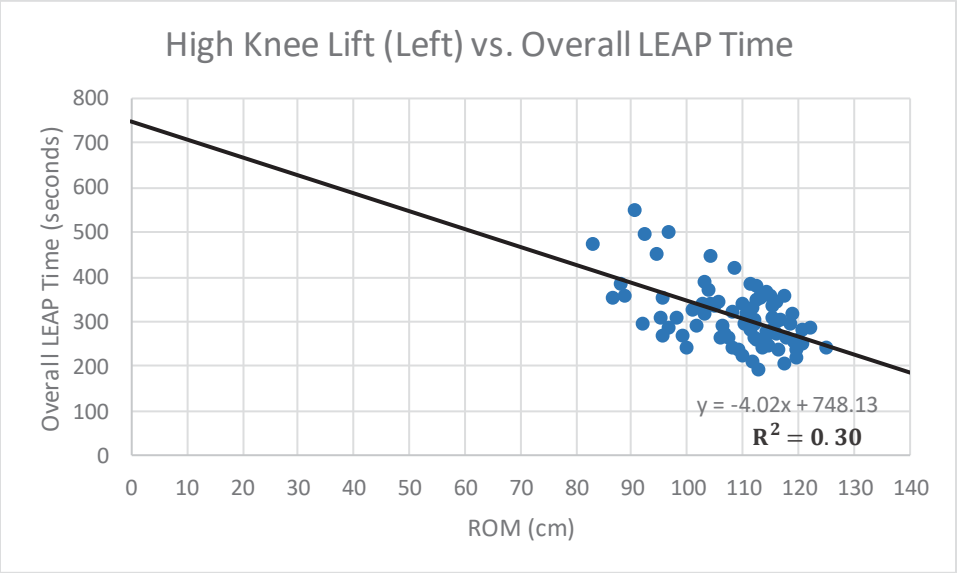

Figure 189: Regression line for Left High Knee Lift vs. Overall LEAP Time

ROM Measure vs. LEAP Course Subjective Rating

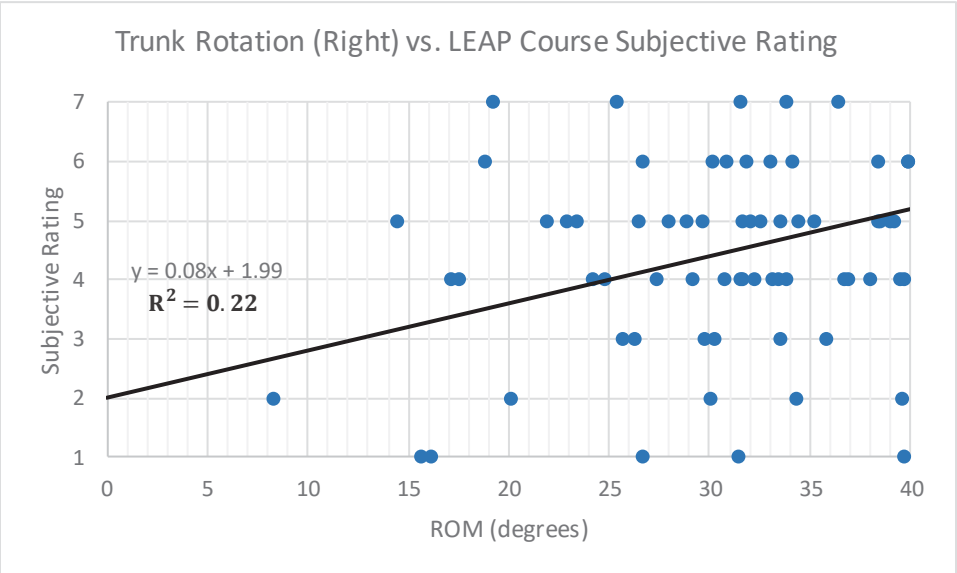

Figure 190: Regression line for Right Trunk Rotation vs. LEAP Course Subjective Rating

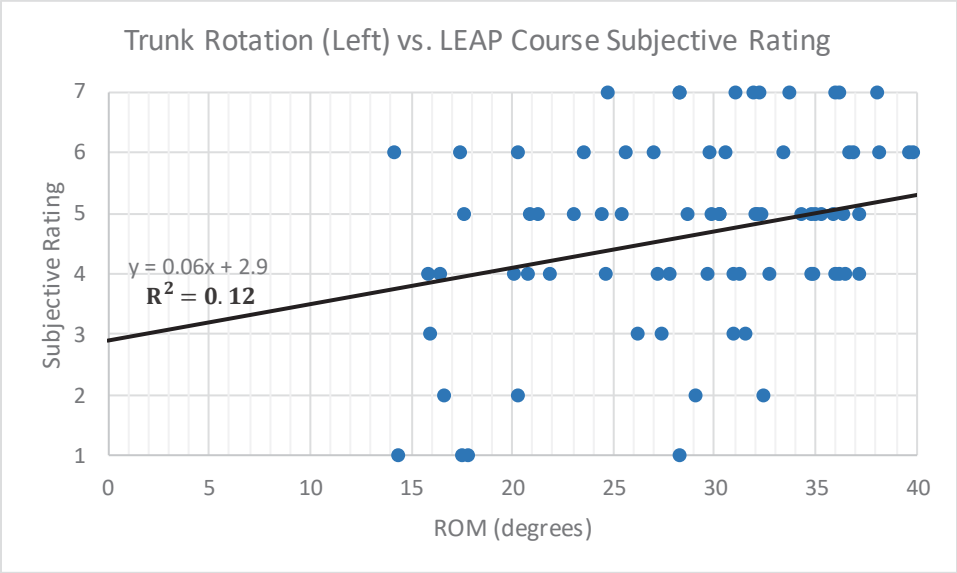

Figure 191: Regression line for Left Trunk Rotation vs. LEAP Course Subjective Rating

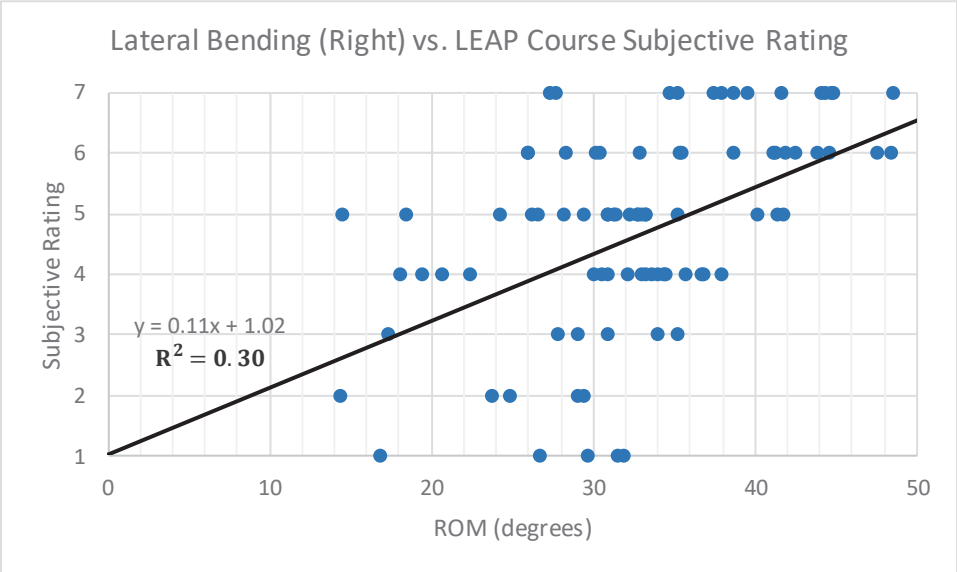

Figure 192: Regression line for Right Lateral Bending vs. LEAP Course Subjective Rating

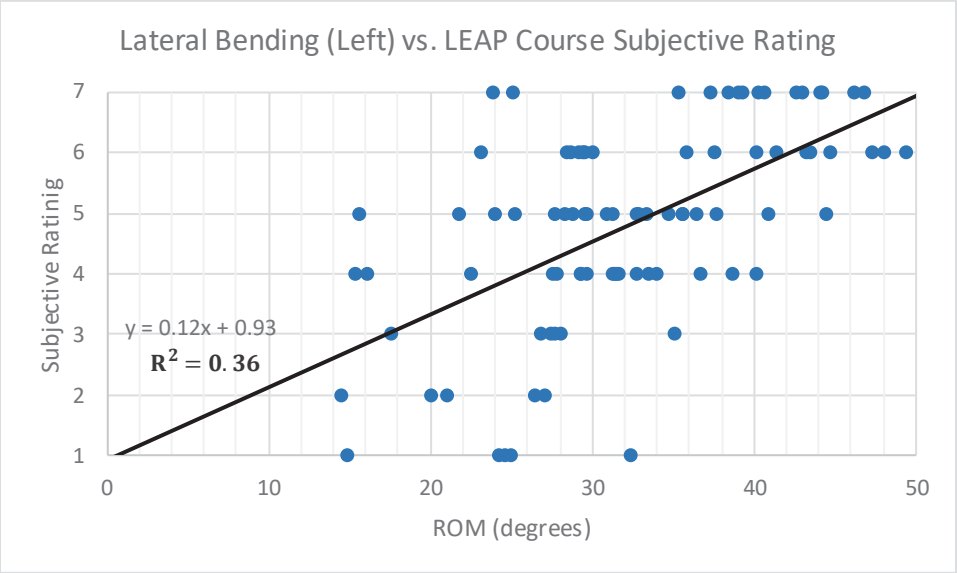

Figure 193: Regression line for Left Lateral Bending vs. LEAP Course Subjective Rating

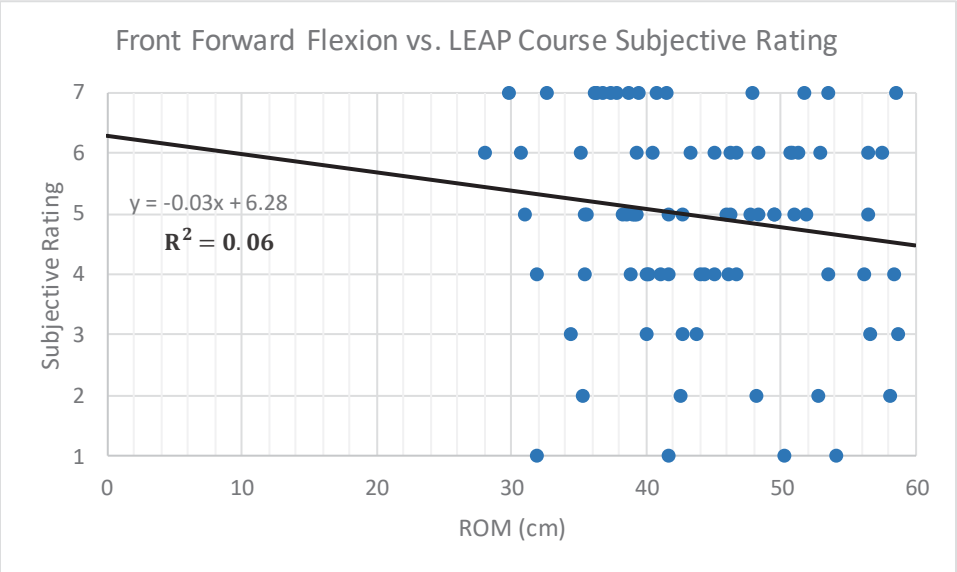

Figure 194: Regression line for Front Forward Flexion vs. LEAP Course Subjective Rating

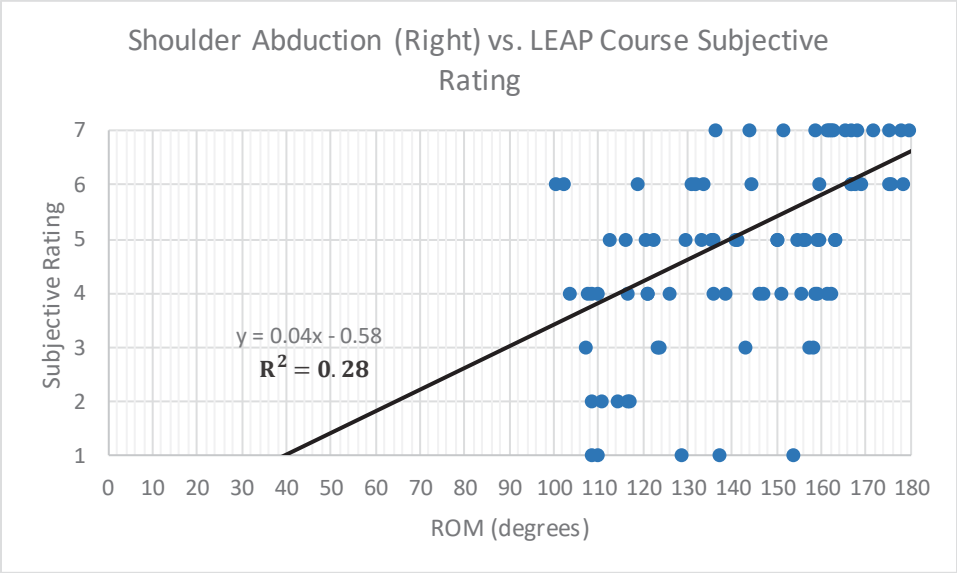

Figure 195: Regression line for Right Shoulder Abduction vs. LEAP Course Subjective Rating

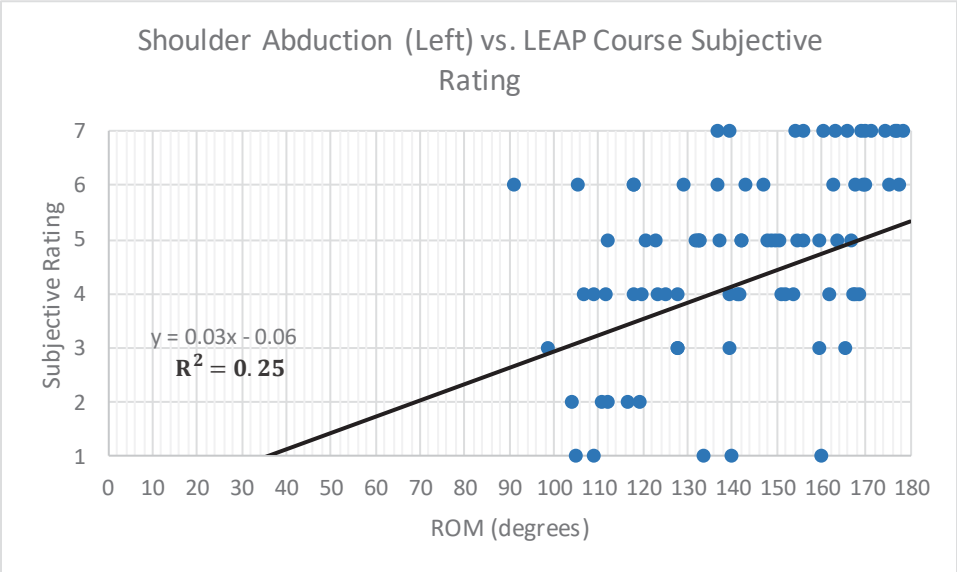

Figure 196: Regression line for Left Shoulder Abduction vs. LEAP Course Subjective Rating

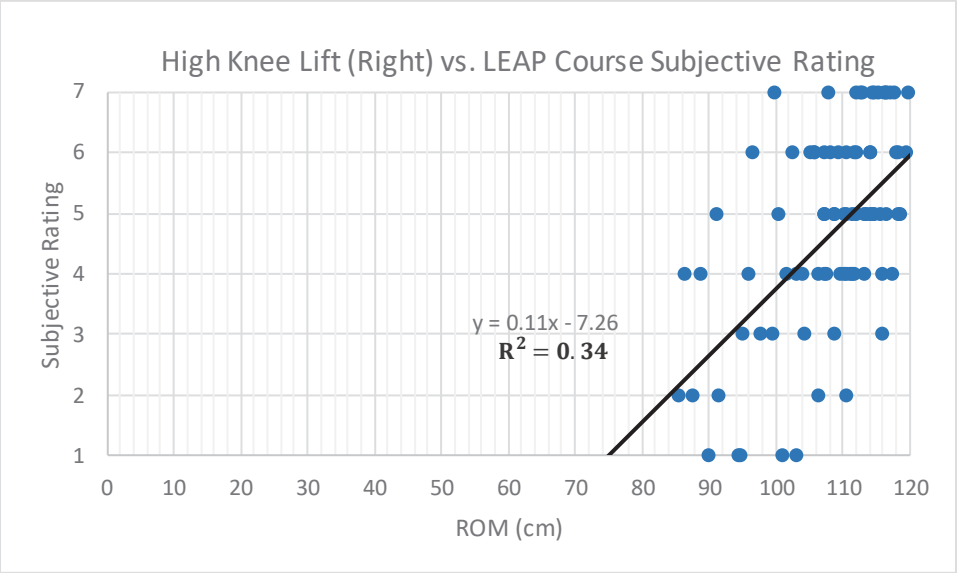

Figure 197: Regression line for Right High Knee Lift vs. LEAP Course Subjective Rating

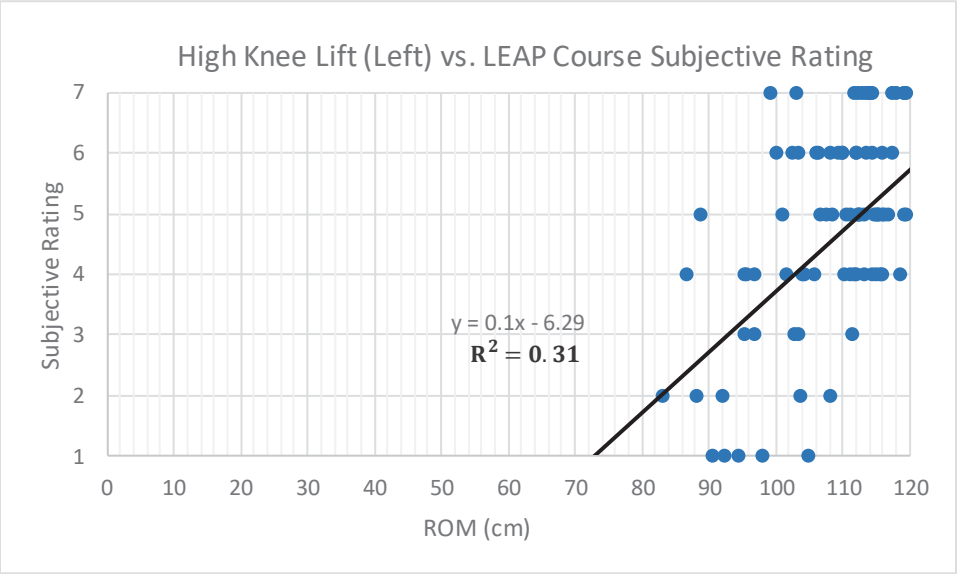

Figure 198: Regression line for Left High Knee Lift vs. LEAP Course Subjective Rating

ROM Measure vs. LEAP Course RPE

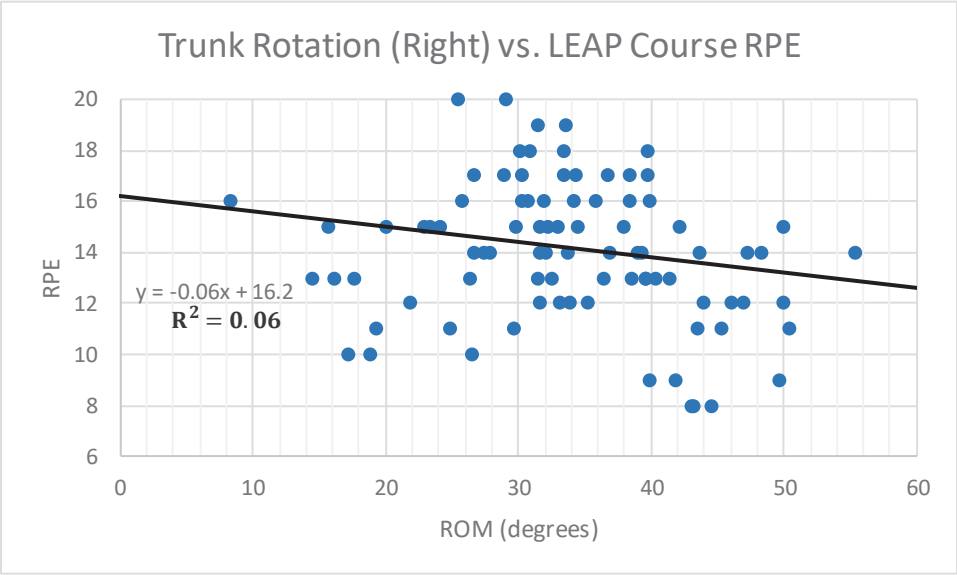

Figure 199: Regression line for Right Trunk Rotation vs. LEAP Course RPE

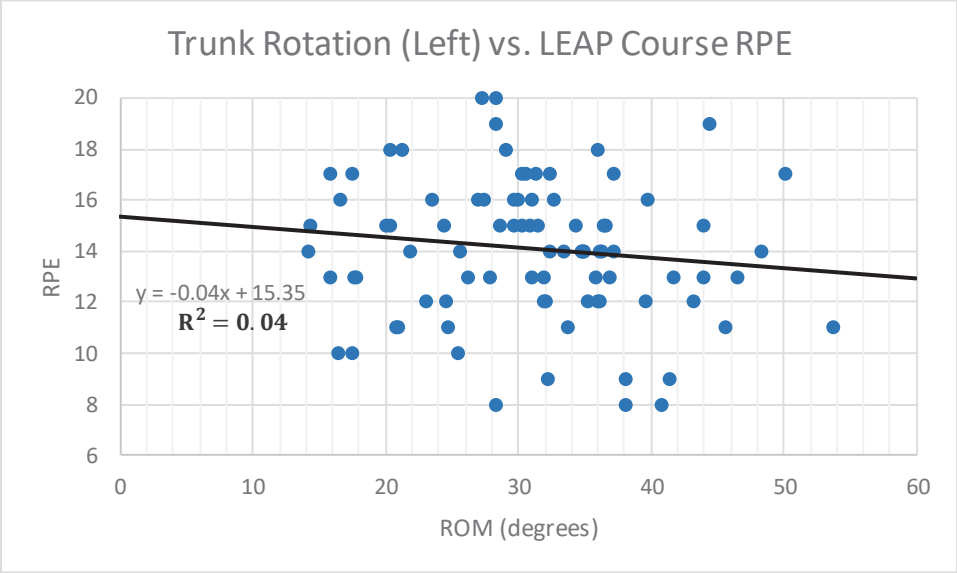

Figure 200: Regression line for Left Trunk Rotation vs. LEAP Course RPE

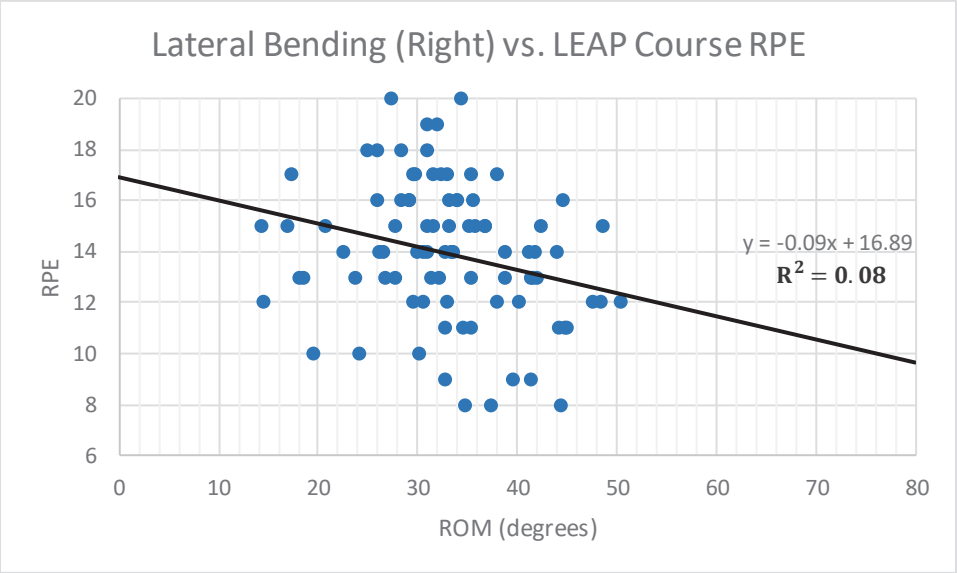

Figure 201: Regression line for Right Lateral Bending vs. LEAP Course RPE

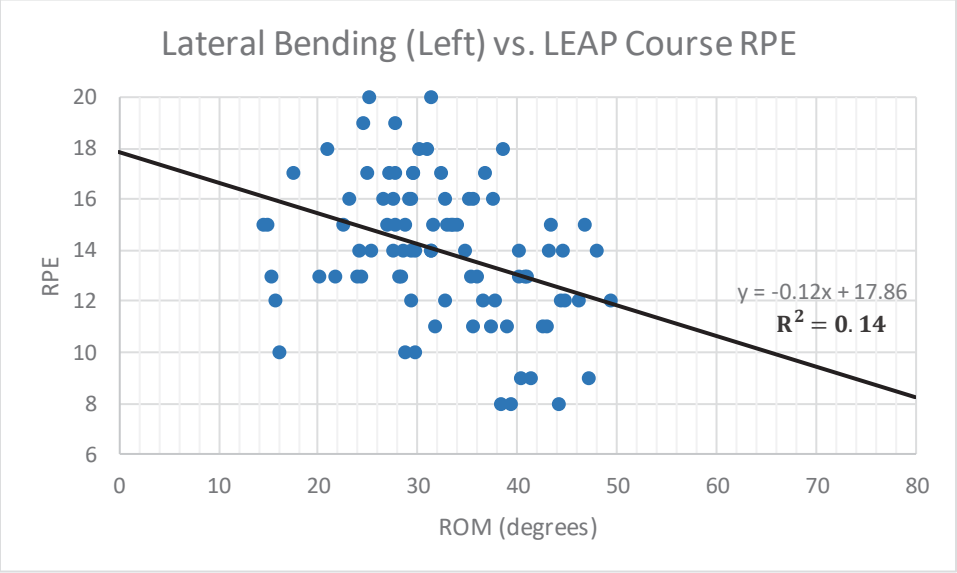

Figure 202: Regression line for Left Lateral Bending vs. LEAP Course RPE

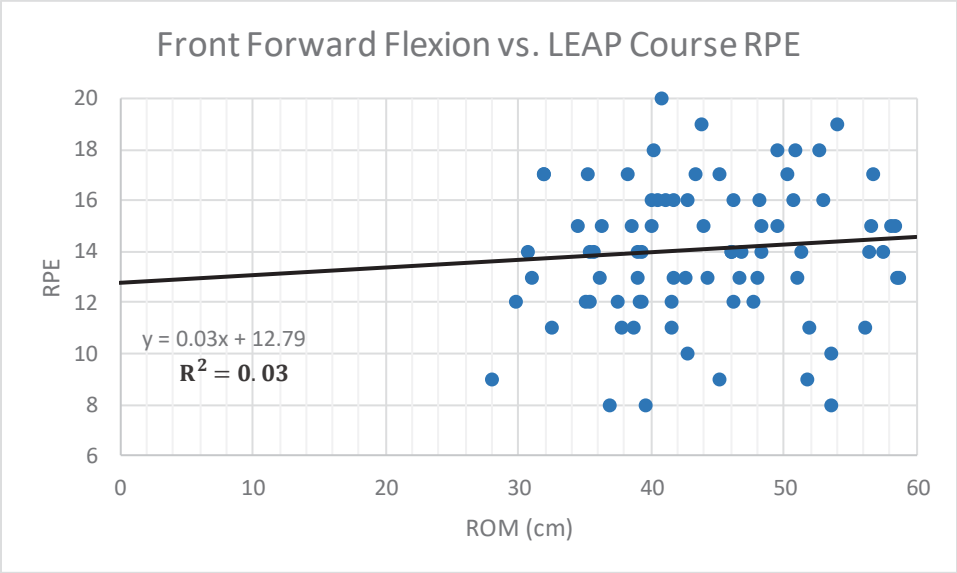

Figure 203: Regression line for Front Forward Flexion vs. LEAP Course RPE

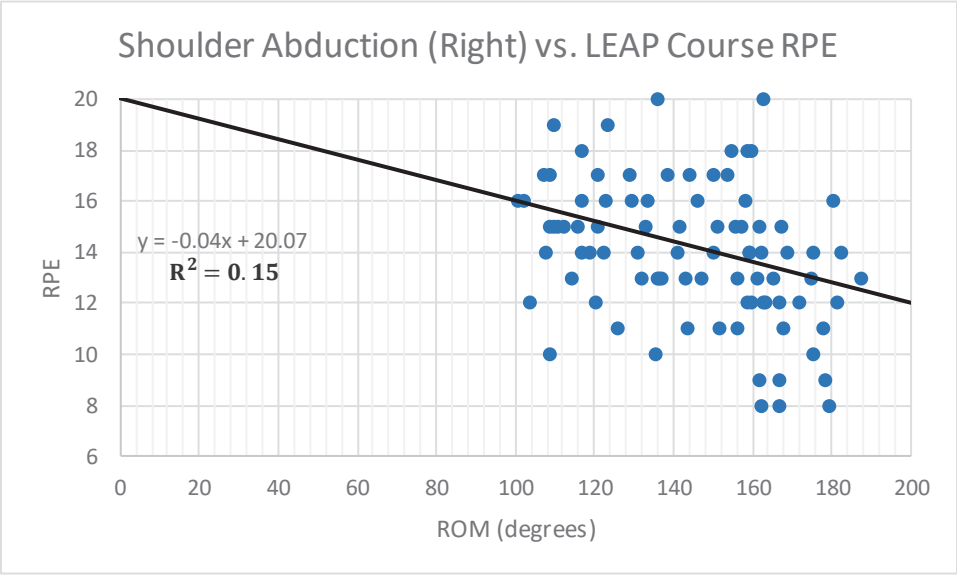

Figure 204: Regression line for Right Shoulder Abduction vs. LEAP Course RPE

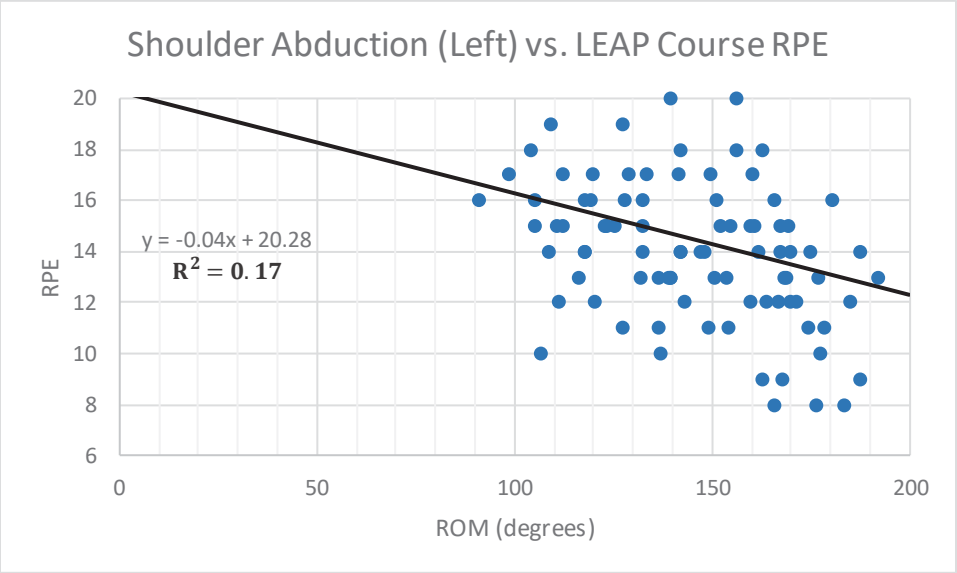

Figure 205: Regression line for Left Shoulder Abduction vs. LEAP Course RPE

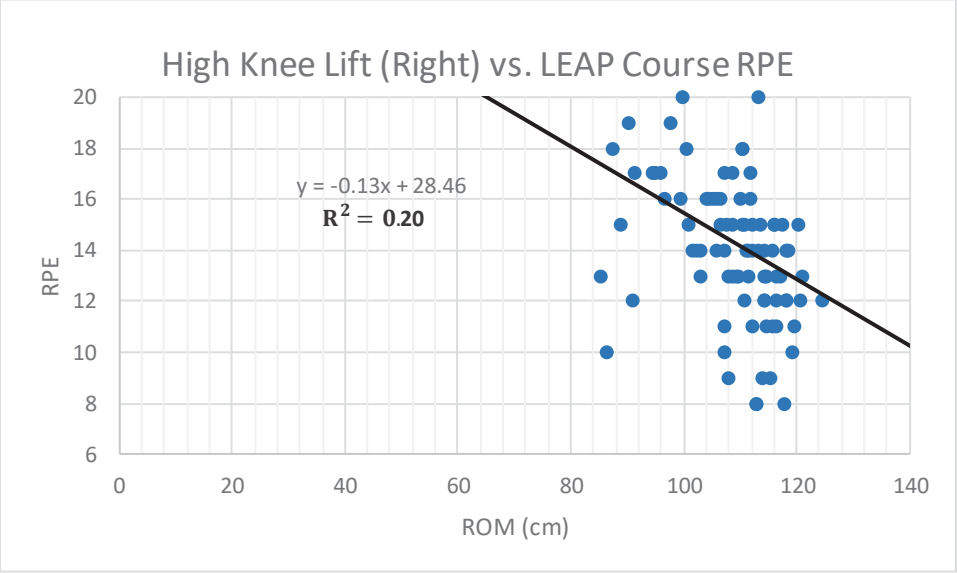

Figure 206: Regression line for Right High Knee Lift vs. LEAP Course RPE

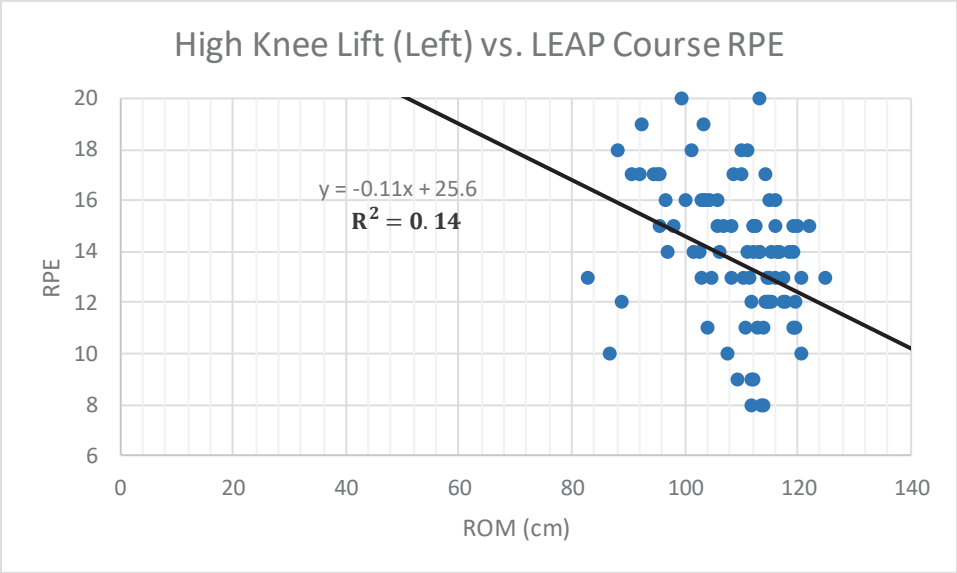

Figure 207: Regression line for Left High Knee Lift vs. LEAP Course RPE

List of Acronyms/Abbreviations

CAF – Canadian Armed Forces

CAN-LEAP – Canadian Load Effects Assessment Program

FPV – Fragmentation Protective Vest

FFO – Full Fighting Order

HR – Heart Rate

ICC – Intra-Class Correlation

IMU – Inertial Measurement Unit

iRoM – Instrumented Range of Motion

LEAP – Load Effects Assessment Program

mCAFT – Modified Canadian Aerobic Fitness Test

MERS – Marine Expeditionary Rifle Squad

MOSID – Military Occupation Specialty Identification Code

PWT – Personal Weapons Test

RCA – Regression Coefficient Analysis

ROM – Range of Motion

RPE – Rating of Perceived Exertion

SME – Subject Matter Expert

TAV – Tactical Vest

USMC – United States Marine Corps

WBGT – Wet Bulb Globe Temperature

This page intentionally left blank.

DOCUMENT CONTROL DATA

*Security markings for the title, authors, abstract and keywords must be entered when the document is sensitive

1. ORIGINATOR (Name and address of the organization preparing the document. A DRDC Centre sponsoring a contractor's report, or tasking agency, is entered in Section 8.) Human Systems Incorporated 111 Farquhar St #202 Guelph, (ON) Canada	2a. SECURITY MARKING (Overall security marking of the document including special supplemental markings if applicable.) CAN UNCLASSIFIED 2b. CONTROLLED GOODS NON-CONTROLLED GOODS DMC A

3. TITLE (The document title and sub-title as indicated on the title page.)

Range of motion measurement reliability for the Canadian Load Effects Assessment Program

4. AUTHORS (Last name, followed by initials – ranks, titles, etc., not to be used)

Morton, A.; Sorgini, C.; Bray-Miners, J; Yu, M.; Sam, N.

5. DATE OF PUBLICATION (Month and year of publication of document.)	6a. NO. OF PAGES (Total pages, including Annexes, excluding DCD, covering and verso pages.)	6b. NO. OF REFS (Total references cited.)
March 2018	245	14

7. DOCUMENT CATEGORY (e.g., Scientific Report, Contract Report, Scientific Letter.)

Contract Report

8. SPONSORING CENTRE (The name and address of the department project office or laboratory sponsoring the research and development.)

DRDC - Toronto Research Centre
Defence Research and Development Canada
1133 Sheppard Avenue West
Toronto, Ontario M3K 2C9
Canada

9a. PROJECT OR GRANT NO. (If appropriate, the applicable research and development project or grant number under which the document was written. Please specify whether project or grant.)	9b. CONTRACT NO. (If appropriate, the applicable number under which the document was written.) W7701-166107/001/QCL
10a. DRDC PUBLICATION NUMBER (The official document number by which the document is identified by the originating activity. This number must be unique to this document.) DRDC-RDDC-2018-C120	10b. OTHER DOCUMENT NO(s). (Any other numbers which may be assigned this document either by the originator or by the sponsor.)

11a. FUTURE DISTRIBUTION WITHIN CANADA (Approval for further dissemination of the document. Security classification must also be considered.)

Public release

11b. FUTURE DISTRIBUTION OUTSIDE CANADA (Approval for further dissemination of the document. Security classification must also be considered.)

12. KEYWORDS, DESCRIPTORS or IDENTIFIERS (Use semi-colon as a delimiter.)

CanLEAP; Body armour

13. ABSTRACT/RÉSUMÉ (When available in the document, the French version of the abstract must be included here.)

Abstract

The Canadian Load Effects Assessment Program (CAN-LEAP) was created to study the implications of “Soldier Burden” on mobility and combat tasks and to determine the threshold at which a degradation in performance occurs. In addition to completing the mobility course and ancillary stands, the flexibility of each soldier while wearing the various equipment configurations is characterized. These Range of Motion (ROM) measurements encompass movements such as trunk rotation, lateral bending, trunk flexion, hip flexion, and shoulder abduction. To date, a standardized approach to taking ROM measures has not been developed. Of the seven experimental studies that have taken place at DRDC-Toronto, there have been four different ROM approaches used, making it difficult to consistently relate ROM to mobility performance. In order to better understand the association between ROM and operational performance, a standardized, accurate, and reliable ROM approach must be developed.

Thirty regular force volunteers participated over six weeks of data collection. Each week a new set of participants completed range of motion exercises in three different equipment conditions and completed the CAN-LEAP course in six different equipment conditions. The first three conditions included a baseline condition, a full fighting order (FFO) condition, and an extended-FFO condition, while the last three conditions were slight modifications to the first three. Participants not only completed multiple runs of the CAN-LEAP course but they also participated in five ROM stations where multiple range of motion measurements were taken using different ROM methods. In addition to completing the typical CAN-LEAP analysis to determine the effect of wearing extended body armour, multiple statistical analysis techniques were employed to determine the effect on soldier ROM of: extended body armour, running the LEAP course, and doffing/donning equipment. An Analysis of Variance (ANOVA) was used to determine the effect on soldier ROM of wearing extended body armour while a combination of ANOVAs and intra-class correlations were employed to determine which methods were most reliable when taking the various ROM measures. Linear regression models were computed using a two-stage cluster bootstrap technique to determine the strength of the relationship between ROM measures and CAN-LEAP performance metrics

Significant differences were observed between conditions in total obstacle course time and individual obstacle times, subjective ratings of performance, ratings of perceived exertion and, to a lesser degree, marksmanship and the other ancillary stands. As expected, soldiers posted the fastest course times in the slick condition and the slowest course times in the more encumbered extended armour condition. While the overall course times and subjective ratings of performance showed a significant decrease in timings and ratings between the extended body armour and the traditional body armour, only select course obstacles showed this statistically significant difference. Significant differences were also observed between conditions in all ROM measures. As expected, soldiers had the greatest ROM in the slick condition and typically had the lowest ROM in the fully encumbered condition. The only ROM measures that showed a significant decrease in ROM between the extended body armour and the traditional body armour were front forward flexion and high knee lift. While all measurement methods were deemed to have good reliability, the Natick protocol of ROM measurement was deemed to be the most reliable measurement method for front forward flexion, high knee lift, and shoulder abduction while the iRoM electronic system was deemed to be the most reliable measurement method for trunk rotation and lateral bending. Right and left high knee lift were found to be most strongly related to obstacle course time, while for subjective ratings it was right/left high knee lift and right/left lateral bend. There was little relationship found between ROM and ratings of perceived exertion

Résumé

Le Programme canadien d'évaluation des effets des charges (PCEEC) vise à étudier les incidences du « fardeau du soldat » sur sa mobilité et sur l'exécution des tâches de combat, ainsi qu'à déterminer le seuil où on assiste à une détérioration du rendement. En plus de les soumettre au parcours d'évaluation de la mobilité, ainsi qu'aux épreuves complémentaires, on doit caractériser l'agilité de chacun des soldats chargés de diverses configurations d'équipement. Ces mesures de l'amplitude articulaire (AA) incluent celles de mouvements comme la rotation du tronc, la flexion latérale, la flexion du tronc, la flexion de la hanche et l'abduction de l'épaule. Jusqu'à présent, aucune démarche standard n'a été élaborée pour permettre de mesurer l'AA. Quatre approches distinctes ont été utilisées lors des sept études expérimentales menées à RDDC Toronto, ce qui a compliqué la tâche d'établir une corrélation entre l'AA et la mobilité. On doit mettre au point une approche standard, précise et fiable pour mesurer l'AA afin de mieux comprendre le rapport entre celle-ci et le rendement opérationnel.

Trente membres de la force régulière se sont portés volontaires pour participer à une collecte de données durant six semaines. Chaque semaine, un nouveau groupe de participants effectuait une série d'exercices d'AA avec trois différentes charges d'équipement et terminait le PCEEC avec six différentes charges. Les trois premiers exercices comportaient une charge de référence, l'attirail de combat complet (ACC), puis une charge additionnelle à l'ACC. Les trois derniers exercices ne comportaient que de légères modifications aux trois premiers. Les participants ont effectué le parcours du PCEEC à maintes reprises en plus de se livrer à des exercices d'AA à cinq épreuves, exercices qui ont servi à mesurer diverses méthodes d'AA. Outre l'analyse typique du PCEEC pour déterminer les effets du port du vêtement de protection balistique allongé, de nombreuses techniques d'analyse statistique ont été employées pour déterminer comment le fait de porter le vêtement, d'effectuer le parcours de l'EEC, puis de revêtir et de retirer l'équipement a des effets sur l'AA des soldats. On a procédé à une analyse de la variance pour déterminer les effets du port du vêtement sur l'AA des soldats et combiné une analyse de la variance et de corrélations intra-classes pour déterminer les méthodes de mesure de l'AA les plus fiables. Des modèles de régressions linéaires ont été calculés au moyen de la méthode bootstrap par grappes à deux degrés pour évaluer la solidité du rapport entre les mesures d'AA et les paramètres de rendement du PCEEC.

On a constaté des différences majeures entre les conditions relatives au temps total qu'il a fallu aux participants pour terminer le parcours d'obstacles et le temps obtenu par chacun, la cote subjective de rendement, la mesure de perception de l'effort et, dans une moindre mesure, l'adresse au tir et les autres épreuves complémentaires. Comme prévu, les participants ont affiché l'AA la plus élevée sans leur équipement et la plus faible lorsqu'ils portaient le vêtement de protection allongé. Malgré une diminution marquée de la durée globale du parcours et de la cote subjective de rendement entre le vêtement de protection balistique allongé et le vêtement traditionnel, on n'a constaté cette différence statistique importante que dans certains parcours d'obstacles. On a également observé des différences significatives avec ou sans équipement pour toutes les mesures d'AA. Comme prévu, les soldats ont affiché l'AA la plus élevée sans leur équipement et la plus faible avec tout l'équipement. On n'a constaté une diminution de l'AA entre le vêtement de protection allongé et le vêtement traditionnel que lors de la flexion avant et du lever du genou. Bien que toutes les méthodes de mesure aient été jugées fiables, le protocole Natick de mesure de l'AA s'est révélé le plus fiable pour la flexion avant, le lever du genou et l'abduction de l'épaule, tandis que le système électronique iRoM a été jugé la méthode de mesure la plus fiable pour la rotation du tronc et la flexion latérale. On a constaté un rapport plus étroit entre la durée du parcours à obstacles et le lever du genou droit et gauche, tandis que pour la cote subjective de rendement, le rapport était plutôt entre le lever du genou droit/gauche et la flexion latérale gauche et droite. On a observé un faible lien entre l'AA et le degré d'effort estimé.